TECHNISCHE UNIVERSITÄT MÜNCHEN

Institut für Experimentelle Genetik

Helmholtz Zentrum München, Neuherberg

Regulatory mechanisms underlying atopic dermatitis:

Functional characterization of the *C11orf30/LRRC32* locus and analysis of genome-wide expression profiles in patients

Judith Manz

Am Ende wird alles gut.
Wenn es nicht gut wird, ist es noch nicht das Ende.

(Oscar Wilde)

TABLE OF CONTENTS

SUMMARY

Atopic dermatitis (AD) is one of the most common chronic inflammatory skin disorders. It results from a complex interaction of genetic and environmental factors. In recent years, much research effort has been put into the identification of genetic mechanisms underlying AD; however, our understanding of the complex susceptibility to this disorder is yet incomplete. To this point, genome-wide association studies (GWAS) on AD have identified 34 genetic susceptibility loci, including common risk variants and several candidate genes playing key roles in immune-mediated pathways and defective epidermal barriers. Even though many risk genes and susceptibility loci are known, the causal functional variants underlying these association signals are still poorly identified and characterized: an almost ubiquitous problem that has become one of the greatest challenges in the "post-GWAS" era. Thus, comprehensive fine-mapping of the loci and functional studies are needed in order to refine the association signals.

The first objective of the present thesis was therefore to characterize the functionality of the common variants located at the widely replicated AD-risk locus 11q13.5, which lies between the two suggestive candidate genes *leucine rich repeat containing 32* (*LRRC32*) and *chromosome 11 open reading frame 30* (*C11orf30*): the regulatory impacts of the GWA lead SNP rs7927894 and its proxy SNP rs2155219 — a further potential functional SNP known to be associated with allergic traits — on gene regulation and differential DNA-protein binding were assessed using luciferase reporter gene and electrophoretic mobility shift assays. Secondly, targeted resequencing of the 11q13.5 locus identified a rare *LRRC32* coding variant (rs79525962/A407T) which was the target of further functional characterization including SNP-dependent changes in protein levels of *LRRC32* using flow cytometry and subcellular localization of the mutated protein. Lastly, the gene expression profiles in skin of AD patients and controls were determined to distinguish new target genes based on cutaneous expression data.

The results implicated a moderate *cis*-regulatory effect of the rs7927894 risk allele on the expression levels of *LRRC32* in whole blood cells but not in skin tissue. The proxy SNP rs2155219 (together with rs34455012indel and rs11236797C>A) exhibited enhancing activity on a minimal promoter and on the native *LRRC32* promoter in an allele- and cell-type-specific manner and EMSA experiments identified SP1 as transcription factor involved in differential binding. Functional investigation of the low-frequency *LRRC32* variant rs79525962/A407T revealed regulatory impact on expression levels of the *LRRC32* encoding protein GARP (glycoprotein A repetitions predominantly), a receptor on human regulatory T cells that binds and activates latent TGFβ. Overexpression assays in CD4+CD25- T cells demonstrated a significant reduction in GARP surface expression (P= 0.040) together with intracellular retention

of the mutated protein (P= 0.020) that were confirmed by subcellular protein localization studies in Cos-7 cells. Notably, comparable analyses in CD4+CD25- T cells obtained from AD patients carrying the A407T variant strongly support the results. Expression profiles in AD patients and controls identified new target genes that are differentially expressed in non-lesional skin (*S100A9, SPRR2F, SPPR2G, PI3, CA2, CCL8, CCl23, PTGDS*) and thereby might contribute to the early stage development of AD.

The results of this thesis indicate that both common and infrequent variants underlie the association signal for AD on chromosome 11q13.5, and that *LRRC32*/GARP is the causal gene affected. These findings contribute to the understanding of the biological basis of the disease and, together with the future investigation of the newly identified biomarkers, might lead to the development of preventive and therapeutic interventions.

ZUSAMMENFASSUNG

Die atopische Dermatitis (AD) ist eine der am häufigsten vorkommenden chronisch entzündlichen Hauterkrankungen. Sie entsteht durch eine komplexe Interaktion genetischer und umweltbedingter Faktoren. In den letzten Jahren wurde ein hoher Forschungsaufwand betrieben um die genetischen Mechanismen, die der atopischen Dermatitis unterliegen, zu erforschen; jedoch ist das Verständnis zur komplexen Entstehung dieser Erkrankung immer noch unvollständig.

Bis heute sind durch genomweite Assoziationsstudien (GWAS) 34 Suszeptibiltätsloci der atopischen Dermatitis identifiziert worden. Diese beinhalten häufig vorkommende Risikovarianten und verschiedene Kandidatengene, die in immun-vermittelten Signalwegen und bei der Störung der epidermalen Hautbarriere eine maßgebliche Rolle spielen. Viele dieser Risikogene und Suszeptibiltätsloci sind bereits bekannt, aber nur wenige der funktionellen kausalen Varianten, die diesen Assoziationen unterliegen, sind identifiziert und charakterisiert. Dies stellt ein geradezu allgegenwärtiges Problem dar, das eine der größten Herausforderungen der „Post-GWAS" Ära widerspiegelt. Aus diesem Grund sind eine umfassende Feinkartierung der assoziierten Region und funktionelle Analysen zur Aufklärung der ursächlichen Varianten und deren molekularen Auswirkungen unabdingbar.

Das erste Ziel dieser Arbeit war daher die Untersuchung der Funktionalität häufig vorkommender Varianten des AD-assoziierten Gen-Lokus auf Chromosom 11q13.5, welcher die beiden möglichen Kandidatengene *LRRC32* (*leucine rich repeat containing 32)* und *C11orf30* (*chromosome 11 open reading frame 30)* umfasst: Der regulatorische Einfluss auf die Genexpression und die DNA-Bindungsfähigkeit von Proteinen des Einzelnukleotidaustausches (*single nucleotide ploymorphism*, SNP) rs7927894, der die stärkste Assoziation in der GWA zeigte, sowie seines Proxys - SNP rs2155219 (eine weitere mögliche funktionelle Variante, die mit allergischen Merkmalen assoziiert ist) - wurde mittels Luciferase Reportergen- und DNA-Protein-Bindungs-Assays (EMSA) untersucht. Die gezielte Re-Sequenzierung des Lokus identifizierte eine seltene Variante (rs79525962/A407T) im codierenden Bereich des *LRRC32* Gens. Die funktionelle Charakterisierung dieser Variante, insbesondere die SNP-abhängige Veränderung der Proteinmengen, die mittels Durchflusszytometrie und subzellulärer Lokalisierung des mutierten Proteins ermittelt wurde, stellte das zweite Ziel dieser Arbeit dar. Eine Untersuchung der Genexpression in Hautgewebe von AD Patienten und Kontrollprobanden diente im letzten Schritt zur Aufklärung von neuen Zielgenen basierend auf spezifischen Expressionsunterschieden in der Haut.

Die Ergebnisse zeigten einen moderaten *cis*-regulatorischen Effekt des rs7927894 Risikoallels auf die *LRRC32*-Expression in Vollblut aber nicht in Hautgewebe. Der proxy SNP rs2155219 (zusammen mit rs34455012indel und rs11236797C>A) bewirkte eine verstärkte Allel- und Zelltyp-spezifische Aktivität des Minimalpromoters und des nativen *LRRC32*-Promoters. Die DNA-Protein-Bindungs-Assays identifizierten SP1 als involvierten Transkriptionsfaktor mit unterschiedlichen Bindungsaffinitäten. Die funktionelle Untersuchung der seltenen *LRRC32* Variante rs79525962/A407T zeigte eine regulatorische Wirkung auf die Expression des *LRRC32* codierenden Proteins GARP (glycoprotein A repetitions predominately). Dieses repräsentiert einen humanen Rezeptor, welcher inaktives TGFβ auf regulatorischen T-Zellen bindet und folglich aktiviert. Experimente in GARP-überexprimierenden CD4+CD25- T-Zellen verdeutlichten einen signifikanten Rückgang der GARP-Expression auf der Zelloberfläche (P= 0.040) zusammen mit einer intrazellulären Anhäufung des mutierten Proteins (P= 0.020). Vergleichbare Experimente in CD4+CD25- T-Zellen von AD Patienten, die die A407T Mutation tragen, sowie subzelluläre Lokalisierungsexperimente in Cos-7 Zellen bestätigten die zuvor gezeigten Ergebnisse. Die Expressionsanalysen in Haut der AD Patienten und Kontrollprobanden identifizierten neue Zielgene mit unterschiedlicher Expression in nicht-lesionaler Haut (*S100A9, SPRR2F, SPPR2G, PI3, CA2, CCL8, CCl23, PTGDS*), welche möglicherweise an der frühen Krankheitsentstehung der atopischen Dermatitis beteiligt sein können.

Die Ergebnisse dieser Arbeit verdeutlichen, dass sowohl die häufig als auch selten vorkommenden Varianten dem Assoziationssignal der atopischen Dermatitis auf Chromosom 11q13.5 unterliegen, und dass *LRRC32*/GARP ein beteiligtes kausales Gen darstellt. Diese Erkenntnisse leisten einen wertvollen Beitrag zum biologischen Verständnis der Erkrankung und können gemeinsam mit einer weiteren Untersuchung der neu identifizierten Biomarker die Entwicklung von Präventionsmaßnahmen und therapeutischen Interventionsstrategien unterstützen.

LIST OF ABBREVIATIONS

A	adenine		**EMSA**	electrophoretic mobility shift assay
AD	atopic dermatitis		**ENCODE**	ENCyclopedia of DNA Elements
AMP	antimicrobial peptide		**ER**	endoplasmatic reticulum
Ala	alanine		**eSNP**	expressed SNP
BH	Bonferroni Holm		**eQTL**	expression quantitative trait loci
bp	base pairs		**FBS**	fetal bovine serum
C	cytosine		**FC**	fold change
CA2	carbonic anhydrase 2		**FcεRI**	high-affinity IgE receptor
cDNA	complementary DNA		**FcεRI***A*	alpha chain of the high affinity receptor for IgE
chr	chromosome		**FLG**	filaggrin
ChIP-Seq	chromatin-immuno-precipitation DNA sequencing		**FOXH1**	Forkhead box protein H1
CI	confidence interval		**Foxp3**	Forkhead/winged-helix transcription factor box P3
CRISPR/Cas9	Clustered Regularly Interspaced Short Plaindromic Repeats / Associated Protein 9		**G**	guanine
CTLA-4	cytotoxic T-lymphocyte antigen 4		**GARP**	glycoprotein A repetitions predominant
Cy5	cyanine 5		**GFP**	green fluorescent protein
C11orf30	chromosome 11 open reading frame 30		**GLI1**	zinc finger protein GLI1
ddNTP	dideoxynucleotide triphosphate		**GO**	gene ontology
DEA	differential allelic expression		**GWAS**	genome wide association studies
DEAE	diethylaminoethyl		**H**	histone
DEAF1	deformed epidermal autoregulatory factor-1		**HapMap**	haplotype map
DET	differentially expressed transcript		**HeLa**	Henrietta Lacks cell line
DNA	deoxyribonucleic acid		**HIC1/2**	hypermethylated in cancer protein 1 and 2
DNase1	deoxyribonuclease I		**HS**	hypersensitive site
dNTP	desoxynucleotide triphosphate		**Ig**	immunoglobulin
DMEM	Dulbecco's Modified Eagle Medium		**IL**	interleukin
EASI	Eczema Area and Severity Index		**indel**	insertion/deletion
E.coli	*Escherichia coli*		**INF**	interferon
EDC	epidermal differentiation complex		**INSM1**	insulinoma-associated 1
EDTA	ethylenediamine tetraacetic acid		**kb**	kilo base
			kDa	kilo Dalton
ELISA	enzyme-linked immunosorbent assay		**KORA**	The Cooperative Health Research in the Region of Augsburg

LAP	latent associated protein		**RPMI**	Roswell Park Memorial Institute medium
LB	lysogeny broth		**RT**	room temperature
LD	linkage disequilibrium		**RT-PCR**	real time-polymerase chain reaction
LRR	leucine-rich repeat		**S100A9**	S100 calcium binding protein A9
ma	major		**SAP**	shrimp alkaline phosphatase
MACS	magnetic activated cell sorting		***S. aureus***	staphylococcus aureus
MAF	minor allele frequency		**SCCE**	stratum corneum chymotryptic enzyme
Mb	mega base		**SCORAD**	SCORing index of Atopic Dermatitis
MCS	multiple cloning site		**SD**	standard deviation
MEM	minimal essential media		**SDS**	sodium dodecyl sulfate
MHC	major histocompatibility complex		**sGARP**	soluble form of GARP
mi	minor		**SMAD**	mothers against decapentaplegic homolog
MS	mass spectrometry		**SNP**	single nucleotide polymorphism
mRNA	messenger ribonucleid acid		**SP1**	specificity protein 1
n	number		**SPINK5**	serine protease inhibitor Kazal-type 5
NCBI	National Center for Biotechnology Information		**SPRR2F**	S-mall Proline-Rich Protein 2F
n.s.	not significant		**T**	tymine
OCT1	octamer binding transcription factor 1		**TBE**	tris-borate-EDTA
OD	optical density		**TCR**	T cell receptor
OR	odds ratio		**TF**	transcription factor
PAGE	polyacrylamide gel electrophoresis		**TFBS**	transcription factor binding site
PBS	phosphate buffered saline		**TGFβ**	transforming growth factor beta
PBMCs	peripheral blood mononuclear cells		**Th**	T helper cell
PCR	polymerase chain reaction		**Thr**	threonine
PG	prostaglandin		**TLR**	toll-like receptor
PI3	Peptidase inhibitor 3		**T$_m$**	melting temperature
PMA	phorbol myristate acetate		**TNF-α**	tumor necrosis factor α
PTGDS	prostaglandin D2 synthase		**Treg**	regulatory T cell
p-value	likelihood		**TSLP**	thymic stromal lymphopoietin
q	long arm of chromosome		**U**	unit
r	correlation coefficient		**UCSC**	university of California Santa Cruz
RANTES	regulated on activation, normal T cell expressed and secreted		**UTR**	untranslated region
RIN	RNA integrity number		**UV**	ultraviolett
RLU	relative light units		**WAO**	World Allergy Organization
RNA	ribonucleic acid		**WT**	wildtype
rpm	revolutions per minute			

x g   centrifuge rotor speed in g

ZNF   zinc finger

λ   wavelength

1 INTRODUCTION

1.1 Atopic dermatitis

1.1.1 Clinical features

Atopic dermatitis (AD) is a common chronic or relapsing inflammatory skin disorder mainly characterized by dry skin, intense pruritus and red, crusting, and itching rashes (Weidinger and Novak 2015) (Figure 1). In the majority of cases, AD frequently starts in early childhood before the age of four (often so-called "early-onset atopic dermatitis or eczema") and up to 70 % of patients show a spontaneous remission in early adolescence (Olesen et al. 1996; Williams and Strachan 1998). It can also persist into or even start in adulthood (so-called "late-onset atopic dermatitis or eczema"), making it one of the most prevalent skin diseases throughout all age groups.

The common evolution of atopic dermatitis is characterized by starting from the scalp and proceeding towards the face and cheeks (mostly affected in infants), the neck, the upper extremities, the trunk and finally the lower extremities. A mild occurrence of disease tends to be restricted to the scalp-face-neck regions whereas in severe atopic dermatitis the whole body may be affected (Ring 2005). Affected areas that are characterized by a thin epidermis are prone to penetration of allergens and/or infective agents leading to secondary infections mainly caused by *Staphylococcus (S.) aureus*. Prevalence of skin colonization with *S. aureus* has widely been demonstrated (Leyden et al. 1974; Kong et al. 2012; Park et al. 2013) and often leads to worsening of the disease (Kong et al. 2012; Brussow 2015). Severe infections such as eczema herpeticum (provoked by infection with herpes simplex virus) appear in less than 5 % of patients and are accompanied by monomorphic and widespread eruptions (Wollenberg et al. 2003; Beck et al. 2009).

Figure 1: Facial and flexural atopic dermatitis in an infant and child, respectively (Weidinger and Novak 2015).

No diagnosis parameters based on histological or laboratory measurements are available for this disease, thus the gold standard of diagnosis refers only to clinical assessment parameters. A summary of various AD symptoms and diagnostic criteria are given by Hanifin and Rajka (Hanifin 1980) who describe the major criteria as pruritus, eczematous lesions, dry skin and genetic predisposition. However, these criteria have not been verified in large population-based settings, therefore a more simplified version according to clinical specifications was adapted (Williams et al. 1994a; Eichenfield et al. 2003). Based on this, atopic dermatitis can be diagnosed when pruritus and eczematous lesions are present (with age-specific morphology and distribution) which show a chronic or relapsing history located either at (1) the face, neck, and extensor of infants or children (2) and/or at skin creases such as folds at elbows, behind the knees or the front of the ankles in all age groups. Moreover, important features that support the diagnosis are early age of onset (during the first 2 years of life), skin dryness (xerosis) and a personal and/or family history of atopy. Typical associated features, that are characteristic but not specific, and help to identify the diagnosis are e.g. non-typical vascular changes like facial pallor, hyperlinearity of the palms and soles or orbital darkening. These criteria have been validated in clinical settings with high sensitivity and specificity (Williams et al. 1994a; Williams et al. 1994b; Möhrenschlager M 1998) and are therefore widely applied in epidemiological studies.

The heterogeneity in extent and severity of atopic dermatitis requires adequate parameters for assessment and various methods have been established to date. In 2010, the core outcome domains for atopic dermatitis were defined as patients-reported symptoms, quality of life, long-term control, and clinical signs (Schmitt et al. 2012). Measurements of the core outcome domains need to be valid, sensitive, and practicable to reach a consensus on international trials. Therefore, the global research initiative HOME (Harmonizing Outcomes Measures for Eczema), founded in 2010, aimed to standardize a core set of outcome measurements for atopic dermatitis and identified the Eczema Area and Severity Index (EASI) and the SCORing index of Atopic Dermatitis (SCORAD) as the best methods to assess the clinical signs of atopic dermatitis (Schmitt et al. 2010; Schram et al. 2012; Schmitt et al. 2013). The SCORAD includes an objective score to quantify the extent and intensity of the affected skin and a subjective score to evaluate subjective symptoms like itching and sleeplessness. In contrast to the EASI, the reliability to measure subjective clinical signs with the SCORAD remains unclear. That is why the EASI should be finally preferred as core instrument for assessment of clinical signs in all future AD trails (Schmitt et al. 2014).

1.1.2 Epidemiology of atopic dermatitis

The prevalence of atopic dermatitis has increased by 2- to 3-fold during the past decades. In industrialized countries, atopic dermatitis is now affecting up to 20 % of children and up to 3 % of adults. Recent data suggest that prevalence is still increasing, especially in young children in many low-income countries such as Latin America or South East Asia (Asher et al. 2006; Williams and Flohr 2006; Williams et al. 2008; Deckers et al. 2012; Mallol et al. 2013). In nearly every second patient, AD manifests within the first 6 months of life, in 60 % during the first year and in 85 % of cases before the age of 5 (Illi et al. 2004; Bieber 2008). In the majority of cases the disease clears up before adolescence (Williams and Strachan 1998) but it can also persist until adulthood or even start or reappear later in life (Garmhausen et al. 2013). Indeed, atopic dermatitis in adulthood is less common but then the symptoms are often very prominent and persistent (Sandstrom and Faergemann 2004). In children only one fifth suffers from severe AD; 80 % of affected children have a mild progression of disease (Ballardini et al. 2013). Data from the German Health Interview and Examination Survey for Children and Adolescents (KiGGS, n = 17,450) revealed that the prevalence in Germany ranges in the middle of ranked rates worldwide with a value of 13.2 % (Schmitz et al. 2012).

In addition, emerging comorbidities linked to AD have been frequently reported. Atopic dermatitis may represent the initial step of the so-called "atopic march" describing the increased risk in AD affected children to develop one or more atopic diseases like asthma, food allergy, and/or allergic rhinitis (Spergel 2010b; Zheng et al. 2011). Up to one third of affected children show an increase in prevalence for food allergy (Thomsen 2015) and also the risk for asthma and hayfever is strongly elevated in children suffering from moderate to severe atopic dermatitis (van der Hulst et al. 2007; Spergel 2010a).

1.1.3 Pathophysiology of atopic dermatitis

Atopic dermatitis is considered as a multifactorial disease characterized by a complex, heterogeneous pathogenesis and clinical phenotype, which results from various gene-gene and gene-environment interactions (Bieber 2010; Weidinger and Novak 2015). The two main key features of AD pathophysiology comprise a disturbed skin barrier function and abnormalities of the immune system resulting in cutaneous and systemic inflammation. Both hallmarks are strongly influenced and triggered by hereditary factors and environmental factors (Figure 2) (Bieber 2010; Eyerich and Novak 2013; Nutten 2015; Weidinger and Novak 2015).
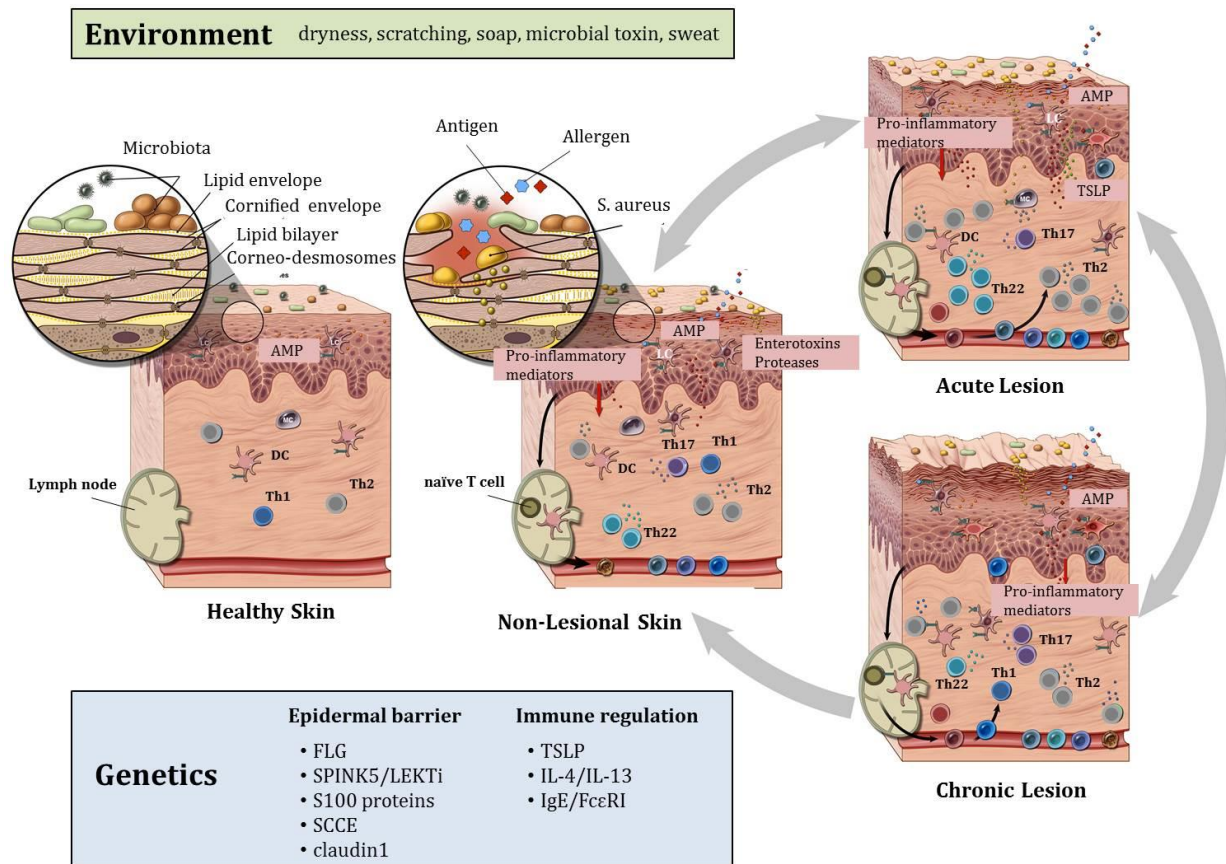
Figure 2: Heterogeneous pathophysiology of atopic dermatitis including barrier and immune abnormalities. AD may be caused by skin barrier disruption or by an impaired immune response influenced by genetic predisposition and environmental factors. Healthy skin comprises an intact and protective epidermal barrier, consisting of a cross-linked lipid-protein structure (cornified envelope) surrounded by lipid mono-and bilayers. Non-lesional (clinically unaffected) skin of AD patients already shows epidermal barrier dysfunction and subclinical inflammation induced by T-cell priming in the lymp nodes after antigen uptake and sequential infiltration of T effector cells. The acute state is mediated by amplified Th2 and Th22 immune responses, an increased colonization with *S. aureus* and progressive barrier disruption. The transition from acute lesional into chronic lesional skin is associated with continued activation of Th2/Th22 cells and additional infiltration of Th1/Th17, progressed epidermal hyperplasia resulting in remarkable cutaneous remodeling and inflammation. AMP= antimicrobial peptides; LC= Langerhans cells; DC= dendritic cell; TSLP= tymic stromal lymphopoietin; Th= T-helper. Adapted from (Weidinger and Novak 2015).

Epidermal barrier function in AD

The epidermal barrier as one of the largest front lines defenses the body against various microbes, allergens and irritants and protects against extensive water loss. The outer epidermal layer (stratum corneum), comprising of corneocytes which are characterized by a strong lipid-protein structure (known as cornified envelope) as well as lipid-enriched intracellular domains, comprises most of the barrier functions (Jensen and Proksch 2009) (Figure 2). Various changes in the epidermal barrier are well established features associated with AD such as altered stratum corneum lipid composition, raised transepidermal water loss, increased pH, disturbed

maturation of lamellar bodies, and altered activity of serine proteases (Ishikawa et al. 2010; Mutanu Jungersted et al. 2010; Levin et al. 2013; Kezic et al. 2014). Whether these epidermal abnormalities represent the primary or secondary effect of the underlying inflammation remained unknown until evidence from genetic studies highlighted the importance in hereditary predetermination of epidermal barrier genes (Barnes 2010). The strongest genetic association for atopic dermatitis so far was identified for the filaggrin gene (*FLG*) located on chromosome 1q21.3, encoding a major component of the epidermal protein-lipid envelope and a key protein in epidermal differentiation. (Marenholz et al. 2006; Palmer et al. 2006; Weidinger et al. 2006; Weidinger et al. 2008b). An early onset of disease and a severe course are characteristic features of *FLG* null mutation carriers. Filaggrin anomalies lead to marked epidermal barrier dysfunction mediated by impaired keratinocyte differentiation, abnormal corneocyte cohesion, increased water loss, impaired lipid formation and higher permeability and susceptibility to infectious agents (Gao et al. 2009; Jungersted et al. 2010; Miajlovic et al. 2010; Gruber et al. 2011; Pendaries et al. 2014). However, the disturbed epidermal function is not exclusively limited to the loss of functional *FLG* protein, as respective mutation carriers are only detectable in a subset of around 30 % of AD patients and even 8 % of the healthy population are carriers of these mutations (Irvine et al. 2011).

Moreover, other epidermal barrier-related genes such as S100 proteins, serine protease inhibitor Kazal-type 5 (*SPINK5*, also known as lymphoepthilial Kazal type-related inhibitor (*LEKT1*)), stratum corneum chymotryptic enzyme (*SCCE/kallikrein 7*) or tight junctions proteins (e.g. *claudin-1*) have been identified as being associated with AD (Moffatt 2004; Vasilopoulos et al. 2004; Glaser et al. 2009; Barnes 2010; Jin et al. 2014). In addition, a disturbed barrier function might also be favored by environmental factors such as washing with soap or other detergents, scratching, sweat and microbial toxins (Kezic et al. 2014).

Immune regulation in AD

Systemic and cutaneous inflammation is the second hallmark of AD caused by various well-characterized immune abnormalities such as increased serum IgE levels, sensitization to allergens, inflammatory cell infiltration, elevated T-helper 2 (Th2) cytokine expression, and decreased expression of anti-microbial peptides (Bieber 2008; Boguniewicz and Leung 2010; Weidinger and Novak 2015). Current pathogenic models assume that the increased permeability due to epidermal barrier dysfunction favors enhanced penetration of environmental allergens followed by interaction with local antigen-presenting Langerhans cells (LC) of the skin. Antigen presentation to naïve T cells (CD4+ cells) provokes a Th2 cell-driven inflammatory response with pro-inflammatory mediators such as interleukin (IL)-4, IL-5, and IL-13 and increased IgE

levels (Ong and Leung 2006). Antigen-primed T cells can be activated in regional lymph nodes or in local skin pools, where they endure as effector memory cells to promote rapid recall responses (Islam and Luster 2012). Antigen-presenting cells in AD are characterized by increased expression of a high infinity receptor for IgE (FcεRI) rapidly after allergen challenge. Binding of IgE to the receptor enables the uptake of allergens and supports a cutaneous inflammatory response (Steinbrink et al. 2009). Strong evidence exists that the regulation of serum IgE levels is genetically predetermined as it has been shown that functional variants of the gene encoding the alpha chain of the high affinity receptor for IgE (*FcεRIA*) strongly correlated with total IgE levels (Weidinger et al. 2008a). Enhanced IgE concentrations may lead to systemic IgE sensitization and the transition from the non-atopic to the atopic form of the disease.

The invasion of allergens due to disrupted epidermis is further implicated by an increased production of thymic stromal lymphopoietin (TSLP) by keratinocytes. TSLP, an IL-7-like cytokine, is known to be a "master switch for allergic inflammation" (Liu 2006) associated with the activation and migration of dendritic cells, Th2-polarization, and B cell differentiation (Ziegler and Artis 2010; Leyva-Castillo et al. 2013). A genetic predetermination of this inflammatory reaction is known since genetic variations in the *TSLP* gene as well as an increased TSLP expression have been strongly associated with AD (Soumelis et al. 2002; Gao et al. 2010). Moreover, the Th2-specific cytokines IL-4 and IL-13 are responsible for the differentiation of allergen-specific Th2 cells as well as the upregulation of adhesion molecules on epithelial cells (Simon et al. 2004; Callard and Harper 2007; Bieber 2010). Unsurprisingly, variants in the genes encoding for IL-4 and IL-13 have been associated with atopic dermatitis and higher IgE serum levels (He et al. 2003; Kabesch et al. 2006; Kayserova et al. 2012). Apart from that, the Th2-dominated microenvironment causes a decrease in expression of antimicrobial peptides (AMPs) (Ong et al. 2002; McGirt and Beck 2006; Howell 2007) and thereby promotes an impaired antimicrobial and permeabilized skin barrier. As a result, AD patients show a high susceptibility to bacterial and viral skin infections and an enhanced colonization with *S. aureus* (Kopfnagel et al. 2013). This feature contributes to exacerbation of the disease by *S. aureus* enterotoxins that provoke IgE-mediated sensitization, loss of suppressor activity of regulatory T cells (Treg), and induce antigen-independent proliferation of T cells (Ganem et al. 2013; Sonesson et al. 2013).

This Th2-mediated AD pathophysiology is mainly present in lesional AD skin of the acute state Although, clinically unaffected (non-lesional) skin looks normal, it already shows signs of low-level inflammation and epidermal barrier dysfunction (Figure 2). Filaggrin deficiency, impaired lipid composition of the stratum corneum, low-grade T effector cell infiltration (Th2 and Th22), increased release of Th2-promoting cytokines all together are typical characteristics of subclinical inflammation in non-lesional AD skin (Suarez-Farinas et al. 2011; Weidinger and

Novak 2015). Acute lesions are predominated by the Th2-mediated inflammation together with upregulation of further terminal differentiation genes (such as *S100A7*, *S100A8*, *S100A9*) and increase in *S. aureus* colonization that contribute to barrier disruption and acute inflammation of the skin. In contrast, in chronic lesions cell infiltration is dominated not only by Th2/Th22 cells but also by Th1/Th17 cells leading to continuous alteration of barrier function, and progression of epidermal hyperplasia and fibrosis (Simon et al. 2014).

Taken together, atopic dermatitis has a heterogeneous clinical phenotype underlying a complex pathophysiology with risk factors that affect the epidermal barrier and the immune system in combination with genetic predetermination and environmental trigger factors. Whether the skin barrier dysfunction conducts immunological abnormalities or vice versa is still unclear. The heterogeneity of the disease is evidenced by its variable clinical occurrence and indicates that different mechanisms might control specific patient subsets (Boguniewicz and Leung 2011; Eyerich and Novak 2013).

1.1.3.1 T-helper subpopulations and the role of regulatory T cells in AD

Different T cell subsets play a pivotal role in atopic dermatitis and each subset captures specific effector functions. Presentation of processed allergens by antigen-presenting cells to naïve CD4+ T cells together with co-stimulatory molecules and signals from cytokine receptors are essential for the differentiation into the T cell subsets, Th1, Th2, Th9, Th17, Th22, and T regulatory (Treg) effector cells (Eyerich and Zielinski 2014). These T cell subsets promote different types of inflammatory responses by producing various and characteristic cytokines (Figure 3).

Th1 cells

Th1 cells are involved in cell-mediated immunity including defense against intracellular microorganisms. Th1 development is usually triggered after contact with intracellular bacteria and the cytokine IL-12 released from naïve CD4+ T lymphocytes. A deregulated Th1 signal cascade results in apoptosis of keratinocytes followed by destruction of tissue in autoimmune disease (e.g. psoriasis, rheumatoid arthritis, asthma) (Skapenko et al. 2005; Jutel and Akdis 2011).

Th2 cells

Secretion of IL-4 leads to the differentiation of naïve T cells into Th2 cells inducing isotype switching to IgE synthesis and mediating of allergic inflammation in atopic dermatitis. The Th2-dominated cytokine environment counter-regulates the Th1-mediated induction of

antimicrobial peptide production in epithelial cells and favors the disruption of the epidermal barrier by downregulating distinct epidermal barrier genes (Albanesi et al. 2007; Howell et al. 2008; Howell et al. 2009). Hence, the Th2-dominated microenvironment largely explains the phenotype of atopic dermatitis in the acute state. However, more chronic AD lesions show a distinct infiltration with newly described T cell subsets such as Th17 and Th22 (Eyerich et al. 2009; Nograles et al. 2009).

Th17 cells

Secretion of IL-1β, IL-23 and transforming growth factor beta (TGFβ) induces Th17 cells generation. These cells secrete their name-giving cytokine IL-17 and thereby mediate protective immunity against extracellular pathogens and control tissue inflammation by recruitment and support of neutrophils survival (Schmidt-Weber et al. 2007). Similar to the Th1 cytokines, IL-17 is known to induce antimicrobial peptides in epithelial cells, however this is antagonized by the Th2 immunity in acute AD skin (Howell et al. 2006; Eyerich et al. 2009).

Th22 cells

Another T-helper cell subset known as Th22 cells, which secretes the signature cytokines IL-22 and TNF-α, show either protective or pathogenic effects in AD. Secretion of IL-22 favors skin integrity and wound healing through keratinocyte migration and proliferation. On the other side, Th22 cells play a role in inflammation by enhancing the TNF-α-induced cytokines and chemokines released by keratinocytes (Trifari et al. 2009; Cavani et al. 2012).

Th9 cells

A novel subset of effector T helper cells, named as Th9 cells, differentiates from naïve CD4+ cells after IL-4 and TGFβ stimulation (Veldhoen et al. 2008). This cell population is characterized by IL-9 release which in turn leads to tissue inflammation in autoimmune diseases (Jutel and Akdis 2011), however, the precise contribution of Th9 cells in AD remains to be clarified.
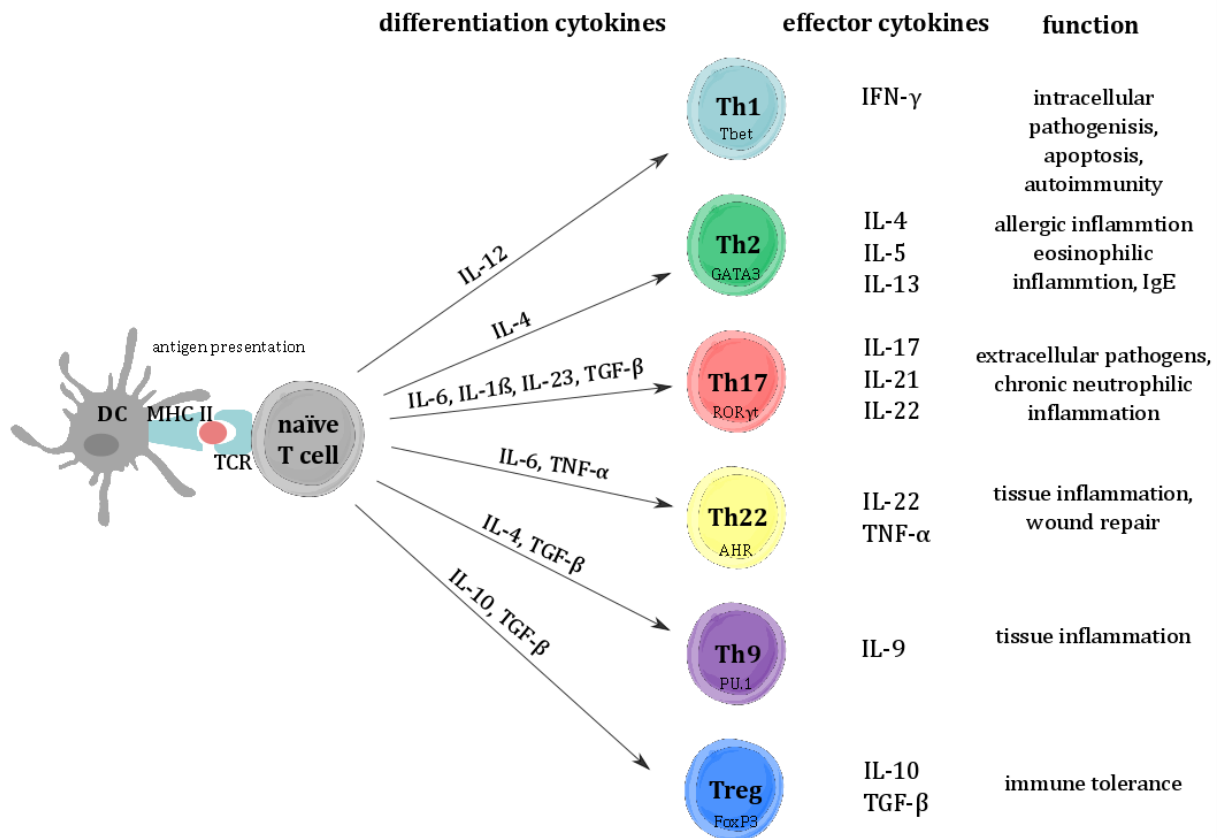
Figure 3: Differentiation of naïve T cells into T-helper (Th) subsets induced by dendritic cells (DC) and respective cytokine environments. Antigen presentation by dendritic cells via major histocompatibility complex II (MHC II) to the T cell receptor (TCR) on naïve T cells, expression of co-stimulatory molecules and cytokine microenvironment leads to differentiation of naïve T cells into various T cell subsets regulated by lineage-specific transcription factors. Based on their individual effector cytokine profiles different effector functions are promoted. DC=dendritic cell, MHC= major histocompatibility complex, TCR= T cell receptor, Th= T-helper cell, IL= interleukin, TGF= transforming growth factor, INF= interferon, TNF= tumor necrosis factor (adapted from (Jutel and Akdis 2011; Eyerich and Zielinski 2014)). Figure was prepared using a template on the Servier medical art website (http://www.servier.com/Powerpoint-image-bank).

Regulatory T cells (Tregs)

The release of IL-10 induces the differentiation of naïve T cells into regulatory T cells. These cells play a key role in maintenance of the immune tolerance and the control of allergic responses. Tregs are characterized by their suppressive IL-10 and TGFβ secretion capacity that drive dampening of immune response through the suppression of T-cell activation, IgE production and suppression of allergic inflammatory effector cells such as mast cells and eosinophils (Jutel and Akdis 2008). Tregs comprise a heterogenic population containing various surface markers and characteristics. Natural Tregs (CD4+CD25+), which originate from the thymus, express the surface marker CD25 (IL-2 receptor alpha chain) and are characterized by constitutive expression of the transcription factor Foxp3 (Forkhead/winged-helix transcription factor

box P3) (Agrawal et al. 2011). In addition to naturally occurring thymic-derived Tregs, so called "adaptive or induced" regulatory T cell subsets, induced by foreign antigens in the periphery, have been described. Members are IL-10-secreting Tr1 cells and TGFβ-induced Th3 cells (Cavani et al. 2001; Wu et al. 2007).

Despite a growing interest in the role of Tregs in the pathogenesis of AD, their precise contribution remains unclear. Evidence that a decrease in Tregs or changes in their functions might influence the pathogenesis of AD comes from clinical syndromes that are associated with Foxp3 mutations. Those loss-of-function mutations lead to a multi-organ inflammatory response including skin inflammation, elevated IgE levels, eosinophilia, and autoimmunity which is linked to Treg deficiency (d'Hennezel et al. 2012). Moreover, stimulation by staphylococcal superantigens, produced by *S. aureus* during colonization of affected AD skin, causes loss of Treg-suppressive activity and favors increase in skin inflammation (Cardona et al. 2006).

The molecular mechanisms underlying Treg-mediated suppression are still also not fully understood. Besides the immunosuppressive effect of Treg-produced cytokines, cell contact-dependent mechanisms may play a significant role in T cell suppression. Natural Tregs constitutively express high cytotoxic T-lymphocyte antigen-4 (CTLA-4), a surface molecule that binds to surface markers (CD80/CD86) on antigen-presenting cells by which T cell activation is inhibited (Wing et al. 2008; Shevach 2009). Another surface molecule that is expressed on activated Tregs, the protein named glycoprotein A repetitions predominant (GARP), has recently been moved into the focus of AD-related research. GARP is a transmembrane protein encoded by the leucine rich repeats containing 32 gene (*LRRC32*) and consists of 662 amino acids with an extracellular domain comprising the name-giving leucine rich repeats (Roubin et al. 1996; Wang et al. 2008). GARP is known to bind the inactive latent form of TGFβ, an immune suppressive cytokine involved in shaping effector T cell populations and a key cytokine in the regulation of inflammatory responses (Banchereau et al. 2012b; Edwards et al. 2013). Through surface anchoring of latent TGFβ, GARP is directly involved in mediating its activation and bioavailability (Tran et al. 2009). Moreover, it has been shown that siRNA induced depletion of GARP leads to reduced suppressive activity and Foxp3 expression in Tregs (Probst-Kepper et al. 2009) demonstrating that GARP presents a key player in the regulatory network of Tregs and their targets during inflammation.

1.1.4 Therapeutic strategies of atopic dermatitis

As a result of the increasing incidence of atopic dermatitis worldwide the burden of healthcare cost increases and the life quality of affected patients is substantially decreased (Plotz et al.

2014). Until today no cure for atopic dermatitis exists, thus, the disease management focusses on improving the symptoms and disease long-term control by addressing pathogenic factors of AD development. AD therapy is largely predominated by epidermal barrier repair with emollients, suppression of inflammatory response using topically applied steroids, calcineurin inhibitors or immunosuppresive agents, and avoidance of allergens to prevent disease exacerbation and flare (Howell et al. 2015; Weidinger and Novak 2015). A typical step-wise approach for AD treatment, as outlined in common guidelines (Akdis et al. 2006; Darsow et al. 2010; Ring et al. 2012), is shown in Figure 4.
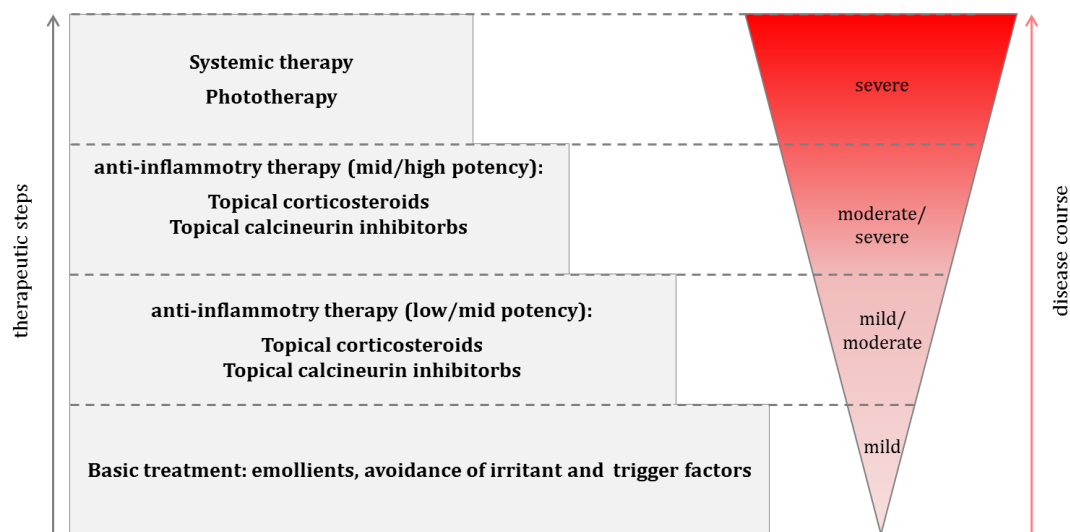
Figure 4: Step-wise approach of atopic dermatitis management. According to severity of the disease different treatment steps addressing key pathological factors are applied. Adapted from (Akdis et al. 2006; Plotz et al. 2014; Weidinger and Novak 2015).

The basic treatment includes the frequent use of emollients, which soften the skin through supply of lipids and sterols and increase skin hydration by reducing evaporation through formation of an occlusive layer (Weidinger and Novak 2015). Application of topical steroids is the first-line anti-inflammatory treatment for acute flares of AD and several randomized controlled trials confirm their efficiency on rapid relief (Hoare et al. 2000). However, prolonged use is associated with several adverse effects such as skin atrophy, acneiform eruptions, rebound flares and the tendency to develop tachyphylaxis (rapid decrease in response to a drug) (Fardet et al. 2007). For this reason, topical corticosteroids should be used carefully and low-potency therapy is preferred especially on skin areas with thinner skin layers and in children (Weidinger and Novak 2015). Topical calcineurin inhibitors (tacrolimus, pimecrolimus) are non-steroidal immunosuppressive agents that are recommended as second option for short-term and occasional treatment (Ring et al. 2008). In contrast to topical corticosteroids, topical calcineurin inhibitors do not induce skin atrophy and are therefore helpful for the application in sensitive

areas with thin skin. Their clinical efficacy is roughly identical with mild to moderate topical steroids (Ashcroft et al. 2005).

In patients with severe AD and refractory manifestation of the disease, systemic immunosuppressive therapy or phototherapy is suggested. Phototherapy represents a second-line intervention in those cases where non-pharmacological and topical measures have failed. Phototherapy is generally considered to be safe and well tolerated, with a low but established number of adverse effects, such as photodamage, xerosis, erythema, actinic keratosis, and sunburn (Patrizi et al. 2015). As a last step, when phototherapy and topical treatment have failed, systemic immunosuppressive therapy is necessary to treat severe and recalcitrant cases of AD. Cyclosporine A, a potent systemic calcineurin inhibitor, represents the most established systemic agent (Schmitt et al. 2007). However, common systemic agents for AD therapy are unspecific and limited both in their application and by causing end-organ toxicities during continuous use. Effective therapeutic alternatives such as targeted immunomodulatory approaches using monoclonal antibodies have strong advantages over conventional pharmacotherapy with less toxicity (Novak and Simon 2011). However, compared to other inflammatory skin diseases (e.g. psoriasis), the effect of those approaches for AD treatment remains uncertain and no biologic therapy is approved for the treatment of AD so far (Howell et al. 2015; Griffiths et al. 2017).

1.1.5 Genetics of atopic dermatitis

Atopic dermatitis is considered a multifactorial disease triggered by a complex interaction between multiple genes. Unlike monogenic disorders, that are caused by mutations in a single gene, AD seems to occur on the basis of variations in a variety of different genes, which do not follow the classical Mendelian inheritance patterns (Glazier et al. 2002). There is substantial evidence that genetic predisposition plays a fundamental role in the development of AD. The importance of genetics in AD is clearly demonstrated by twin studies, which show a considerably higher concordance rate in monozygotic twins (72 %- 86 %) compared to dizygotic twins (21 % - 23 %) (Cookson 2001; Strachan et al. 2001). The overall heritability of AD estimated from all twin studies published after 1970 account for up to 70 % (Elmose and Thomsen 2015). Furthermore, evidence of a positive family history for AD comes from large multiple studies investigating affected patients and their families (Kaiser 2004). Results of these studies showed that children from parents suffering from AD have a higher risk in developing AD than children whose parents have asthma or allergic rhinitis (Moore et al. 2004; Wadonda-Kabondo et al. 2004).

1.1.5.1 Genetic studies in atopic dermatitis

In the past decade, significant progress has been made in the field of genetics by identifying many candidate genes and loci that are linked and associated with atopic dermatitis (Barnes 2010; Hoffjan and Stemmler 2015). Different approaches have been utilized to investigate genetic associations in AD to date.

Linkage studies

Linkage studies, in which the entire genome is screened for chromosome regions linked with the disease in families independently of hypotheses, identified several chromosomal regions (including 1q, 3q, 3p, 4q, 5q, 11p 17q, 18q and 20p) that show linkage to atopic dermatitis (Lee et al. 2000b; Cookson 2001; Haagerup et al. 2004; Guilloud-Bataille et al. 2008; Christensen et al. 2009). However, linkage studies are not able to identify specific genes as the identified linked regions typically enclose a large genomic region encoding many different genes. Moreover, results from linkage studies differ greatly from each other and only very few genetic associations have been reliably replicated in other cohorts (Barnes 2010).

Candidate gene studies

In contrast, to identify responsible genes candidate gene approaches represent a more enhanced method to detect direct gene-disease association across the genome. Genetic markers (single nucleotide polymorphisms (SNP), insertions, deletions) in candidate genes of interest (supposed to be causally involved in the underlying disease) are compared among cohorts with a case-control study design (Risch and Merikangas 1996). A comprehensive review in 2009 (Barnes 2010) recorded 111 AD candidate gene studies so far, whereof 81 candidate genes were analyzed and of which 46 genes showed significant association with AD. Replications of AD association in at least two independent studies have finally been shown for 13 genes. Among these genes, the filaggrin encoding gene (*FLG*) is the only one which consistently associates in more than 20 studies, representing the only established risk gene to date (O'Regan et al. 2008). Two common *FLG* mutations (R501X and 2282del4) represent the strongest genetic risk factors for AD in the European Caucasian population (Baurecht et al. 2007; Rodriguez et al. 2009). However, selection of candidate genes is often based on limited knowledge and single genes are believed to only add small knowledge to the overall heritability (Hirschhorn 2005).

Genome-wide association studies

More recently, genome-wide association studies (GWAS) have been presented as an unbiased approach to replace candidate gene studies and to search for genetic markers influencing

complex traits in large case-control cohorts (Hardy and Singleton 2009). Over the last years, rapid advances in technology have allowed to analyze >1,000,000 SNPs simultaneously in a single scan with chip-based methods in these studies (Spencer et al. 2009). At the end, results comprise significantly different allele frequencies of analyzed SNPs, which are termed as an association of the SNP with the disease, between patients and healthy controls. Threshold of statistical significance in genome-wide association studies are stringent, making it necessary to use a large sample set (Hunter and Kraft 2007).

So far, eight genome-wide association studies on atopic dermatitis have been performed (Esparza-Gordillo et al. 2009; Sun et al. 2011; Hirota et al. 2012; Ellinghaus et al. 2013; Weidinger et al. 2013; Baurecht et al. 2015; Paternoster et al. 2015; Schaarschmidt et al. 2015), identifying more than 30 susceptibility loci tagged by highly associated SNPs (Table 1). Most of the risk genes located in susceptibility loci contribute to the biological function of the epidermal barrier (e.g. *FLG, OVOl1, ACTL9*), are involved in immune mechanisms (e.g. *RAD50/IL13, IL2/IL21, IL18R1/IL18RAP*), tissue response (e.g. *LRRC32, GLB1, ZNF652*), or environmental sensing (e.g. *CARD11, HLA-DRB1/HLA-DQA1*). Evidence from a recently published meta-analysis of 22 European studies, including 21,399 cases and 95,464 controls with multi- ancestry, replicated 16 of the known AD risk loci and identified 11 novel risk loci, bringing the total number of AD risk loci up to 34 so far (Paternoster et al. 2015). The new loci include risk genes with known function in autoimmunity and immune regulation, especially innate host defense as well as T cell activation and specification (*PPP2R3C, IL-7R, STAT3, ZBTB10, ETS1, CD207*).

Further GWA analyses demonstrated that there is substantial genetic overlap between atopic dermatitis and other inflammatory diseases such as asthma (Weidinger et al. 2013; Marenholz et al. 2015), allergic rhinitis (Marenholz et al. 2011) and inflammatory bowel diseases (Schreiber et al. 2005; Barrett et al. 2008). Moreover, meta-analyses of GWA data suggest common genetic risk loci for AD and psoriasis, another common cutaneous inflammatory disorder associated with Type 1-polarized immune response (Weidinger et al. 2013; Baurecht et al. 2015). In general, it seems that many of the identified GWA risk genes have been linked to other immune-mediated diseases and only a few are involved in other atopic traits.

1.1.5.2   AD associated locus 11q13.5 – an pleiotropic locus for atopic diseases

One of the most robust AD-associated regions refers to the 11q13.5 locus that was identified in the first GWAS in 2009 (Esparza-Gordillo et al. 2009). Within this study, 0.5 million SNPs were genotyped in two independent discovery cohorts comprising 939 AD cases and 975 controls (set 1) and 270 independent families with two affected siblings (set 2). Highly associated

genomic regions were subsequently tested in two further independent replication sets (1363 cases and 2739 controls; 1274 cases and 1218 controls for set 3 and 4, respectively). A meta-analysis with all 9500 studied individuals revealed the strongest genome-wide significant association (P= 7.6 x 10^{-10}) with atopic dermatitis for the marker rs7927894 (C>T) at 11q13.5 (Figure 5). Heterozygous carriers of the rs7927894 A risk allele had a 1.16 times higher risk of developing AD (odds ratio (OR) =1.16; 95 % confidence interval (CI):1.02-1.32), whereas homozygous carriers showed a 1.47 times higher risk for AD development (OR=1.47; 95 % CI:1.29-1.68) (Esparza-Gordillo et al. 2010).

The associated SNP rs7927894 is located in an intergenic region 38 kb downstream of the gene *C11orf30* (chromosome 11 open reading frame 30) and 68 kb upstream of the gene *LRRC32* (leucine rich repeat containing 32). *C11orf30* encodes the nuclear protein EMSY which has been shown to be involved in transcriptional regulation, DNA repair, and has recently been reported to play a role in the regulation of interferon-stimulated transcription (Ezell and Tsichlis 2012). Moreover, EMSY acts as a transcriptional repressor of the *BRACA2* (breast cancer 2) gene and mRNA and protein amplification of EMSY has been reported in epithelium-derived ovarian and breast cancer (Brown et al. 2006; Altinisik et al. 2011). The other nearby located gene *LRRC32* encodes the protein GARP, a surface protein highly expressed on regulatory T cells (Wang et al. 2008). As described in chapter 1.1.3.1, regulatory T cells play an important role in maintaining the immune homeostasis and GARP might represent a key factor in this regulatory network during cutaneous inflammation.
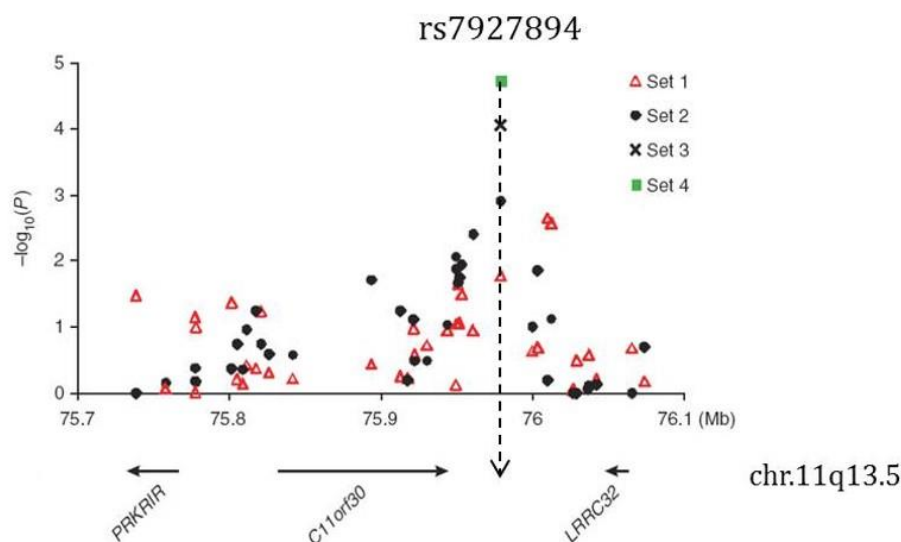
Figure 5: Genome-wide associations for atopic dermatitis on chromosome 11q13.5. The strongest association was observed for rs7927894 (P= 7.6 x 10^{-10}), indicated by vertical dotted line. Location of genes in the 11q13.5 region is indicated by arrows and gene names (based on NCBI build 36). Association results are based on the first genome-wide association study (GWAS) in AD patients. Adapted from (Esparza-Gordillo et al. 2009).

Table 1: Summary of genome-wide association studies for atopic dermatitis (adapted from (Hoffjan and Stemmler 2015; Bin and Leung 2016)

Reference	Study population	Initial sample description	Replication sample description	Region	Genes (newly identified)	Most significant associations (p-value)
Esparza-Gordillo J et al. (2009)	European	939 cases 975 controls, (from 270 families)	2,637 cases 3,957 controls	11q13.5 1q21	C11orf30/LRRC32*§#^ FLG∞≠*#	rs7927894 (8 x10⁻¹⁰) rs6661961 (1.2 x10⁻⁹)
Sun LD et al. (2011)	Han Chinese	1,012 cases 1,362 controls	3,624 cases, 12,197 controls 1,806 European ancestry cases, 3,256 European ancestry controls	5q22.1 20q13.33	TMEM232/SLC25A46* TNFRSF6B/ZGPAT*§#	rs7701890 (3.15 × 10⁻⁹) rs6010620 (3.0 × 10⁻⁸)
Paternoster L et al. (2011)	European (meta-analysis)	5,606 cases 20,565 controls	5,419 cases 19,833 controls	11q13.1 19p13.2 5q31	OVOL1*^ ACTL9^ KIF3A/RAD50/IL13*§^	rs479844 (1.1 × 10⁻¹³) rs2164983 (7.1 × 10⁻⁹) rs2897442 (3.8 × 10⁻⁸)
Hirota T et al. (2012)	East Asian (Japan)	1,472 cases 7,971 controls	1,856 cases 7,021 controls	2q12 6p21.3 11p15.4 3p21.33 3q13.2 7p22 10q21.2 20q13	IL1RL1-IL18R1-IL18RAP*^ GPSM3 (MHC)*^ OR10A3/NLRP1*^ GLB1* CCDC80*^ CARD11* ZNF365*^ CYP24A1/PFDN4*^	rs13015714 (8.35 × 10⁻¹⁸) rs176095 (8.38 × 10⁻²⁰) rs878860 (1.54 × 10⁻²²) rs6780220 (2.77 × 10⁻¹⁶) rs12634229 (1.56 × 10⁻¹⁹) rs4722404 (7.83 × 10⁻⁹) rs10995251 (5.58 × 10⁻²⁰) rs16999165 (1.65 × 10⁻⁸)
Weidinger S et al. (2013)	European	1563 cases 4,054 controls	2,286 cases 3,160 controls	5q31 6q21 11q13	RAD50/IL13* MHC^ LRRC32	rs2158177 (2.65 × 10⁻¹⁰) rs6474 (1.61 × 10⁻⁹) rs2155219 (8.17 × 10⁻⁹)
Ellinghaus D et al. (2013)	European, Japanese, Chinese	2,425 cases 5,449 controls	2,425 cases 5,449 controls	4q27 11p13 16p13.13 17q21.32 1q21.3 2q12.1	IL2/IL21*^ PRR5L*^ CLEC16A*^ ZNF652* LCE3A SLC9A4	rs17389644 (1.30 × 10⁻⁸) rs12295535 (7.96 × 10⁻¹³) rs2041733 (3.44 × 10⁻¹⁵) rs16948048 (2.92 × 10⁻⁹) rs72702813 (1.49 × 10⁻³³) rs759382 (6.01 × 10⁻¹¹)
Baurecht H et al. (2015)	European	2,079 cases 3,867 controls	na	1q21.3 1q21.3	LCE3E^ LCE1E	rs10888499 (5 x 10⁻²⁵) rs77199844 (2 x 10⁻¹⁷)
Schaarschmidt H et al. (2015)	European	924 cases 5506 controls	1383 cases 1728 controls	2q24.3 9p21.3	XIRP2/CYMA3 DMRTA1	rs6720763 (4.37 × 10⁻⁸) rs10738626 (1.45 × 10⁻⁸)
Paternoster L et al.	Multi-ancestry	21,000 cases 95,000 controls	32,059 cases 228,628 controls	14q13.2 11q24.3 1q21.2 8q21.3 10p15.1 5p13.2 2p25.1 2p16.1 17q21.2 3p21.1 2p13.3	PPP2R3C EST1 C1orf51/MRPS21 MIR5708/ZBTB10 IL15RA/IL2RA IL7R/CASPL LINC00299 PUS10 STAT3 SFMBT1/RFT1 CD207/VAX2	rs2038255 (1.8 × 10⁻¹⁰) rs7127307 (3.9 × 10⁻¹⁰) rs7512552 (9.1 × 10⁻¹⁰) rs6473227 (1.4 × 10⁻⁹) rs6602364 (1.5 × 10⁻⁹) rs10214237 (2.9 × 10⁻⁸) rs10199605 (3.4 × 10⁻⁸) rs4643526 (3.5 × 10⁻⁸) rs12951971 (4.1 × 10⁻⁸) rs7625909 (4.9 × 10⁻⁸) rs112111458 (1.4 × 10⁻⁷)

*: gene locus replicated in (Schaarschmidt et al. 2015); §: gene locus replicated in (Ellinghaus et al. 2013); #: gene locus replicated in (Baurecht et al. 2015); ∞: gene locus replicated in (Weidinger et al. 2013); ≠: gene locus replicated in (Sun et al. 2011); ^: gene locus replicated in (Paternoster et al. 2015)

Importantly, the association between rs7927894 and AD has been replicated in an Irish and Austrian study cohort (O'Regan et al. 2010; Greisenegger et al. 2013) and the same locus, however tagged by different lead SNPs, has been associated in further GWAS on atopic dermatitis in the last years (Ellinghaus et al. 2013; Baurecht et al. 2015; Schaarschmidt et al. 2015). Notably, the rs7927894 risk allele has also been associated with Crohn's disease, an inflammatory bowel disease sharing many pathophysiological characteristics with AD including epithelial inflammation, abnormal barrier function, and disturbed immune response (Schreiber et al. 2005; Barrett et al. 2008). Furthermore, association of rs7927894 with atopic asthma and hay fever has been demonstrated by analyzing over 9300 probands of the ALSPAC cohort (Avon Longitudinal Study of Parents and Children birth cohort) (Marenholz et al. 2011). Ferreira et al. reported further association with asthma of a variant (rs7130588) closely located to rs7927894 at the 11q13.5 locus (Ferreira et al. 2011). This proxy SNP is in complete linkage disequilibrium (LD) (r^2= 1) with rs7927894 and the two risk alleles (rs7927894:T and rs7130588:G) that occur on the same haplotype, indicating the same underlying causal variant is responsible for the observed association. Another proxy SNP (rs2155219 G>T) located on 11q13.5 and in high LD with the GWA lead SNP (r^2= 0.722), has been shown to be associated with allergic rhinitis and grass sensitization in four large European adult cohorts comprising up to 12,000 participants (Ramasamy et al. 2011). Interestingly, the same SNP has recently been reported to be associated with reduced expression levels of *C11orf30* and *LRRC32* in white blood cells and adipose tissue (Bonnelykke et al. 2013). In summary, these results indicate that the AD-associated 11q13.5 locus represents a very pleiotropic region not only for atopic dermatitis but also for many other atopic diseases.

1.1.5.3   Follow-up of genome-wide association studies by functional studies

Genome-wide association studies represent a starting point on the way to elucidate and understand the genetic basis of complex traits and common diseases. Even though various risk genes and susceptibility loci are known, the causal functional variants underlying these association signals are still poorly identified and characterized (Hardy and Singleton 2009). Furthermore, GWAS cannot answer the question whether a disease-associated genetic variant is functionally important or serving only as a genetic marker, which is in linkage disequilibrium with the functional variant. For further elucidation of validated association signals and for the identification of causal gene variants, fine mapping of the region and functional analyses are mandatory. Only a small number of identified trait-associated SNPs are located in protein-coding regions (Cargill et al. 1999); approximately 80 % of trait-associated SNPs can be found in intergenic regions and non-coding introns demonstrating a prominent role of these regions on

modulating gene expression (Wray 2003; Hardy and Singleton 2009). A variety of experimental *in vitro* methods (e.g. reporter gene assays, EMSAs, etc.) can be used to investigate the functional significance of these SNPs on gene regulation, RNA stability, protein expression, and control of protein levels (Knight 2003). Comprehensive characteristics of the SNPs using these tools are the key steps in improving our understanding of the mechanisms of disease and in designing effective strategies for risk assessment and treatment.

1.2   Aim of the study

This study aimed to contribute to the post-genome era by exploring the functional properties of the AD-associated locus *C11orf30/LRRC32* at chromosome 11 through elucidation of involved target genes and functional variants underlying the association signal.

The first aim of this thesis was to characterize the functionality of the common AD-associated lead SNP — rs7927894 — and selected potential functional variants being in LD with this SNP: the regulatory impacts of these SNPs on candidate and reporter gene expression in skin and appropriate cell lines were assessed. Further, differential protein-DNA binding patterns and the involvement of transcription factors were investigated and characterized.

The second aim was to study the functional implication of a rare *LRRC32* missense variant that was identified through targeted resequencing of the AD-associated locus. The investigation focused on SNP-dependent changes in mRNA and protein levels of *LRRC32* as well as on the subcellular localization of the mutated protein.

To identify new AD target genes based on expression data, the third aim was to compare the genome-wide expression profiles of lesional and non-lesional skin of AD patients and healthy controls.

2 RESULTS

The following chapter is divided into three parts: the first part covers the functional impact of the AD-associated GWA lead SNP rs7927894 and its proxy SNP rs2155219 mainly on transcriptional activity of candidate gene expression and differential protein binding. The second part focusses on the functional impact of the rare *LRRC32 (*leucine rich repeat containing 32) coding variant rs79525962 on RNA and protein expression levels. The third part presents genome-wide expression profiles in affected and non-affected skin of atopic dermatitis patients compared to healthy controls.

2.1 The GWA lead SNP rs7927894 and its proxy SNPs within the AD-associated 11q13.5 locus

Most of the strongest signals derived from genome-wide association studies (GWAS) are located far away from annotated loci mostly in non-coding and intronic regions (Wray et al. 2003; Freedman et al. 2011). How these identified GWA hits are connected to its associated traits is still unclear and turned out to be one of the greatest challenges in the "post-GWAS" era. The GWA lead SNP rs7927894, identified by the first genome-wide association study on atopic dermatitis (Esparza-Gordillo et al. 2009), is associated with atopic dermatitis and other inflammatory traits and is located in an intergenic region on chromosome 11q13.5 between the two annotated genes *LRRC32* (leucine rich repeat containing 32) and *C11orf30* (chromosome 11 open reading frame 30). Considering a possible regulatory role of this intergenic region (chr11: 75831792-76074500) an intense public database research using UCSC and ENCODE databases (http://www.genome.ucsc.edu/ENCODE/) revealed a conserved and potentially high regulatory region (termed as 7x Regulatory Potential, regulatory potential scores calculated from alignment of seven mammals using ESPERR (evolutionary and sequence pattern extraction through reduced representations, (Taylor et al. 2006)) including DNase1 hypersensitivity clusters, promoter- and enhancer-associated histone marks (H3K4Me1), and different conserved transcription factor binding sites (all from Chip-seq data, ENCODE project) (Figure 6). Rs7927894 is located not directly in, but in between several peaks of high regulatory potential.
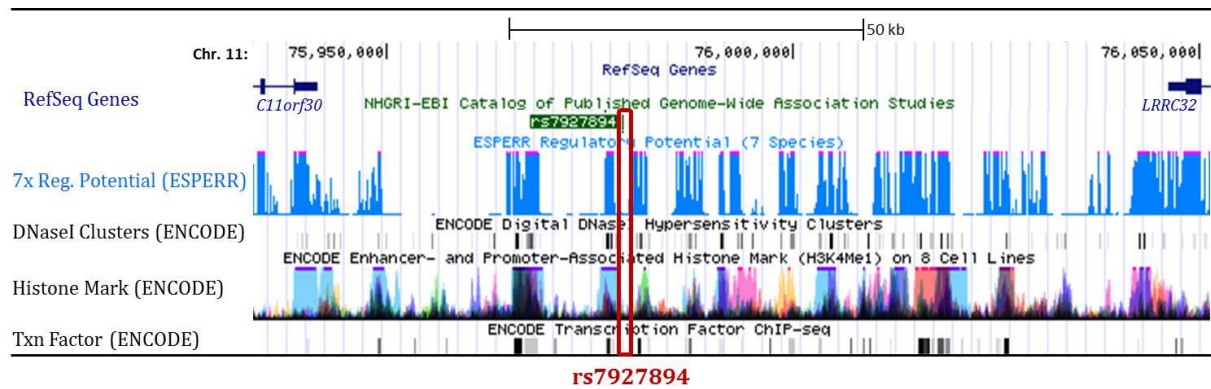
Figure 6: Functional regulatory database analysis of the AD-associated GWA lead SNP rs7927894 containing intergenic region using UCSC Genome Browser (NCBI36/hg18 chr11:75922950-76054392). SNP is located close to high regulatory regions (7x Reg. Potential, ESPERR), DNaseI Hypersensitivity Cluster (ChIP-seq, ENCODE), enhancer- and promoter-associated Histone marks (H3K4Me1, ChIP-seq, ENCODE) and transcription factor binding sites (ChIP-seq, ENCODE). SNP location is outlined by red box. ESPERR= evolutionary and sequence pattern extraction through reduced representations; ENCODE= ENCyclopedia of DNA Elements.

2.1.1   Allelic expression analysis of *LRRC32* and *C11orf30* transcripts depending on rs7927894

The impact of the GWA lead SNP rs7927894 on candidate gene expression was initially assessed by expression analysis in the KORA F4 study. Existing genotype data of rs7927894 and expression data of the two neighboring genes *LRRC32* and *C11orf30* in the KORA F4 cohort (n=739) were analyzed in order to detect a genotype-specific impact of rs7927894 on transcript levels of *C11orf30* and *LRRC32*. A significant rs7927894-dependent lower expression level (P= 0.0055) of *LRRC32* was observed in minor T allele (risk allele) carriers compared to major C allele (non-risk) carriers. No rs7927894-dependent expression difference was observed for *C11orf30* transcript levels. However, this analysis was conducted in whole blood which might be not the adequate cell system for analyses in the context of AD.

To investigate *cis*-regulation of variants on gene expression levels within the tissue of interest, e.g. skin, allelic expression analysis exhibits an alternative and complementary approach. This technique compares the relative expression of the two alleles in one single individual resulting in detection of skewed and non-skewed allelic expression of investigated genes (Serre et al. 2008; Berulava and Horsthemke 2010). For this purpose, RNA from individuals who are heterozygous for the investigated SNP and heterozygous for an expressed SNP (eSNP) located in *C11orf30* and *LRRC32*, respectively, were used. The eSNP serves as tagging marker within the respective gene and eSNP selection was carried out in co-operation with Andrew Johnson from the National Heart, Lung, and Blood Institute (NHLBI) by interrogation (2 Mb around

rs7927894) of an eSNP database, consisting of published associations between gene transcript levels and genotypes of nearby SNPs in *cis* of various tissues and cell types (Kottgen et al. 2013). For *LRRC32*, an eSNP (rs3781701) located in the 3' untranslated region (UTR) and for *C11orf30* an intronic eSNP (rs2282611) was selected. Allele-specific gene expression was measured in skin samples of five individuals using fluorescence-tagged single-nucleotide primer extension assays. Allelic RNA expression levels were determined by comparing the number of genomic DNA molecules for each allele (ratio expected to be 1:1), with the number of allelic mRNA molecules within the same individual.

Since no proxy SNPs of rs7927894 are present which are in high linkage disequilibrium (LD) with selected eSNPs, allelic expression patterns were additionally determined in control samples that were heterozygous for the eSNP but homozygous for the associated SNP. Available genotype combinations and allelic imbalance in analyzed individuals and controls are shown in Figure 7: if the AD-associated SNP affects gene expression, an allelic expression imbalance of the candidate genes (*LRRC32* or *C11orf30*) tagged by the eSNP would be observed in rs7927894 heterozygotes, but not in rs7927894 homozygotes (control samples). Similar degrees of skewing in rs7927894 hetero- and homozygous individuals demonstrate that the gene expression of *LRRC32* and *C11orf30* is not affected by the rs7927894 genotype.

	SNP of interest	eSNP		DEA "causal" SNP
individuals	+/-	+/-	DAE	SNP of interest
controls	+/+ or -/-	+/-	no DAE	
individuals	+/-	+/-	DAE	eSNP/proxy SNP
controls	+/+ or -/-	+/-	DAE	

Figure 7: Scheme of genotype combinations and differential allelic expression (DAE) patterns in analyzed individuals and control individuals. The SNP of interest is responsible for expression imbalance if there is a DAE in heterozygous individuals but not in control samples. If there is DAE in both samples, the eSNP or any proxy SNP might be responsible for the detected expression imbalance. DAE: differential allelic expression; eSNP: expressed SNP; +/-: heterozygous alleles; +/+ or -/-: homozygous alleles.

As shown in Figure 8 relative transcript levels of *LRRC32* as well as *C11orf30* were slightly skewed by rs7927894 in skin of five individuals. However, control samples (c1 and c2) showed the same allelic expression patterns for both *LRRC32* and *C11orf30* compared to rs7927894 heterozygous individuals. This indicates that the differential expression is not affected by the rs7927894 genotype, but possibly by other *cis*-regulatory variants, which might be in LD with the expressed SNP.
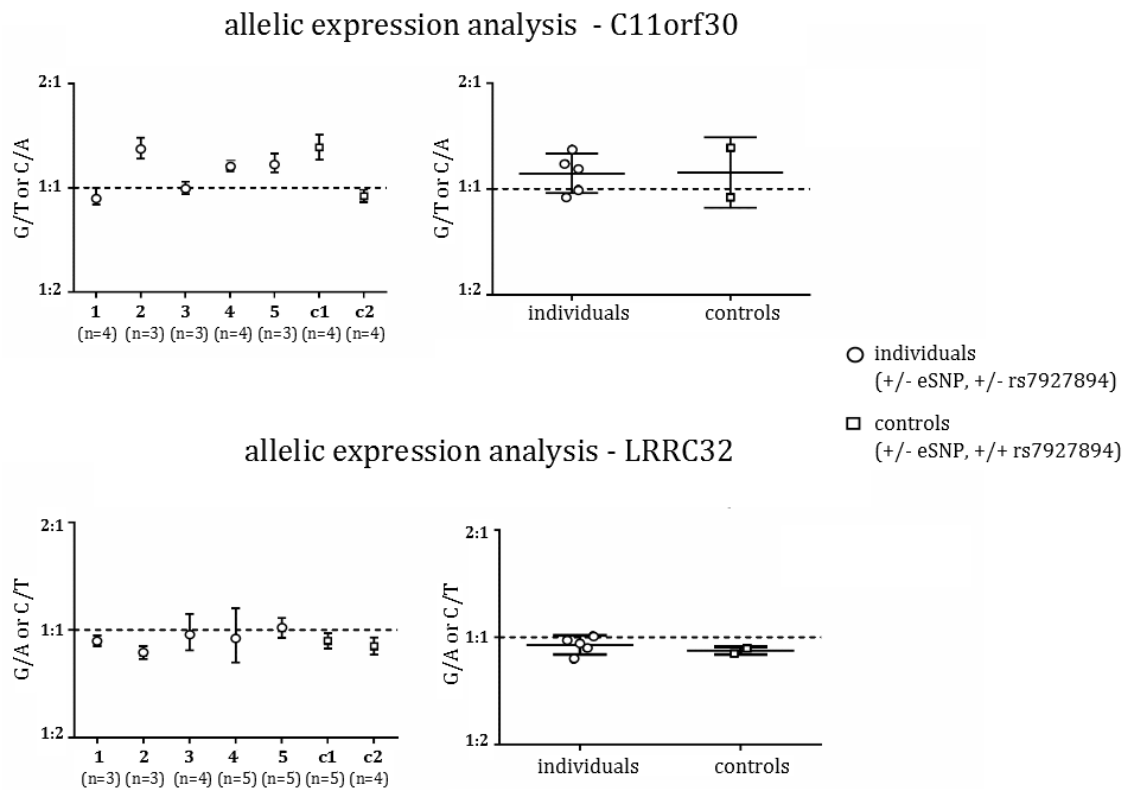
Figure 8: Allele-specific expression analysis of *C11orf30* and *LRRC32* in skin dependent on rs7927894 genotype. Each dot represents one individual heterozygous for the AD-associated SNP rs7927894 and for the respective expressed SNP (eSNP) of *LRRC32* or *C11orf30* (numbered 1 to 5). Controls (c1, c2) are homozygous for rs7927894 and heterozygous for the eSNP. For both genes, the ratio of the two alleles in each individual is skewed, independent of the rs7927894 genotype.
+/-: heterozygous alleles; +/+ or -/-: homozygous alleles.

2.1.2   Characterization of rs7927894 proxy SNPs within the 11q13.5 locus

In addition to the lead SNP, several proxy variants were identified and further analysis was focused on five proxy variants highly associated with rs7927894 ($r^2 > 0.7$) (Table 2). All proxy SNPs have a minor allele frequency (MAF) > 35 % and are located at the 11q13.5 locus: rs7130588 and rs6592645 in the 3' UTR of *C11orf30*, the other three proxy SNPs (rs7927997, rs2926914, rs2155219) are intergenic variants.

Table 2: Detailed genomic information about GWA top hit rs7927894 and five proxy SNPs on chr. 11q13.5

SNPs	Gene	Chr. Location of SNP *	Position	Alleles	MAF **	r^2 (rs7927894)	Distance [bp] (rs7927894)
rs7927894	C11orf30/LRRC32	Chr11:7630316	intergenic	C/T	37.5 %	1	0
rs7927997	C11orf30/LRRC32	Chr11:76301375	intergenic	C/T	36.7 %	0.965	59
rs7926914	C11orf30/LRRC32	Chr11:76301255	intergenic	G/T	38.3 %	0.965	61
rs7130588	C11orf30	Chr11:76270683	C11orf30 3' UTR	A/G	36.7 %	0.965	30633
rs6592645	C11orf30	Chr11:76271005	C11orf30 3' UTR	A/G	36.7 %	0.897	30311
rs2155219	C11orf30/LRRC32	Chr11:76299194	intergenic	G/T	45 %	0.722	2122

* dbSNP Genome Build 37.5; ** MAF=minor allele frequency (pilot_1_CEU_low_coverage_panel); SNP considered for further investigation is highlighted in red (rs2155219)

Comprehensive computational analysis and literature research revealed one out of five as potential candidate SNP for further investigation. Rs2155219 is known to be associated with allergic traits like grass sensitization and allergic rhinitis (Ramasamy et al. 2011). Interestingly, association with reduced expression levels of *C11orf30* and *LRRC32* dependent only on the rs2152219 genotype and not on the GWA lead SNP in white blood cells was detected within the EAGLE consortium (EArly Genetics and Lifecourse Epidemiology Consortium) (Bonnelykke et al. 2013). Therefore, detailed database analysis with the UCSC Genome Browser and prediction of allele-specific impact of rs2155219 on transcription factor binding sites (TFBS) was performed (Figure 9). Data from the ENCODE project provided evidence for high regulatory potential of rs2155219 in contrast to rs7927894 represented by location in clusters of high regulatory regions like DNase1 hypersensitive sites and promoter- and enhancer-associated histone marks (Figure 9A). To predict TFBS, an *in silico* analysis of the SNP surrounding region was carried out using the Genomatix MatInspector software with standard settings (Cartharius et al. 2005). This program utilizes a library of position weight matrices derived from a large set of known binding sites from several publications. Binding sites of corresponding transcription factors namely SP1 (specificity protein 1), INSM1 (insulinoma-associated 1) as well as ZNF (zinc finger protein), and GLI1 (zinc finger protein GLI1/glioma-associated oncogene) both located on the reverse complementary DNA strand, were predicted to get lost when the minor (T) allele of rs2155219 is present (Figure 9B). This might be due to the fact that the variant rs2155219 is directly located in the matrix core sequence of all four corresponding transcription factors binding motifs (Figure 10) showing high matrix similarities (0.958, 0.879, 0.920, and 0.994 for INSM1, SP1, GLI1, and ZNF, respectively). In comparison, the DEAF1 (deformed epidermal autoregulatory factor-1) binding site is lacking and the HIC1/2 (hypermethylated in cancer protein 1 and 2) and FOXH1 (forkhead box protein H1) binding sites, both on the opposite DNA strand, are predicted to be present for rs7927894 minor T allele (Figure 9B). However, only the core binding sequence of DEAF1 (matrix similarity= 0.783) and HIC1/2 (matrix

similarity= 0.968) are affected by rs7927894 (Figure 10). The functional *in-silico* analyses showed evidence that rs2155219 might play a role in gene regulation and that the GWA lead SNP rs7927894 may not be the most appropriate variant for functional investigation. To this end, rs2155219 was chosen for further detailed functional analysis.
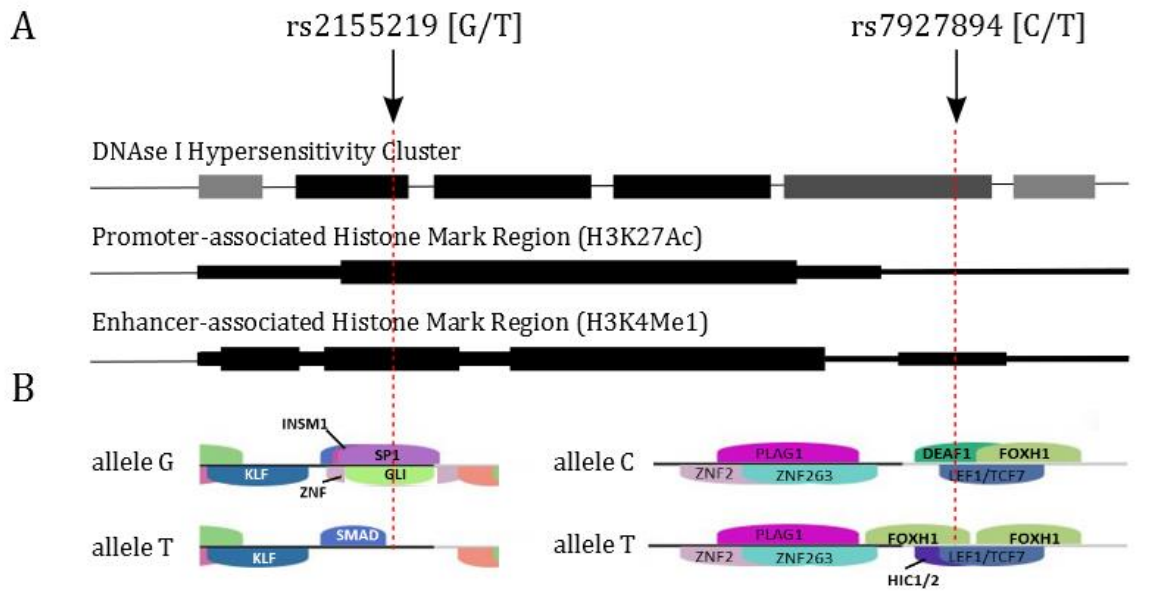

Figure 9: Schematic representation of rs7927894 and rs2155219 in transcriptional regulatory regions including DNase1 Hypersensitivity Clusters and Histone Mark Regions (A). Adpated from UCSC Genome Browser; output based on ENCODE data *(*https://genome.ucsc.edu/ENCODE/). A black box indicates the extent of the regulatory region. The darkness is proportional to the maximum signal strength observed. **Schematic representation of rs7927894 location in comparison to rs2155219 and predicted allele-specific transcription factor binding sites (B)** Four binding sites (SP1, GLI, ZNF, INSM1) get lost when minor T allele of rs2155219 is present. HIC1/2 and FOXH1 binding sites are present and DEAF1 binding site get lost when the minor T allele of rs7927894 exists. Adapted from Genomatix MatInspector software output (Cartharius et al. 2005) . Arrows display position of SNPs.
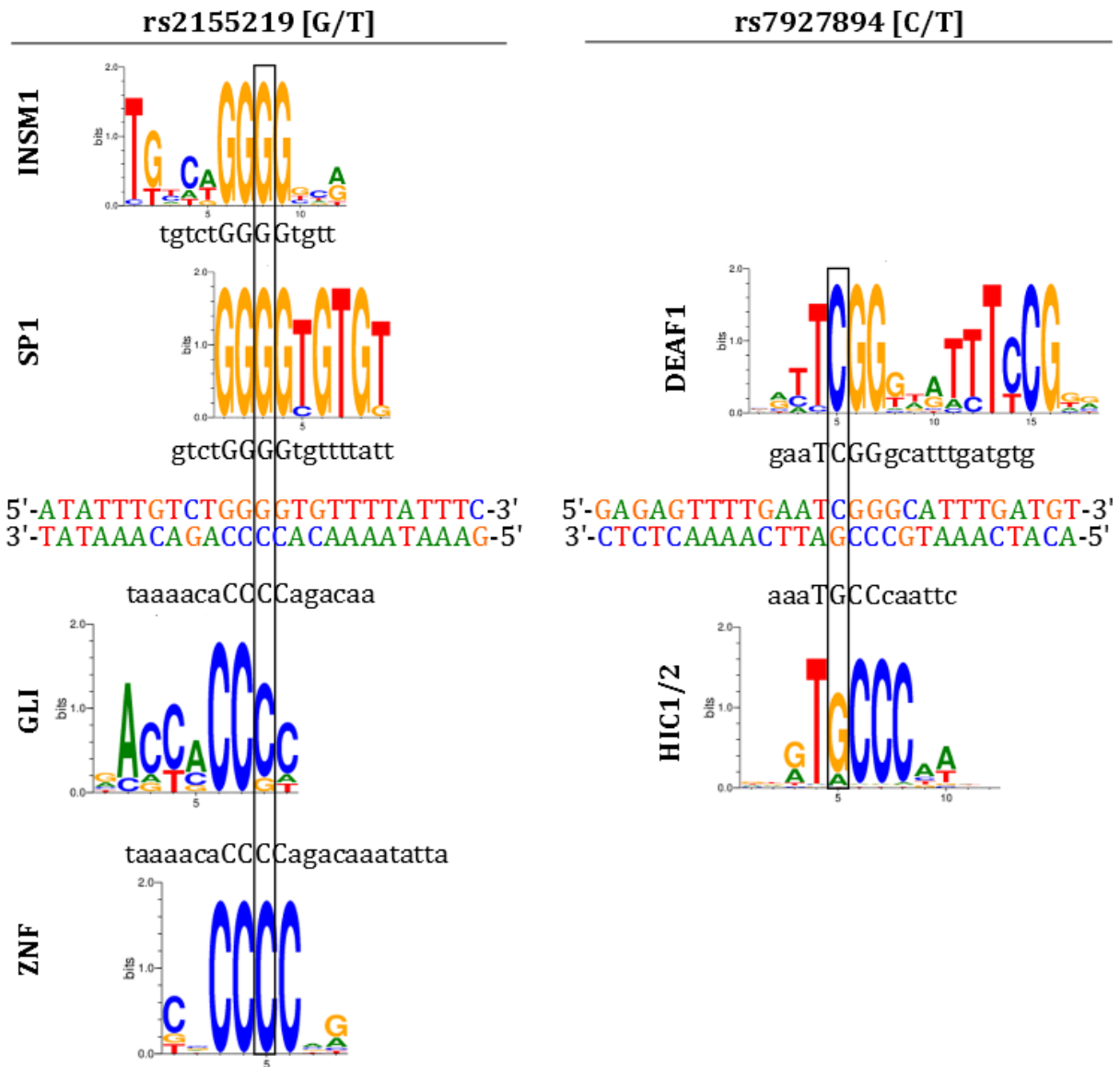
Figure 10: Binding motifs and consensus sequences of predicted transcription factors that show different binding properties for rs2155219 and rs7927894. DNA sequences (shown in coloured letters) containing either rs2155219 (GRCh37/hg19: chr11: 76,299,182-76,299,206) or rs7927894 (GRCh37/hg19: chr11: 76,301,304-76,301,329) are depicted. Position of SNP is indicated by box. Position weight matrices (PWM) and IUPAC consensus sequences for INSM1, SP1, GLI, ZNF, DEAF1, and HIC1/2 (black letters) identified with the MatInspector software, are shown. Nucleotides in capitals represent the core binding motif; nucleotides in small letters denote the conserved binding motif. Blue C = cytosine, green A = adenine, red T= thymine, yellow G= guanine.

2.2 Functional impact of SNP rs2155219 in the 11q13.5 locus

2.2.1 Allele-specific effect of rs2155219 on promoter regulation

For functional investigation of rs2155219 on promoter regulation, transcriptional activity of the SNP-surrounding sequence was analyzed via luciferase reporter assays. A 459 bp sequence around rs2155219 was cloned into the multiple cloning site (MCS) of a pGL4.23 vector using appropriate restriction sites. This vector carries the multiple cloning site upstream of a minimal promoter regulating the firefly luciferase gene. The insert length was chosen based on computational analysis of the region in order to cover high regulatory regions (mainly DNase1 hypersensitivity sites) around the polymorphism rs2155219. To analyze allele-specific differences in transcriptional activity due to rs2155219, different inserts containing either the major (ma) or minor (mi) allele were designed (Figure 11) and obtained fragments were analyzed via luciferase reporter gene assay in the cell lines HaCaT (human keratinocyte), A549 (human alveolar basal epithelium), HeLa (human cervical cancer), and Jurkat (human T lymphocyte). HaCaT cells are human immortal keratinocytes and appropriate cells to study AD-related specific mechanisms. The same applies to Jurkat cells, an immortalized T lymphocyte cell line. The human alveolar basal epithelium cell line A-549 was selected to investigate lung epithelium specific effects as the 11q13.5 locus has also shown to be associated with asthma (Marenholz et al. 2011). As another epithelium cell line and mainly as negative control, the common HeLa cells, derived from cervical cancer, were chosen.

For each cell line appropriate experimental conditions were evaluated and adapted. Normalization was performed related to the signal of the transfection control plasmid pGL4.74, which constitutively expresses renilla luciferase. Finally, data from SNP construct was normalized to the read of the transfected empty vector (without insert), which was set to 100 % response. Results represent data of three biological and technical replicates.
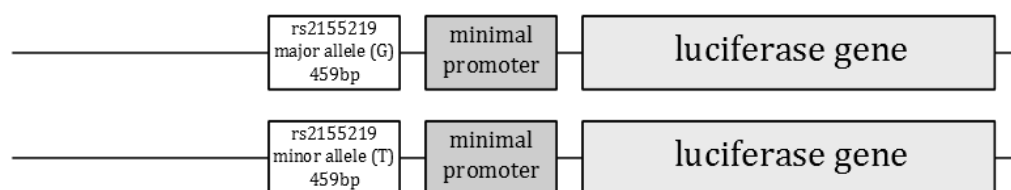

Figure 11: Schematic representation of cloned pGL4.23 minimal promoter contructs used for luciferase reporter gene assay (5' → 3' orientation). A 459 bp sequence surrounding rs2155219 (GRCh37/hg19: chr11: 76298922-76299380) with either major G or minor T allele was cloned in front of the minimal promoter and firefly luciferase gene.

In Jurkat cells, the rs2155219T minor allele exhibited a strong repressing activity on minimal promoter activity compared to the empty vector (42 % decrease of luciferase activity) while the major allele-sequence (G allele) had no significant influence on transcriptional regulation (Figure 12). In contrast, a 1.5-fold increase in luciferase activity was obtained by the minor allele in HaCaT cells compared to the empty vector, whereas again no effect was observed for the major allele. In A549 and HeLa cells both alleles acted as repressors on minimal promoter activity with no allele-specific differences.
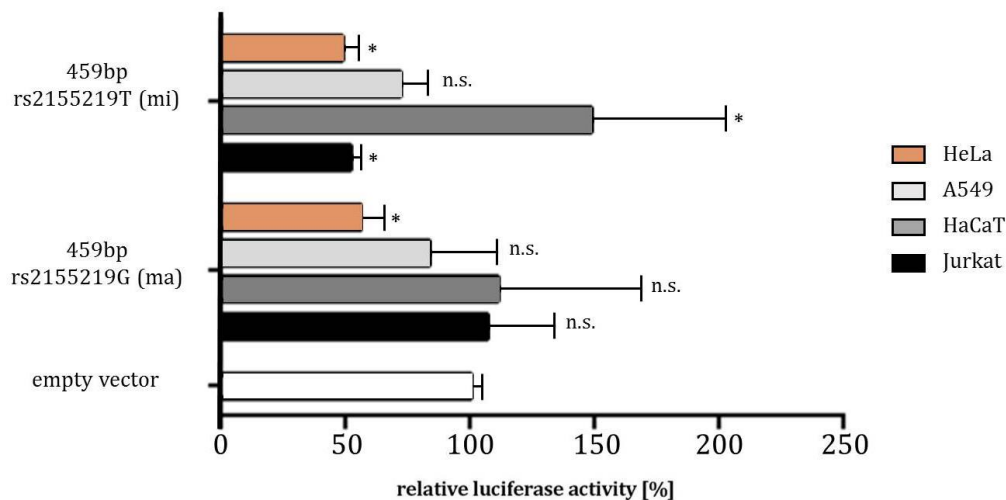
Figure 12: Cell-type specific regulatory activity of a 459 bp-rs2155219 surrounding region on a minimal promoter. Assays were performed in HeLa epithelial cells, A549 bronchial epithelial cells, HaCaT keratinocyte cells and Jurkat T cells with luciferase reporter gene constructs carrying the major non-risk (G) and minor risk (T) allele of rs2155219 in front of a minimal promoter. The AD-associated T allele of rs2155219 showed significantly higher minimal promoter activity in HaCaT cells and significantly lower activity in Jurkat and HeLa cells compared to the non-risk allele. P-values are given for each construct in comparison to the empty vector without any insert. P-values were derived from linear mixed-effects models. * P<0.05; n.s. = not significant; n=3 (biological and technical replicates); ma= major; mi= minor; empty vector= minimal promoter vector without insert.

To include a bigger context of regulatory regions, an 1142 bp SNP-surrounding sequence (GRCh37/hg19 chr11: 76298922-76300063) covering several transcription factor binding sites and more DNase1 hypersensitivity clusters was analyzed via luciferase reporter assays with the corresponding major and minor allele of rs2155219. It has to be taken into account that within this 1142 bp-sequence not only the SNP rs2155219 but two additional interesting variants are located: rs11236797 C>A and rs34455012indel. The main characteristics of these variants are listed in Table 3. The intergenic polymorphism rs11236797 is a known proxy SNP of rs2155219 in high LD (r^2= 0.9) located 456 bp upstream. The variant rs34455012 with a minor allele

frequency of 46.4 % causes a 7 bp (CCAGTAT) deletion or insertion, respectively, and is located 658 bp upstream of rs2155219.

Table 3: Genomic information about rs11236797 and rs34455012

SNP	Gene	Chr. Location of SNP	Position	Alleles	MAF**	r^2 (rs2155219)[+]	Distance [bp] (rs2155219)
rs11236797	C11orf30/ LRRC32	Chr11: 76588605	intergenic	C/A	36.9 %	0.9	456
rs34455012	C11orf30/ LRRC32	Chr11: 76588801-76588807	intergenic	- /CCAGTAT	46.4 %	-	658

* dbSNP Genome Build 38.2; ** MAF=minor allele frequency (1000genomes, pilot_1_CEU_low_coverage_panel)

The regulatory activity of the SNP haplotypes in detail namely - rs2155219 major allele (G), rs1123797 major allele (C) and rs34455012 insertion (CCAGTAT) - or - rs2155219 minor allele (T), rs1123797 minor allele (A) and rs34455012 deletion - were analyzed via luciferase reporter assays in Jurkat, HaCaT, A549, and HeLa cells (Figure 13).
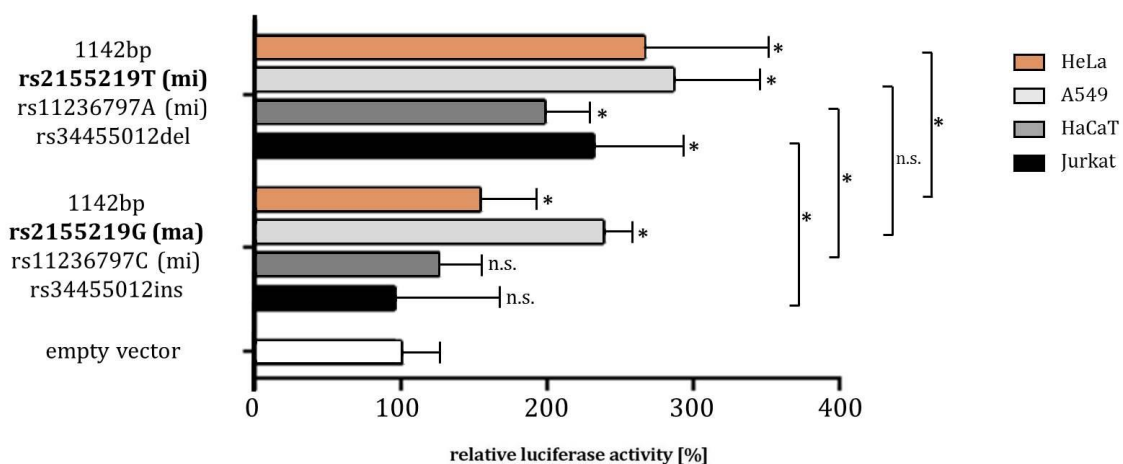
Figure 13: Enhancing activity of a 1142 bp-rs2155219 surrounding region (including two additional variants (rs11236797C>A; rs34455012indel) on a minimal promoter. Luciferase assays were performed in HeLa (n=8), A549 (n=3), HaCaT (n=4), and Jurkat cells (n=6) with luciferase reporter gene constructs carrying the major non-risk (G) and minor risk (T) allele of rs2155219, including rs34455012 (insCCAGTAT>del) and rs11236797(C>A) in front of a minimal promoter. The AD-associated minor allele of rs2155219 in combination with rs34455012del and rs12236797A showed significantly higher minimal promoter activity compared to the non-risk allele (in concert with rs34455012ins and rs12236797C allele) in all investigated cell lines. P-values are given for each construct in comparison to the empty luciferase vector. P-values were derived from linear mixed-effects models (otherwise noted in brackets). * P<0.05; n.s. = not significant; ma= major; mi= minor; empty vector= minimal promoter vector without insert.

Reporter vector constructs containing the SNP combination rs2155219G - rs1123679C and rs34455012ins revealed slightly enhancing activity on a minimal promoter in HaCaT, A549, and HeLa cells (1.3-, 2.4-, 1.5-fold increase in luciferase activity, respectively) compared to the empty vector. No difference in luciferase activity was observed in Jurkat cells. An even higher enhancing effect was observed for the rs2155219T allele in combination with rs12236797A and rs34455012del compared to the empty vector in Jurkat, HaCaT, A549, and HeLa cells (2.4-, 1.9-, 2.8-, and 2.6-fold increase in luciferase activity, respectively). In addition, a SNP-dependent enhancing activity on the minimal promoter was observed for the minor T allele of rs2155219 (together with rs1123679A and rs334455012del) compared to the rs2155219 major G allele (in concert with rs12236797C allele and rs34455012ins) in all cell lines.

In order to test whether the orientation of the insert is essential for the capability to activate a minimal promoter, the two insert sequences were cloned in a reverse complementary orientation into the same reporter vector. Inverse sequence constructs were tested in all four cell lines and data were normalized to the empty vector (Figure 14). The above shown enhancing effects (Figure 13) were completely abolished after the sequence orientation change and even turned into a strong repression in Jurkat, HaCaT and HeLa cells. In A549 cells no significant difference in luciferase activity compared to the empty vector was seen.
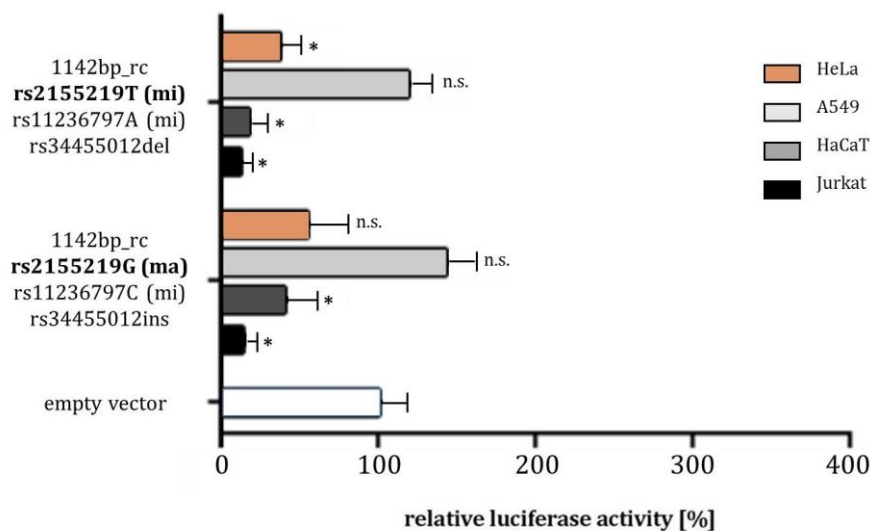

Figure 14: Reverse complementary 1142 bp-rs2155219 surrounding sequence showing orientation specificity on activation of a minimal promoter. Luciferase assays were performed in HeLa, A549, HaCaT, and Jurkat cells with luciferase minimal promoter vectors carrying the reverse complementary sequence including major non-risk (G) and minor risk (T) allele of rs2155219 (together with rs11236797(C>A) and rs34455012 (insCCAGTAT>del)). The sequence turned into a strong repressor in HeLa, HaCaT, and Jurkat cells and showed no significant effect in A549 cells. P-values are given for each construct in comparison to the empty luciferase vector. P-values were derived from linear mixed-effects models. n=3; * P<0.05; n.s. = not significant; ma= major; mi= minor; rc= reverse complementary; empty vector= minimal promoter vector without insert.

Results of reverse complementary controls demonstrate an orientation- and cell type-specific effect of the 1142 bp SNP sequence, however, the causal enhancing variant responsible for the effect could not be determined, yet. For this purpose, different combinations of SNP haplotypes of the 1142 bp-sequence were explored by two additional reporter constructs (Figure 15). The first two constructs, named (1) and (2), include the major or and minor SNP combinations of rs2155219, rs11236797, and rs34455012 as explained before. Construct (3) only differs from construct (2) in the allele of rs2155219 and thus includes rs2155219G (ma), rs11236797A (mi), and rs34455012del. The last construct (4) represents a rs2155219G (ma), rs11236797C (ma) and rs34455012ins haplotype and was used in comparison to construct (3) to figure out if an allele-specific effect of rs11236797 exists. Comparison between construct (1) and (4) revealed potential effects based on the indel rs34455012. All reporter constructs together were tested via luciferase assay in Jurkat, HaCaT, A549 and Hela cells and luciferase activity was normalized to the empty vector. P-values were analyzed for each construct in comparison to the empty vector and among each construct.
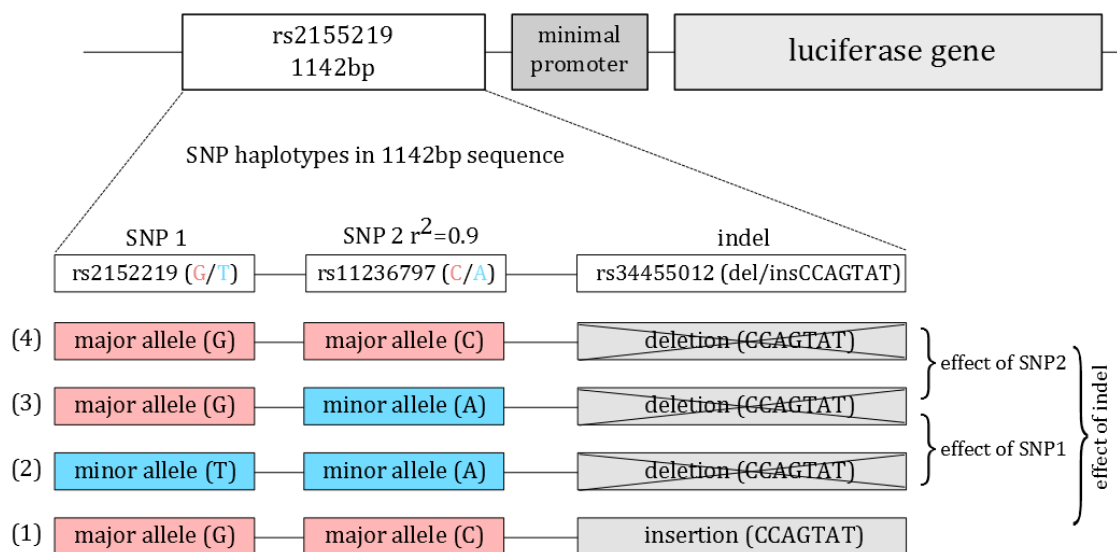
Figure 15: Cloned pGL4.23 minimal promoter constructs used for luciferase assay (5'→3' orientation. A 1142 bp rs2155219 surrounding sequence with different haplotypes of SNP 1 (rs2155219 G>T), SNP 2 (rs11236797 C>A) and indel (rs34455012 del>insCCAGTAT). Parentheses indicate the polymorphisms combinations compared.

In HaCaT keratinocyte cells luciferase activity was significantly higher with all tested constructs, except construct (1) (1.27-fold increase in luciferase activity, not significant), compared to the empty vector (Figure 16). Comparison between construct (2) and (3) revealed significant increase in luciferase activity (1.3-fold increase) dependent on rs2155219. The strongest enhancement of promoter regulation was exhibited by construct (4). When compared to the empty vector a 3.91-fold increase in luciferase activity was seen. Compared to construct (3) a 1.42-fold higher activity was observed dependent on rs11236797. However, the strong enhancing activity of construct (4) was mainly due to rs34455012 which can be revealed from the 3-fold increase in luciferase activity when comparing construct (1) and (4).
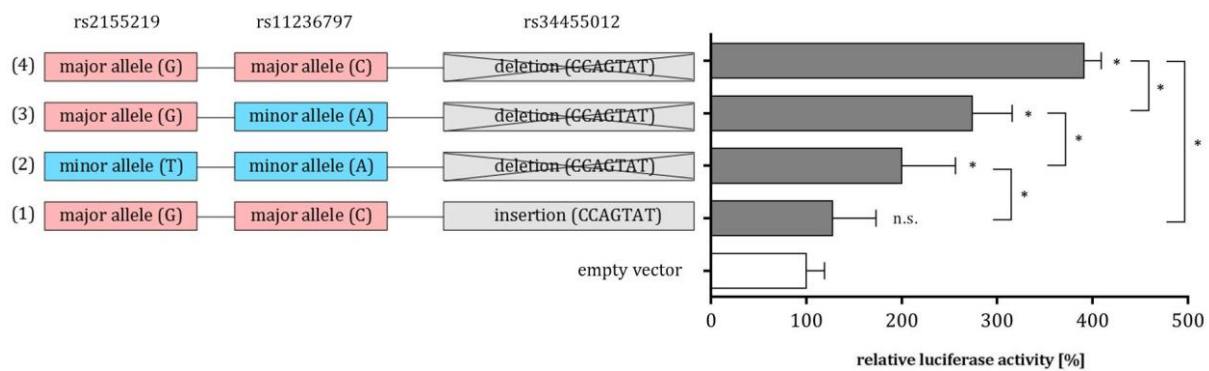
Figure 16: Enhancing activity of a 1142 bp sequence harbouring different haplotypes of rs2155219, rs11236797, and rs34455012 on a minimal promoter in HaCaT cells (n=4). Haplotypes of construct (1), (2), (3), and (4) revealed 1.27-, 1.99-, 2.74-, and 3.91-fold higher luciferase activity, respectively, compared to the empty vector without any insert. P-values (*P< 0.05) are given for each construct in comparison to the empty luciferase vector or otherwise denoted in brackets. P-values were derived from linear mixed-effects models. n.s. = not significant; empty vector= minimal promoter vector without insert.

The same analysis in human T lymphocytes (Jurkat cells) revealed a different result indicating a cell-type specific effect of the investigated variants (Figure 17). Compared to the empty vector only construct (2) containing rs2155219T, rs11236797A, and rs34455012del showed a moderate enhancing effect (1.9-fold increase in luciferase activity) compared to the empty vector. Comparison between construct (2) and (3) revealed a weak reduction of luciferase activity, which was not significant. Between construct (3) and (4) no difference in luciferase activity was detected. A 1.7-fold higher promoter activity of construct (4) in comparison to construct (1) points to rs34455012 depended promoter activity.
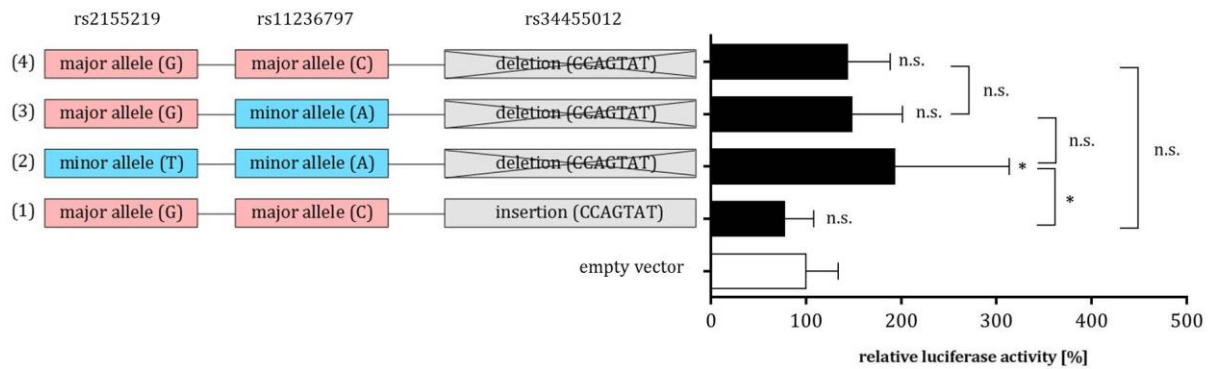
**Figure 17: Regulatory activity of a 1142 bp sequence harbouring different haplotypes of rs2155219, rs11236797, and rs34455012 on a minimal promoter in Jurkat cells (n=6).** Haplotypes of construct (1), (2), (3), and (4) revealed slightly lower (84.9 % luciferase activity), 1.91-, 1.48-, and 1.44-fold higher luciferase activity, respectively, compared to the empty vector without any insert. P-values are given for each construct in comparison to the empty luciferase vector or otherwise noted in brackets. P-values were derived from linear mixed-effects models. *P<0.05; n.s. = not significant; empty vector= minimal promoter vector without insert.

In A459 cells, all four constructs exhibit a strong and significant enhancing effect on promoter activity (Figure 18). Rs2155219-dependent effect on luciferase activity was visible by a significant increase (1.4-fold) between construct (2) and construct (3); however, rs11236797 featured no significant difference when comparing signals of construct (3) and (4). In contrast, the rs34455012 deletion was found to behave as strong activator of promoter activity (1.7-fold) in A549 cells.
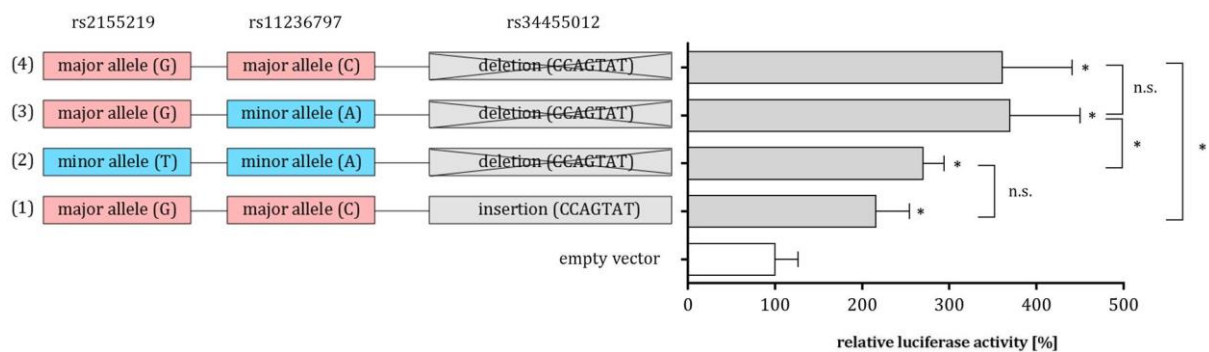
Figure 18: Strong enhancing activity of a 1142 bp sequence harbouring different haplotypes of rs2155219, rs11236797, and rs34455012 on a minimal promoter in A549 cells (n=3). Haplotypes of construct (1), (2), (3), and (4) revealed 2.35-, 2.79-, 3.94-, and 3.87-fold higher luciferase activity, respectively, compared to the empty vector without any insert. P-values are given for each construct in comparison to the empty luciferase vector or otherwise noted in brackets. P-values were derived from linear mixed-effects models. *P<0.05; n.s. = not significant; empty vector= minimal promoter vector without insert.

Similar to A549 cells all constructs revealed significant enhancer activity compared to the empty vector in HeLa cells (Figure 19). Neither rs2155219 nor rs11236797 revealed significant differences in luciferase activity when constructs (2) and (3), and (3) and (4), respectively, were compared. Though, the rs34455012 deletion in construct (4) featured a moderate enhancing activity (1.5-fold) compared to the insertion in construct (1).
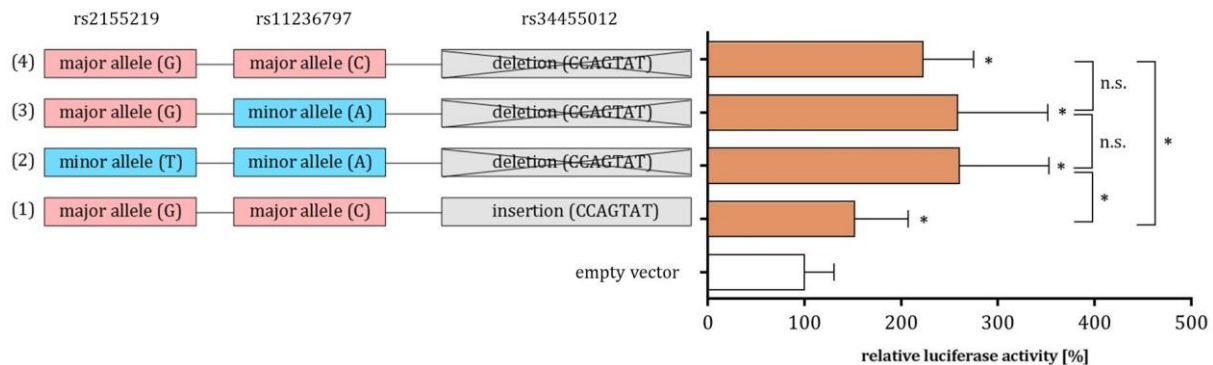

Figure 19: Strong enhancing activity of a 1142 bp sequence harbouring different haplotypes of rs2155219, rs11236797, and rs34455012 on a minimal promoter in HeLa cells (n=8). Haplotypes of construct (1), (2), (3), and (4) revealed 1.52-, 2.60-, 2.58-, and 2.23-fold higher luciferase activity, respectively, compared to the empty vector without any insert. P-values are given for each construct in comparison to the empty luciferase vector or otherwise noted in brackets. P-values were derived from linear mixed-effects models. *$P<0.05$; n.s. = not significant; empty vector= minimal promoter vector without insert.

2.2.2   Regulatory effect on native *LRRC32* and *C11orf30* promotors

After having shown that the 1142 bp sequence with SNP rs2155219 (in combination with rs11236797 and rs34455012) features enhancing activity on a minimal promoter it was obvious to investigate the impact of this sequence on the native promoters of the two neighbouring genes *LRRC32* and *C11orf30*. First, the promoter sequences were identified with the Genomatix software tool *gene2promoter*: A verified 844 bp and 711 bp promoter sequence for *C11orf30 and LRRC32*, respectively, were selected, amplified from genomic DNA and cloned into the promoter-free luciferase vector pGL4.12. Activity of each promoter construct was evaluated via luciferase reporter assays in 4 cell lines. Both promoter constructs showed high activity in all tested cell lines: the *LRRC32* promoter revealed a 5.1-, 5.7-, 10.1, and even 18.4-fold increase in luciferase activity compared to the empty vector without promoter in Jurkat, HaCaT, A549, and HeLa cells, respectively (Figure 20A). Very strong activity of the *C11orf30* promoter was identified in all

investigated cells showing increase in luciferase of at least 100-fold activity in comparison to the activity of the promoter-free vector (Figure 20).
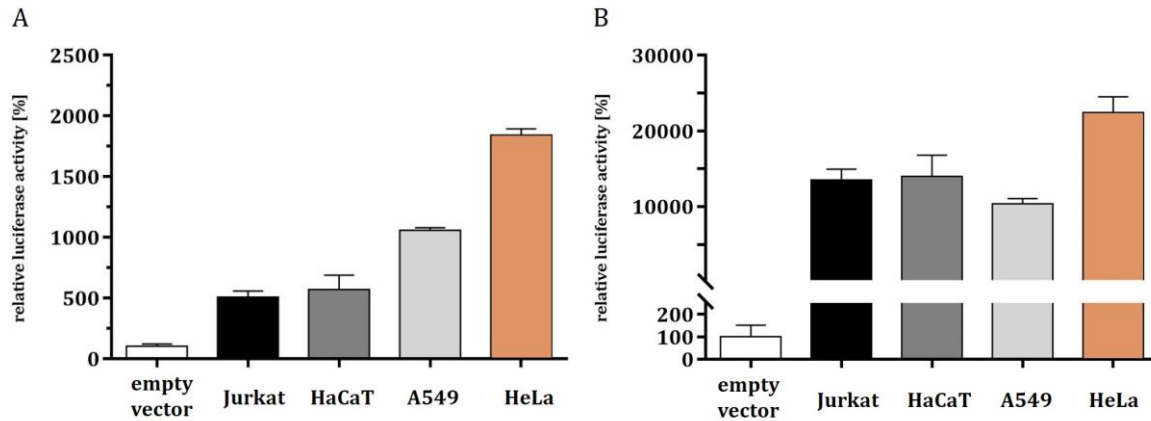

Figure 20: Strong activity of native *LRRC32* and *C11orf30* promoters in Jurkat, HaCaT, A549, and HeLa cells. Luciferase assays were performed with constructs containing a putative promoter sequence for *LRRC32* (A) (711 bp) or *C11orf30* (B) (844 bp), respectively. Data are normalized to the empty pGL4.12 vector without promoter, which was set 100 %. Both promoters revealed high activity in Jurkat, HaCaT, A549, and HeLa cells (5.1-, 5.7, 10.6, 18.4-fold increase in luciferase activity for *LRRC32* promoter; 135.1-, 139.8-,103.7-, and 224.2-fold increase in luciferase activity for *C11orf30* promoter); n=3 (biological and technical replicates); empty vector= promoter-free luciferase vector pGL4.12.

In the second step, to investigate whether the1142 bp-enhancer sequence exhibits regulatory impact on the native promoters, the two enhancing sequences according to the haplotypes rs2155219G - rs11236797C - rs34455012insCCAGTAT and rs2155219T - rs11236797A - rs34455012del were cloned in front of the native gene promoters and promoter activities were measured subsequently by assaying for the luciferase reporter gene. Both constructs revealed a significant increase of *LRRC32* promoter activity in Jurkat, HaCaT, A549 and HeLa cells compared to the native *LRRC32* promoter without enhancer. Except for Jurkat cells, the higher activity was observed for the rs2155219G - rs11236797C - rs34455012insCCAGTAT haplotype in comparison to the other haplotype with the strongest increase shown in HaCaT keratinocytes (2.1-fold and 1.7-fold higher luciferase activity compared to empty vector or the other haplotype, respectively). In contrast, neither the rs2155219G - rs11236797C - rs34455012insCCAGTAT nor the rs2155219T - rs11236797A - rs34455012del haplotype exhibited regulatory effect on the *C11orf30* promoter in all investigated cell lines (Figure 21).
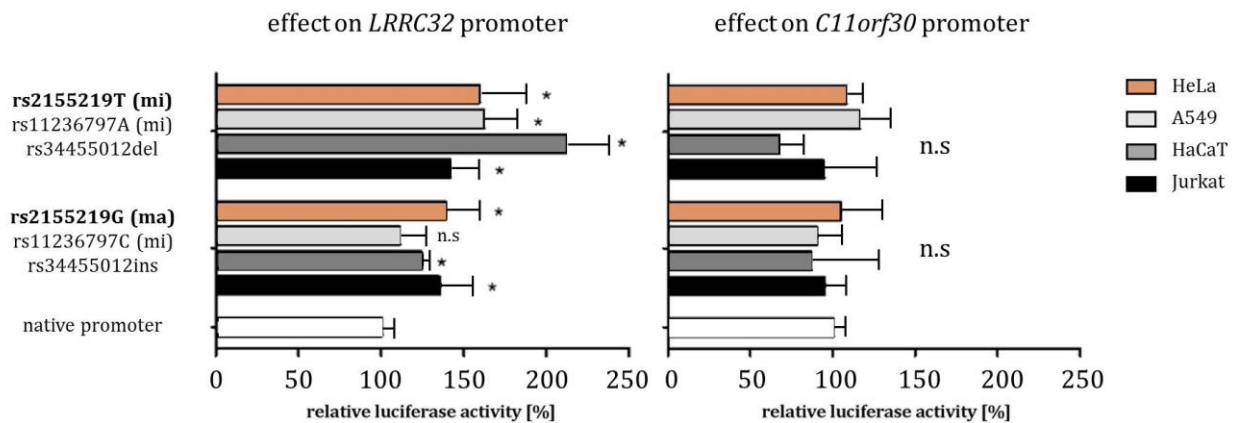
Figure 21: Significant enhancing activity of a 1142 bp-rs2155219 surrounding region (including two additional variants (rs11236797C>A; rs34455012indel)) only on the native *LRRC32* promoter and not on the *C11orf30* promoter. Assays were performed in Jurkat (n=6), HaCaT (n=4), A549 (n=4), and HeLa cells (n=6) with luciferase reporter gene constructs carrying the major non-risk (G) and minor risk (T) allele of rs2155219, including rs34455012 (insCCAGTAT>del) and rs11236797(C>A) in front the native *LRRC32* or *C11orf30* promoters, respectively. Reporter vector constructs containing rs2155219T together with rs34455012del and rs12236797A acted as weak enhancer on the native *LRRC32* promoter and showed no effect on *C11orf30* promoter activity compared to the native promoters. P-values are given for each construct in comparison to the native promoter vector. P-values were derived from linear mixed-effects models. *P<0.05; n.s. = not significant; empty vector= native *LRRC32* or *C11orf30* promoter vector without insert.

2.2.3   Candidate gene expression in skin in dependence of rs2155219 genotype

After having shown that the investigated variant rs2155219 has regulatory impact on the native *LRRC32* promoter, candidate gene expression levels (*LRRC32* and *C11orf30*) dependent on rs2155219 genotype were determined in skin tissue. For analysis, a subset of AD skin samples (n=15; lesional and non-lesional skin as a part of the Ambitious study; see 4.6.2) and skin from healthy controls (n=17) were used. Unfortunately, expression data of *C11orf30* did not match quality criteria (detection P-value > 0.01) and were excluded. For *LRRC32*, a genotype-dependent shift was detected resulting in higher *LRRC32* expression levels in homozygous major G allele carriers compared to heterozygous and homozygous minor T allele carriers in lesional skin (Figure 22). The same shift was detected in control samples whereas no difference in expression levels was identified in non-lesional skin samples. Overall, baseline expression was clearly higher in cases compared to controls.
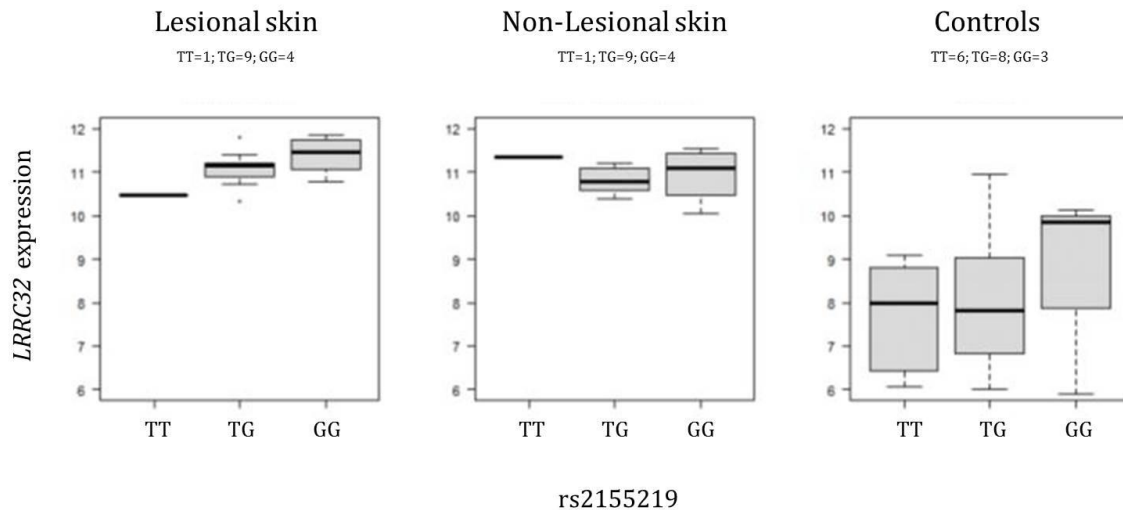
Figure 22: Rs-2155219-dependent expression levels of LRRC32 in skin. A genotype-dependent shift towards homozygous G allele carriers was detected in lesional skin and control samples. Similar genotype-dependent expression levels were observed in non-lesional skin. Considerable higher baseline expression levels were observed in cases compared to controls. Figure shows $\log_2$-transformed LRRC32 expression (y-axis) versus rs2155219 genotype (x-axis) in cases (n=14) and controls (n=17); data not significant. GG= homozygous major alleles for rs2155219; TG= heterozygous alleles for rs2155219; TT= homozygous minor alleles for rs2155219.

2.2.4   Analysis of differential protein-DNA binding patterns

To further investigate the impact of rs2155219 on DNA binding ability of nuclear proteins, electrophoretic mobility shift assays (EMSA) with allele-specific oligonucleotides for rs2155219 were performed. EMSA experiments were carried out using nuclear protein extracts from Jurkat cells, an immortalized human T lymphocyte cell line suitable for analyzing T cell specific mechanisms. In addition, results from luciferase assays indicated potential cell-type specific effects on transcriptional activity in Jurkat cells with a stronger activity in case of the rs2155219 T minor than the major G allele.

Differential protein binding patterns were observed in EMSA experiments with labeled probes carrying the major G allele compared to the minor T allele of rs2155219 (Figure 23, lane 3 and 10). Specific binding of DNA-protein complexes was analyzed by competition with increasing concentrations (10- and 100-fold excess) of unlabeled probes containing either the major or minor allele of rs2155219. Competition analyses demonstrated a decrease in band intensities to the point of disappearance of complexes when competing with the major allele (Figure 23, lane 4-7, 11-14). Competition with probes of the common transcription factor OCT1 showed constant band intensities (Figure 23, lane 8-9, 15-16) indicating specific binding of a nuclear protein or complex with a lower binding capacity to the minor allele. Probes without nuclear extract did

not reveal any protein-DNA binding (Figure 23, lane 1-2). Computational analysis revealed transcription factor SP1 as a potential candidate affected by rs2155219 (Figure 9). In order to figure out whether SP1 is included in the protein binding complex, SP1 competition and supershift experiments were conducted. The addition of SP1 competitor oligonucleotides resulted in disappearance of the band of rs2155219 major allele-protein complexes (Figure 23, lane 17-18). Supershift experiments using an SP1 antibody identified a decrease in band intensity of the complex and resulted in two additional new bands (Figure 23, lane 20, indicated by arrowhead). The negative control using an IgG antibody did not reveal any supershift. These results indicate an rs2155219 allele-specific protein-DNA interaction and identified SP1 as potential transcription factor involved in differential binding.
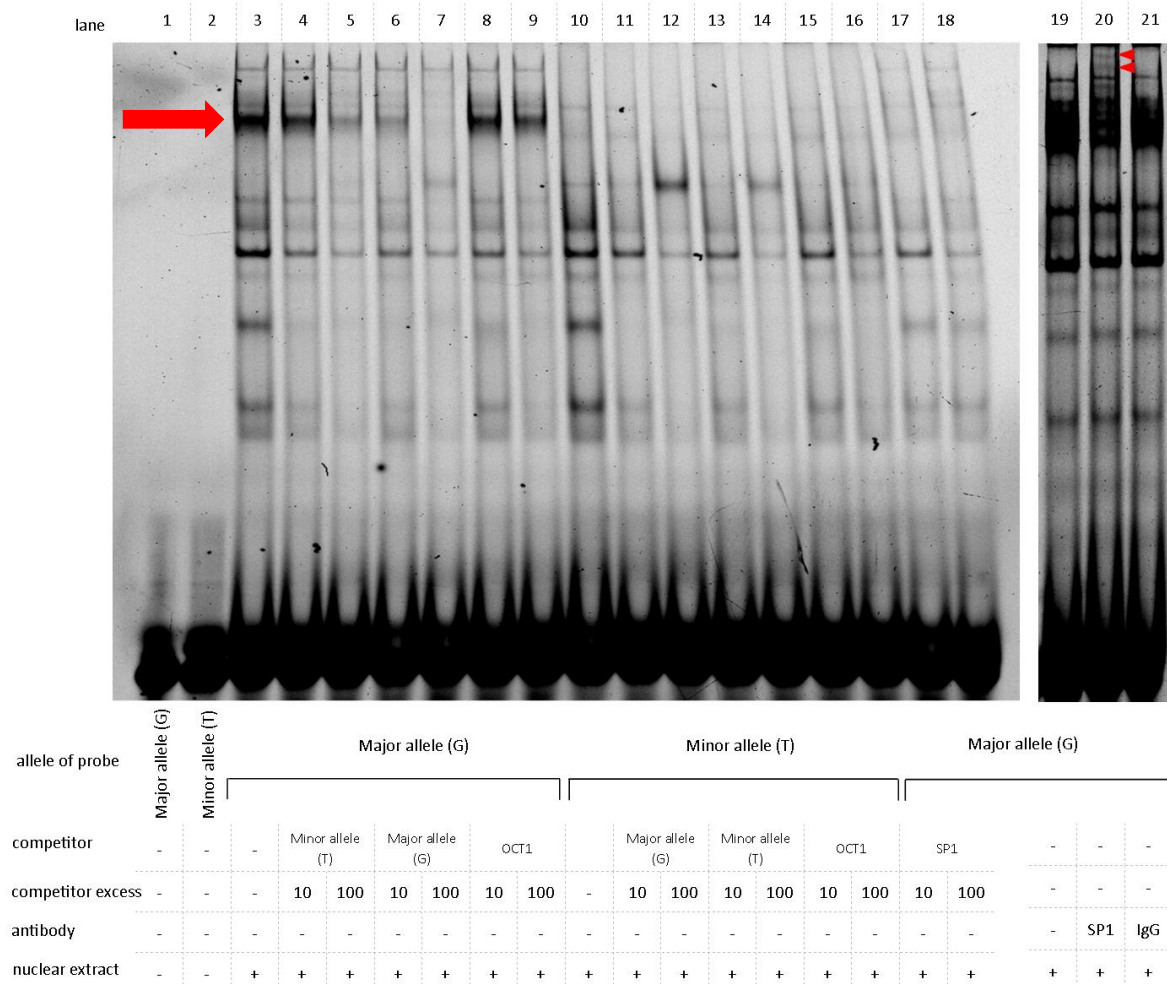
Figure 23: Allele-specific protein-DNA interaction of the SNP rs2155219 and identification of SP1 as differential binding protein in Jurkat nuclear extracts. Labeled oligonucleotides carrying the major non-risk allele (G) or minor risk allele (T) of rs2155219, showed differential protein binding (lane 3, 10, 19) (DNA protein complex, indicated by arrow). Competition experiments were performed with complementary unlabeled oligonucleotides (lane 4-9, 11-18). Supershift with an SP1 antibody resulted in two additional bands (lane 20 (indicated by arrowheads). Oligonucleotides without nuclear extract did not reveal any protein-DNA binding (lane 1-2).

2.3 Functional impact of *LRRC32* coding variant rs79525962

Results of this part are published in Manz *et al.* (Manz et al. 2016).

2.3.1 Targeted resequencing of 11q13.5 locus and identification of low frequency missense variants

During thesis progress, the basis of the second part was developed in cooperation with the group of Prof. Dr. Stephan Weidinger from the "Universitätsklinikum Schleswig-Holstein". They performed a targeted resequencing approach on the AD-associated 11q13.5 locus including the two genes *C11orf30* and *LRRC32* to refine earlier observed 11q13.5 disease association signals. Starting with next generation sequencing of 11q13.5 (chr11:75,800,000-76,070,000; NCBI36/hg18) in 31 atopic dermatitis patients enriched for low frequency risk variants followed by validation with Sanger sequencing identified two coding variants (A407T/rs79525962, R518W/rs142940671) in *LRRC32* with minor allele frequencies < 0.01 (based on 1000 genomes). Four additional rare missense variants (R312C/rs371900727, S411R/rs201431152, R414W (without annotation in dbSNP 132), R652C/rs143082901) were further identified in 100 independent AD cases by enlarged screening of the coding regions of *LRRC32*. For *C11orf30*, no rare missense variants were detected. Furthermore, all six *LRRC32* variants were subjected to association testing in an independent set of 2,193 German AD cases and 2,197 control subjects from the German population-based POPGEN cohort. The POPGEN cohort comprises comprehensive genetic and epidemiological data for several complex diseases of a defined population set in northern Schleswig-Holstein (Krawczak et al. 2006). Association testing revealed significant excess of *LRRC32* variants in individuals with AD compared to healthy individuals. The variant A407T/rs79525962 was identified as the most frequent associated variant with an OR of 1.46 (95 % CI 1.11 – 1.92; P= 0.007). This missense variant is located in the coding sequence of *LRRC32* and is causing an amino acid change from alanine to threonine (Ala (**G**CC) →Thr (**A**CC)) Interestingly, A407T/rs79525962 is in high linkage disequilibrium with rs2155219 (D'=1) and other previously reported GWAS risk SNPs for inflammatory and atopic traits within 11q13.5. Thus, this variant was an interesting candidate for further functional characterization.

2.3.2   Protein modelling and bioinformatics prediction of missense variants

In order to predict functional impact of the identified *LRRC32* missense variants structural protein modelling and bioinformatics prediction was performed by Prof. Weidinger and his group. The *LRRC32* encoding protein GARP (glycoprotein A repetitions predominant) is a member of the Toll-like receptor (TLR) family and it is constituted of an N-terminal extracellular leucine-rich repeat (LRR) domain (including 21 LRRs), a transmembrane domain and a short cytoplasmic domain. Protein modelling was performed based on the Toll-like Receptor Regulator CD180 (PDB ID 3b2d, chain A) because both proteins share the same characteristics (e.g. number of conserved disulfide bridges, LRR repeats, and a missing intracellular signaling domain. The extracellular domain of GARP is predicted to fold into an alpha/beta horseshoe shape, in which leucine-rich beta-strands form a characteristic concave inner surface (Figure 24). This domain, comprising the 21 LRRs, harbors a continuous asparagine ladder within the LRR repeats, leading to uniform beta sheet angles typical for a structural TLR subgroup (Manavalan et al. 2011).
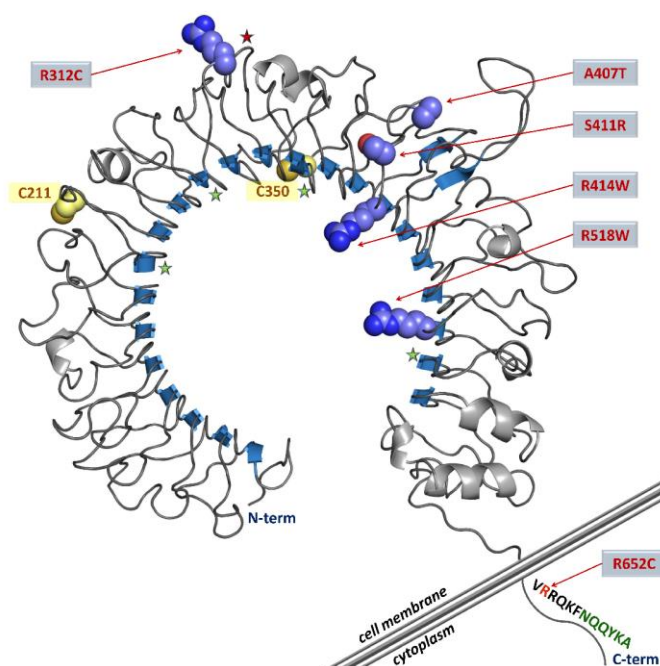
Figure 24: Structural protein model of glycoprotein A repetitions predominant (GARP). The extracellular LRR repeat domain is visualized in cartoons. The cell membrane and intracellular domain of GARP are depicted schematically. All identified variants are displayed in grey boxes and position is denoted by red arrows: variant positions in the extracellular domain are shown in blue spheres. Cysteines forming disulfid bridges with TGFβ1 are shown as yellow spheres. N-glycosylation sites are marked with asterisks (green: predicted, red: verified). In the cytoplasmic tail a potential PDZ binding motif is highlighted in green letters. Annotation of the LRR motifs was facilitated by the LRRFinder(Offord and Werling 2013). The structural model of GARP was created and refined using the WHATIF web interface (Hekkelman et al. 2010). PyMOL was used for superimposition and visualization of protein structures (http://www.pymol.org/; The PyMOL Molecular Graphics System, Version 1.2r3pre, Schrödinger, LLC). Protein modeling was performed by Prof. Weidinger and colleagues. Adapted from (Manz et al. 2016).

Different functional N-glycosylation sites have been verified or predicted for GARP (Chen et al. 2009) (Figure 24, green and red asterisks, respectively), and binding of latent TGFβ1 via two disulfide bridges has been shown for the cysteins C192 and C331 (Wang et al. 2008) (Figure 24, highlighted in yellow). The variant A407T/rs79525962 harbors a T instead of an A allele, causing a conformational change from the hydrophobic amino acid alanine to the larger and polar amino acid threonine. Functional and Protein stability prediction (obtained by the ELM webserver(Dinkel et al. 2012) and PoPMuSiC(Dehouck et al. 2011)) for A407T/rs79525962 revealed that this variant is likely to obstruct proper protein folding or hamper post-translational modifications necessary for protein transport. Taken together, structural protein modelling and bioinformatics analysis predicted a disruption of protein transport upon this variant, and this finding provided the basis for further molecular and functional characterization of rs79525962.

2.3.3   Impact of rs79525962/A407T on RNA level

To investigate whether the SNP rs79525962 (G>T) causing mutation A407T influences mRNA expression, the abundance of *LRRC32* including rs79525962**G** (further named as wildtype (WT) *LRRC32*) and *LRRC32* including rs79525962**T** (further named as A407T *LRRC32*) were determined by semi-quantitative RT-PCR in different cell lines. RNA was extracted from HeLa, Cos-7 and CD4+CD25- T cells transfected with either WT *LRRC32*- or A407T *LRRC32*-expression plasmids, reverse transcribed and amplified by end-point RT-PCR using transcript specific primers (Figure 25, 2054 bp fragment). Amplification of the housekeeping gene *β-actin* was used as control. The three different cell lines for investigation of cell type-specific differences in *LRRC32* mRNA expression were selected for the following reasons: Cos-7 cells were mainly chosen because of high transfection efficiency, HeLa cells as control cell line and CD4+CD25- T cells as cell type of interest as GARP, the protein encoded by *LRRC32*, is known to act as surface receptor on regulatory T cells (Wang et al. 2009).

In all cell lines, no difference in mRNA expression levels between wildtype *LRRC32* and A407T *LRRC32* was detected (Figure 25). With untransfected cells as template and when using water instead of DNA (negative control), no amplification was observed. The amplification of *β-actin* (884 bp fragment) was equal in untransfected as well as in overexpressed cells demonstrating high quality of cDNA and experimental success. In addition, a light *LRRC32* expression in untransfected CD4+CD25- cells indicates endogenous expression of *LRRC32* in CD4+CD25- T cells.
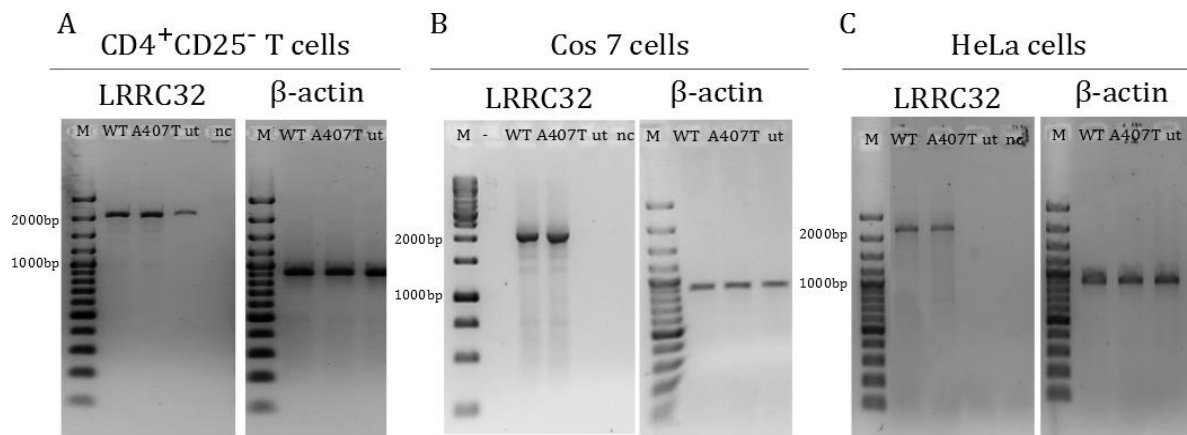
Figure 25: mRNA Expression of *LRCC32* wildtype (WT), *LRRC32* including SNP rs79525962 (A407T) and human *ß-actin* in CD4+CD25- Tcells, Cos-7, and HeLa cells. RNA was prepared from *LRRC32* wildtype-, *LRRC32* A407T-transfected cells, and untransfected cells (ut), reverse transcribed and amplified by endpoint RT-PCR. No expression difference on RNA level was observed between wildtype and A407T *LRRC32* (2054 bp fragment). Amplification of *ß-actin* (884 bp fragment) was equal in all samples and served as control. nc= negative control (water instead of cDNA), M= DNA Ladder.

2.3.4 Impact of rs79525962/A407T on protein level

2.3.4.1 GARP protein expression determined by Western Blot analysis

To examine the expression of the *LRRC32* encoded protein GARP, Western Blot analysis was performed in Cos-7 cells transiently transfected with different plasmids encoding either WT *LRRC32* or A407T *LRRC32*. To visualize potential differences between wildtype and mutated (A407T) GARP, Cos-7 cells were used because of high transfection efficiency. Different protein fractions containing cytosolic proteins (cp), membrane proteins (mp), or total protein (tp) were generated from GARP-overexpressing cells. Protein fractions obtained from cells transfected with the empty vector (without GARP encoding sequence) were used as negative control. Moreover, recombinant human GARP, known to own a size of 70-80 kDa, served as positive control. In addition, expression of green fluorescent protein (GFP) was assessed for normalization because GARP and GFP were translated from a single bicistronic mRNA while using the pIRES-AcGFP expression vector.

Since GARP protein is known to be a cell surface membrane protein, analysis of expression differences was focused on the membrane fraction: no difference in GARP protein expression was detected between wildtype GARP and A407T GARP in membrane protein lysates of overexpressed Cos-7 cells (Figure 26). In addition, equal expression levels were found in total protein lysates of wildtype GARP and A407T GARP. No GARP expression was detected in

cytosolic proteins fractions. Whereas wildtype and A407T GARP appeared as a single protein band with the expected molecular mass between 70 and 80 kDa in membrane Cos-7 homogenates, an additional band of 65 kDa was visible in case of total protein lysate. Green fluorescent protein (GFP) appeared as protein band with the expected molecular mass of 30 kDa in cytosolic and total protein fractions. GFP expression did not reveal differences in expression levels between WT and A407T GARP expressing cell lysates, indicating equal efficiency of transfection and sample preparation.
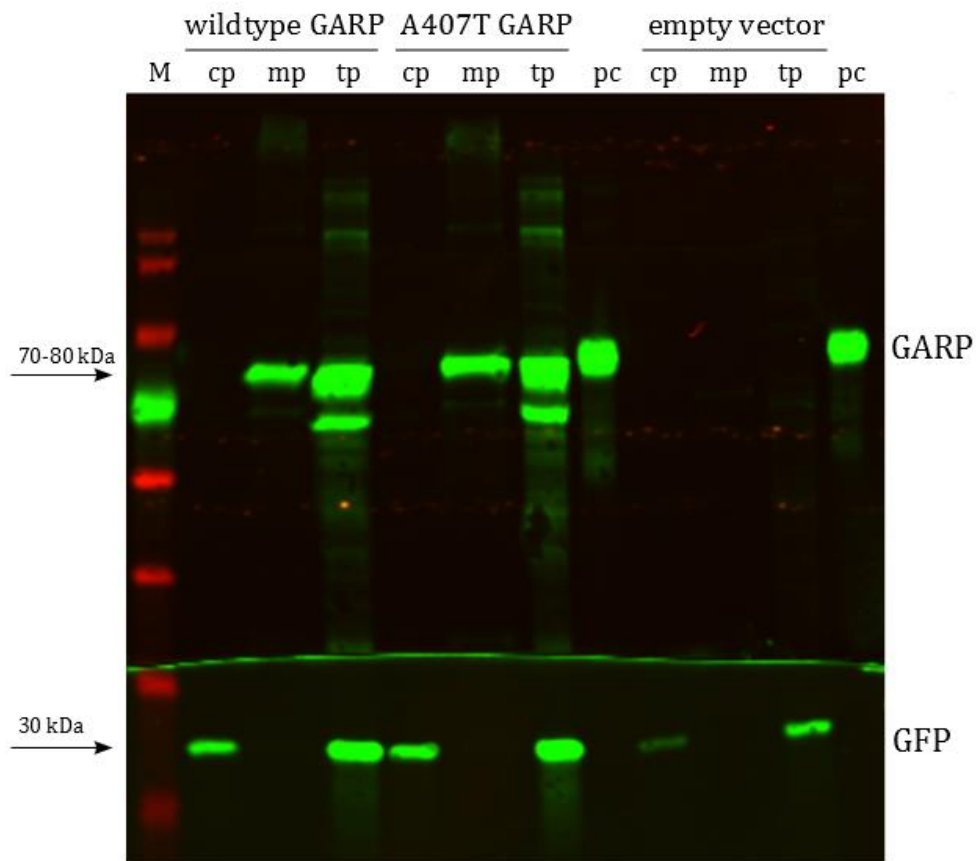
Figure 26: Western Blot analysis on Cos-7 cell lysates after 48 h overexpression of wildtype GARP and A407T GARP mutation. Cytoplasmic (cp), membrane (mp) and total (tp) protein fractions of wildtype GARP- and A407T GARP-overexpressed Cos-7 cells were analyzed by Western blotting using a GARP-specific monoclonal primary antibody (Plato-1, mouse IgG2b) and an IR dye-labeled secondary antibody (goat anti-mouse IRDye 800CW). No difference in GARP protein expression was observed between wildtype and A407T GARP in membrane and total protein lysates. Recombinant human GARP (72 kDa) was used as positive control (pc). Cos-7 cell lysates transfected with emtpy vector served as negative control. Green fluorescent protein (GFP) staining was used for normalization of total protein and cytoplasmic protein fractions.

However, the measured fraction used up to now covers not only protein of the cell surface but of all occurring membranes in a cell (integral membrane proteins and membrane-associated proteins). To focus only on outer cell membranes (where GARP is expressed) surface protein fractions for Western Blot analysis were prepared. For this purpose, cell surface proteins of GARP transfected Cos-7 cells were labeled using a periodate oxidation and aniline-catalyzed oxime ligation (PAL)-based procedure followed by biotinylation of cell surface-sialylated glycoproteins which were then captured by streptavidin-coupled beads. This specific plasma membrane (mp) fraction together with the nuclei (nuc), and cytosolic (cyt) protein fractions generated after transfection from wildtype- and A407T GARP-overexpressing Cos-7 cells were analyzed by Western Blot. For GARP detection a specific monoclonal antibody (Plato-1, mouse IgG2b) and an IR dye-labeled secondary antibody (goat anti-mouse IRDye 800CW) were applied. Protein fractions obtained from cells transfected with the empty vector (without GARP encoding sequence), and hybridization only with secondary antibody served as negative controls. Recombinant human GARP protein was used as positive control. Detection of GFP signals using an anti-GFP antibody was performed to check transfection efficiency and for normalization.

Wildtype and A407T GARP proteins appeared as a single protein band with the expected molecular masses of 70-80 kDa. Surprisingly, a strong GARP expression was observed in the cytosolic fraction than in the membrane and nuclei fractions (Figure 27). However, no marked difference was detected between wildtype GARP and A407T GARP expression in all analyzed fractions. Similar expression level of GFP protein in cytosolic fractions indicated equal transfection efficiency of the GARP-pIRES-AcGFP expression vectors. Neither GARP nor GFP protein was detected in protein lysates of Cos-7 cells transfected with empty vector and after hybridization only with secondary antibodies (data not shown).
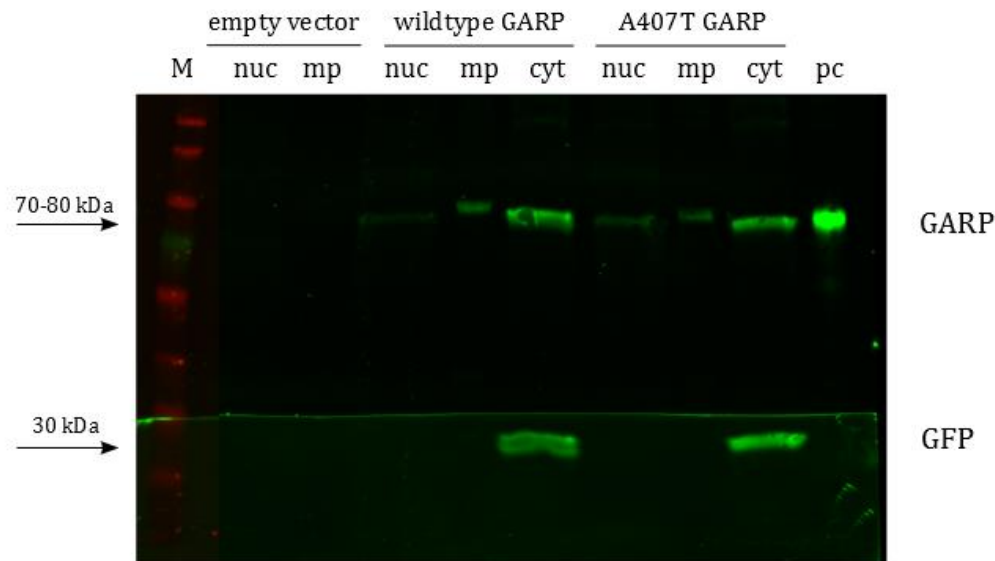
Figure 27: Western Blot analysis on Cos-7 cell fractions – including specific cell surface (plasma membrane (mp)) protein fraction - after 48 h overexpression of wildtype GARP and A407T GARP mutation. Plasma membrane proteins were obtained after biotinylation of membrane proteins and captured by streptavidin-coupled beads. Nuclei (nuc), plasma membrane (mp) and cytosolic (cyt) protein fractions of wildtype GARP- and A407T GARP-overexpressed Cos-7 cells were analyzed by Western Blot using a GARP-specific monoclonal primary antibody (Plato-1, mouse IgG2b) and an IR dye-labeled secondary antibody (goat anti-mouse IRDye 800CW). Equal amount of GARP protein expression was observed between wildtype and A407T GARP in all fractions. Recombinant human GARP (72 kDa) was used as positive control (pc). Cos-7 cell lysates from cells treated with the empty vector served as negative control. Green fluorescent protein (GFP) staining was used for normalization of cytoplasmic fractions.

2.3.4.2   Subcellular localization of GARP in HeLa and Cos-7 cells

In order to gain additional insight into characteristics of the mutated protein subcellular localization studies in HeLa and Cos-7 cells overexpressing wildtype and A407T GARP were performed using immunocytohistochemistry. After transfection of cells with either wildtype GARP or A407T GARP expressing pIRES-AcGFP vectors and permeablization, intracellular GARP staining of transfected cells was conducted using an anti-human GARP IgG2b antibody followed by a goat anti-mouse Alexa-Fluor488 secondary antibody. Extracellular staining was conducted without permeabilization. Nuclei were counterstained with Hoechst 33342 dye and outer cell membrane staining was performed by using the CellLight® Plasma Membrane-RFP BacMam 2.0 reagent, a construct which expresses a red fluorescence protein fused to the myristolyation/palmitoylation sequence from Lck tyrosine kinase after transfection into the cells. However, transfection and thereby red staining of plasma membrane was only successful in HeLa cells (Figure 28B). In both cell lines, localization of GARP protein on the cell surface and accumulation of protein in the cytosol was seen. On the cell surface, decreased localization of GARP protein was observed in A407T GARP compared to wildtype GARP expressing cells

(Figure 28A+B, cell surface). On the other hand, higher retention of mutated GARP was detected compared to WT GARP expressing cells in the cytosol (Figure 28A, intracellular).
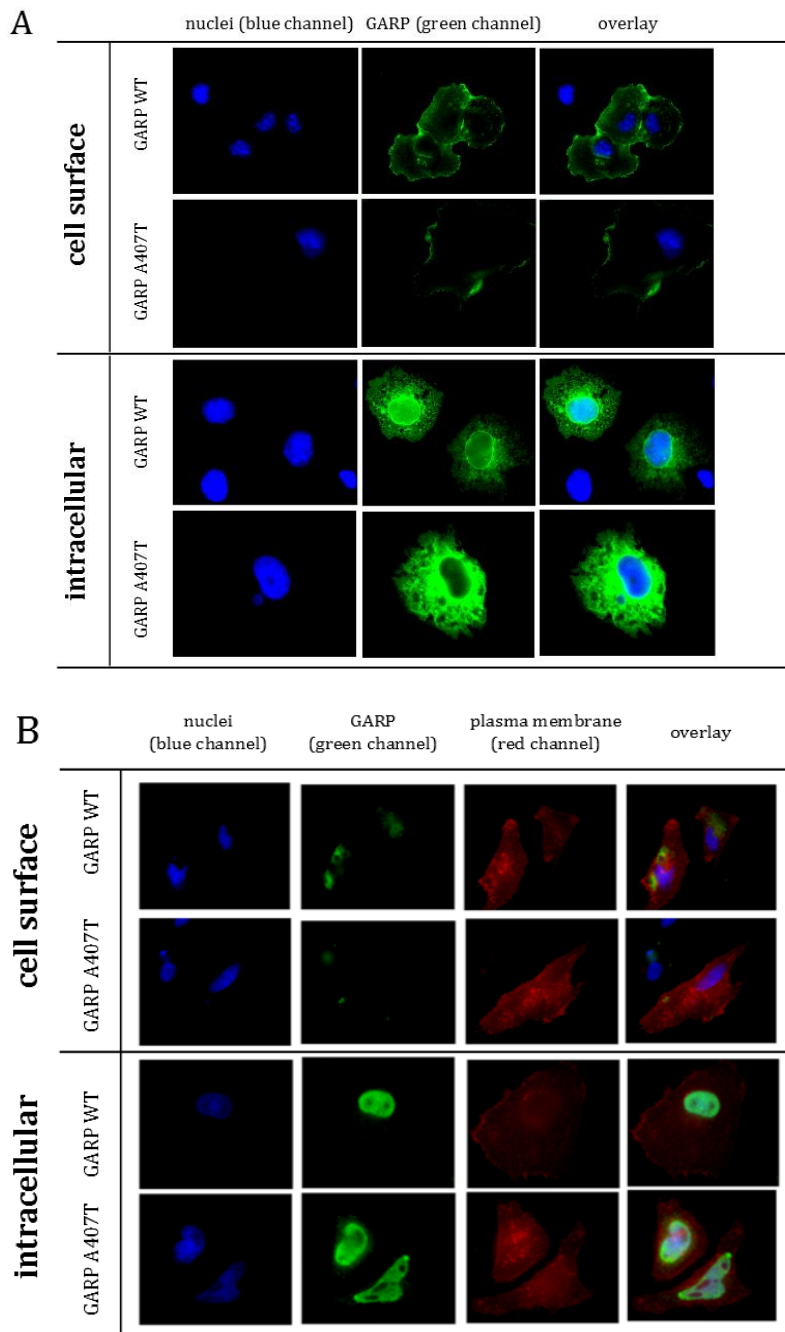
Figure 28: Cell surface and intracellular localization of wildtype (WT) and mutated GARP (A407T) on transiently transfected Cos-7 (A) and HeLa (B) cells. Nuclei were stained using Hoechst 33342 dye (blue channel); GARP was stained using anti-human GARP IgG2b /goat anti-mouse Alexa-Fluor488 antibody (green channel); plasma membrane was stained using CellLight® Plasma Membrane-RFP BacMam 2.0 reagent (only visible in HeLa cells; red channel). Reduced expression of mutated GARP on the cell surface was observed in both cell lines compared to protein expression in wildtype GARP expressing cells. Intracellular staining revealed high amount of protein in the cells with higher retention of mutated GARP at least in Cos-7 cells. Images were collected on a Zeiss Axiophot fluorescence microscope with an AxioCam MRm CCD sensor (40x magnification).

2.3.4.3 GARP protein expression determined by flow cytometric analysis (FACS)

After having shown by immunohistochemistry that mutated GARP expression on the cell surface might be reduced compared to non-mutated protein expression, the next step was to examine the expression differences via flow cytometric analysis. For this purpose, Cos-7 cells were again transiently transfected with either wildtype GARP or A407T GARP expressing vectors, stained with a mouse allophycocyanine-conjugated anti-human GARP antibody followed by flow cytometric analysis. To verify the transfection efficiency, GFP signals of transfected cells were analyzed without antibody staining. For Statistical analysis log-transformed percentage of GARP-positive cells were calculated and the three groups – untransfectetd control cells (ctrl), wildtype GARP (WT), and mutant GARP (A407T) expressing cells were compared by ANOVA following a Bonferroni-Holm (BH) corrected post-hoc analysis. A slightly lower GARP surface expression (P_{BH}= 0.3538) was identified on A407T GARP compared to wildtype GARP expressing Cos-7 cells (Figure 29). GARP surface expression on untransfected control cells was low. GFP signals to determine transfection efficiency showed no deviation between WT and A407T GARP-overexpressing cells (GFP positive cells: 46.6 ± 12.1 % and 45.7 ± 9.3 % for WT and A407T transfected cell population, respectively), thus, normalization was not necessary.

FACS analysis in Cos-7 cells showed that there might be a difference in cell surface expression between WT and A407T GARP. Cos-7 cells, however, originate from monkey kidney and might not represent the right model for the human situation. Thus, GARP expression was also investigated in a human cell system. For this, the non-regulatory CD4+ CD25- T cell population was chosen. It is widely known that GARP surface expression is up-regulated in regulatory T cells (CD4+CD25+) after activation and remains at a low level in the non-regulatory fraction (CD4+CD25-) (Tran et al. 2009; Wang et al. 2009). The non-regulatory CD4+CD25- T cell population was selected for further experiments due to its very low endogenous GARP expression and because of sufficient cell numbers that could be obtained after isolation from peripheral blood of healthy donors.

Results of four independent experiments using cells of four independent healthy donors revealed a significant lower GARP protein expression on the cell surface (P_{BH}= 0.0436) of A407T expressing cells compared to WT expressing CD4+CD25- T cells (Figure 30). No GARP signals were detected on unstained cells that served as negative control. A slight expression was observed on untransfected but stained cells (Ctrl) indicating a weak endogenous GARP expression in CD4+CD25- cells. Moreover, GFP signals showed no deviation between WT GARP and A407T GARP-overexpressing cells (GFP positive cells: 16.7 ±3.9 % and 14.8 ± 5.2 % for WT and A407T transfected cell population, respectively).
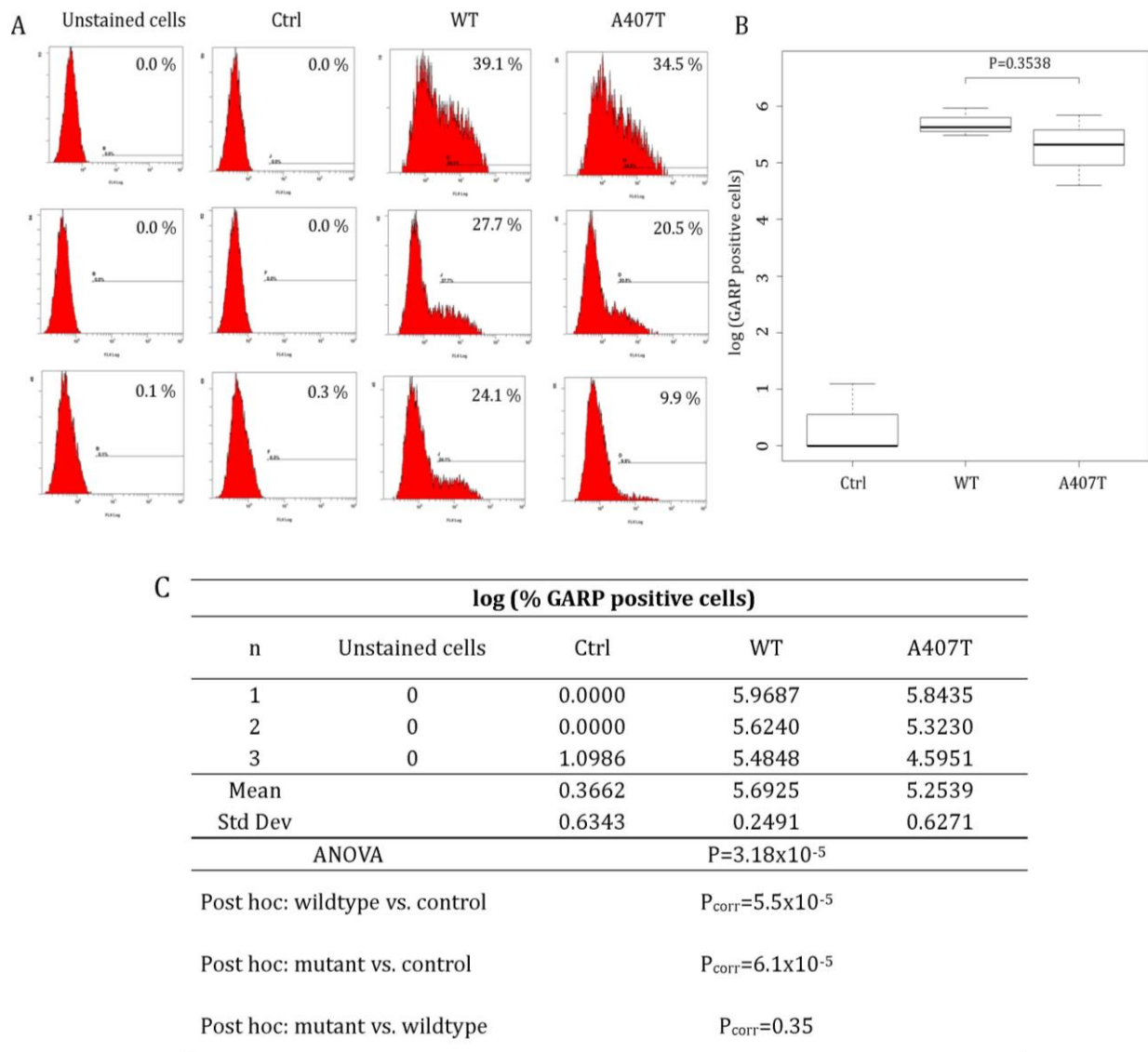
Figure 29: Slighty lower expression of mutant GARP on the surface of transiently transfected Cos-7 cells. Both wildtype GARP (WT) or A407T GARP (A407T) were overexpressed in Cos-7 cells and GARP surface expression was measured by flow cytometry. Histograms show fluorescence intensity (x axis) versus cell number (y axis). The values in the respective histograms indicate percentage of GARP-positive cells (A). Boxplots display log-transformed percentage of GARP-positive cells (mean ± SD), which were normalized by the percentage of unstained cells (B). Table indicates all values of three independent experiments and corresponding p-values. Statistical analysis was performed using ANOVA following a Bonferroni-Holm (BH) corrected post-hoc analysis (C).
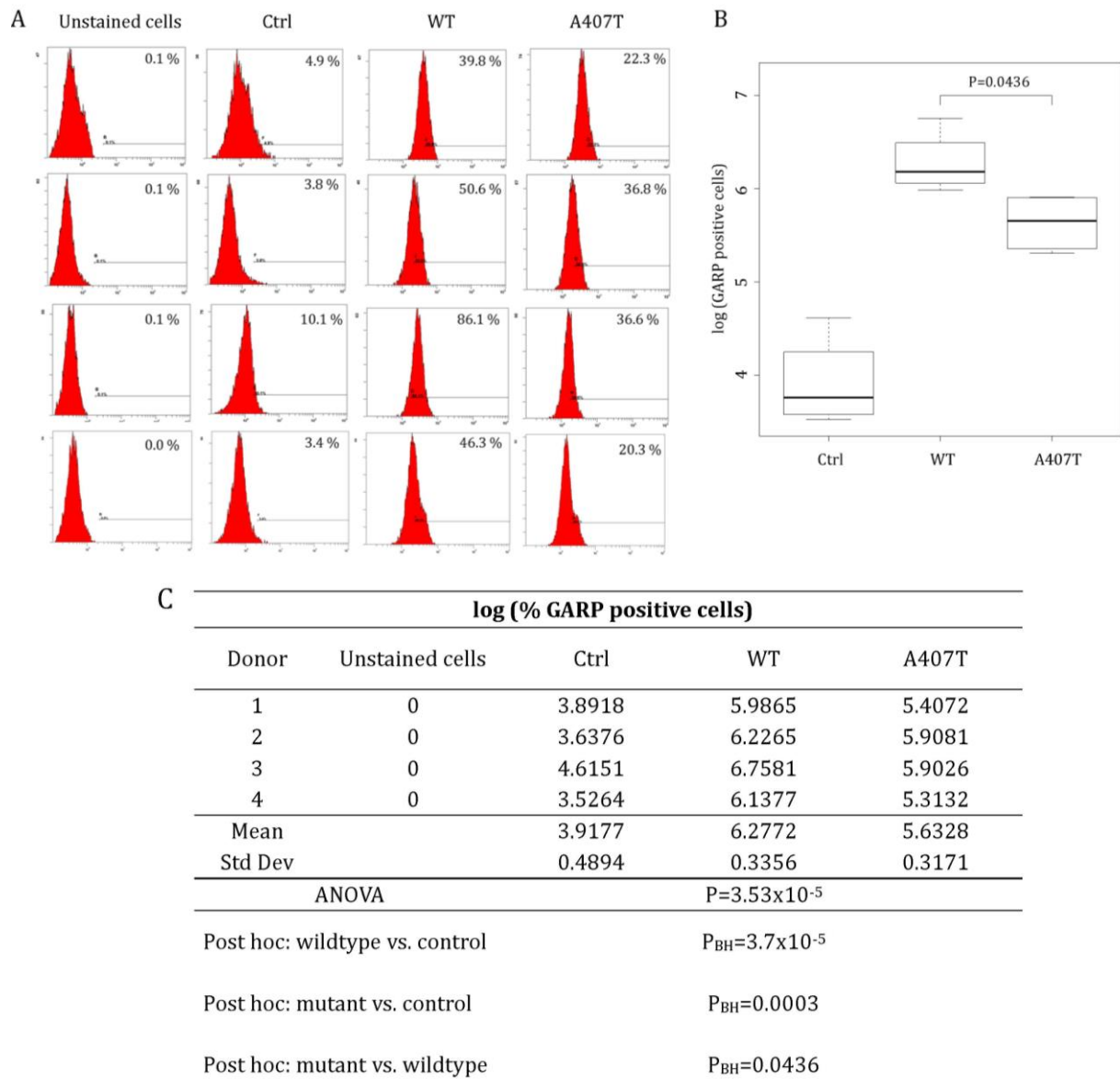
Figure 30: **Significant lower mutant GARP surface expression in transiently transfected CD4+CD25-T cells of four healthy donors analyzed by flow cytometry.** Both wildtype GARP (WT) or A407T GARP (A407T) were overexpressed in CD4+CD25- T cells and GARP surface expression was measured by flow cytometry. Histograms show fluorescence intensity (x axis) versus cell number (y axis). The values in the respective histograms indicate percentage of GARP-positive cells (A).Boxplots display log-transformed percentage of GARP-positive cells (mean ± SD), which were normalized by the percentage of unstained cells (B). Table indicates all values of three independent experiments and corresponding p-values. Statistical analysis was performed using ANOVA following a Bonferroni-Holm (BH) corrected post-hoc analysis (C).

To examine whether the observed reduced surface expression of A407T GARP might be due to intracellular accumulation of the protein, antibody staining and FACS analysis in CD4+CD25- T cells overexpressing wildtype and A407T GARP was conducted after permeabilization of the cells. A significantly higher intracellular amount of mutated protein (P_{BH}= 0.0202) was detected in comparison to the expression of wildtype GARP within the cell (Figure 31). Again, low levels of GARP were detected in unstained cells, but high intracellular expression was observed in untransfected control cells. In summary, these results revealed a significant lower expression of mutated GARP on the cell surface in combination with a higher intracellular abundance when compared to non-mutated GARP.
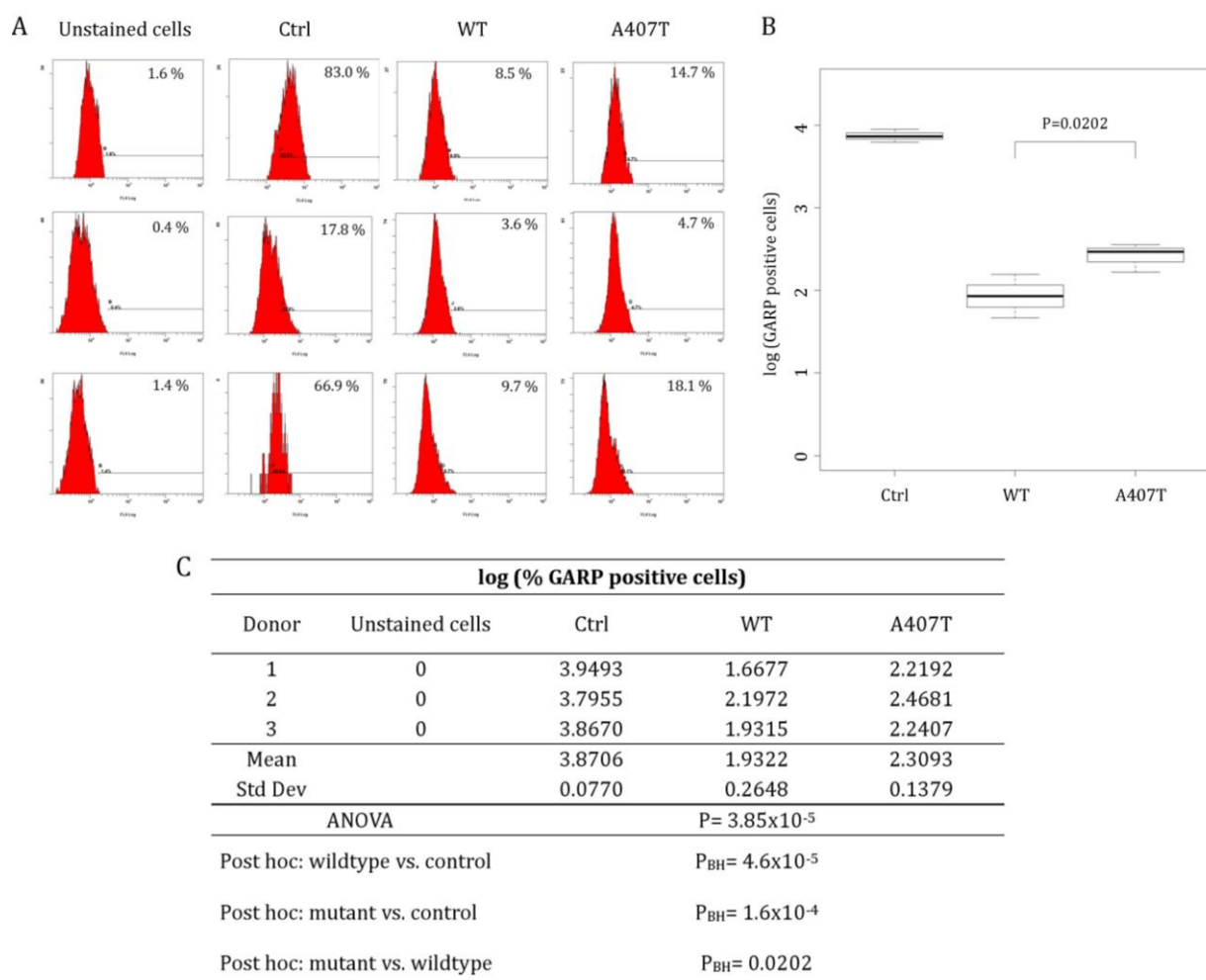
Figure 31: Significant higher intracellular mutant GARP expression in transiently transfected CD4+CD25- T cells of three healthy donors analyzed by flow cytometry. Both wildtype GARP (WT) or A407T GARP (A407T) were overexpressed in CD4+CD25- T cells and intracellular GARP expression was measured by flow cytometry after permeabilization. Histograms show fluorescence intensity (x axis) versus cell number (y axis). The values in the respective histograms indicate percentage of GARP-positive cells (A). Boxplots display log-transformed percentage of GARP-positive cells (mean ± SD), which were normalized by the percentage of unstained cells (B). Table indicates all values of three independent experiments and corresponding p-values. Statistical analysis was performed using ANOVA following a Bonferroni-Holm (BH) corrected post-hoc analysis (C).

2.3.4.4 FACS analysis of CTLA-4, FOXP3 and Neuropilin as specific regulatory T cell markers

To further investigate whether the observed GARP expression differences show any alteration of T cell function, different regulatory T cell markers (CTLA-4, FOXP3, Neuropilin) were measured via flow cytometry. Data were log-transformed and normalized to the unstained cells. Measurement revealed a significant lower expression of CTLA-4 (P= 0.03) as well as a tendency for reduced FOXP3 and Neuropilin expression in A407T GARP transfected compared to wildtype transfected CD4+CD25- T cells (Figure 32).
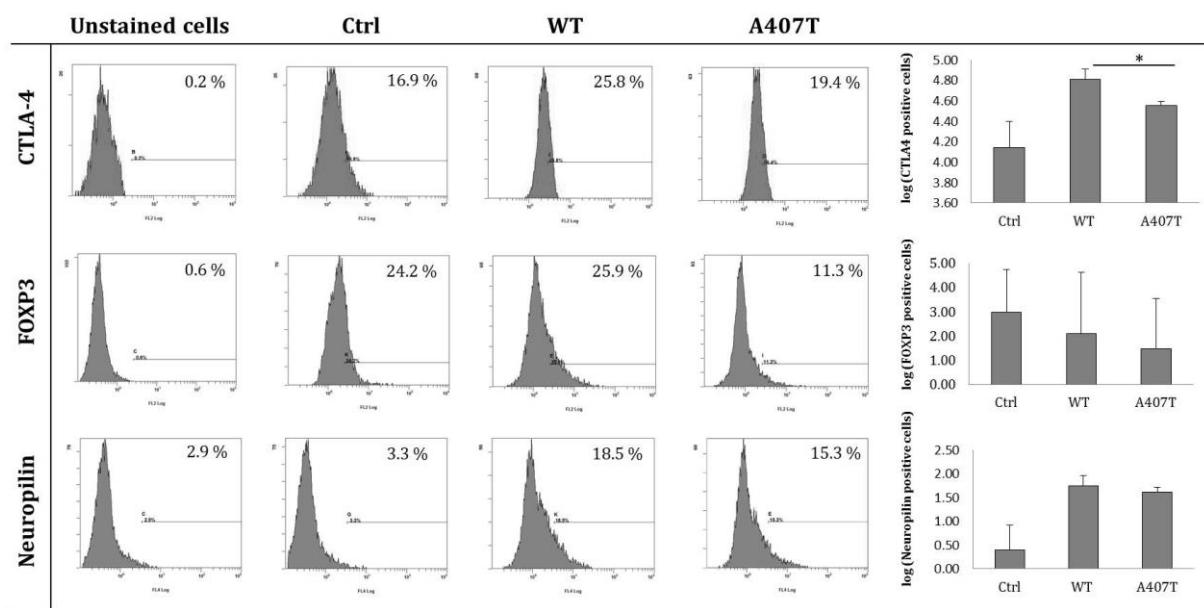
Figure 32: Expression phenotype analysis of A407T GARP transfected CD4+CD25- T cells compared to wildtype (WT) transfected cells using flow cytometric analysis (n=3). Both wildtype GARP (WT) or A407T GARP (A407T) was overexpressed in CD4+CD25- T cells and CTLA-4, FOXP3, and Neuropilin expression was measured by flow cytometry using specific antibodies. Significant reduction in CTLA-4 expression (P= 0.0342) was detected in A407T GARP expressing cells compared to WT GARP expressing cells. Histograms show fluorescence intensity (x axis) versus cell number (y axis). The values in the respective histograms indicate percentage of GARP-positive cells. Diagram bars display log-transformed percentage of respective Treg marker-positive cells normalized to the unstained cells (error bars show 95 % CI).*P> 0.05; n=3).

2.3.5 Analysis of soluble GARP via enzyme-linked immunosorbent assay (ELISA)

In literature it is described that GARP encodes a surface receptor on activated T regulatory cells that binds latent TGFβ and modulates peripheral tolerance and T effector cell function (Wang et al. 2008). Interestingly, it has recently been shown that not only the anchored GARP exerts regulatory function but also recombinant soluble GARP (sGARP) which can bind to recombinant latent TGFβ, and causes suppressive bioactivity *in vitro* (Hahn et al. 2013). Hence, there is an intriguing possibility that the soluble form may exist naturally, and could be a potential biomarker for various cancers or autoimmune conditions. To explore whether the GARP mutation might have any influence on shedding GARP/TGFß complexes from the cell surface, soluble GARP concentration in cell culture supernatant of wildtype and A407T GARP overexpressing CD4+CD25- cells were measured via ELISA. Twenty-four hours post transfection nearly similar concentration of soluble GARP in cell culture supernatant of transiently transfected T cells (0.211 ng/ml and 0.228 ng/ml GARP for WT GARP- and A407T GARP-expressing cells, respectively) and untransfected control cells (0.205 ng/ml GARP) was detected (Figure 33).
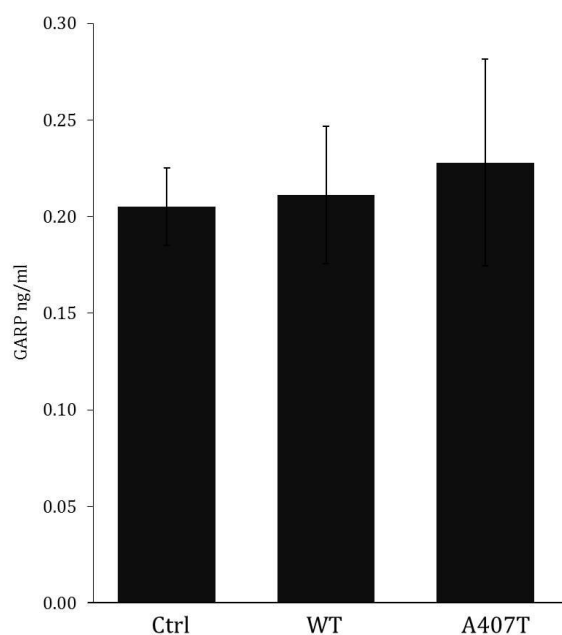
Figure 33: Comparable soluble GARP concentration in cell culture supernatants of transiently transfected CD4+CD25- T cells. Both wildtype GARP (WT) or A407T GARP (A407T) was overexpressed in CD4+CD25- T cells and soluble GARP concentration in cell culture supernatants was measured by ELISA 24h post transfection. Untransfected CD4+CD25- T cells were used as control (Ctrl). Bars show mean ± SD; n=4.

2.4 Cutaneous mRNA expression patterns in atopic dermatitis

To obtain a deeper insight into the genetic architecture of atopic dermatitis not only based on genetic data of the associated and previously investigated locus on chromosome 11q13.5 but on the whole genome, this part of the project was set out to compare the gene expression of lesional (AL) and non-lesional (AN) skin from atopic dermatitis (AD) patients with that of healthy controls (NN).

2.4.1 RNA quality assessment of samples isolated from skin biopsies

Skin samples of AD patients from lesional and non-lesional skin were obtained from the previously reported Ambitous study (Hotze et al. 2014) (Atopic Dermatitis Biomarker Identification Trial in omalizumab Usage, ClinicalTrials.gov identifier: NCT01179529), a prospective observational trial aimed to identify potential biomarkers for AD patient subgroups that benefit from an anti-IgE treatment with omalizumab (Xolair®, Novartis). Skin biopsies before treatment (lesional (n=19) and non-lesional skin samples (n=19)) were used for this investigation. Skin biopsies from healthy controls (n=27) were recruited at the "Department of Dermatology at the University Hospital, TU München".

Since the success of expression analysis relies upon having high, quality RNA samples, it is important to check quality parameters before starting the analysis. Quality assessment criteria included concentration measurement (determined by a Nanodrop spectrophotometer, minimum of 400 ng required) and RNA integrity (determined by RIN value, cut-off was set > 5.5). Control samples revealed an average RNA integrity number of 6.3 and an average total RNA concentration of 3.84 µg. RNA samples from lesional and non-lesional skin showed an average RIN value of 6.7 and 5.8, respectively, together with an average concentration of 10.88 µg and 5.95 µg in lesional and non-lesional samples, respectively (Table 4).

Since most of the samples exhibited a low RNA integrity (RIN value < 6.5), PCR-amplification of the housekeeping gene *β-actin* was performed as additional quality step for all samples with RIN values < 6.5. Visual inspection of the electropherogram (consisting of weak and strong PCR bands) decided whether the *β-actin* amplification was sufficient (strong band, equated with high quality) or not (weak band, equated with low quality). For quantification the same amount of every PCR product was applied to the gel, however, evaluation was done based on discretion of the doctoral candidate.

As shown in Figure 34, for example, even though the Bioanalyzer electropherogram showed minor degradation (based on the 28S RNA peak) resulting in low RIN values, *β-actin* was amplified sufficiently in most of the samples. However, if the *β-actin*-amplification was not sufficient (indicated by PCR bands of weak intensity), the samples were excluded from further analysis. All samples with RIN values > 6.5 were directly used for further analysis without additional *β-actin* amplification step.
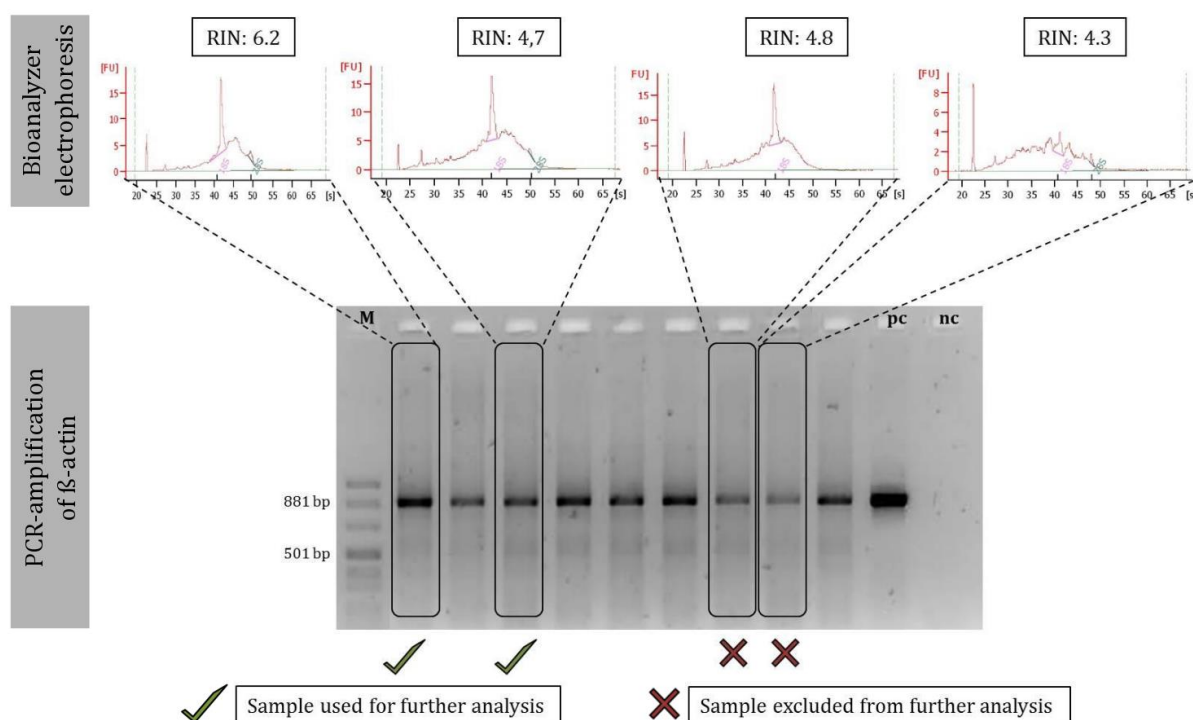

Figure 34: Two-step quality control of RNA samples isolated from skin biopsies. Electropherograms and RNA integrity number (RIN) were generated by the Agilent Bioanalyzer software. As additional quality control step, *β-actin* amplification (884 bp fragment) was performed via RT-PCR of samples with RIN values < 6.5. Samples were excluded from further analyses if *ß-actin* amplification was not sufficiently detectable (weak intensity of PCR fragment). M= DNA ladder, pc= positive control (high quality cDNA); nc= negative control (water instead of cDNA template).

Table 4: Quality parameters of RNA samples isolated from skin (before and after quality control)

	Controls			Cases					
				lesional skin			non-lesional skin		
	RIN	**conc.**	**n**	**RIN**	**conc.**	**n**	**RIN**	**conc.**	**n**
Before QC	6.3	3.84 μg	27	6.7	10.88 μg	19	5.8	5.95 μg	19
After QC	6.6	3.90 μg	21	6.8	10.98 μg	15	6.0	6.76 μg	15

RIN= RNA integrity number; conc. = total RNA concentration, n= number of samples; QC= quality control

In summary, after quality control 14 samples did not match the quality criteria and were excluded from further analysis; therefore 51 samples remained for genome-wide expression analysis. All quality parameters of samples before and after quality control are summarized in Table 4.

2.4.2 Quality control of gene expression data

After successful RNA isolation, whole-genome expression profiles were generated with the Illumina HumanHT-12 v4 Expression BeadChip and data was collected and visualized with the Illumina GenomeStudio software (Gene Expression Module). To analyze the reliability and application efficiency of generated expression data, several data quality parameters need to be fulfilled (Table 5).

The number of detected genes represents a good overall quality control indicator. Based on the calculated detection p-value, that represents the confidence that a transcript is expressed above the background, a transcript is called "detected" (p-value ≤ 0.01). As a rule, high quality data exhibit more than 10,000 detected genes with a p-value threshold of 0.01. In the present analysis, the average of detected genes reached 13318 ± 497 and 12965 ± 809 in controls and AD cases, respectively (Table 5). Suitable parameters to visualize the overall strength of the measured signal are the "signal average" and the "signal-to-noise-ratio". The signal average describes the average signal for the sample across all probes and should be at least higher than the background signal (> 300). All samples showed a high signal average (1039 ± 89 and 1033 ± 91 for controls and cases, respectively) with low variation between the samples. The signal-to-noise-ratio, calculated by dividing the ninety-fifth percentile average intensity across all probes (P95) by the fifth percentile average intensity across all probes (P5), demonstrates a high intensity of the measured signal compared to the background when the value is equal 10 or higher. Control and cases reached clearly higher signal-to-noise-ratios, namely 52 ± 6 and 53 ± 8, respectively (Table 5).

Table 5: Data quality control parameters (Mean ± SD)

	Controls (n=21)	Cases (n=30)	Reference value
Detected genes (0.01)	13318 ± 497	12965 ± 809	> 10000
Signal average	1039 ± 89	1033 ± 91	> 300
Signal-to-noise ratio (P95/P05)*	52 ± 6	53 ± 8	> 10
Negative signal (background)	114 ± 15	115 ± 18	< 300

*P05= fifth percentile average intensity across all probes; P95= ninety-fifth percentile average intensity across all probes

2.4.3 Genome-wide expression differences between non-lesional (AN) and lesional (AL) AD skin and healthy controls (NN)

For investigation of genome-wide differences in expression profiles a quality controlled-subset of AD cases (lesional and non-lesional skin samples, each with n=15) together with healthy controls (n=21), matched by age and sex, were selected. The study characteristics of cases and controls including mean age, sex, and mean SCORAD (SCORing index Atopic Dermatitis) scores are listed in Table 6.

Table 6: Study population

	Controls (n=21)	Cases (n=15)
Mean age (SD)	25.83 (5.67)	46.87 (13.12)
Sex (male/female)	7 / 14	8 / 7
Mean SCORAD score at inclusion (SD)		50.27 (17.42)

SD: standard deviation

After quality control of data (see 2.4.2), differences in $\log_2$-expression levels between cases and controls were compared using the Welch-test. The following pairwise comparisons were analyzed to define the AD phenotype: AL/NN (lesional skin of cases vs. controls), AN/NN (non-lesional skin of cases vs. controls), AL/AN (cases lesional vs. non-lesional) representing "inflammation genes", "unique genes of non-inflamed AD skin" and "pairwise inflammation genes within the same individual", respectively. Only transcripts with a fold change (FC) value > 2 and P_{FDR} < 0.05 were selected and considered as genome-wide differentially expressed (DET). Statistical analysis was performed in cooperation with Dr. Hansjörg Baurecht of the "Universitätsklinikum Schleswig-Holstein".

A total of 10,572 transcripts were expressed in the epidermis and pairwise comparison of AL/NN, AN/NN and AL/AN revealed 250, 14 and 51 transcripts with genome-wide significant differential expression (DET) (P_{FDR} <0.05, fold change >2) (Appendix Table I-III). Off these DETs, three genes (*S100A9, SPRR2F, PI3/elafin*) were found to be consistently upregulated in all three comparisons. Furthermore, 9 upregulated (S100A7, SPRR2G, C1QB, CA2, *CCL23, CCL8, LYPD2, MARCO, MS4A4A*) and one downregulated (PTGDS) genes were identified in AL/NN and AN/NN as well as 30 upregulated and 11 downregulated genes in AL/NN and AL/AN (Figure 35, Table 7).
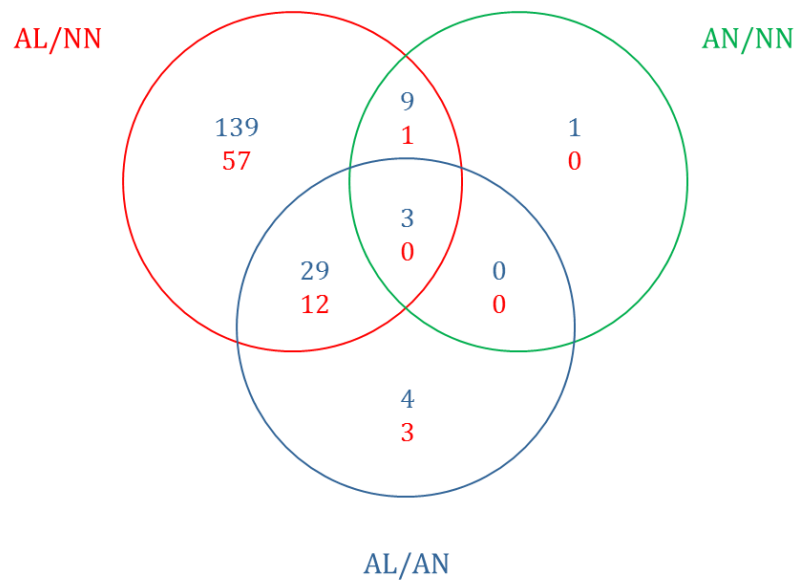
Figure 35: Venn diagram of significantly differentially expressed genes in lesional (AL) and non-lesional (AN) skin in comparison with healthy controls (NN). Numbers of upregulated genes are displayed in blue, numbers of downregulated genes in red. δ> $\lvert 1 \rvert$, q< 0.05.

Table 7: Regulated genes found in pairwise gene expressions comparison of AN/NN, AL/NN and AL/AN (P$_{FDR}$ <0.05, fold change >2)

AN/NN	AL/NN	AL/AN
S100A9, SPRR2F, PI3		
S100A7, SPRR2G, C1QB, CA2, CCL23, CCL8, LYPD2, MARCO, MS4A4A *PTGS*		
	ADAM19, CARHSP1, CHI3L2, ECGF1, EPSTI1, FABP5, FCN1, GPR68, HS3ST3A1, IFI27, IFI6, IL7R, ISG15, LRP8, MGC102966, MMP9, MX1, NAMPT, NELL2, NETO2, NP, POL3S, RPL29, S100A8, SERPINB1, SPRR1B, SRGN, TNC, TNFRSF12A, UPP1 *AQP9, C5orf4, CACNA1H, CLDN23, HS.374278, HS.554507, LEPR, LOC202134, PLLP, RORC, TMEM99*	

blue: upregulated genes; red: downregulated genes; AL: lesional skin; AN: non-lesional skin; NN: controls

2.4.4 Functional enrichment analyses of gene sets

In order to identify functional gene classes (gene ontology (GO) terms or KEGG pathways) that are over-represented in the analyzed gene set, functional enrichment analyses were performed with the software DAVID (Huang da et al. 2009). Afterwards, identified functional annotations were subsequently clustered to groups of functional clusters. In general, functional enrichment

analysis was restricted to the annotation categories KEGG_PATHWAY, GOTERM_BP (GO Biological Process), GOTERM_CC (GO Cellular Component) and GOTERM_MF (GO Molecular Function).

Functional enrichment analyses

Intersecting genes between the two comparisons AL/NN and AN/NN can be interpreted as unique "AD-related genes" since they are common between inflamed skin and non-affected skin of AD patients. On the other hand, the overlap between AL/NN and AL/AN can be considered as differentially regulated "inflammation genes". Therefore, functional enrichment analyses were focused on enriched functional gene classes which were common for genes of the described intersections.

Results of DAVID analyses revealed two highly enriched gene ontology terms, "defense response" (GO term 0006952) and "extracellular region" (GO term 0005576), which were common between AL/NN and AN/NN. Seven genes (*CCL8, CCL23, C1QB, S100A9, S100A7, CA2, PI3)* of the shared 12 upregulated genes and the one downregulated gene (*PTGDS)* were included (Table 8). The same functional annotation "extracellular region" (GO term 0005576) was also most significantly enriched between AL/NN and AL/AN including 11 (FCN1, IL7R, ISG15, LEPR, LRP8, MMP9, NELL2, PI3, POL3S, SRGN, TNC) of the shared genes (Table 8).

Clustering of functional groups

Subsequent clustering of enriched functional annotations to groups using DAVID revealed seven highly enriched annotation clusters (enrichment score (ES) > 2.2) for AL/NN (Figure 36). By considering only annotation clusters consisting of enriched terms meeting a corrected significance threshold (p_{BH} < 0.05), reduced the results to the first three clusters which could be termed as "Defense response", "Extracellular space" and "Plasma membrane". For AN/NN three highly enriched functional annotation clusters (ES > 2.1) were observed, termed as "Epidermis development", "Defense response" and "Immune response". However, none of the functional annotations met the corrected significance threshold. Finally, for AL/AN three enriched functional annotation clusters (ES > 1.3; "Extracellular space", "Extracellular matrix" and "Enzyme inhibitor activity") were identified, off which none of the functional annotations met a corrected significance threshold as well.
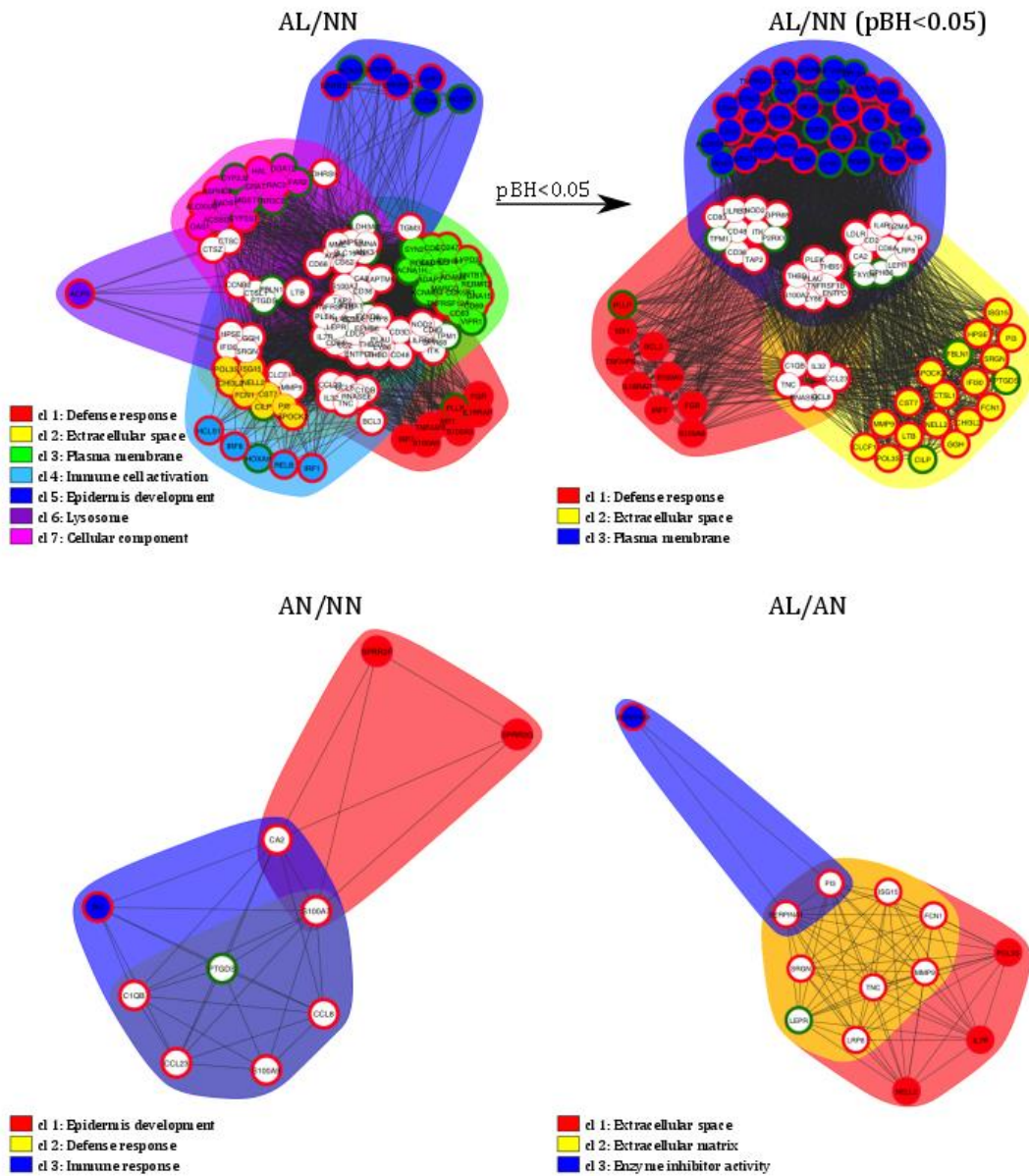
Figure 36: Functional annotation cluster derived from DAVID gene enrichment analysis for lesional skin vs. controls (AL/NN), non-lesional skin vs. controls (AN/NN), and lesional skin vs. non-lesional skin (AL/AN). Functional clusters are dedicated by different colours. Gene names in red circles display upregulated genes; gene names in green circles downregulated gene transcripts. Corresponding genes are listed in Appendix Table IV-VI.

Table 8: Intersecting genes between AL/NN and AN/NN as well as AL/NN and AL/AN which contribute to enriched terms

Lesional/Controls (AL/NN) versus Non-lesional/Controls (AN/NN)						
Gene	most sign. enriched common GO term	further enriched common GO terms	Diff AL/NN	P$_{FDR}$ AL/NN	Diff AN/NN	P$_{FDR}$ AN/NN
CCL8	0006952~defense response (BP)	0009611/0006954/0005615/0005576/0044421	1.597	0.0020	1.082	0.0015
CCL23	0006952~defense response (BP)	0009611/0006954/0005615/0005576/0044421	1.825	2.6E-04	1.427	0.0131
C1QB	0006952~defense response (BP)	0009611/0006954/0005576/0044421	1.510	3.0E-05	1.050	0.0042
S100A9	**0006952~defense response (BP)**	**0009611/0006954**	**3.160**	**1.2E-06**	**1.894**	**0.0070**
S100A7	0006952~defense response (BP)	0005576	4.050	5.2E-07	3.161	8.1E-04
CA2	0005576~extracellular region (CC)	0005615/0044421	1.711	5.6E-06	1.307	0.0048
PTGDS	0005576~extracellular region (CC)		-1.241	6.4E-04	-1.344	0.0317
PI3	0005576~extracellular region (CC)	0044421	**4.999**	**1.5E-05**	**1.922**	**0.0175**
Lesional/Controls (AL/NN) versus Lesional/Non-lesional (AL/AN)						
Gene	most sign. enriched common GO term	further enriched common GO terms	Diff AL/NN	P$_{FDR}$ AL/NN	Diff AL/AN	P$_{FDR}$ AL/AN
FCN1	0005576~extracellular region (CC)	0005615/0044421	1.093	0.0377	1.373	0.0216
IL7R	0005576~extracellular region (CC)	0005576	1.932	3.3E-05	1.058	0.0185
ISG15	0005576~extracellular region (CC)	0005615/0044421	1.249	2.3E-04	1.250	0.0043
LEPR	0005576~extracellular region (CC)	0005615/0044421	-1.495	0.0013	-1.554	0.0027
LRP8	0005576~extracellular region (CC)	0005615/0044421	1.259	1.6E-04	1.092	0.0017
MMP9	0005576~extracellular region (CC)	0005615/0044421	1.501	0.0044	1.349	0.0189
NELL2	0005576~extracellular region (CC)		1.962	3.1E-06	1.529	0.0097
PI3	**0005576~extracellular region (CC)**	**0044421**	**4.999**	**1.5E-05**	**3.077**	**0.0027**
POL3S	0005576~extracellular region (CC)		2.880	2.2E-05	1.935	0.0035
SRGN	0005576~extracellular region (CC)	0005615/0044421	1.357	0.0015	1.102	0.0077
TNC	0005576~extracellular region (CC)	0044421	1.735	2.3E-05	1.290	0.0028

Genes indicated in bold are DETs in three comparisons: AL/NN, AN/NN and AL/AN.
0006952= defense response (BP); 0005576= extracellular region (CC); 0005615= extracellular space (CC); 0006954= inflammatory response (BP); 0009611= response to wounding (BP); 0044421= extracellular region part (CC)
BP= biological process; MF= molecular function; CC= cell compartment

3   DISCUSSION

During the past decade, genome-wide association studies (GWAS) have reformed the world of genetics by their huge power to comprehensively detect genetic association between gene variants and complex phenotypes and diseases (Welter et al. 2014). Although, GWAS have provided useful findings about genetic factors contributing to complex diseases, the causal variants and disease-causing mechanisms that lead to the disease onset are still almost unclear. To understand the functional consequences of these identified variants, functional characterization of associated loci is perhaps the greatest challenge in the "post-GWAS" era.

It has long been recognized that heritable factors contribute to the development of atopic dermatitis (AD) and many candidate genes and susceptibility loci of atopic dermatitis have been identified by GWAS within the last years (Esparza-Gordillo et al. 2009; Sun et al. 2011; Hirota et al. 2012; Ellinghaus et al. 2013; Weidinger et al. 2013; Baurecht et al. 2015; Paternoster et al. 2015; Schaarschmidt et al. 2015). This study focuses on the widely replicated *C11orf30/LRRC32* AD-risk locus (11q13.5) that comprises a robust site of association of common intergenic risk variants. However, which of the identified variants is responsible for the association signal and which candidate genes are affected is not answered yet. Hence, the focus of this work has been dedicated to characterize the susceptibility region on 11q13.5 by investigating the functional implications of risk variants underlying the association signal: the GWA lead SNP (rs7927894), selected proxy SNPs (rs2155219, rs11236797 and rs34455012indel) and a rare coding variant (rs79525962).

3.1   The AD-associated polymorphism rs7927894 is not associated with allelic expression imbalance of *C11orf30* and *LLRC32* in skin tissue

Nearly 90 % of the identified GWA lead SNPs are located intronic or intergenic, mainly in chromosome regions with high regulatory potential (Welter et al. 2014). Therefore, it is not unlikely that these SNPs are able to influence gene regulation of genes in proximity. In fact, it has been shown that trait-associated SNPs are more probable associated with expression quantitative trait loci (eQTL) than non-associated SNPs (Nicolae et al. 2010). Thus, eQTL analysis of *LRRC32* and *C11orf30* in peripheral blood of the KORA F4 cohort was considered to analyze the impact of rs7927894 on transcript levels of genes in its proximity. The results presented here indicate a moderate *cis*-regulatory effect of the rs7927894 risk allele on *LRRC32* expression

but not on *C11orf30* transcript levels. However, this analysis was conducted in whole blood which might be not the suitable cell system for analyses in the context of atopic dermatitis. RT-PCR analysis of 17 human tissues showed nearly ubiquitous expression of *C11orf30* and *LRRC32* and also revealed expression in AD-relevant tissues such as skin (Esparza-Gordillo et al. 2009). However, equivalent SNP-dependent gene expression analyses in AD-related tissues demand high sample numbers to achieve statistically reliable results with high statistical power. This is often very challenging as high sample numbers are difficult to achieve, especially for not easy accessible tissues like skin.

In that case, the *cis*-regulating impact of a SNP on the particular transcript level can be measured by allelic expression analysis in heterozygous individuals using an expressed SNP (eSNP) as a marker (Yan et al. 2002; Pastinen and Hudson 2004; Serre et al. 2008; Berulava and Horsthemke 2010). For this approach only a few subjects are needed and comparing the relative expression of the two alleles in one single individual implicate several advantages: allelic transcript levels are compared within the same genetic and cellular context (e.g. environmental factors, amount of transcription factors), which increases the sensitivity to detect *cis*-acting effects (Pastinen and Hudson 2004; Pastinen et al. 2006). Since genetic heterogeneity in humans is high, studies often fail to identify *cis*-regulatory effects using gene expression data. These effects are possibly hampered by individual differences in *trans*-acting regulation that swamp *cis*-regulatory signals (Serre et al. 2008). Hence, the comparison of alleles within rather than between samples nullifies possible *trans*-acting regulatory effects and provides furthermore an internally controlled situation (Knight 2006; Serre et al. 2008; Pastinen 2010). In this study results of allelic expression analysis in skin revealed that relative transcript levels of *LRRC32* and *C11orf30* were slightly skewed by rs7927894, however, homozygous control samples showed the same allelic expression patterns for both genes. This indicates that the differential expression is not affected by the rs7927894 genotype itself but rather might be affected by the eSNP or by other *cis*-regulatory variation in LD.

The eSNP selection might be a possible point of criticism. On the one hand the selection was carried out by interrogation of an established eSNP database that consists of known associations between gene transcript levels and genotypes of *cis*-regulatory SNPs (Kottgen et al. 2013), on the other hand, for selection of heterozygous skin samples, information about the eSNP genotype is required and the eSNP needs to be captured by the utilized genotyping array. Therefore, the selection was limited, especially for the eSNP tagging *LRRC32*. In contrast, the eSNP selected for *C11orf30* was already successfully applied to allelic expression studies of candidate breast cancer genes (Maia et al. 2009). Moreover, a common SNP (MAF> 5 %) is required to increase the power in detecting allelic imbalance of genes (Serre et al. 2008); but this was in concordance with both selected eSNPs, having a high allele frequency (33.9 % and 20.6 % for *LRRC32* eSNP

and *C11orf30* eSNP, respectively; based on 1000genomes). At the same time, it should be noted that in allelic studies the abundance of each allele from a heterozygous individual is analyzed using RT-PCR and primer extension with fluorescent nucleotides. Thus it has to be kept in mind that artefactual allelic imbalance might occur which is caused by stochastic RT-PCR amplification of one allele (Pastinen and Hudson 2004) or simply result from random silencing of one of the two alleles.

Since the effects of SNPs on RNA expression are often very subtle it is not surprising that candidate gene expression analysis experiments may not give a clear answer. Nevertheless the data suggest that the GWA lead SNP does not have a distinct regulatory impact on *LRRC32* and *C11orf30* expression in skin tissue and it is likely that other variants are involved.

3.2 Rs7927894 versus rs2155219 – a proxy SNP as potential regulatory variant

Since the International Haplotype Map (HapMap) project, which was conducted to analyze common patterns of DNA polymorphisms in the human genome (International HapMap 2005), identified that major parts of the human genome are arranged in blocks consisting of polymorphisms in strong linkage disequilibrium (LD) (so called LD blocks), it is known that GWA lead SNPs are usually tagged by multiple correlated variants in LD (Gabriel et al. 2002). The design of genotyping chips used in GWAS benefit from the known LD structure while only a subset of SNPs in LD have to be genotyped, however, identification of the functional and causal SNP responsible for the underlying signal is hampered. Looking at the investigated locus 11q13.5, LD structure obtained from HapMap data sets (Phase 1 and 2; http://hapmap.ncbi.nlm.nih.gov/index.html.en) shows correlation of the AD-associated lead SNP rs7927894 with a set of variants on both sides of the SNP (Figure 37). The majority of variants in LD (D'> 0.8) in a 750 kb surrounding region of rs7927894 are located intergenic between *C11orf30* and *LRRC32*. Some SNPs are located in the 3' region of *LRRC32* or in *C11orf30* itself, and a few correlated polymorphisms can be found in the intergenic region between *C11orf30* and the upstream protein kinase encoding gene *PRKRIR*. Hence, LD data alone did not reveal, which of the proxy SNPs is of prior interest and on which of the two genes should be focused in further studies.
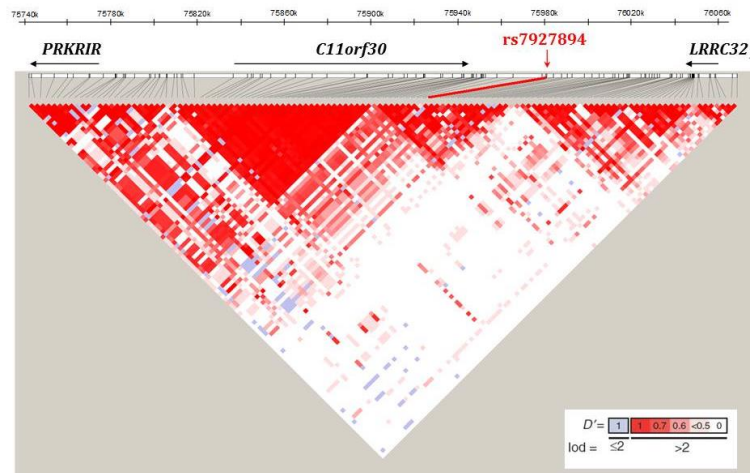
Figure 37: Linkage disequilibrium (LD) structure and genes in the AD-associated region on chromosome 11q in the CEU HapMap population. The AD-associated SNP rs7927894 is correlated with many variants on both sides of the SNP (D'>0.8). Disequilibrium coefficient values for HapMap data were generated with Haploview. Figure modified from (Esparza-Gordillo et al. 2009).

Therefore, comprehensive computational analysis and literature research was focused on highly correlated proxy SNPs, and rs2155219 was selected as potential candidate SNP based on the analyses. Evidence from several studies supported that rs2155219 is an interesting proxy SNP for further investigation. This variant initially yielded genome-wide significant evidence of association with atopic dermatitis (OR= 1.36, P= 8.17 x 10^{-09}) in a large panel of Northern European AD cases (Weidinger et al. 2013). Further studies showed association of rs2155219 with various phenotypes such as grass sensitization (OR= 1.22, P= 9.4 × 10^{-09}), allergic rhinitis (OR= 1.17, P= 3.8 × 10^{-08}) (Ramasamy et al. 2011) and recently also with poly-sensitization of 4 allergens (OR= 2.27, P= 0.003) (Amaral et al. 2015). Bonnelykke and colleagues demonstrated association of rs2155219 T allele with allergic sensitization (OR= 1.13, P= 1.4 x 10^{-18}) and showed significant reduced expression levels for the two neighboring genes *C11orf30* (P= 4.2 x 10^{-26}) and *LRRC32* (P= 7.1 x 10^{-06}) in white blood cells (Bonnelykke et al. 2013).

These results are consistent with the performed eQTL analysis on *LRRC32* expression in skin within this project where lower expression levels were observed in homozygous rs2155219 T allele carriers compared to G allele carriers in lesional skin. Due to the small power of the study (low sample size) the effect was not significant, however, the direction of effect was similar as reported previously by Bonnelykke *et al.*, illustrating that this SNP has allele-specific regulatory impact on *LRRC32* gene regulation. Unfortunately, no analysis could be performed dependent on *C11orf30* transcript levels due to quality criteria, and no RNA was left for supplementary single gene measurements. Thus no prediction can be made on regulation of this gene. In regard to *LRRC32*, considerable higher baseline *LRRC32* expression levels were

observed in cases compared to controls, which underline that *LRCC32* expression is regulated by rs2155219 during AD but also indicate that other regulatory factors might have additional impact on *LRRC32* expression.

In order to understand gene regulation and to characterize non-coding regions that are likely to harbor regulatory features, extensive knowledge of transcriptional regulatory elements is essential. This can be investigated by interrogation of data from the ENCODE (Encyclopedia of DNA Elements) project, a huge research collaboration project that aims to set up a comprehensive summary of functional and regulatory elements to understand and interpret regulation in the human genome (Consortium 2004; Consortium 2011; Consortium 2012). The potential regulatory impact of rs2155219 in the 11q region was verified by the location within ENCODE-predicted regulatory regions such as DNase1 hypersensitive sites and promoter-and enhancer-associated histone marks (H3K27Ac, H3K4Me1). DNase1 hypersensitive sites represent chromatin structures that are more susceptible to endonuclease digestion (e.g. by DNAse1) than surrounding chromatin. The altered chromatin structure at hypersensitive sites allows access to DNA sequences and therefore these sites represent important regions for regulation of gene expression or chromosome function (Sabo et al. 2004; Sabo et al. 2006; Thurman et al. 2012). A histone mark characterizes a chemical modification (e.g. methylation or acylation) of a specific histone protein present in chromatin. Additionally, this modification has impact on gene expression by changing how accessible the chromatin is to transcription (Heintzman et al. 2007).

Compared to the GWA lead SNP rs7927894 the proxy SNP rs2155219 is directly located in such predicted regulatory regions and therefore represented a promising candidate for functional investigation. Furthermore, the *in silico* analysis of putative transcription factor binding sites (TFBS) showed that rs2155219 is predicted to alter the binding of the several transcription factors in an allele-dependent manner and might thereby directly interfere with transcriptional processes. Interestingly, some of these transcription factors have already been related to skin-mediated processes. For instance, a member of the GLI transcription factors – GLI2 - has shown to be a potent oncogene in epidermal cells (Sheng et al. 2002) and is known to be expressed in human keratinocytes where on the one hand it executes repressing activity on epidermal differentiation genes and on the other hand activates keratinocytes proliferation in normal skin (Regl et al. 2004).

The most promising candidate is transcription factor SP1 as its gene expression has been shown to be reduced in skin of AD patients. Moreover, SP1 silencing in cells results in keratinocyte expression profile changes (Bin et al. 2011a; Bin et al. 2011b). In contrast, INSM1 has not yet been associated with atopic dermatitis or skin-related issues. This transcription factor is known to be involved in the control of gene expression in various endocrine cell types as well as in

regulating the development of cells in the central and peripheral nervous systems (Gierl et al. 2006; Osipovich et al. 2014).

Indeed, the bioinformatic analyses revealed evidence that rs2155219 plays an important role in the regulation of gene expression; however, bioinformatics analyses can only infer binding potential of transcription factors, but not the functionality of the investigated sequence. Therefore, a predicted TFBS is not necessarily a functional site. Furthermore, most of the data were generated from large-scale genomic methods (e.g. CHIP-seq) and have to be cautiously interpreted due to the production of unwanted artifacts or false-positives because of the large amount of experiments. Although, bioinformatics strategies are a helpful tool to identify transcriptional regulatory elements and TFBS, nevertheless, these methods will not replace the need for experimental verification, and functionality can ultimately be proven only by laboratory experiments with defined settings. Therefore, the following focus was set on functional investigation of the selected proxy SNP rs2155219 to determine its regulatory impact at the *C11orf30/LRRC32* gene locus.

3.2.1 Rs2155219 alters the DNA binding ability to SP1 transcription factor in Jurkat cells

To verify bioinformatics predictions, electromobility shift assays (EMSAs) were performed. Results of EMSA experiments clearly demonstrated allele-specific protein-DNA interactions of rs2155219 and nuclear proteins from Jurkat cells with less binding capacity of the rs2155219 minor effect allele. Competition experiments with high excess of unlabeled major allele oligonucleotides and when using the common transcription factor OCT1 underlined binding specificity. Furthermore, SP1 supershift and competition experiments revealed SP1 binding to the polymorphic site of rs2155219. This is consistent with previously performed bioinformatic analysis predicting the loss of the SP1 transcription factor binding site if the rs2155219 minor T allele is present. This might be due to the fact that the SP1 matrix core sequence (gtctGG**G**tgt → gtctGG**T**Gtgt) is directly disrupted by rs2155219 (G>T) and thereby explains the lower binding capacity to the minor allele which is in agreement with the EMSA results supporting the specificity of SP1 binding. Interestingly, supershift experiments using an SP1 antibody revealed new protein complexes consisting of two additional upper bands that is consistent with earlier studies showing the same effect (Xu and Rogers 2007; Kretschmer et al. 2014). Using an isotype control (same antibody class as SP1 antibody) emphasized SP1 binding specificity and excluded that the binding effect is caused only by the isotype of the antibody. On the basis of the results, it

can be proposed that SP1 is part of the shown protein-DNA complex with lower binding affinity to the rs2155219 minor effect allele.

SP1 is a well-described cellular transcription factor belonging to the SP/XKLF (Specificity protein/kruppel-like factor) family and it is known to be involved in regulation of various cellular functions including immunological processes (Kadonaga et al. 1987; Li et al. 2004). As previously mentioned decreased SP1 gene expression levels have been demonstrated in skin biopsies of AD patients by Bin and colleagues (Bin et al. 2011a). Furthermore, they showed that SP1 deficiency results in increased levels of specific proteases (belonging to the KLK family) of the stratum corneum followed by higher TSLP levels representing a typical pathogenic state in atopic dermatitis (Bin et al. 2011b). Therefore, SP1 deficiency is directly linked to atopic dermatitis and may play a pivotal role in its pathogenesis.

Furthermore, SP1 appears as an established binding partner for many other transcription factors. Co-operation of SP1 with SMAD proteins at promoter sequences, for instance, has been reported to increase expression of TGFβ signaling genes (Poncelet and Schnaper 2001). Therefore, it is not unlikely that further protein complex partners might exist which could be identified through further EMSA and supershift experiments. Computational analyses provide predicted transcription factors, differentially regulated by rs2155219, on which should be focused in further studies. However, supershift experiments are reliant on the availability of the protein epitope to the antibody after DNA-protein complex formation and not every protein domain is accessible for antibody binding. Thus, selection and concentration of the antibody make up a critical point. Verification of established proteins such as SP1 as well as identification of new binding partners using mass spectrometry is therefore mandatory and should be the focus of further investigation.

3.2.2 The rs2155219 risk allele shows regulatory activity at the *C11orf30/LRRC32* gene locus

The functional relevance of rs2155219 on transcriptional regulation was analyzed in four different cell lines (Jurkat, HaCaT, A549, and HeLa cells) using luciferase reporter gene assays with two different insert lengths (459 bp and 1142 bp). The 459 bp insert reporter vectors demonstrated that the rs2155219 minor T allele acted as weak enhancer in HaCaT keratinocytes, whereas the same allele shows weak repressing of minimal promoter activity in Jurkat cells. In contrast, the 1142 bp sequence acted as a strong enhancer in all four cell lines. This difference might be explained by additional regulatory elements (TFBS and DNase1

hypersensitivity clusters) that are included in the 1142 bp sequence, which might favor the stronger regulatory impact on promoter activity.

The strongest effect (280 % increase in luciferase activity compared to empty vector) with the 1142 bp insert sequence was detected in A549 cells. This human lung adenocarcinoma epithelial cell line is widely used as a model to study asthma-related mechanisms in transfection assays (Liu et al. 2009; Birben et al. 2012; Marcos-Vadillo and Garcia-Sanchez 2016) and was selected due to the known association of the 11q13.5 locus with asthma (Ferreira et al. 2011; Marenholz et al. 2011). Despite the fact that the 1142 bp sequence acted as enhancer in all cell lines, the effect sizes were different indicating tissue-specific transcriptional regulation of the reporter gene. Tissue specificity of transcriptional regulation is not uncommon, and various studies have demonstrated cell-type or tissue-specific regulatory effects on gene expression (Dimas et al. 2009; Powell et al. 2012). Especially in complex diseases, SNPs are more likely to be associated in a tissue-dependent manner, probably due to tissue-specific expression patterns of involved transcription factors (Fu et al. 2012).

Since luciferase assays are artificial *in vitro* procedures to study promoter activity, it was of interest whether the insert orientation had influenced the minimal promoter activity. Reporter constructs containing the 1142 bp enhancer sequence in reverse complementary orientation showed completely abolished previous shown enhancing effects on promoter activity in all cell lines and thereby demonstrated the orientation-specific impact of the 1142 bp enhancer sequence. Nevertheless, it cannot be fully excluded that the enhancing effect might have been caused by the insertion itself. For this, the investigation of an additional negative control such as a reporter gene vector containing a "desert site" – a sequence without any specific predicted regulatory potential - would help to underline the concluded orientation and sequence specificity in further experiments.

When comparing the effect of both rs2155219 alleles to activate the minimal promoter, the stronger effect was observed for the minor T allele demonstrating an allele-specific regulatory impact of rs2155219. However, it has to be taken into account that two additional variants are located in the 1142 bp sequence (rs11236797 C>A and rs34455012indel). Therefore, the effect is not exclusively limited to rs2155219 and the additional variants might also contribute to the enhancing activity of the sequence. Investigation of different SNP allele combinations, to elucidate the involved variant responsible for the effect, did not point out one single variant but rather indicate that the combination of all genetic variants determines the observed regulatory activity (results are summarized in Figure 38). The variant rs11236797 is in high linkage disequilibrium with rs2155219 ($r^2 = 0.9$; based on 1000genomes release March 2012) representing rather a highly correlated proxy SNP tagging the association signal than a causal functional variant itself. It is apparent that the rs34455012 7 bp deletion favors higher activity

in all cell lines and demonstrates significant allele-specificity in HaCaT, A549 and HeLa cells (Figure 38). Insertions/deletions (indels) are the second most frequent variation in the human genome after SNPs (Weber et al. 2002; Mills et al. 2006; Genomes Project et al. 2015) and indels in functionally important regions may affect gene regulation and function. Several coding indel polymorphisms, for instance, have been associated with human diseases such as the Fragile X syndrome (Warren et al. 1987) or cystic fibrosis (Collins et al. 1987), as well as the 2282del4 of the filaggrin gene which is associated with AD (Weidinger et al. 2006). According to the 1000 genomes database the genotype frequency of rs34455012 is 53.6 % for the deletion and 46.4 % for the CCAGTAT insertion, however, in spite of the possible regulatory effect that was shown in luciferase experiments within this study, association testing in about 2000 AD cases versus 2000 controls did not reveal any association with atopic dermatitis (personal communication S. Weidinger, Christian-Albrechts-Universität zu Kiel). LD calculation retrieved from this data showed that rs34455012 and rs2155219 are in high LD (D'= 1) indicating location in the same haplotype block, however, their r^2-value of 0.16 implied that these variants are not good predictors of each other.
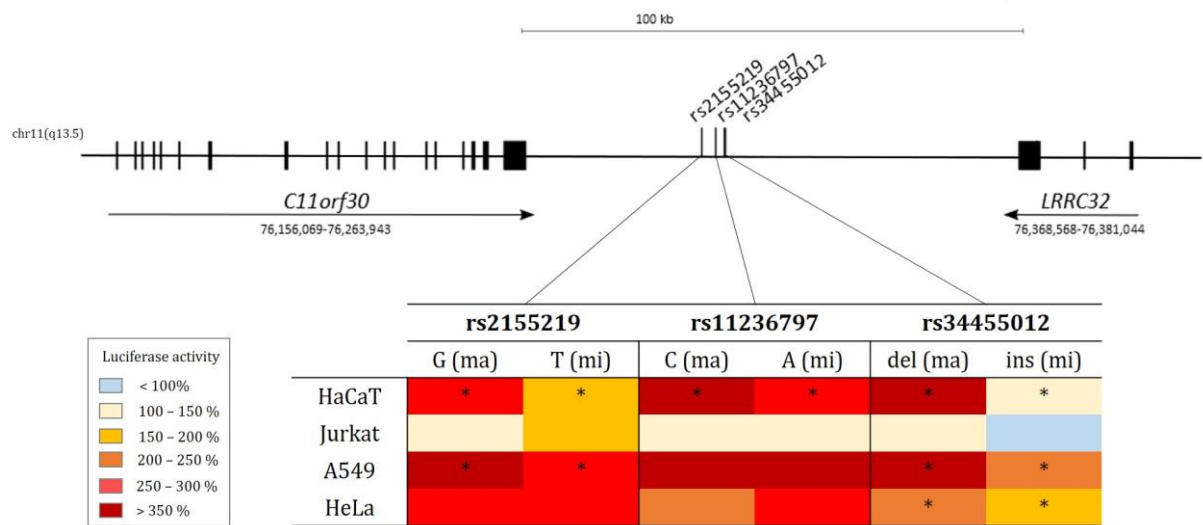
Figure 38: Schematic structure of the human *C11orf30/LRRC32* locus including the genomic location of rs2155219, rs11236797, and rs34455012 and their luciferase activity in HaCaT, Jurkat, A549, and HeLa cells. The genomic position of each gene is given below the arrows (NCBI database build GRCh37.5). * significant allele-specific difference in luciferase activity (P<0.05). Luciferase activity was normalized to empty vector (without insert) which was set 100 %.

With regard to rs2155219, an allele-specific effect was observed in HaCaT, Jurkat, and A549 cells, however, only in Jurkat cells the minor T allele provoked higher luciferase activity compared to the major G allele (Figure 38). Jurkat cells are immortalized T lymphocytes and represent a commonly used cell system to study immunological mechanisms. On the basis of the

results, it seems that the rs2155219 T allele might be involved in *cis*-regulation of T cell specific mechanisms. As mentioned above it is already known that along with atopic dermatitis rs2155219T is associated with other immunological phenotypes such as grass sensitization and allergic rhinitis, however, the underlying molecular mechanisms have not been identified yet. Interestingly, the 11q13.5 located gene *LRRC32* encodes a surface receptor on regulatory T cells and plays a key role in modulation of immune-regulatory responses (Wang et al. 2008; Probst-Kepper et al. 2009). Furthermore, rs2155219-dependent regulation of *LRRC32* transcript levels has already been demonstrated in white blood cells (Bonnelykke et al. 2013) and was confirmed with own data in skin tissue. In this context, it might be possible that rs2155219 might also be involved in T cell specific gene regulation of *LRRC32* or other relevant immunological genes.

To analyze the rs2155219-dependent transcriptional regulation of *LRRC32* and *C11orf30*, reporter assays with the native gene promoter sequences were performed. Interestingly, analysis of the native *LRRC32* promoter activity dependent on rs2155219T (in combination with rs11236797A and rs34455012del) confirmed expected regulatory impact. The *LRRC32* promoter was significantly activated in all cell lines resulting in elevated luciferase activity compared to the native promoter without enhancer, whereas no effect on *C11orf30* promoter activity was seen. However, an allele-specific activity compared to the rs2155219 G allele (in combination with rs11236797C and rs34455012ins) was only observed in HaCaT keratinocytes and not in Jurkat cells as expected.

In general, it has to be mentioned that the enhancement in reporter gene expression was quite low in these experiments. Precursor experiments showed that the selected promoter sequences were strongly active in Jurkat, HaCaT, A549 and HeLa cells. Especially the *C11orf30* promoter sequence revealed up to 100-fold higher activity in comparison to the activity of the promoter-free vector. Therefore, it is possible that the high activity might capture the enhancing effect, which shows comparatively lower activity.

Taken together, on the basis of the results it can be proposed that all investigated variants together contribute to the identified regulatory activity, however, rs2155219 represents the "lead variant" showing the highest regulatory impact and might therefore possibly be a functional variant underlying the observed GWA signal. Native promoter studies identified *LRRC32* as a potential causative gene involved.

3.2.3   Limitations of reporter gene assays

Luciferase based promoter assays represent an easy and fast way to study promoter regulation and genetic variation in living cells, however, there are also several challenges in using these

functional assays. The fragment sizes used in reporter gene assays are typically small in order to analyze single variant specific effects and to avoid masking of allelic effects in a longer fragment (Tokuhiro et al. 2003). However, essential regulatory elements can be widely dispersed but need to interact with each other, thus, reporter assay inserts do not necessarily represent the genomic context *in vivo* (Maston et al. 2006). Furthermore, it is always possible that the used cell culture system does not match the physiological conditions (e.g. presence of transcription factors and co-factors) needed to activate the regulatory element or that the activation might be induced by additional stimulating factors. Moreover, it is not guaranteed that the *in vivo* activity of the endogenous counterpart to the reporter gene might be the same due to differences in chromatin structures and methylation status that might influence binding of transcription factors and thus level of expression (Knight 2003). Epigenetic variations (specifically DNA methylation) are known to have an essential impact on transcriptional regulation and evidence from epigenetic studies in AD skin lesions (Rodriguez et al. 2014) highlights the importance of epigenetic modulation and its contribution to the pathogenesis of AD. In addition, it should be considered that also other regulatory mechanisms such as small regulatory RNAs (e.g. microRNAs) or long noncoding RNAs (lncRNAs) exist, which might have an additional influence on gene regulation.

Furthermore, the transient transfection might be another limitation of reporter assays as within a transfected cell, the plasmid DNA exists in a highly artificial amount that might influence the natural activity of regulatory elements (Knight 2003). Within this study, a lipid-based transfection method was applied and lipid-DNA complexes often accumulate resulting in low transfection efficiency (Liu et al. 1997). However, for normalization a dual luciferase reporter assay was used and luciferase activity of the test plasmid was normalized against the luciferase activity of a control vector. Advanced methods such as the nucleofectin technique where the test plasmid is transported directly into the cell nucleus (Gresch et al. 2004) or gene editing methods like CRISPR/Cas9 (Clustered Regularly Interspaced Short Plaindromic Repeats/Associated Protein 9) where a RNA-guided endonuclease protein is used for sequence-specific DNA cleavage (Mali et al. 2013), are useful alternative approaches to enable high transfection efficiency.

3.3 Do low frequency functional variants underlie the 11q association signal?

Genome-wide association studies provide an efficient strategy to assess common variants in large population studies and to identify trait-associated variants. For atopic dermatitis 34 AD susceptibility loci, tagged by associated common SNPs have been identified until now.

However, despite the promising results in identifying potential functional variants, they explain only less than 20 % of the estimated heritability of atopic dermatitis (Esparza-Gordillo et al. 2009; Sun et al. 2011; Hirota et al. 2012; Ellinghaus et al. 2013; Weidinger et al. 2013; Baurecht et al. 2015; Paternoster et al. 2015; Schaarschmidt et al. 2015). One possible reason for the missing heritability might be explained by rare variants (usually defined with a minor allele frequency of less than 5 %) which often show valuable allelic heterogeneity at causal loci (Kryukov et al. 2007; McClellan et al. 2007). However, one limitation of GWAs is that these studies are under powered to detect such rare alleles or lack appropriate proxies in genotyping arrays. Thus, a resequencing approach is needed for fine-mapping of associated loci and to identify potential functional rare variants.

The targeted resequencing approach on the AD-associated 11q13.5 locus revealed significant excess of *LRRC32* missense variants in individuals with AD and identified the variant rs79525962 (A407T), located in the coding sequence of *LRRC32*, as the most frequent associated variant (MAF< 0.01). Little is known about this polymorphism - especially the functional properties have not been investigated yet. When having a look at previously reported GWA risk variants for inflammatory and atopic traits it shows that the rare variant rs79525962 is in high LD (D'= 1) (Manz et al. 2016) underlining the location in the same haplotype block of the association and thereby demonstrating a candidate of potential high functionality.

3.3.1   rs79525962 does not influence *LRRC32* mRNA expression but alters GARP protein levels

The investigated missense variant rs79525962 causes an amino acid change from alanine to threonine (Ala (GCC) → Thr (ACC)) and might have direct impact on *LRRC32* mRNA expression levels and/or GARP protein expression. Using semi-quantitative RT-PCR, equal levels of *LRRC32* mRNA were shown for WT LRRC32 (rs79525962**G**) and A407T LRRC32 (rs79525962**T**) transfected HeLa, Cos-7, and CD4+CD25- T cells. Appropriate controls (negative control and amplification of β-actin) assure reliability of the results and validate high cDNA quality. On the one hand, the results confirm known ubiquitous *LRRC32* mRNA expression levels of different tissues and cell types (Esparza-Gordillo et al. 2009; Manz et al. 2016); on the other hand, rs79525962 does not cause *LRRC32* mRNA expression changes and, thus, might not interfere with *LRRC32* mRNA synthesis, maturation or degradation.

Flow cytometric analyses (FACS) in Cos-7 cells raised evidence that the variant has impact on the protein level by showing slightly lower expression of GARP protein on the cell surface of A407T LRRC32 transfected cells in comparison to WT LRRC32 transfected Cos-7 cells. Likewise,

subcellular localization of GARP protein confirmed lower surface expression in A407T LRRC32 transfected Cos-7 cells by using immunohistochemistry. In addition, a significantly higher amount of mutated protein was observed within the cells indicating that rs79525962 might influence protein transport upon the cell surface. Interestingly, the protein seems to be accumulated in the endoplasmatic reticulum (ER), where protein translation, folding, post-translational modification, and preparation for protein transport take place, since strong staining was observed in close proximity to the cell nucleus. Based on the results, it might be possible that rs79525962 is directly involved in changes of ER-mediated protein processes which finally result in lower GARP expression on the cell surface where it acts as latent TGFβ binding receptor. For preliminary experiments, Cos-7 cells were used because of high transfection efficiency and easy handling; however, they do not represent the cell type of target where the protein GARP is known to be active. GARP exerts its function on regulatory T cells (CD4+CD25+ T cells) (Stockis et al. 2009; Tran et al. 2009), however, the non-regulatory fraction was chosen for further transfection experiments due to their very low endogenous GARP levels (Tran et al. 2009; Wang et al. 2009) and because these cells could be isolated in a sufficient number which was necessary for functional FACS analysis. FACS analysis in CD4+CD25- T cells validated previous shown results and highlighted a significant regulatory impact of rs79525962 on GARP expression levels in the target cell system.

On the other hand, Western Blot analysis verified the presence of GARP after transient transfection but showed nearly similar expression levels of mutated and wildtype protein in the surface protein fractions. Besides lower sensitivity compared to FACS analysis, quantification of protein levels determined by Western Blot analysis is a huge problem and disadvantage of the method. Although, sophisticated software analysis tools allow to semi-quantify Western Blot protein expression (Taylor et al. 2013), the method has still a high demand in terms of experimental setup and optimization of the experimental conditions (e.g. protein isolation, sample loading, buffer consumption, blotting procedure, antibody concentration, etc.). Furthermore, the results showed that GARP expression in the outer membrane fractions was quite low and interestingly, the highest GARP expression was observed in the cytosolic fraction. This might indicate that most of the protein had not yet been transported to the outer membrane and probably an extended transfection period (e.g. 72 hours) would have been an appropriate addition. Even though no significant changes in expression levels were detectable, Western Blot results demonstrated that the protein quality was sufficient (i.e. no degradation, digestion or multimerisation of protein was visible) and might not be affected by the mutation as both proteins (mutated and WT GARP) appeared as clear bands with the expected molecular masses of 70-80 kDa, which was in agreement with recombinant human GARP used as positive control. For quantification and additional identification of proteins present in the sample, high-

resolution mass spectrometry would be the method of choice. However, given the fact that the FACS analysis showed significant and robust results in target cells, which could be verified by localization studies, and that mass spectrometry is much more expensive and also more technically challenging, mass spectrometry analysis was not taken into further consideration within the scope of the project.

3.3.2 rs79525962 might impair immune mechanisms by regulating GARP protein expression

GARP is a membrane protein first identified and highly expressed on the surface of activated regulatory T cells (Wang *et al.* 2008; Tran *et al.* 2009), but recently also other cell types such as platelets, melanoma cells and mesenchymal stromal cells with GARP surface expression have been identified (Wang et al. 2008; Tran et al. 2009; Carrillo-Galvez et al. 2015; Hahn et al. 2016). GARP functions as a receptor of TGFβ by binding its inactive latent form and thereby regulating its activation and availability. TGFβ is known as a pleiotropic cytokine, playing a key role in immune regulation through activation of Treg differentiation and suppression of T effector cells (Banchereau et al. 2012a). Notably, dysregulated TGFβ signaling has been related to the pathology of several allergic phenotypes in humans, including atopic dermatitis (Frischmeyer-Guerrerio et al. 2013).

However, knowledge about the functional contribution of GARP to the suppressor function of Tregs via TGFβ is still limited and it seems that both proteins interact in a complex manner to promote their anti-inflammatory effects. It is known that GARP directly anchors the secreted biologically latent form of TGFβ (homodimer consisting of mature TGFβ noncovalently bound to the latency-associated protein (LAP)) to the surface of regulatory T cells. The release of mature TGFβ from the surface GARP/latent TGFβ complex is mediated through various signals including proteolysis and contact to integrin αvβ6 or αvβ8 expressing cells (Wang et al. 2012; Robertson and Rifkin 2013). Biologically active TGFβ is then able to act in an autocrine or paracrine manner on Tregs themselves or other target immune cells, respectively, by binding to the TGFβ1 receptor and thereby execute its immune-modulatory function (Tran et al. 2009; Banchereau et al. 2012a; Wang et al. 2012). Several lines of evidence point out that GARP plays a fundamental role in the immunosuppressive function of regulatory T cells. It has been shown that siRNA induced depletion of GARP leads to reduced suppressive activity of Tregs and lower Foxp3 expression, the major transcription factor in Tregs, whose dysfunction is associated with systemic autoimmune disease in humans (Wildin et al. 2001; Probst-Kepper et al. 2009).

Likewise, anti-GARP antibodies against a specific epitope within GARP/TGFβ1 complexes were able to block active TGFβ1 production by human Tregs (Cuende et al. 2015).

Apart from surface anchoring, a study by Gauthy and colleagues (Gauthy et al. 2013) identified soluble GARP/latent TGFβ complexes *in vitro*, possibly due to proteolytic shedding from the cell surface. Although the mechanism of this shedding process is not yet known, further studies recently showed that a recombinant produced soluble form of GARP (sGARP) is able to bind free latent TGFβ and enhance its activation. Furthermore, application of sGARP to naïve CD4+ cells represses their proliferation and effector cytokine production, which could in turn be suppressed by an antibody-mediated blockade of the TGFβ receptor (Hahn et al. 2013; Fridrich et al. 2016). In line with these observations, ELISA experiments within this study using supernatants of wildtype and mutant *LRRC32*/GARP transfected T cells revealed low levels of soluble GARP in cell supernatants, however, no concentration differences between the groups were observed. Therefore, it can be proposed that lower GARP surface expression in A407T LRRC32 transfected T cells is not due to increased shedding of GARP from the surface.

Besides GARP, various surface markers are known to be upregulated on activated Tregs, contributing to T cell suppression by cell contact-dependent mechanisms. For instance, natural Tregs constitutively express high cytotoxic T-lymphocyte antigen-4 (CTLA-4), a surface molecule that binds to surface markers (CD80/CD86) on antigen-presenting cells by which T cell activation is inhibited (Wing et al. 2008; Shevach 2009). Furthermore, Neuropillin (CD304) another surface marker on Tregs (Bruder et al. 2004; Corbel et al. 2007) is able to support the interaction between regulatory T cells and antigen-presenting cells during antigen recognition (Sarris et al. 2008). Results presented here revealed that in A407T LRRC32 transfected CD4+CD25- T cells significant lower expression of CTLA-4 and a tendency towards a reduced Neuropillin expression was shown compared to T cells expressing intact GARP protein. In addition, Foxp3 expression was decreased, indicating an overall dampening of the Treg gene signature in A407T LRRC32 transfected CD4+CD25- T cells.

On the basis of the results, it can be proposed that the investigated variant rs79525962 (A407T) has a significant impact on GARP protein levels probably by impeding correct protein folding, post-translational modification and/or membrane transportation inside the cell, leading to a significant extracellular reduction of GARP protein on CD4+CD25- T cells and a simultaneously intracellular protein accumulation. This assumption is strongly supported by further experiments in AD patients carrying the A407T mutation, which were conducted by a cooperation partner (Prof. Dr. Natalija Novak, Universitätsklinikum Bonn) and combined in the recently published paper included in this thesis (Manz et al. 2016). Experiments in AD patients carrying the A407T variant showed that GARP surface expression levels were significantly reduced in unstimulated CD4+CD25- and CD4+CD25+ T cells as well as after activation with

TGFβ into GARP+FOXP3+ regulatory T cells as compared to cells from wildtype carriers. Furthermore, CD4+CD25- T cells obtained from mutation carriers showed a lower conversion rate into GARP+FOXP3+ regulatory T cells. Together, these data obtained from AD patients carrying the A407T variant strongly support the functional *in vitro* results presented in the thesis, with less GARP surface expression caused by the missense variant A407T of *LRRC32*. Thus, results of the functional assays were directly placed into the disease context of atopic dermatitis involving the variant A407T as a new GARP regulating factor. In future studies site-specific genome-editing techniques such as CRISPR/Cas9 can be a useful tool to analyze if this effect is caused exclusively by the mutation itself. Such further studies then have to determine the effects of the *LRRC32* missense variant on GARP function and the suppressive capability of Treg cells in the context of cutaneous inflammation.

Taken together, the results of this study underline the immunological type of AD pathophysiology by identifying LRRC32/GARP as involved causal gene, which is regulated by common and rare AD-risk variants. Furthermore, the transcription factor SP1, which was found to be involved in rs2155219 allele-dependent differential binding, represents a well-known key regulator of immunological processes and its deficiency is directly linked to atopic dermatitis (Li et al. 2004; Bin et al. 2011b). In addition, the 11q13.5 locus has already been associated with related immunological diseases like asthma (Marenholz et al. 2011), and Crohn's disease (Barrett et al. 2008) supporting the fact that this locus contributes to a common inflammatory pathway involved in the development of several immunological diseases.

3.4   Genome-wide cutaneous mRNA expression analysis in atopic dermatitis

Since the main part of this thesis was focused on the functional characterization of AD-associated variants and the identification of target genes based on genetic data, the last part of the study included a genome-wide expression analysis in skin of AD patients (either non-lesional (AN) and/or lesional (AL)) compared to the skin of healthy controls (NN). The main aim of this part was to identify further target genes based on skin-specific expression data that are involved in the pathophysiology of atopic dermatitis and might function as selective biomarkers for the early and progressed stage of the disease.

3.4.1 Signature genes of the AD phenotype are involved in keratinization and skin inflammation

The pathophysiology of atopic dermatitis is complex and characterized by epidermal barrier dysfunction and excessive immunological alterations resulting in a heterogeneous clinical phenotype. The encoded proteins of the three consistently upregulated genes in all three comparisons (AN/NN, AL/NN, AL/AN), namely *S100A9* (S100 calcium binding protein A9)*, SPRR2F* (Small Proline-Rich Protein 2F)*, and PI3* (Peptidase inhibitor 3, skin-derived/elafin), are known biomarkers of the keratinocyte structure (S100A9 and SPRR2F) and the inflammatory skin phenotype (PI3/elafin) in AD (Thijs et al. 2015).

S100A9 is a member of the epidermal differentiation complex (EDC) where it exhibits protective function of the skin via antimicrobial activities and modulation of immune response. Furthermore, S100A9 plays a role in regulating and promoting the epidermal response to epidermal injury, since S100A9 levels strongly increase after epidermal injury (Thorey et al. 2001; Eckert et al. 2004). The results of the present study confirm the known overexpression of *S100A9* in lesional skin shown in various studies (Suarez-Farinas et al. 2011; Gittler et al. 2012; Rodriguez et al. 2014; Correa da Rosa et al. 2015) and suggest also overexpression in non-lesional skin of AD patients. Similar findings were observed in a German acne cohort comparing expression levels by RT-PCR of involved skin to non-involved skin of acne patients (Kelhala et al. 2014). The same differential expression was shown for *S100A7* belonging to the same gene family as *S100A9*. Results of this study are in concordance with other studies showing an upregulation of *S100A7* expression levels both in non-lesional and lesional AD skin (Suarez-Farinas et al. 2011; Gittler et al. 2012).

Similarly, the present analysis revealed consistent upregulation of a further structural protein, namely SPRR2F (small-proline rich protein 2F) in all three comparisons. SPRR2F belongs to a group of 11 specific cornified envelope precursor proteins (two *SPRR1*, seven *SPRR2*, one *SPRR3*, and one *SPRR4* genes), encoded by a multigene family and clustered within the epidermal differentiation complex (Gibbs et al. 1993; Marenholz et al. 1996). The SPRR proteins are known to be expressed in skin and oral mucosa (De Heller-Milev et al. 2000; Lee et al. 2000a) and evidence from immunohistochemistry experiments early revealed that expression changes are common under pathophysiological conditions of keratinization and skin inflammatory disorders (Koizumi et al. 1996). However, upregulation of SPRR2F was only shown in mucosa lesions of patients with severe trachoma, an infectious disease of the conjunctiva, but have not been identified in skin lesions of AD so far (Burton et al. 2011). Indeed, two other SPRR genes - *SPRR1A* and *SPRR2C* - are known to be highly expressed in skin lesions of chronic AD patients (Jarzab et al. 2009). Interestingly, phylogenetic relationships between human SPRR genes

inferred a homogeneous clade of all seven SPRR2 genes with a closer link between the known AD-associated *SPRR2C* and *SPRR2F* (Carregaro et al. 2013), which was shown to be highly upregulated for the first time in this study. *SPRR2G*, another SPRR gene that was found to be upregulated in non-lesional and lesional AD skin, seems to be an ancestral member of this phylogenetic clade and is known to be expressed in unaffected skin (Kypriotou et al. 2012) but, so far as this is known, have not been described related to skin pathologies like AD before.

The third consistently upregulated gene *PI3* (Peptidase inhibitor 3, skin-derived/elafin) encodes a known serine protease inhibitor mainly produced by keratinocytes (Pfundt et al. 1996). PI3, that is highly upregulated by inflammatory stimuli, shows antimicrobial activity and contributes to the immune homeostasis of the skin by inhibiting polymorphonuclear leucocyte-derived proteinases (Alkemade et al. 1994; Nakane et al. 2002). PI3 is absent in normal human skin, but it is highly upregulated upon barrier disruption or inflammation in inflammatory disorders such as psoriasis (Schalkwijk et al. 1993; Nonomura et al. 1994). However, PI3 expression is also present in AD lesions, even though compared to psoriasis the expression is much lower (Nomura et al. 2003; de Jongh et al. 2005). The present analysis identified PI3 as differentially expressed gene in lesional AD skin, that was in agreement with findings by Suárez-Fariñas (Suarez-Farinas et al. 2011; Suarez-Farinas et al. 2013), but also suggest overexpression in non-lesional skin which was not shown by others before.

3.4.2 Dysregulation of potential precursor genes in non lesional AD skin

Although, clinically unaffected (non-lesional) skin of AD patients looks normal at first sight, it has been shown that non-lesional skin demonstrates an intermediate phenotype between normal and lesional skin with distinct differences (Suarez-Farinas et al. 2011). Signs of low-level inflammation supported by infiltration of inflammatory T cells, and decreased hydration and impaired lipid synthesis leading to epidermal barrier dysfunction are known processes of the early disease stage and have been identified in non-lesional in comparison to healthy skin (Werner and Lindberg 1985; Hamid et al. 1994; Jensen et al. 2004). Expression profiling of non-lesional and lesional AD skin in comparison to healthy skin will help to identify further biomarkers of disease activity that can be reversed by successful disease treatment. Apart from treating the active disease state, biomarkers of the early stage may help to stop disease progression or even prevent the disease initiation. Differentially expressed genes in non-lesional skin might therefore be an interesting target in biomarker research.

The present analysis identified 14 significantly differentially expressed genes in non-lesional skin compared to skin of healthy controls, whereof 13 genes were also included in the AL/NN

analysis indicating potential precursor genes which already show expression changes in the early stage of the disease. Functional enrichment analysis and subsequent clustering of enriched functional annotations to groups assigned the genes to functional classes of "Epidermis development" (SPRR2F, SPRR2G, CA2, S100A7), "Defense response" (S100A7, S100A9, CCL8, CCL23, C1QB, PTGDS) and "Immune response" (S100A7, S100A9, CCL8, CCL23, C1QB, PTGDS, PI3, CA2), which are all well-known involved processes of AD development.

Among the above discussed structural proteins SPRR2F and SPRR2G, which show upregulation in non-lesional skin for the first time, another potential precursor gene, encoding the enzyme carbonic anhydrase 2 (CA2), was identified and assigned to the "epidermis development" cluster. CA2 is a metalloenzyme that catalyzes the reversible hydration of carbon dioxide and is thereby involved in the maintenance of water transport and the cellular pH in various tissues including skin (Geers and Gros 2000; Mastrolorenzo et al. 2003; Boron 2004). Several microarray analyses showed overexpression of CA2 in lesional AD skin (Nomura et al. 2003; de Jongh et al. 2005), which were confirmed by Kamsteeg and colleagues showing increase in CA2 expression on mRNA level as well as on protein levels using Western Blot and ELISA (Kamsteeg et al. 2007). They further showed that CA2 expression was strongly induced by Th2 cytokines *in vitro*; however, none of these studies investigated the CA2 expression levels in non-lesional skin. This analysis showed a 2.5-fold higher expression of CA2 in non-lesional skin compared to healthy skin and identified CA2 as potential gene of the early AD development.

The skin of AD patients is characterized by elevated pH values and alkalization affects the skin barrier leading to an altered function (Eberlein-Konig et al. 2000; Hachem et al. 2003). The blockage of CA2 causes a reduction of the intracellular pH in different cell types (Kniep et al. 2006); therefore it might be possible that CA2 upregulation in AD skin contribute to abnormalities in pH levels and epidermal barrier function as an early epidermal response to Th2 cytokine environment. However, further studies are needed to clarify the role of CA2 upregulation and its physiological consequences in AD development.

Two other genes assigned to the "Defense response" and the "Immune response" clusters are the chemokines CCL8 and CCL23 that belong to the CC-chemokine family and regulate cell trafficking during homeostasis and inflammation (Hwang et al. 2005). Both are known inflammatory chemokines which have been reported in relation to AD. A study by Bao et al., for instance, demonstrated a higher CCL8 expression in human keratinocytes after IL-4 stimulation *in vitro* (Bao et al. 2013). IL-4 promotes differentiation of Th2 cells, which are predominant in AD, and also mutations in IL-4 and its receptor have been associated with AD (Hershey et al. 1997; He et al. 2003; Hassan et al. 2007). IL-4 transgenic mice can be used as a mouse model for human AD since epidermal overexpression of IL-4 causes inflammatory skin lesions, which meet the human AD diagnostic criteria, in these mice. Expression analysis in pre-lesional skin, as they

defined as "no obvious skin abnormality on clinical observation" revealed increased CCL8 expression compared to controls (Bao et al. 2016), which is consistent with results of the present study, showing the same results in human non-lesional skin. In contrast another study showed upregulation of CCL23 expression directly in the epidermis of AD patients, however, they did not distinguish between lesional and non-affected AD skin (Novak et al. 2007). Surprisingly, they additionally identified CCL23 levels in plasma of atopic individuals, indicating that CCL23 expression might have the potential as novel AD biomarker, which could be emphasized by the present study in which increased CCL23 expression levels were observed in non-lesional skin representing the early AD development.

The only differentially expressed gene which was downregulated in non-lesional skin compared to healthy skin encodes the enzyme prostaglandin D2 synthase (PTGDS) which catalyzes the conversion of prostaglandin H2 (PGH2) to prostaglandin D2 (PGD2) (Urade and Hayaishi 2000). Prostaglandin D2 represents a major prostanoid of activated mast cells that has been implicated in various allergic inflammatory diseases. A study by Fujitani et al. showed that overexpression of PTGDS resulted in a Th2-dominated lung inflammation and eosinophilia in a transgenic mouse model (Fujitani et al. 2002). Furthermore, inflammatory skin responses were shown to be reduced in a mutant mouse model, carrying a targeted disruption of the PGD2 receptor on Th2 cells, as well as in mice administered with an inhibitor of the prostaglandin D2 synthase. Histological screening revealed that both blocking of the PTGDS enzyme and blockage of the PGD2 receptor leads to reduced infiltration of lymphocytes, eosinophils, and mast cells and suggests an important role of PTGDS in cutaneous inflammation. Speculatively, in this regard downregulation of PTGDS, as identified in the present analysis, might contribute to an anti-inflammatory response of the epidermis. Interestingly, this kind of "protective factor" could not resist against the upcoming massive inflammation during AD progression since downregulation of PTGDS in lesional skin became less compared to non-lesional skin. PTGDS may thus have potential as a therapeutic target for AD treatment, which needs to be further investigated in studies with larger sample sizes.

In summary, this study provides new and confirms known potential target genes that are involved in AD pathophysiology, that help to characterize lesional and non-lesional skin of AD patients. One major disadvantage makes up the sample size of the study, and extended randomized clinical trials are strongly needed for further investigation to replicate identified genes. Furthermore, independent replication and validation of the results at mRNA or protein level should be the target of further studies. However, skin biopsies represent a not easy accessible sample type and isolation of RNA from skin biopsies presents a challenge because of the high presence of RNases that quickly degrade RNA in the sample. That is one reason why RNA quality of skin samples in this study was partially lowered. However, self-adapted two step

quality control including RNA integrity and *β-actin* amplification helped to screen and to identify samples useful for downstream analysis. Finally, quality control of expression data confirmed usability.

Taken together, the results point out new AD biomarkers based on expression data in skin, which might be useful a contribution to the diagnosis and treatment strategies of AD. Especially, DETs found to be regulated in non-lesional skin might be beneficial targets for disease-specific therapeutics that can not only help to improve the active disease but also prevent its initiation.

3.5 Conclusion

This thesis establishes a basis for the understanding of the functional properties of the AD-associated *C11orf30/LRRC32* locus through characterization of common and rare risk variants and their regulatory impact on transcript levels of genes in proximity. Analysis of gene expression profiles in AD patients revealed potential biomarkers that provide new insights into disease development and might support development of preventive and therapeutic interventions.

Functional investigation of the GWA lead SNP rs7927894 demonstrated a *cis*-regulatory effect of the rs7927894 risk allele on *LRRC32* RNA expression levels in whole blood cells but not in skin tissue. Further analysis of a selected candidate regulatory SNP tagging the association signal (rs2155219) highlighted that this common variant (in concert with rs11236797C>A and rs34455012indel) has allele- and cell-type specific enhancing activity on minimal promoters as well as on the native *LRRC32* promoter but not on the *C11orf30* promoter in different human cell lines. EMSA experiments identified SP1 as a nuclear transcription factor showing allele-dependent differential binding to the polymorphic site of rs2155219.

Targeted resequencing of the *C11orf30/LRRC32* locus identified an AD-associated rare variant (rs79525962), located in the coding sequence of *LRRC32*. This variant showed strong regulatory influence on protein expression of the *LRRC32* encoding protein GARP on the surface of human T cells. Comparable analysis in mutation carriers strongly support the results of the *in vitro* studies and put the findings into the context of atopic dermatitis. Based on genetic data, this study characterized two new functional variants underlying the association signal and identified *LRRC32* as causal gene involved.

Further target genes were identified through analysis of genome-wide expression profiles in skin of AD patients and controls. Expression data confirmed known biomarkers of the keratinocyte structure (*S100A9* and *SPRR2F*) and the inflammatory skin phenotype (*PI3/elafin*),

and revealed new target genes that are differentially expressed in non-lesional skin (*S100A9, SPRR2F, SPPR2G, PI3, CA2, CCL8, CCl23, PTGDS*) and thereby might contribute to the early stage development of AD.

Taken together, the results of this thesis provide new insights into the complex pathophysiology of AD by identification of new functional variants and involved target genes and thereby contribute functional comprehension useful for future drug development and personalized medicine.

3.6 Outlook

Functional investigation of the common variant rs2155219 underlined its regulatory impact (in concert with rs11236797 and rs34455012) on *LRRC32* native promoter activity in different cell types. Allele-specific *LRRC32* expression studies dependent on the rs2155219 genotype in AD-related tissues should be the subject of further investigation to confirm the results on the expression levels. In addition to SP1, other transcription factors involved in differential binding to the polymorphic site of rs2155219 should be analyzed using electrophoretic mobility shift assays and mass spectrometry. Furthermore, *in vivo* binding of SP1 transcription factor using ChIP-Seq could be an additional subject of future studies.

Further investigation into the *LRRC32* coding variant rs79525962 should be focused on the interaction and binding of the mutated GARP protein and TGFβ. Feasible *in vitro* approaches could be immunoprecipitation of the GARP/TGFβ complex using specific antibodies followed by SDS-PAGE and Western Blot detection and/or FACS analysis of the latent associated protein (LAP), which forms a complex with TGFβ when it is bound to GARP on the surface of Tregs. Moreover, to determine the functional effect of mutated GARP on responder T cells, *in vitro* Treg suppression assays would be a helpful tool and should be the target of further investigations. On the other hand, additional investigation of intracellular TGFβ-induced signals transduction with SMAD-reporter constructs could provide new insights into intracellular mechanisms related to GARP dysfunction. Furthermore, the tracking of intracellular GARP movement, using fluorescent markers (e.g. GFP), would help to identify targets of disturbed GARP post-translational modifications and transport.

Genome-wide expression results should be replicated and validated by an independent cohort using RNA-sequencing and the main findings should also be validated by different methods, e.g. qPCR. It is possible that the analysis of gene expression patterns in skin tissue is confounded by the mixture of the different cell types existing in skin, especially if the cell type of interest is not the predominant component (e.g. in lesional skin infiltrating T cells are predominant) (Mesko et

al. 2011). Therefore, gene expression analysis in peripheral blood mononuclear cells, for instance, should be considered as an alternative target cell type in further studies. This approach would not only be less invasive but could also potentially identify differentially regulated genes which could be used as new biomarkers with better translation into the clinical setting.

4   METHODS

4.1   Working with organisms

4.1.1   Working with eukaryotic cell lines

4.1.1.1   Cultivation of used cell systems

HeLa

HeLa is an adherent human cerivix carcinoma cell line (Scherer et al. 1953). HeLa cells were cultivated in MEM (minimal essential media) containing 10 % FBS (fetal bovine serum), 100 U/ml penicillin, and 100 µg/µl streptomycin under sterile conditions at 37 °C with 5 % CO_2 in a humidified atmosphere.

Jurkat

Jurkat is a suspension cell line of immortalized T lymphocytes (Schneider et al. 1977). Jurkats were maintained in RPMI-1640 medium (Roswell Park Memorial Institute medium) containing 10 % FBS, 2 mM L-glutamine, 100 U/ml penicillin, and 100 µg/µl streptomycin at 37 °C and 5 % CO_2 in a humidified atmosphere.

A-549

A-549 is a human carcinoma alveolar basal epithelial cell line (Giard et al. 1973). A-549 cells were grown in MEM containing 10 % FBS, 100 U/ml penicillin, and 100 µg/µl streptomycin under sterile conditions at 37 °C with 5 % CO_2 in a humidified atmosphere.

HaCaT

HaCaT is an immortalized keratinocyte cell line from adult human skin (Boukamp et al. 1988). HaCaT cells were grown in DMEM supplemented with 10 % FBS, 100 U/ml penicillin, and 100 µg/µl streptomycin under sterile conditions at 37 °C with 5 % CO_2 in a humidified atmosphere.

Cos-7

Cos-7 is an adherent fibroblast-like cell line derived from monkey kidney tissue (Jensen et al. 1964). Cos-7 cells were cultivated in DMEM supplemented with 10 % FBS, 100 U/ml penicillin,

and 100 µg/µl streptomycin under sterile conditions at 37 °C with 5 % CO_2 in a humidified atmosphere.

4.1.1.2 Maintenance of cell culture

Thawing of cells

Cryopreserved cell aliquots were thawed in a 37 °C water bath and diluted in 10 - 15 ml of fresh medium. The cells were centrifuged at 1000 x g for 1 min and the cell pellet was resuspended in 6 ml of fresh medium and incubated in a T25 cell culture flask overnight. At a confluence of 80 - 100 %, cells were transferred to a T75 cell culture flask for further cultivation.

Culturing/splitting of cells

Cells were split at a confluence of 80 % - 100 %, approximately three times a week. Adherent cells (HeLa, A-549, HaCaT and Cos-7 cells) were first washed with 1x phosphate buffered saline (PBS) (10 mM sodium-phosphate buffer pH 7.4, 150 mM NaCl) followed by trypsinization with 1 ml trypsin-EDTA. After a few minutes incubation at 37 °C, trypsinization was stopped by adding fresh medium, cells were resuspended and part of the cell suspension was transferred to a new cell culture flask. Depending on cell growth rate, cell type or appropriate cell number required for an experiment, different splitting ratios were used (typically 1:3 – 1:6). For splitting of suspension cells (e. g. Jurkats) 15 - 20 ml culture medium was removed and one half of the remaining cell suspension was transferred to a new T75 cell culture flask and filled up with fresh medium to a final volume of 30 ml.

Cryopreservation of cells

For cryopreservation, cells were washed with PBS and trypsinized if necessary (adherent cells). An automated cell counter (Cellometer Auto T4, Peqlab) was used for determination of cell numbers. Cell suspension with a cell number of 5 x 10^6 cells was then centrifuged for 1 minute at 500 x g and the cell pellet was suspended in freezing medium supplemented with 20 % FBS and 10 % DMSO. Cells were transferred into Cryo Tube™ vials and cooled down to - 80 °C in steps of 1 °C per minute using a Mr. Frosty Freezing Container in a -80 °C freezer. For long time storage, cell aliquots were stored in liquid nitrogen tanks.

4.1.1.3 Transfection of eukaryotic cells

Transfections of DNA plasmids into the cells were performed using lipophilic carrier supported transfection procedures, mainly based on the manufacturer's protocols, however optimized for all used cell lines. For optimal transfection efficiency, the cell layer should be 50 – 70 % confluent at the time of transfection. Hence, cells were seeded in a 12-well plate 24 hours prior transfection at an appropriate cell density. Cell concentration was assessed by counting the cells with a Cellometer® Auto T4 Cell Counter. For luciferase reporter assays, several pGL4.23- and pGL4.12 vector-based plasmids (firefly luciferase as reporter) and control vector pGL4.74 (renilla luciferase as constitutive reporter) were used. All transfection conditions that were applied for transfection of reporter gene constructs in HeLa, Jurkat, A-549, and HaCaT cells are listed in Table 9 and Table 10. Briefly, corresponding amounts of test and control vectors together with transfection reagent were incubated in appropriate volumes of medium without further supplements for 20 minutes at room temperature. After the incubation, the formed lipid-DNA complexes were added to the cells in a drop wise manner and incubated for 32 hours at 37 °C in a 5 % CO_2-atmosphere.

Table 9: Reporter Assay transfection protocol for pGL4.23 constructs (12-well format)

Cell line	Cell density* [cells/ml]	Transfection reagent (TR)	Ratio TR[µl]: DNA[µg]	Test vector [ng]	Control vector pGL4.74 [ng]	Medium
HeLa	1×10^5	FuGene 6	1.5 : 0.5	500	50	50 µl MEM
Jurkat	4×10^5	Mirus IT	1 : 2	2000	50	100 µl RPMI
A-549	2×10^5	ViaFect	1.5 : 0.5	500	50	100 µl MEM
HaCaT	2×10^5	Lipofectamine 2000	2.5 : 1	1000	50	100 µl DMEM

*seeded 24 hours prior transfection; 1ml volume/well

Table 10: Reporter Assay transfection protocol for pGL4.12 constructs (12-well format)

Cell line	Cell density* [cells/ml]	Transfection reagent (TR)	Ratio TR[µl]: DNA[µg]	LRRC32 Promoter [ng]	C11orf30 Promoter [ng]	Control vector pGL4.74[ng]	Medium
HeLa	1×10^5	FuGene 6	1.5 : 0.5	500	50	50/5+	50 µl MEM
Jurkat	4×10^5	Mirus IT	1 : 2	750	500	50	100 µl RPMI
A-549	2×10^5	ViaFect	0.8 : 0.2	750	200	50	100 µl MEM
HaCaT	2×10^5	ViaFect	1.5 : 0.5	500	100	50	100 µl DMEM

*seeded 24 hours prior transfection, 1ml volume/well; +ng of control vector used for LRRC32Prom. construct/C11orf30 Prom. construct, respectively

4.1.2 Working with primary cells

4.1.2.1 Isolation of CD4+CD25- cells

Human peripheral blood mononuclear cells (PBMCs) were isolated from peripheral blood of healthy donors by a Ficoll density gradient centrifugation (Lymphoprep™, Amersham Biosciences) at the Universitätsklinikum Schleswig-Holstein (UKSH). EDTA-blood was mixed with PBS up to 100 ml, every 20 ml of the mixture were layered carefully on 25 ml of the lymphocyte separation medium (LSM 1077) in a 50 ml Falcon tube and centrifuged for 30 minutes at 480 x g. with the brake set to off. After centrifugation, PBMCs were visible as a white layer at the plasma/LSM interface, which was isolated and washed 3 times with 30 ml 2 mM EDTA-PBS. Cells were counted to prepare appropriate volume of beads for magnetobead separation using the CD4+CD25+ Regulatory T Cell Isolation Kit© of Miltenyi Biotec. Freshly isolated PBMCs were separated into CD4+CD25+ and CD4+CD25- T cells using MACS (magnetic activated cell sorting, Miltenyi Biotec) according to the manufacturer's protocol. The isolation procedure was performed in cooperation with Dr. Agatha Schwarz at the UKSH Hautklinik.

4.1.2.2 Transfection of primary cells using DEAE-dextran

The non-regulatory CD4+CD25- T cell fractions were transiently transfected with pIRES2-AcGFP1 plasmids carrying either the coding sequence of human wildtype GARP or the mutated A407T GARP using an adapted diethylaminoethyl (DEAE)-dextran protocol as described elsewhere (Gulick 2001). Briefly, 2×10^6 CD4+CD25- T cells were seeded in 6-well plates and incubated with 20 µl of 10 mg/ml DEAE-dextran solution and 2.5 µg plasmid DNA in 1 ml serum free RPMI medium at 37 °C in a humidified atmosphere. After 4 h incubation cells were washed twice with growth medium supplemented with 10 % fetal calf serum followed by stimulation with 5 µg/ml phorbol myristate acetate (PMA) and 10 ng/ml Concanavalin A (ConA, both from Sigma-Aldrich). The cells were incubated at 37 °C for 24 h, harvested and subjected to flow cytometric analysis.

4.1.3 Working with Escherichia coli

4.1.3.1 Cultivation and maintenance

Liquid *E.coli* DH5α or Top10 cultures were cultivated in growth medium (lysogeny broth (LB) medium) containing appropriate antibiotic (50 µg/ml ampicillin or 50 µg/ml kanamycin). To

obtain single colonies for PCR screen, liquid E. coli cultures were spread on agar plates based on lysogeny broth (LB) containing 50 µg/ml ampicillin or kanamycin and incubated overnight at 37 °C. After incubation, single bacterial clones were transferred from agar plates into 100 – 200 µL LB-medium without antibiotics (LB$_0$) using sterile pipet tips and cultured for two hours during vigorous shaking (200 rpm). These small scale cultures were then used for PCR screen (see 4.1.3.3). For plasmid enrichment, inoculation of liquid media (from small scale cultures or glycerol stocks) was performed using sterile pipet tips and bacteria cultures were grown overnight in a shaking incubator (200 rpm) at 37 °C.

LB$_0$ medium:	10 g NaCl
	10 g BACTO Peptone
	5 g Yeast extract
	ad 1000 ml H$_2$O (pH 7.4)
solid agar plates:	add 1,5 % (w/v) agar-agar

4.1.3.2   Short and long-term storage

For short-term storage (up to some month) agar plates containing bacterial colonies were sealed with Parafilm M® and stored at 4 °C. For long-term storage, glycerol stocks were prepared by mixing sterile 80 % glycerol and liquid culture (1:1, v/v) in a cryogenic tube and keeping this at - 80 °C for several years.

4.1.3.3   Transformation of chemo-competent *E.coli* and Colony Screen-PCR

For transformation of plasmid DNA into *E.coli*, 200 ng of plasmid DNA (e.g. ligation product) was added to 100 µl freshly thawed (on ice) chemo-competent *E.coli* and incubated for 20 minutes on ice. Cells were heat-shocked at 42 °C for 45 seconds and subsequently chilled on ice for two minutes. 150 µl of LB-medium without antibiotics were added and cells were incubated at 37 °C for one hour with vigorous shaking (1000 rpm). After incubation, 50 µl of transformation mixture was plated on LB agar plates supplemented with suitable antibiotics and incubated overnight at 37 °C. Several clones were picked and screened via PCR for existence of transformed plasmid and insertion of fragment. For screening PCR vector primers and the in house produced Taq-polymerase and corresponding PCR-buffer (100 mM Tris-HCl (pH9), 500 mM KCl, 15 mM MgCl$_2$) were used and PCR conditions were applied according to chapter 4.2.5.1. Bacterial clones carrying the right insert were subjected to plasmid isolation procedures followed by sequencing of plasmid DNA to verify the insert.

4.2 DNA-based molecular methods

4.2.1 Isolation and purification procedures

4.2.1.1 Isolation of plasmid DNA from bacteria

Depending on the volume of liquid culture and corresponding amount of plasmid DNA, two different scales for the isolation of plasmid DNA from *E.coli* were used. The NucleoSpin® Plasmid Kit (Macherey&Nagel) was used for small scale preparations, with a 6 ml overnight culture according to the manufacturer's protocol. DNA was eluted two times with 25 µl Ampuwa® water (Fresenius). The NucleoBond® Xtra Midi Kit (Macherey&Nagel) was utilized for medium scale preparations with 50 ml of overnight culture according to the manufacturer's protocol. The DNA from medium scale preparations was dissolved in 100 µl Ampuwa® water. DNA concentration was measured with a NanoDrop and DNA and was stored at -20 °C.

4.2.1.2 Purification of dsDNA from solution

Purification of PCR products was performed with the Wizard® SV Gel and PCR Clean-up System (Promega) according to the manufacturer's protocol with slight modifications. First and second washing steps were carried out with 600 µl and 400 µl membrane wash solution, respectively, and DNA was eluted two times with 20 µl Ampuwa® water. DNA concentration was measured using NanoDrop and DNA was stored at -20°C.

4.2.1.3 Purification of dsDNA from agarose gels

Purification of DNA from agarose gels after electrophoresis was conducted with the Wizard® SV Gel and PCR Clean-up System. First, the DNA bands were cut out using a scalpel and the DNA containing gel slices were dissolved and purified according to the manufacturer's protocol with the same modification listed in 4.2.1.2. Elution was performed with 20 - 30 µl Ampuwa® water.

4.2.1.4 Purification of sequencing PCR products

Prior to sequencing, sequencing PCR reaction products have to be purified in order to remove excess of dNTPs and fluorescence-labeled ddNTPs, which would interfere with the sequencing process. For purification the Montage™ SEQ96 Sequencing Reaction Cleanup Kit (Millipore) was used according to the manufacturer's protocol. Elution of PCR products from the filter membrane was performed with 25 µl of injection solution.

4.2.2   Quality assessment of nuclei acids

4.2.2.1   Quantification of nucleic acids by measuring optical density

For quantification, the optical density of nucleic acids was measured at λ= 260 nm (1 OD corresponds to 50ng/µl DNA or 40ng/µl RNA, respectively) with a NanoDrop spectrophotometer (ND 1000, PeqLab). To verify good DNA purity, an A260/A280 ratio of 1.7-2.0 (ensures that the samples is free of protein contamination) and an A260/A230 ratio of more than 1.5 (ensures exclusion of salt and phenol contamination) should be present.

4.2.2.2   Qualitative determination of DNA by agarose gel electrophoresis

For quality determination and separation of DNA fragments after PCR gel electrophoresis was performed. 1.5 % agarose in 1x TBE buffer (w/v) was commonly used for gel preparation. To visualize DNA bands under UV illumination, 0.025 % (v/v) of nucleic acid staining solution (Midori Green, Biozym) was added. Electrophoretic separation was conducted in a constant electric field with a voltage of 100 V for 30 - 60 minutes. DNA fragments were visualized under UV illumination (λ = 254 nm) by a gel documentation system (Bio vision Gel documentation, PeqLab).

10x TBE buffer	108 g Tris/ 89mM
	55 g boric acid/89mM
	9.3 g EDTA in 1 l H20/2 mM (pH 8.0)

4.2.3   Cloning strategies

DNA inserts for luciferase- and expression vectors were generated by PCR amplification from human genomic DNA or a bought genomic *LRRC32* cDNA clone. The PCR products were cloned via two restriction sites into appropriate plasmid vectors. Finally, all constructs were verified by sequencing. Table 11 shows all cloning products that were generated during this thesis.

Table 11: Summary of cloning products

Vector backbone	Insert sequence	variant (allele)
pGL4.23	459 bp	rs2155219 (G)
pGL4.23	459 bp	rs2155219 (T)
pGL4.23	1142 bp	rs2155219 (G) rs11236797 (C) rs34455012 (CCAGTAT)
pGL4.23	1142 bp	rs2155219 (T) rs11236797 (A) rs34455012 (del)
pGL4.23	1142 bp	rs2155219 (G) rs11236797 (A) rs34455012 (del)
pGL4.23	1142 bp	rs2155219 (G) rs11236797 (C) rs34455012 (del)
pGL4.23	1142 bp reverse complementary	rs2155219 (G) rs11236797 (C) rs34455012 (CCAGTAT)
pGL4.23	1142 bp reverse complementary	rs2155219 (T) rs11236797 (A) rs34455012 (del)
pGL4.12	LRRC32 promoter 711 bp	-
pGL4.12	C11orf30 promoter 844 bp	-
pGL4.12	LRRC32 promoter 711 bp	rs2155219 (G) rs11236797 (C) rs34455012 (CCAGTAT)
pGL4.12	LRRC32 promoter 711 bp	rs2155219 (T) rs11236797 (A) rs34455012 (del)
pGL4.12	C11orf30 promoter 844 bp	rs2155219 (G) rs11236797 (C) rs34455012 (CCAGTAT)
pGL4.12	C11orf30 promoter 844 bp	rs2155219 (T) rs11236797 (A) rs34455012 (del)
pIRES2-AcGFP1	LRRC32 1988 bp	rs79525962 (T)
pIRES2-AcGFP1	LRRC32 1988 bp (A407T)*	rs79525962 (C)

del= deletion; *: non-synonymous variant leads to an amino acid change at pos. 407 (Ala→Thr)

4.2.3.1   Cloning via two restriction sites

PCR-amplified DNA fragments were inserted either into the vector pGL4.23, pGL4.12 or pIRES2-AcGFP1 via two restriction sites. Digestion of inserts and vectors with the restriction enzymes resulted in complementary "sticky" ends that allowed targeted and site-directed ligation. Details on used vectors, inserts and appropriate restriction enzymes are listed in Table 12. Briefly, 1 µg

of DNA (insert and vector) was digested in 20 µl reaction volumes together with appropriate concentrations of buffer, BSA and 10 – 20 U enzymes overnight at 37 °C. After incubation, the reaction was stopped by heat-inactivation for 20 minutes at 65 °C.

Table 12: Cloning protocol for reporter vector constructs

Vector	Insert	Restriction enzyme	Buffer (NEB)*	BSA+
pGL4.23	rs2155219 rs11236797 rs34455012 459 bp or 1142 bp	Bgl II Hind III	2	-
pGL4.12	LRRC32 promoter C11orf30 promoter	Bgl II Hind III	2	-
pGL4.12 LRRC32 promoter C11orf30 pomoter	rs2155219 rs11236797 rs34455012 1142bp	KpnI SacI	1	10 %
pIRES2-AcGFP1	LRRC32 1988 bp LRRC32 1988 bp (A407T)	XhoI SacII	2	

*Buffer provided by New England Biolabs; +bovine serum albumin

4.2.3.2   Ligation

T4 DNA Ligase was used for ligation of vectors and inserts. 150 ng of vector DNA and a five times molar excess of insert DNA were mixed and incubated with enzyme, 1 x T4 DNA ligase buffer, and H_2O to a final volume of 20 µl. The ligation reaction was incubated at room temperature for three hours. Ligated products were then used for transformation into chemo-competent *E.coli* (see 4.1.3.3).

4.2.4   Dual Luciferase Assay

HeLa, Jurkat, A549, and HaCaT cells were seeded at an appropriate cell density and transfected with different luciferase constructs as described in chapter 4.1.1.3 (see Table 9 and Table 10). For normalization 50 ng of the pGL4.74 vector, which constitutively expresses renilla luciferase, was co-transfected. Luciferase activity was measured 32 hours post transfection using the Promega Dual-Luciferase Assay Kit according to the manufacturer's protocol. Cell lysis of adherent cells (HeLa, A549, and HaCaT) was performed with 200 µl 1 x passive lysis buffer (supplied by DLR Assay, Promega) per well after washing the cells once with 1 x PBS. After gentle shaking in the plate for 30 minutes, the cells were frozen at – 80 °C overnight. Cell lysis of

HaCaT cells was supported by scraping the cells with a cell scraper. To harvest Jurkat cells, cell suspension was transferred to a 2 ml Eppendorf tube and centrifuged for 3 minutes at 300 x g. Cell pellet was washed two times with PBS and finally cell lysis was performed with 200 µl 1 x passive lysis buffer during gentle shaking for 30 minutes followed by freezing the lysates at – 80 °C overnight. Luciferase activity was measured with the GloMax®-Multi Detection System (Promega) by using 20 µl of thawed cell lysate and 50 µl reagents from the Dual Luciferase Assay Kit with a 2-second premeasurement delay and a 5-second measurement period according to the manufacturer's instructions. Experiments were performed at least three times in analytical triplicates. Relative promoter activity was generated by calculating intensity ratios of firefly/renilla luciferase activity. Normalization on the empty vector (carrying no insert) was applied to show the overall effect of the investigated sequence on the minimal promoter or the native *LRRC32* or *C11orf30* promoters. For statistical analysis first Kolmogorov-Smirnov-tests were performed to test for normality of distribution. Showing no significant deviation from normal distribution linear mixed effect models (LME, R-software) with random intercept were used in order to identify statistically significant differences in regulatory activity/promoter activity between the different constructs.

4.2.5 PCR-based methods

4.2.5.1 Polymerase chain reaction (PCR)

Polymerase chain reactions were performed in 25 µl and 50 µl reactions containing 0.2 mM dNTP-mix, 1 µM each of forward and reverse transcript-specific primer, and 0.5 – 2.5 U of Pfu Turbo DNA polymerase (Strategene) in supplied 1 x PCR buffer. Human genomic DNA, plasmid DNA, bacteria culture or primary PCR were used as templates. For screening PCRs with bacterial cultures, the in-house produced Taq-polymerase and the corresponding PCR-buffer (100 mM Tris-HCl (pH9), 500 mM KCl, 15 mM $MgCl_2$) was applied. The cycling program started with an initial denaturing step of 10 minutes at 95 °C followed by 35 cycles with 30 seconds at 95 °C, 30 seconds at the appropriate annealing temperature (usually 3 °C below primers melting temperature), 1 minute for each amplified kb at 72 °C, one final cycle at 72 °C for 10 minutes and hold on 6 °C. For difficult to amplify fragments (e.g. GC-rich templates), the Phusion® High-Fidelity DNA Polymerase (NEB) was used according to the manufacturer's instructions. The PCR products were mixed 1:1 with 6x Loading Dye (15 % Ficoll 400, 0.25 % bromophenol blue, 0.25 % xylene cyanol FF) and analyzed together with a DNA marker for the appropriate fragment length by electrophoresis on a 1.5 % agarose gel as described in chapter 4.2.2.2. All used primers are listed in Appendix Table VII.

4.2.5.2   PCR mutagenesis

SNP-surrounding sequences needed for cloning of plasmids were amplified from human genomic DNA or genomic *LRRC32* cDNA clone containing the major alleles of investigated SNPs. Single point mutations to insert the minor instead of major allele were performed via PCR mutagenesis followed by Fusion PCR (Figure 39). Forward and reverse primers were designed to contain the desired point-mutation in the middle of the primer sequence (Figure 39A, p3_for and p2_rev). Two PCR reactions were performed, one using the general forward primer (p1_for) together with the reverse point-mutation included primer (p2_rev), the other one using the forward point-mutation included primer (p3_for) together with the general reverse primer (p4_rev) resulting in two new fragments both including the induced point mutation (Figure **39**B). PCR conditions were applied as described in chapter 4.2.5.1. PCR products were analyzed on a 1.5 % agarose gel, purified with the Wizard® SV Gel and PCR Clean-up Kit and used as targets for Fusion PCR.

Fusion PCR was applied in order to combine DNA fragments produced via PCR mutagenesis to obtain a DNA fragment including site-directed point mutation. The two gained amplicons of the first PCR were used as template and PCR was carried out together with the general PCR primers (p1_for and p4_rev) flanking the entire sequence of the final product. Final PCR amplicon was analyzed on a 1.5 % agarose gel, purified, and verified via sequencing. For difficult to amplify sequences point-mutations into plasmid DNA were carried out by using the QuikChange® Site-Directed Mutagenesis kit (Stratagene) according to the manufacturer's instructions.
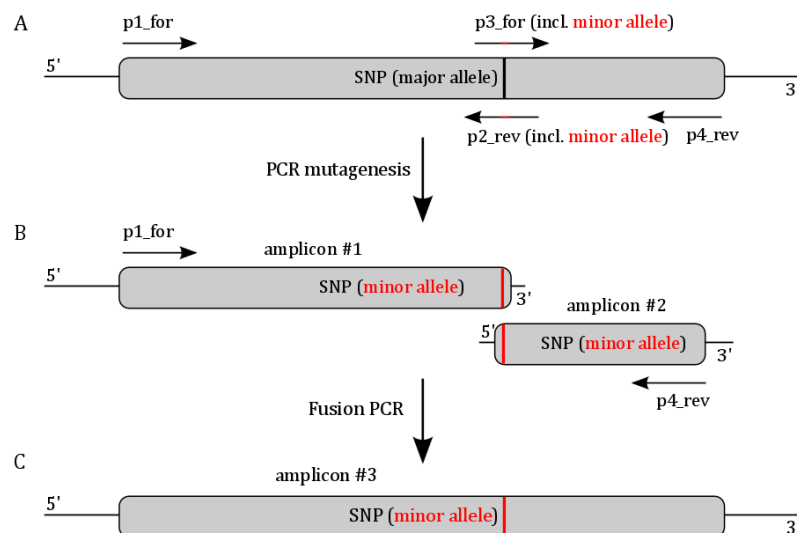
Figure 39: Allele change in DNA insert using PCR mutagenisis and Fusion PCR. (A) Primer pair with desired point mutation in the middle was used in separate PCR reactions: (B) amplicon #1 was amplified using the general forward primer (p1_for) together with the reverse point-mutation included primer (p2_rev), amplicon #2 was generated using the forward point-mutation included primer (p3_for) together with the general reverse primer (p4_rev). (C) PCR product with desired allele change of SNP as a result of Fusion PCR. for= forward; rev= reverse.

4.2.5.3   DNA sequencing

To identify and verify DNA sequences or DNA plasmids DNA sequencing was carried out by Sanger sequencing. Sequencing reaction was conducted using the BigDye® Terminator v3.1 Cycle Sequencing Kit (Applied Biosystems) according to the manufacturer's instructions. The PCR reaction included 0.2-2 µl template DNA (10 ng per 1kb template DNA sequence), 2 µM sequencing primer, 1 µl BigDye® Terminator v3.1 (containing fluorescence-labeled ddNTPs in 1 x sequencing buffer), and ultrapure LiChrosolvR water for chromatography (Merck) up to a volume of 5 µl. The PCR conditions started with an initial denaturation for five minutes at 95 °C followed by 35 cycles for 30 seconds at 95 °C, 45 seconds at 3° C below primer melting temperature, and four minutes at 60 °C. Subsequently, PCR products were purified using the Montage™ Seq96 Sequencing Reaction Cleanup Kit (Millipore) as described in chapter 4.2.1.4 and analysed with the ABI PRISM® 3730 DNA Analyzer (Applied Biosystems).

4.2.5.4   cDNA synthesis and end-point-RT (reverse transcriptase) PCR

For first strand cDNA synthesis 1 µg of RNA was reverse transcribed using oligo(dT)$_{18}$ primers and the RevertAid RT Reverse Transcription Kit (Thermo Scientific) according to the manufacturer's protocol. The cDNA synthesis reaction was then diluted to a ratio of 1:5 with H_2O. 2 µl of the diluted cDNA synthesis reaction mixture was used as template for subsequent RT-PCR in 50 µl total volume. End-point RT-PCR was carried out in a RoboCycler (Stratagene) using Pfu Turbo DNA polymerase (Stratagene) with an initial step of 10 minutes at 95 °C followed by 35 cycles with 30 seconds at 95 °C, 45 seconds at the appropriate annealing temperature, 1 minute for each amplified kb at 72 °C and one final cycle at 72 °C for 10 minutes. For cDNA quality assessment amplification of human β-actin was performed with 25 amplification cycles. PCR products were visualized on a 1.5 % agarose gel (containing 0.0025 % Midori Green (Biozym) using a Bio Vision Gel documentation system.

4.3   RNA-based molecular methods

4.3.1   Isolation of RNA from cell culture

RNA was isolated from different transfected and non-transfected mammalian cells (HeLa, CD4+CD25- T cells, and Cos-7) 48 hours post transfection using the RNeasy Mini Kit (Qiagen) in combination with a DNase I digestion treatment according to the manufacturer's protocol. The QIAshredder spin-columns (Qiagen) were used for homogenization of cell lysates according to

the manufacturer's instructions. Finally, total RNA was eluted two times with 25 µl RNase-free H$_2$O.

4.3.2 Isolation of RNA from skin biopsies

Skin biopsies were first cut to small pieces with a scalpel followed by homogenization with the Precellys® 24 homogenizer (PeqLab) in two cycles of 30 seconds at 6500 rpm and 20 seconds rest period in between using 1.4 mm ceramic beads (CK14) in 300 µl Homogenization Buffer (Buffer RLT, RNeasy Mini Kit, Qiagen). After homogenization, lysates with beads were centrifuged for 2 minutes at 18 000 x g and the supernatant was subjected to RNA isolation procedure using the RNeasy Mini Kit according to the manufacturer's protocol. DNase I digestion treatment was performed and total RNA was eluted two times with 25 µl RNase-free H$_2$O. RNA was stored in aliquots at -80 °C.

4.3.3 RNA quantification and integrity

RNA concentration was assessed with a Nanodrop spectrophotometer. RNA integrity was analyzed on the Agilent Bioanalyzer using the Agilent RNA 6000 Nano Kit according to the manufacturer's protocol. All RNA samples with RIN (RNA integrity number) values < 5.5 were excluded from further analysis.

4.3.4 Differential allelic expression analysis

To identify potential *cis*-regulatory effects of SNP rs7927894 on gene transcription of the genes *LLRC32* and *C11orf30*, allele-specific gene expression was performed using fluorescence-tagged single-nucleotide primer extension assays (Figure 40). RNA samples from skin biopsies of five individuals that were heterozygous for the atopic dermatitis (AD)-associated SNP rs7927894 as well as for an expressed SNP (eSNP) located in the coding region of *LRRC32* or *C11orf30* were used for the analysis. In addition, two control individuals, which were only heterozygous for the eSNP and homozygous for the associated SNP, were analyzed.

The eSNP was used as tag SNP for the appropriate gene transcript and eSNP criteria included: coding SNP, minor allele frequency > 0.1, and correlation with SNP of interest. Expressed SNP selection was carried out in co-operation with Andrew Johnson from the National Heart, Lung, and Blood Institute (NHLBI) by interrogation of an eSNP database to find all eQTL (expression quantitative trait loci) associations within a 2 Mb-surrounding region of the associated SNP of interest. Correlation between potential eSNPs and the SNP of interest was evaluated and finally

rs3781701 and rs2282611 were selected for further analyses for *LRRC32* and *C11orf30*, respectively. 200 ng of appropriate RNA samples (homozygous for SNP of interest and eSNP) were reverse transcribed together with DNaseI digestion treatment and 300 – 400 bp fragments flanking the eSNP were generated by RT-PCR using the GoTaq® DNA Polymerase (Promega) in a 50 µl reaction volume according to the manufacturer's protocol. Cycler settings were used as follows: 2 minutes at 95 °C, 35 cycles of 30 seconds at 95 °C, 30 seconds at appropriate annealing temperature (Tm$_{LRRC32}$ = 64 °C; Tm$_{C11orf30}$ = 52 °C), and 40 seconds at 72 °C, followed by one cycle at 72 °C for 5 minutes. PCR products were purified with the Wizard® SV Gel and PCR Clean-up System and then used as templates for single base primer extension assays using the ABI PRISM® SNaPshot™ Kit (Applied Biosystems). Extension primers were designed to anneal to the sequence adjacent to the SNP. Reaction mixture consists of 0.2 pmol of DNA, 0.2 µM of extension primer, 5 µl SNaPshot Mix filled up with water to a final volume of 10 µl. Reaction was carried out in a thermocycler for 3 seconds at 96 °C followed by 25 cycles for 10 seconds at 96 °C, 5 seconds at the appropriate extension primer annealing temperature (Tm_ext$_{LRRC32}$ = 61 °C; Tm_ext$_{C11orf30}$ = 51 °C), and 30 seconds at 60 °C and finally hold at 10 °C. Addition of fluorescence dye-labeled ddNTPs (included in SNaPshot Mix) resulted in single base extension to the annealed primer and termination. To remove unincorporated dNTPs, shrimp alkaline phosphatase (SAP) treatment was performed with 1 µl enzyme (1 U/µl) for 60 minutes at 37 °C and enzyme activity was stopped after 15 minutes at 75 °C. Samples (0.8 µl of SAP-treated PCR reaction) were mixed with 0.5 µl Gene Scan™ 120 LIZ® Size standard (Applied Biosystems) and 9 µl of Hi-Di™ Formamide (Applied Biosystems) heated for 5 minutes at 95 °C, immediately cooled down on ice and the reaction products were analyzed by gel capillary electrophoresis on ABI PRISM® 3730 DNA Analyzer (Applied Biosystems). Data analysis was carried out with Gene Mapper® 4.0 software and allelic ratios were manually calculated after export to Microsoft Excel. Genomic DNA samples from the same individuals, where the allelic ratio is expected to be 1:1, were analyzed in the same manner and ratios were used for normalization. Allelic ratios above or below 1 indicated differential allelic expression of gene transcripts. Experiments were performed up to 5 times, first two repeats were conducted in cooperation with Tea Berulava from the Institute of Human Genetics at the University of Essen. All used primer sequences are listed in Appendix Table VII.
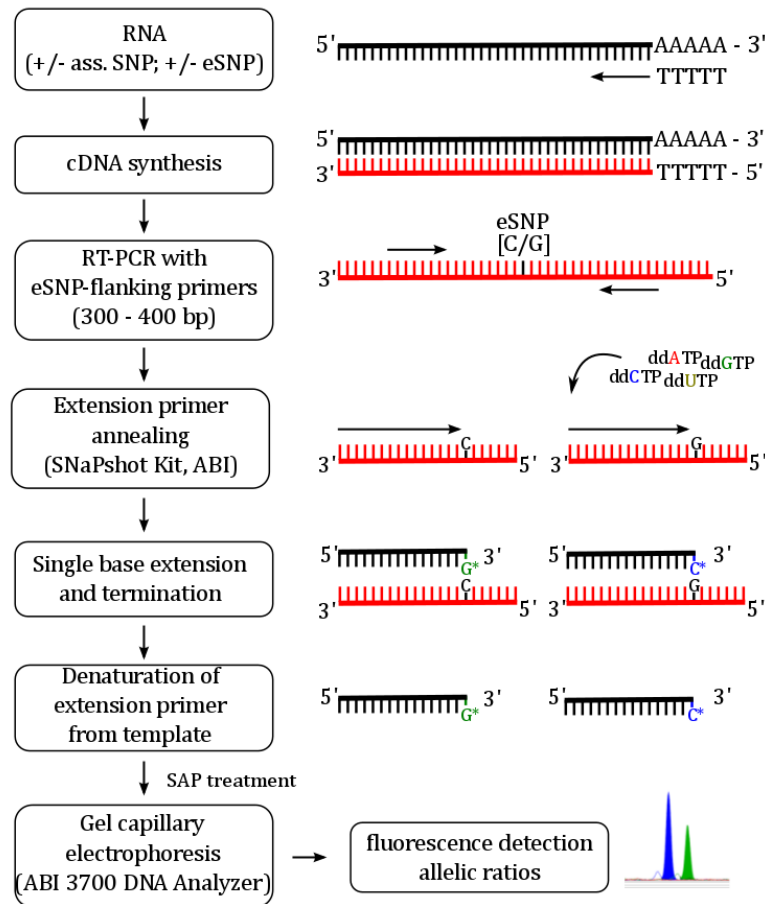
Figure 40: Differential allele-specific gene expression analysis using fluorescence-tagged single-nucleotide primer extension assays. RNA sample (heterozygous for associated SNP and eSNP) was reverse transcribed into cDNA followed by amplification of eSNP-flanking sequence. PCR products, fluorescence dye-labeled ddNTPs and extension primer were used for single base primer extension assay resulting in single base extension and termination of sequence. Shrimp alkaline phosphatase (SAP) treatment was performed to remove unincorporated dNTPs. Products were analyzed by gel capillary electrophoresis on a ABI 3700 DNA Analyzer and allelic ratios were calculated after fluorescence detection.

4.4 Protein chemistry

4.4.1 Nuclear protein extracts

Jurakt cells were stimulated with 25 ng/ml phorbol myristate acetate (PMA) and 500 ng/ml ionomycin for 6 hours and nuclear extracts were prepared using the Nuclear Extraction Kit (Active Motif) according to the manufacturer's protocol. The concentration of total protein was determined via the Pierce™ BCA Protein Assay Kit (Thermo Fisher Scientific) according to the manufacturer's protocol.

4.4.2 Electrophoretic Mobility Shift Assay (EMSA)

Electrophoretic shift assays were performed in order to analyze the predicted allele-specific alterations in transcription factor binding. Cy5-labeled and complementary unlabeled oligonucleotides (100 pMol/µl) containing the major or minor allele of investigated SNPs or the consensus sequences for SP1 and OCT1 were annealed for 2 minutes at 95 °C followed by 10 minutes at 76 °C and then slowly cooled down to room temperature. Resulting labeled double-stranded DNA probes were purified via 12 % polyacrylamide gel electrophoresis. Binding reaction was carried out using 6.6 µg of nuclear extract in 1 x binding buffer and 0.5 µg poly dI-dC filled up with water to a total volume of 10 µl for 10 min at 4 °C. 1 ng of labeled probe was added without or together with 10 times or 100 times excess of competitor oligonucleotides and further incubated for 20 minutes at 4 °C. After incubation, the reaction was stopped by adding 1 µl of loading dye. Protein-DNA complexes were separated on a 5.3 % polyacrylamide gel by electrophoresis in 0.5 x Tris-borate-EDTA (TBE) buffer for 10 min at 180 V followed by 3 hours at 240 V. Band patterns were visualized by scanning the gel ($\lambda = 633$ nm) with the Thyphoon Trio + imager (GE Healthcare Life Sciences). For supershift experiments 0.1 µg of a SP1 antibody was added to the reaction mixture following the standard binding reaction and incubated for another 45 minutes at 4 °C. IgG isotype antibody (0.1 µg) was used as control. Experiments were performed at least three times. All oligonucleotides were purchased from Metabion and are listed in Appendix Table VII.

12 % non-denaturing gel (oligo purification)	25 ml 1x TBE
	15 ml acrylamide/bisacrylamide (40 %w/v)
	1562.5 µl 80 % v/v glycerol
	7 ml H_2O
	375 µl 10 % APS
	25 µl TEMED
5.3 % non-denaturing gel (Protein separation)	25 ml 1x TBE
	6.5 ml acrylamide/bisacrylamide (40 %w/v)
	1562.5 µl 80 % v/v glycerol
	15.5 ml H_2O
	375 µl 10 % APS
	25 µl TEMED

1x binding buffer   4 % v/v Glycerol

                                                     1 mM MgCl2

                                                     0.5 mM EDTA

                                                     0.5 mM DTT

                                                     50 mM NaCl

                                                     10 mM TrisHCl pH7.5

10x Loading Buffer   250 mM Tris/HCl pH7.5

                                                     40 % v/v Glycerol

                                                     0.2 % Orange G

4.4.3 Protein over-expression in mammalian cells

For functional investigation of the coding *LRRC32* SNP rs79525962 (A407T) LRRC32/GARP protein expression was performed via transient plasmid transfection. pIRES2-AcGFP1 expression vector constructs carrying either the coding sequence of the human wildtype GARP or the human mutated A407T GARP were transiently transfected into different mammalian cells (CD4+ CD25- T cells, HeLa, and Cos-7 cells). CD4+ CD25- T cells were transfected using an adapted DEAE-dextran method as described in chapter 4.1.2.2. Lipophilic carrier supported transfection procedures were applied for HeLa and Cos-7 cells and all transfection conditions are listed in Table 13. Briefly, indicated cell numbers were seeded in a 6-well format at the appropriate cell density, 24 hour prior transfection. 1200 ng of plasmid DNA together with 3.6 µl of corresponding transfection reagent were incubated in 100 µl of medium without supplements for 20 minutes at room temperature. The formed lipid-DNA complexes were added to the cells in a drop wise manner and incubated for 48 hours at 37 °C in a humid 5 % CO_2-atmosphere.

Table 13: Transfection protocol using pIRES2-AcGFP2 expression vector

Cell line	Cell number [cells/2ml]	Transfection reagent	Ratio TR[µl]: DNA[µg]	DNA [ng]	medium[µl]
HeLa	4×10^4	FuGene 6	3 : 1	1200	100 MEM
Cos-7	0.5×10^5	X-treme Gene 9	3 : 1	1200	100 DMEM

4.4.4 Protein purification and isolation

Depending on the application different isolation procedures were applied. For total protein isolation over-expressing cells were washed with cold PBS before the cells were coated with 250 µl PBE solution per well (500 mM EDTA, 0.25 g BSA ad 50 ml PBS, sterile-filtered) to gently detach the cells without trypsination. Treatment was carried out for 15 minutes at 4 °C while gently rocking the plates several times. Another 250 µl PBE/well were added in order to detach cells completely. Cell preparations were centrifuged for 10 minutes at 5000 x g and cell pellets were frozen at – 80 °C until use.

For isolation of membrane proteins and separation from cytosolic proteins the Mem-PER Eukaryotic Membrane Protein Extraction Reagent Kit (Pierce Biosciences) was used according to the manufacturer's protocol. Briefly, 5×10^6 cells were harvested by scraping the cells off the surface with a cell scraper followed by centrifugation at 300 x g for 5 minutes. Cell pellet was washed with 3 ml of Cell Wash solution, centrifuged again at 300 x g for 5 minutes and washing step was repeated with 1.5 ml of Cell Wash solution. Permeabilization of cells was performed by resuspension of the cell pellet in 0.75 ml Permeabilization Buffer and incubation for 10 minutes at 4 ° C with constant mixing. After centrifugation for 15 minutes at 16000 x g the supernatant containing the cytosolic protein fraction was removed and immediately stored at – 80 °C. Remaining pellet was resuspended in 0.5 ml of Solubilization Buffer, incubated at 4 °C for 30 minutes with constant mixing and supernatant with solubilized membrane and membrane-associated proteins was removed after centrifugation for 15 minutes at 4 °C and immediately stored at – 80 °C.

4.4.5 Preparation of specific plasma membrane fraction from cell culture cells

Cell surface proteins of GARP transfected Cos-7 cells were first labeled using a periodate oxidation and aniline-catalyzed oxime ligation (PAL)-based procedure followed by biotinylation of cell surface-sialylated glycoproteins which were then captured by streptavidin-coupled beads as described elsewhere (Graessel et al. 2015). Briefly, after 48 hours after transfection the cells were washed once with prewarmed PBS, once with PBS supplemented with 1 M CaCl$_2$/MgCl$_2$ (pH 6.7) and then added to 500 µl biotinylation mix (0.5 M NaIO$_4$, 500 µM aminooxy-biotin, 0.5 M aniline ad PBS supplemented with 1 M CaCl$_2$/MgCl$_2$ (pH 6.7)) and incubated on a shaker for 30 minutes at 4 °C in the dark. For quenching, glycerol was added to a final concentration of 1mM for additional 5 minutes. Cells were washed with cold 1 x TBS and carefully scraped into 100 µl lysis buffer (1 % Nonidet P-40, 10 mM NaCl, 10 mM Tris-HCl, pH 7.6, in ddH$_2$O) and frozen at – 80 °C. For preparation of plasma membrane fractions, lysed cells were thawed on ice for 15 minutes, vortexed several times in between, followed by centrifugation for 10 minutes at

6000 x g at 4 °C. The supernatant was diluted 1:5 with 1 x TBS and subsequently incubated with 10 µl prewashed streptavidin beads (Strep-Tactin Superflow 50 % suspension, IBA GmbH) in LoBind tubes (Eppendorf) for 2.5 hours at 4 °C on a rotator to bind biotinylated cell surface proteins to high-affinity streptavidin beads. After binding, samples were centrifuged at 2000 x g for 1 minute, and bead-protein complexes were washed with different buffers (à 200 µl) in the following order : washing buffer (diluted 1:5 with 1 x TBS); 0.5 % SDS in PBS supplemented with 1 M $CaCl_2/MgCl_2$ (pH 6.7); UC buffer (6 M urea, 100 mM Tris-HCl, pH 8.5); 5 M NaCl (high-salt); 100 mM Na_2CO_3 (pH 11.3); and 50 mM Tris-HCl (pH 8.5). Centrifugation steps during the washing procedure were performed at 2000 x g for 2 minutes. The supernatant was discarded and the proteins were eluted from beads with 30 µl 2 x Laemmli buffer incubated for 15 minutes at room temperature on a shaker followed by 5 minutes at 70 °C with gentle shaking (650 rpm). After centrifugation at 2500 x g for 2 minutes, the supernatant containing the plasma membrane proteins were used for Western Blot analysis. Protein fraction procedure was performed in cooperation with Dr. Christine von Törne and Jennifer Behler from the "Research Unit of Protein Science, Helmholtz Zentrum München."

4.4.6   Protein quantification

The concentration of total protein was determined via the Pierce™ BCA Protein Assay Kit (Thermo Fisher Scientific) according to the manufacturer's protocol. For total protein determination, cell pellets were first resuspended in 30 – 50 µl PBS containing EDTA-free protease inhibitor and cell disruption was conducted with four cycles of 30-seconds ultrasonication pulses and 30-seconds ice bath. Protein concentration of enriched membrane and cytosolic fractions were measured directly after thawing the samples on ice.

4.4.7   Sodium dodecyl sulfate polyacrylamide gel electrophoresis (SDS-PAGE)

For separation of denaturized proteins according to their electrophoretic mobility, sodium dodecyl sulfate polyacrylamide gel electrophoresis (SDS-PAGE) was used. First, protein samples were diluted 1:5 with 5 x Laemmli loading buffer and denatured by incubation for 10 minutes at 95 °C. Six µg of denatured protein samples or 0.7 µl of PageRuler Prestained Protein Ladder (Thermo Fisher Scientific) were loaded on lanes of a gel (consisting of 5 % stacking gel and 10 % separating gel; 9 x 6.5 cm) and separated in running buffer at 80 V for 60 minutes. Gels were either stained with Coomassie Brilliant Blue (and destained with 5 % MeOH, 7.5 % acetic acid, 87.5 % ddH_2O) or blotted onto a PVDF membrane as described below (see 4.4.8).

Separation gel (10 %):	3.3 ml Rotiphorese Gel 30
	2.5 ml separation gel buffer
	4.2 ml MilliQ-H$_2$0
	10 µl TEMED
	100 µl 10 % APS

Stacking gel (5 %):	1.7 ml Rotiphorese Gel 30
	2.5 ml stacking gel buffer
	5.8 ml MilliQ-H$_2$0
	5 µl TEMED
	50 µl 10 % APS

10x SDS running buffer	0.25 M Tris
	2 M Glycin
	1 % (w/v) SDS

| Separation gel buffer | 1.5 M Tris/HCL, pH 8.8 |
| | 0.5 % (w/v) SDS |

| Stacking gel buffer | 0.5 M Tris/HCL, pH 8.8 |
| | 0.5 % (w/v) SDS |

5x Laemmli loading buffer	300 mM Tris/HCL pH 8.8
	50 % (v/v) glycerol
	10 % (w/v) SDS
	25 % (v/v) β-mercatoethanol
	0.05 % Comassie Brilliant Blue G25

Coomassie Brilliant Blue	0.05 % (w/v) Coomassie Brilliant Blue R250
	10 % (v/v) acetic acid
	40 % (v/v) methanol

4.4.8 Immunoblotting (Western Blot)

Western Blots were carried out in order to detect specific proteins with antibodies after protein overexpression in several cell lines. After separation of proteins with SDS-PAGE the gel was equilibrated for 15 minutes in transfer-buffer and the PVDF membrane was activated in methanol first, followed by transfer of separated proteins from the gel onto a PVDF membrane (Immobilon FL, Millipore) via semi-dry-blot in transfer-buffer at 20 V for 60 minutes. Afterwards, the membrane was blocked with 50 % Odyssey Blocking Buffer (TBS) in TBS for 1 hour at room temperature. For detection of specific proteins, incubation with primary antibody (GARP: LRRC32, mAb (Plato-1, mouse IgG2b) 1:1000; GFP: anti-GFP (3H9) in-house production 1:40) was then carried out in 50 % Odyssey Blocking Buffer (TBS) in TBS-T overnight at 4 °C and protected from light. After incubation, the blot was washed three times with 1 x TBS-T for 10 minutes, followed by incubation with IR-dye labeled secondary antibody (goat anti-mouse IRDye 800CW (LI-COR) 1:30000 and goat anti-rat (H+L) 790CW (Dianova) 1: 40000) in 50 % Odyssey Blocking Buffer (TBS) in TBS-T for 3 hours. After washing three times for 10 minutes with 1 x TBS-T, signals were detected via an Odyssey infrared imaging system (LI-COR). For testing antibody specificity, membranes were only incubated with secondary antibodies after transfer and blocking. 15 ng of recombinant human LRRC32/GARP protein (R&D Systems) was used as positive control. Experiments were repeated at least three times.

Blot Buffer	48 mM Tris
	39 mM glycin
	0.0375 % (m/v) SDS
	20 % (v/v) methanol
10 x TBS (pH 7.4)	100 mM Tris
	1500 mM NaCl
1x TBS-T (0.1 %)	1x TBS + 0.1 % Tween20

4.5 Immunological methods

4.5.1 Subcellular localization studies

For visualization of potential differences between wildtype and mutated GARP protein expression, HeLa and Cos-7 cells were used for subcellular localization studies because of high transfection efficiency and morphological benefits relating to high cell volume.

Cells were grown on glass coverslips in a 6-well plate and transiently transfected with pIRES2-AcGFP1 plasmids carrying either the coding sequence of human wildtype GARP or mutated GARP as described in chapter 4.4.3. For counterstaining the plasma membrane CellLight® Plasma Membrane-GFP BacMam 2.0 reagent (Molecular Probes), a Lck tyrosine and RFP (red fluorescence protein) fusion construct that provides specific targeting to the cellular plasma membrane, was directly added to the transfected cells after 24 hours and incubated for at least additional 16 hours at 37 °C. After 48 hours incubation in a humidified atmosphere at 37 °C and 5 % CO_2, cells were fixed in 3.7 % formaldehyde in PBS for 10 minutes at 37 °C and blocked with 3 % BSA in PBS for 30 minutes. For intracellular staining fixed cells were additionally permeabilized for 5 minutes using 0.5 % Triton X-100 in PBS prior to blocking with BSA. Fixed cells were stained with anti-human GARP IgG2b antibody (Enzo Life Sciences, 1:200 in 3 % BSA/PBS) followed by goat anti-mouse Alexa-Fluor488 (Thermo Fisher Scientific, 1:1000 in 3 % BSA/PBS) secondary antibody. Nuclei were counterstained with Hoechst 33342 dye (Thermo Fisher Scientific, 1:5000 in PBS) for 2 minutes. Washing of cells was performed with PBS after each step. Coverslips were rinsed and mounted on slides using VectaShield mounting medium (Vector Laboratories). Images were collected on a Zeiss Axiophot fluorescence microscope with an AxioCam MRm CCD sensor and analyzed by the Axio Vision release 4.8 software.

4.5.2 Flow cytometric analysis (FACS)

Extracellular and intracellular GARP expression of transiently transfected Cos-7 and CD4+CD25- T cells was investigated by FACS analysis. Twenty-four hours after transfection and after taking off the cell culture supernatant for further analysis, cells were harvested with ice-cold PBS and blocked with 3 % bovine serum albumin (BSA) in PBS for 30 minutes at 4 °C. To permeabilize cells for intracellular staining, cells were resuspended in BD Cytofix/Cytoperm™ solution (Becton Dickinson) and incubated for 20 minutes at 4 °C. After incubation, permeablized cells were washed twice with 1 x BD Perm/Wash™ buffer (centrifugation at 300 x g for 5 minutes) and stained with 5 µl of a mouse allophycocyanine-conjugated anti-human GARP antibody (BioLegend) for 3 hours. For extracellular staining cells were directly incubated with anti-human GARP antibody after blocking and washing the cells two times with PBS supplemented

with 2 mM EDTA and 0.5 % BSA. After antibody staining, cells were washed again with PBS (containing 2 mM EDTA and 0.5 % BSA), resuspended in 100 µl PBS/EDTA/BSA Buffer and analysed with the FC500 Flow cytometer (Beckman Coulter). To verify the transfection efficiency, GFP signals of transfected cells were analysed directly after cell harvest without antibody staining. Data of FACS analysis were analysed with the CXP analysis software (Beckman Coulter). Unstained cells were used as normalization control. Experiments were performed at least 3 times with freshly isolated CD4+CD25- T cells from healthy independent donors. FACS analysis was performed in cooperation with Dr. Agatha Schwarz from the "Universitätsklinikum Schleswig-Holstein" in Kiel.

4.5.3 Enzyme-linked immunosorbent assay (ELISA)

Human soluble GARP from cell culture supernatants of transfected CD4+CD25- cells was analysed by conventional sandwich ELISA using 96-well plates coated with GARP-specific antibody according to the manufacturer's protocol (BioLegend).

4.6 Population and patient-based approaches

4.6.1 Cooperative Health Research in the Region of Augsburg (KORA)

The KORA (Cooperative Health Research in the Region Augsburg) study is a population-based cohort study of 18,000 adults performed in Southern Germany (in and around the city of Augsburg). The focus of the study is to examine the genetic basis and incidence of many chronic diseases (e.g. cardiovascular diseases, diabetes mellitus, allergies and asthma) in the study population (Holle et al. 2005; Wichmann et al. 2005). The KORA study includes four cross-sectional health surveys (S1 – S4), which were performed as five year intervals, since 1984. Two of the surveys (S3 and S4 examined in 1994/1995 and 1999/2001, respectively) have been followed up resulting in the two follow-up studies F3 (2004/2005) and F4 (2006/2008) including 3,988 and 4,227 participants, respectively (Holle et al. 2005). The studies were approved by the Ethics Committee of the Bavarian Medical Association and all participants supplied written informed consent. Expression analysis dependent on lead SNP rs7927894 was assessed in a subset of the KORA F4 study (n=739).

4.6.2 Atopic Dermatitis Biomarker Identification Trial in Omalizumab Usage (Ambitious study)

The Ambitious study (ClinicalTrials.gov identifier: NCT01179529) is an investigator-initiated prospective single-arm observational 28-week trial aimed to identify potential biomarkers for identification of AD patient subgroups that benefit from an anti-IgE treatment with Omalizumab (Xolair®, Novartis). Within the Ambitious study a target population of 20 adults (nine men/eleven women) aged between 23 and 76 were enrolled. Exhaustive description of study desgin, inclusion and exclusion criteria, and patient characteristics are described elsewhere (Hotze et al. 2014). Among others, skin biopsies of lesional and non-lesional skin before and after Omalizumab treatment were collected at the „Klinikum rechts der Isar, Dermatologie/Biederstein, TU München" according to standardized operating procedures. Within the scope of this thesis, skin biospies before treatment were used for allelic expression and genome-wide expression pattern analyses in atopic dermatitis. Controls were recruited at the "Department of Dermatology at the University Hospital, TU München".

4.7 Genome-wide gene expression analysis

4.7.1 Sample Preparation

To investigate genome-wide differences in expression profiles of atopic dermatitis skin biopsies from lesional and non-lesional skin of AD patients (Ambitious study) RNA was isolated using the RNeasy Mini Kit as described above (see 4.3.2). RNA concentration was assed using a NanoDrop 1000 spectrophotometer (PeqLab) and RNA integrity was verified using a RNA 6000 Nano Kit on the Agilent 2100 Bioanalyzer. RNA samples with a RNA integrity number< 5.5 were excluded.

4.7.2 Illumina gene expression analysis

Whole-genome expression profiles were generated with the Illumina HumanHT-12 v4 Expression BeadChip (Illumina) according to the manufacturer's protocol. In brief, 400ng of RNA were reverse transcribed into cDNA followed by second strand synthesis and purification of cDNA. *In vitro* transcription into cRNA and biotin-UTP labeling was performed using the Illumina TotalPrep-96 RNA Amplification Kit (Ambion). 3 µg of labeled cRNA was hybridized to the Illumina HumanHT-12 v4 Expression Bead Chip. Chips were washed, detected, and scanned according to the manufacturer's instructions. Data collection and visualization were performed with the Illumina GenomeStudio 2011.1 Gene Expression Module 1.9.0 software.

4.7.3 Statistical analysis and differential expressed gene (DEG) analysis

For expression analysis, the raw data exported from the Illumina GenomeStudio software were analyzed by R-software. The data were subject to background correction, variance stabilizing transformation and normalization using the quantiles method (Du et al. 2008). Differences in $\log_2$-expression levels between cases and controls were compared using the Welch-test. For comparison of gene expression data within the same individual, the t-test for paired samples was applied. Only transcripts with a fold change (FC) value > 2 and P_{FDR} < 0.05 were selected and considered as genome-wide differentially expressed (DET).

Functional enrichment analyses were performed with DAVID (Huang da et al. 2009) using the following settings: uploaded gene lists displayed the official gene symbol; annotations were limited to those of *Homo sapiens*; DAVID default *Homo sapiens* whole-genome background and pre-built Illumina HumanHT-12_V3 array background were used to identify enriched functional annotations with differentially expressed transcripts such as GO terms (focused on major categories: biological process (bp), cellular compartments (cp) and molecular function (mf)) or KEGG pathways, which were subsequently clustered to groups of functional annotations (functional clusters). For enriched functional annotations Benjamini–Hochberg corrected P values (P_{BH}) were presented and for functional clusters the respective enrichment score (=mean(-$\log_{10}(P_{funct.\ annot.})$)) was calculated. Functional enrichment analysis was restricted to the annotation categories KEGG_PATHWAY, GOTERM_BP (GO Biological Process), GOTERM_CC (GO Cellular Component) and GOTERM_MF (GO Molecular Function). Statistical analysis was performed in cooperation with Dr. Hansjörg Baurecht (Universitätsklinikum Schleswig-Holstein, Hautklinik Kiel).

4.8 Bioinfomatics

4.8.1 DNA sequence analysis

DNA sequence analysis was performed with various tools: BioEdit Sequence Alignment Editor (Ibis Biosciences) was used for visualization of ABI sequencing data shown as electropherograms. The Vector NTI® (Thermo Fisher Scientific) software tool AlignX was used for sequence alignment of sequenced products (e.g. plasmid DNA after cloning insert of interest) with respective reference sequences. Transcriptional regulatory regions like DNase 1 hypersensitivity clusters and promoter- and enhancer-associated histone mark regions (H3K27Ac and H3K4Me1, respectively) were analyzed by using the ENCyclopedia of DNA

Elements (ENCODE) data (Consortium 2004) visualized with the UCSC Genome Browser (Miller et al. 2007).

4.8.2 Transcription factor binding site (TFBS) and promoter analysis

For prediction of allele-specific transcription factor binding sites dependent in the SNPs rs7927894 and rs2155219 surrounding region the Genomatix *SNPInspector* and *MatInspector* software (Cartharius et al. 2005), 2005], that utilizes a library of position weight matrices derived from a large set of known binding sites from several publications, was used. To investigate the native promoters of *C11orf30* and *LRRC32* in the 11q13.5 genomic region, i.e., to identify putative functional promoter sequences, the Genomatix software tool G*ene2Promoter* was used.

5 MATERIAL AND ORGANISMS

5.1 Cell lines

Cell line	Company	Accession number
HeLa	DMSZ	ACC57
Jurkat	DMSZ	ACC282
A-547	DMSZ	ACC107
HaCaT	kindly provided by Anja Uhmann, University Göttingen, Germany	
Cos-7	kindly provided by Dr. Agatha Schwarz, Hautklinik Kiel, Universitätsklinikum Schleswig-Holstein, Germany	

5.2 Bacteria strains

E. coli DH5α (Stratagene)

F- endA1 glnV44 thi-1 recA1 relA1 gyrA96 deoR nupG Φ80d*lacZ*ΔM15 Δ(*lacZYAargF*) U169, hsdR17(rK- mK+), λ–

E. coli TOP10 (Invitrogen)

F- mcrA Δ(mrr-hsdRMS-mcrBC) φ80lacZΔM15 ΔlacX74 nupG recA1 araD139 Δ(ara-leu)7697 galE15 galK16 rpsL(StrR) endA1 λ-

5.3 Genomic clone

IMAGE ID 30344529/AT99 C06 (M13F)   Source BioScience LifeSciences

5.4 Vectors

For detailed vector maps information see Appendix Figure I-IV

pGL4.23[*luc2/minP*]	Promega
pGL4.12[*luc2CP*]	Promega
pGL4.74[*hRluc/TK*]	Promega
pIRES2-AcGFP1	Clontech Laboratories

5.5 Enzymes

5.5.1 General enzymes

Trypsin-EDTA	Gibco
T4 DNA Ligase	New England Biolabs
DNase1	Qiagen
shrimp alkaline phosphatase	usb

5.5.2 Polymerases

Pfu turbo polymerase (2.5 U/µl)	Stratagene
Phusion® High-Fidelity DNA Polymerase	New England Biolabs
GoTaq® DNA Polymerase	Promega

5.5.3 Restriction endonucleases

BglII	New England Biolabs
HindIII	New England Biolabs
KpnI	New England Biolabs
SacI	New England Biolabs

5.6 Marker

GeneRuler 100 bp DNA Ladder	Thermo Fisher Scientific
pUC Mix Marker, 8 (VIII)	Fermentas
PageRuler ™ Prestained Protein Ladder	Thermo Fisher Scientific
Gene Scan™ 120 LIZ® Size standard	Applied Biosystems

5.7 Antibodies

Human antibody	Company	Product-Number
LRRC32, mAb (Plato-1, mouse IgG2b)	Enzo Life Sciences	ALX-804-867
anti-mouse IRDye® 800CW (goat)	Licor	926-32210
anti-GFP (3H9) (rat)	in-house production	
anti-rat IgG (H+L) Alexa Fluor 790 (goat)	Dianova	112-665-143
APC anti-human GARP (LRRC32)	BioLegend	352506

5.8 Chemicals

Chemical	Company
Acetic acid	Merck
Acrylamide	Roth
Agarose	Biozym
Ammoniumperoxidsulphate (APS)	Merck
Ampicillin	Sigma-Aldrich
Ampuwa water	Fresenius Kabi
Bacto-agar	BD Biosciences
Biotin	Sigma-Aldrich
Boric acid	Alfa Aesar
Bovine serum albumin (BSA)	Roth
CellLight® Plasma Membrane-GFP BacMam 2.0	Molecular Probes
Comassie Brilliant Blue G25	Biomol
cOmplete™, EDTA-free Protease Inhibitor	Sigma-Aldrich
Concanavalin A	Sigma-Aldrich
Diethylaminoethyl (DEAE)-dextran	Sigma-Aldrich
Dimethylsulfoxide (DMSO)	Sigma-Aldrich
Difco™ Yeast extract	BD Biosciences
dNTPs	Fermentas
Dithiothreitol (DTT)	Fermentas
DMEM	Gibco
EDTA	Merck
Ethanol	Merck
Fetal bovine serum (FBS Gold)	PAA
Fetal calf serum	PAN Biotech

Fugene6 Transfection Reagent	Promega
L-Glutamine	Invitrogen
LiChrosolv® water for chromatography	Merck
Lymphoprep™	PROGEN Biotechnik GmbH
Glycerol	neoLab
Glycine	Biomol
HEPES	Biomol
Hoechst 33342 dye	Thermo Fisher Scientific
Kanamycin	Sigma-Aldrich
Lipofectamine 2000 Transfection Reagent	Thermo Fisher Scientific
6x Loading Buffer	Fermentas
β-Mercaptoethanol	Sigma-Aldrich
Magnesium chloride	Sigma-Aldrich
Magnesium sulfite	Sigma-Aldrich
MEM	Gibco
Midori Green	Biozym
ODEYSSEY Blocking Buffer	LI-COR
Orange G	Sigma-Aldrich
Penicillin-Streptomycin	Gibco
Phorbol myristate acetate (PMA)	Sigma-Aldrich
Poly[d(I-C)]	Roche Diagnostics
Potassium chloride	Merck
Potassium acetate	Merck
2-Propanol	Merck
Rotriphorese® Gel 40 (37,5:1)/30 (37,5:1)	Roth
RPMI1640	Gibco
SDS	Roth
Sodium chloride	Merck
Sodium phosphate	Merck
Tetramethylethylenediamine (TEMED)	Sigma-Aldrich
TransIT®-Jurkat Transfection Reagent	Mirus
Tris	Merck
Triton X-100	Thermo Fisher Scientific
Trypsin-EDTA	Gibco
VectaShield mounting medium	Vector Laboratories
ViaFect Transfection Reagent	Promega
X-treme GENE 9	Roche Diagnostics

5.9 Consumable supplies

Cellstar plastic pipettes 5 ml/ 10 ml/ 25 ml	Greiner bio-one
Cell scraper	Cyto one
Cover slip 22x22 mm	Roth
Cryo Tube™ Vials	Nunc
Dishes 94/16 with vents (100 mm)	Greiner bio-one
Falcons 15 ml/ 50 ml	BD
Falcon Round-Bottom Tubes	BD
Falcon U-Bottom Plate	BD
Immobilon FL	Millipore
LumiNunc™ 96 well plates	Nunc
Multiwell Plate (6 well, 12 well)	Greiner bio-one
Parafilm M® Laboratory Film	Pechiney Plastic Packaging
PCR softstrips 0.2 ml	Biozym
Pipet Tips Diamond Tower Pack	Gilson
Protein LoBind® tubes	Eppendorf
QIAshredder spin-columns	Qiagen
Safe-Lock Tubes 1.5 ml/ 2.0 ml	Eppendorf
Safe-Lock Tubes 1.5 ml, black	A. Hartenstein
StableStak Racks (20μl, 200μl, 1000μl)	Mettler Toledo
SuperFrost® Plus 25x75x1 mm	Menzel Gläser
TC Flask (T25/T75)	Greiner bio-one

5.10 Kits

ABI PRISM® SNaPshot™ Kit	Applied Biosystems
BCA™ Protein Assay Kit	Thermo Fisher Scientific
BigDye terminator v3.1 cycle Sequencing Kit	Applied Biosystems
CD4+CD25+ Regulatory T Cell Isolation Kit©	Miltenyi Biotec
Dual-Luciferase® Reporter Assay	Promega
HumanHT-12 v4 Expression BeadChip Kit	Illumina
Human Soluble GARP/LRRC32 ELISA Kit	BioLegend
Illumina TotalPrep-96 RNA Amplification Kit	Ambion
Mem-PER Eukaryotic Membrane Protein Extraction Reagent Kit	Pierce Biosciences

Montage™SEQ96 Sequencing Reaction Cleanup Kit	Millipore
Nuclear Extraction Kit	Active Motif
NucleoSpin® Plasmid Kit	Macherey-Nagel
NucleoBond® Xtra Midi Kit	Macherey-Nagel
PAXgene® Blood RNA Kit	Qiagen
QuikChange® Site-directed mutagenesis kit	Stratagene
RevertAid RT Reverse Transcription Kit	Thermo Fisher Scientific
RNeasy® Mini kit	Qiagen
Wizard®SV Gel and PCR Clean-up System	Promega

5.11 Laboratory Equipment

ABI PRISM® 3730 DNA analyzer	Applied Biosystems
AutoMACS® Pro Seperator	Miltenyi Biotec
BeadArray Reader	Illumina
Bio vision Gel documentation	PeqLab
Cellometer® Auto T4	PeqLab
Centrifuge Universal 32R	Hettich Centrifuges
Centrifuge Rotana Typ 3500	Hettich
Duomax 1030	Herdolph Instruments
FC500 Flow cytometer	Beckman Coulter
GenAmp® PCR System 9700	Applied Biosystems
GenesisRSP150	Tecan
GloMax®-Multi Detection System	Promega
Haake K20 + Haake DC10 Kühlbad	ThermoHaake
Heat Sealer ALPS50V	Thermo Fisher Scientific
Heraeus Freso™ 21 centrifuge	Thermo Fisher Scientific
Hybridization oven	Illumina
Hybex Microarray Incubation System	SciGene
Incubator Hera cell	Heraeus Instruments
Jitterbug™ Microplate Incubator Shaker	Boekel Scientific
Laminar Flow HERA safe	Heraeus
Magnetic Stand-96	Ambion
Maxigel System	Biometra
Microscope Primo Vert	Zeiss

Microscope Axiophot	Zeiss
Micropipettes	Rainin
Mikro200	Hettich Centrifuges
Mini-PROTEAN III	BioRad
Mr. Frosty Freezing Container	Thermo Fisher Scientific
NanoDrop ND 1000 Spectrophotometer	PeqLab
ODYSSEY® Infrared Imaging System	LI-COR
pH Meter 766 calimatric	Knick
Power PAC 200/300	BioRad
Precellys® 24 homogenizer	PeqLab
Robocycler 96	Stratagene
Rotanta 46S	Hettich Centrifuges
Semidry Blotter	Biorad
Shaker Innova 4230	New Brunswick Scientific
Special accuracy weighting machine BP2215	Satorius
Standard Power Pack P25 T	Biometra
SubCellR GT electrophoresis chamber	BioRad
Thermomixer comfort	Eppendorf
Scanner Typhoon Trio +	GE Healthcare
UV-VIS Spectrophotometer DU530	Beckman
Vacutainer	Nalgene
Vacuum pump	Millipore
Vortex-Genie® 2	Scientific Industries
Water bath Lauda A100	Lauda
Water bath VWB 12	VWR

5.12 Programs and computer software

5.12.1 Online tools and databases

BioEdit (free alignment program): *http://www.mbio.ncsu.edu/BioEdit/bioedit.html*

BLAST (Basic Local Alignment Search Tool): *http://www.ncbi.nlm.nih.gov/BLAST*

dbSNP (SNP datbase):*http://www.ncbi.nlm.nih.gov/projects/SNP/*

Ensemble Genome Browser: http://www.ensembl.org/index.html

ENCODE (Encyclopedia of DNA elements): http://genome.ucsc.edu/ENCODE/

Genomatix (MatInspector, SNPInspector, gene2promoter): *http://www.genomatix.de/*

HapMap project homepage: *http://www.hapmap.org*

Metabion Oligonucleotide Calculator: *http://www.metabion.com/biocalc/index.html*

NCBI (National center of Biotechnology Information): *http://www.ncbi.nlm.nih.gov/*

SNAP (SNP Annotation and Proxy Search Tool):

http://www.broadinstitute.org/mpg/snap/ldsearch.php

UCSC Genome Bioinformatics Browser: *http://genome.ucsc.edu/*

UniProt (Universal Protein Resource): http://www.uniprot.org/

1000 Genomes: http://www.1000genomes.org/

5.12.2 Computer software

Adobe Illustrator, Adobe

Adobe Photoshop, Adobe

Axio Vision release 4.8 software, Carl Zeiss

CXP analysis software, Beckman Coulter

DNA Baser v3.5.0, Heracle BioSoft (sequence assembly software)

GeneMapper® Version 4.0, Applied Biosystems

GenomeStudio 2011.1 Gene Expression Module 1.9.0 software

GloMax® 96 Microplate Luminometer Software version 1.9.2, Promega

Inkscape 0.48

LIC-COR Odyssey application software v3.0, LI-COR

Microsoft Office 2010

NanoDrop version 3.1.0, NanoDrop Technologies

R-software

VectorNTI, Invitrogen

Vision-Capt, Bioprofil (Gel documentation software)

6 REFERENCES

Agrawal R, Wisniewski JA, Woodfolk JA. 2011. The role of regulatory T cells in atopic dermatitis. *Current problems in dermatology* **41**: 112-124.

Akdis CA, Akdis M, Bieber T, Bindslev-Jensen C, Boguniewicz M, Eigenmann P, Hamid Q, Kapp A, Leung DY, Lipozencic J et al. 2006. Diagnosis and treatment of atopic dermatitis in children and adults: European Academy of Allergology and Clinical Immunology/American Academy of Allergy, Asthma and Immunology/PRACTALL Consensus Report. *Allergy* **61**: 969-987.

Albanesi C, Fairchild HR, Madonna S, Scarponi C, De Pita O, Leung DY, Howell MD. 2007. IL-4 and IL-13 negatively regulate TNF-alpha- and IFN-gamma-induced beta-defensin expression through STAT-6, suppressor of cytokine signaling (SOCS)-1, and SOCS-3. *Journal of immunology* **179**: 984-992.

Alkemade JA, Molhuizen HO, Ponec M, Kempenaar JA, Zeeuwen PL, de Jongh GJ, van Vlijmen-Willems IM, van Erp PE, van de Kerkhof PC, Schalkwijk J. 1994. SKALP/elafin is an inducible proteinase inhibitor in human epidermal keratinocytes. *J Cell Sci* **107** (Pt 8): 2335-2342.

Altinisik J, Karateke A, Coksuer H, Ulutin T, Buyru N. 2011. Expression of EMSY gene in sporadic ovarian cancer. *Molecular biology reports* **38**: 359-363.

Amaral AF, Minelli C, Guerra S, Wjst M, Probst-Hensch N, Pin I, Svanes C, Janson C, Heinrich J, Jarvis DL. 2015. The locus C11orf30 increases susceptibility to poly-sensitization. *Allergy* **70**: 328-333.

Ashcroft DM, Dimmock P, Garside R, Stein K, Williams HC. 2005. Efficacy and tolerability of topical pimecrolimus and tacrolimus in the treatment of atopic dermatitis: meta-analysis of randomised controlled trials. *Bmj* **330**: 516.

Asher MI, Montefort S, Bjorksten B, Lai CK, Strachan DP, Weiland SK, Williams H, Group IPTS. 2006. Worldwide time trends in the prevalence of symptoms of asthma, allergic rhinoconjunctivitis, and eczema in childhood: ISAAC Phases One and Three repeat multicountry cross-sectional surveys. *Lancet* **368**: 733-743.

Ballardini N, Kull I, Soderhall C, Lilja G, Wickman M, Wahlgren CF. 2013. Eczema severity in preadolescent children and its relation to sex, filaggrin mutations, asthma, rhinitis, aggravating factors and topical treatment: a report from the BAMSE birth cohort. *The British journal of dermatology* **168**: 588-594.

Banchereau J, Pascual V, O'Garra A. 2012a. From IL-2 to IL-37: the expanding spectrum of anti-inflammatory cytokines. *Nature immunology* **13**: 925-931.

Banchereau J, Pascual V, O'Garra A. 2012b. From IL-2 to IL-37: the expanding spectrum of anti-inflammatory cytokines. *Nature immunology* **13**: 925-931.

Bao L, Shi VY, Chan LS. 2013. IL-4 up-regulates epidermal chemotactic, angiogenic, and pro-inflammatory genes and down-regulates antimicrobial genes in vivo and in vitro: relevant in the pathogenesis of atopic dermatitis. *Cytokine* **61**: 419-425.

Bao L, Zhang H, Mohan GC, Shen K, Chan LS. 2016. Differential expression of inflammation-related genes in IL-4 transgenic mice before and after the onset of atopic dermatitis skin lesions. *Mol Cell Probes* **30**: 30-38.

Barnes KC. 2010. An update on the genetics of atopic dermatitis: scratching the surface in 2009. *The Journal of allergy and clinical immunology* **125**: 16-29 e11-11; quiz 30-11.

Barrett JC, Hansoul S, Nicolae DL, Cho JH, Duerr RH, Rioux JD, Brant SR, Silverberg MS, Taylor KD, Barmada MM et al. 2008. Genome-wide association defines more than 30 distinct susceptibility loci for Crohn's disease. *Nature genetics* **40**: 955-962.

Baurecht H, Hotze M, Brand S, Buning C, Cormican P, Corvin A, Ellinghaus D, Ellinghaus E, Esparza-Gordillo J, Folster-Holst R et al. 2015. Genome-wide comparative analysis of atopic dermatitis and psoriasis gives insight into opposing genetic mechanisms. *American journal of human genetics* **96**: 104-120.

Baurecht H, Irvine AD, Novak N, Illig T, Buhler B, Ring J, Wagenpfeil S, Weidinger S. 2007. Toward a major risk factor for atopic eczema: meta-analysis of filaggrin polymorphism data. *The Journal of allergy and clinical immunology* **120**: 1406-1412.

Beck LA, Boguniewicz M, Hata T, Schneider LC, Hanifin J, Gallo R, Paller AS, Lieff S, Reese J, Zaccaro D et al. 2009. Phenotype of atopic dermatitis subjects with a history of eczema herpeticum. *The Journal of allergy and clinical immunology* **124**: 260-269, 269 e261-267.

Berulava T, Horsthemke B. 2010. The obesity-associated SNPs in intron 1 of the FTO gene affect primary transcript levels. *European journal of human genetics : EJHG* **18**: 1054-1056.

Bieber T. 2008. Atopic dermatitis. *The New England journal of medicine* **358**: 1483-1494.

Bieber T. 2010. Atopic dermatitis. *Annals of dermatology* **22**: 125-137.

Bin L, Howell MD, Kim BE, Streib JE, Hall CF, Leung DY. 2011a. Specificity protein 1 is pivotal in the skin's antiviral response. *The Journal of allergy and clinical immunology* **127**: 430-438 e431-432.

Bin L, Kim BE, Hall CF, Leach SM, Leung DY. 2011b. Inhibition of transcription factor specificity protein 1 alters the gene expression profile of keratinocytes leading to upregulation of kallikrein-related peptidases and thymic stromal lymphopoietin. *The Journal of investigative dermatology* **131**: 2213-2222.

Bin L, Leung DY. 2016. Genetic and epigenetic studies of atopic dermatitis. *Allergy Asthma Clin Immunol* **12**: 52.

Birben E, Sackesen C, Turgutoglu N, Kalayci O. 2012. The role of SPINK5 in asthma related physiological events in the airway epithelium. *Respiratory medicine* **106**: 349-355.

Boguniewicz M, Leung DY. 2010. Recent insights into atopic dermatitis and implications for management of infectious complications. *The Journal of allergy and clinical immunology* **125**: 4-13; quiz 14-15.

Boguniewicz M, Leung DY. 2011. Atopic dermatitis: a disease of altered skin barrier and immune dysregulation. *Immunological reviews* **242**: 233-246.

Bonnelykke K, Matheson MC, Pers TH, Granell R, Strachan DP, Alves AC, Linneberg A, Curtin JA, Warrington NM, Standl M et al. 2013. Meta-analysis of genome-wide association studies identifies ten loci influencing allergic sensitization. *Nature genetics* **45**: 902-906.

Boron WF. 2004. Regulation of intracellular pH. *Adv Physiol Educ* **28**: 160-179.

Boukamp P, Petrussevska RT, Breitkreutz D, Hornung J, Markham A, Fusenig NE. 1988. Normal keratinization in a spontaneously immortalized aneuploid human keratinocyte cell line. *The Journal of cell biology* **106**: 761-771.

Briggs MR, Kadonaga JT, Bell SP, Tjian R. 1986. Purification and biochemical characterization of the promoter-specific transcription factor, Sp1. *Science* **234**: 47-52.

Brown LA, Irving J, Parker R, Kim H, Press JZ, Longacre TA, Chia S, Magliocco A, Makretsov N, Gilks B et al. 2006. Amplification of EMSY, a novel oncogene on 11q13, in high grade ovarian surface epithelial carcinomas. *Gynecologic oncology* **100**: 264-270.

Bruder D, Probst-Kepper M, Westendorf AM, Geffers R, Beissert S, Loser K, von Boehmer H, Buer J, Hansen W. 2004. Neuropilin-1: a surface marker of regulatory T cells. *European journal of immunology* **34**: 623-630.

Brussow H. 2015. Turning the inside out: The microbiology of atopic dermatitis. *Environmental microbiology* doi:10.1111/1462-2920.13050.

Burton MJ, Rajak SN, Bauer J, Weiss HA, Tolbert SB, Shoo A, Habtamu E, Manjurano A, Emerson PM, Mabey DC et al. 2011. Conjunctival transcriptome in scarring trachoma. *Infect Immun* **79**: 499-511.

Callard RE, Harper JI. 2007. The skin barrier, atopic dermatitis and allergy: a role for Langerhans cells? *Trends in immunology* **28**: 294-298.

Cardona ID, Goleva E, Ou LS, Leung DY. 2006. Staphylococcal enterotoxin B inhibits regulatory T cells by inducing glucocorticoid-induced TNF receptor-related protein ligand on monocytes. *The Journal of allergy and clinical immunology* **117**: 688-695.

Cargill M, Altshuler D, Ireland J, Sklar P, Ardlie K, Patil N, Shaw N, Lane CR, Lim EP, Kalyanaraman N et al. 1999. Characterization of single-nucleotide polymorphisms in coding regions of human genes. *Nature genetics* **22**: 231-238.

Carregaro F, Stefanini AC, Henrique T, Tajara EH. 2013. Study of small proline-rich proteins (SPRRs) in health and disease: a review of the literature. *Archives of dermatological research* **305**: 857-866.

Carrillo-Galvez AB, Cobo M, Cuevas-Ocana S, Gutierrez-Guerrero A, Sanchez-Gilabert A, Bongarzone P, Garcia-Perez A, Munoz P, Benabdellah K, Toscano MG et al. 2015. Mesenchymal stromal cells express GARP/LRRC32 on their surface: effects on their biology and immunomodulatory capacity. *Stem Cells* **33**: 183-195.

Cartharius K, Frech K, Grote K, Klocke B, Haltmeier M, Klingenhoff A, Frisch M, Bayerlein M, Werner T. 2005. MatInspector and beyond: promoter analysis based on transcription factor binding sites. *Bioinformatics* **21**: 2933-2942.

Cavani A, Albanesi C, Traidl C, Sebastiani S, Girolomoni G. 2001. Effector and regulatory T cells in allergic contact dermatitis. *Trends in immunology* **22**: 118-120.

Cavani A, Pennino D, Eyerich K. 2012. Th17 and Th22 in skin allergy. *Chemical immunology and allergy* **96**: 39-44.

Chen R, Jiang X, Sun D, Han G, Wang F, Ye M, Wang L, Zou H. 2009. Glycoproteomics analysis of human liver tissue by combination of multiple enzyme digestion and hydrazide chemistry. *Journal of proteome research* **8**: 651-661.

Christensen U, Moller-Larsen S, Nyegaard M, Haagerup A, Hedemand A, Brasch-Andersen C, Kruse TA, Corydon TJ, Deleuran M, Borglum AD. 2009. Linkage of atopic dermatitis to chromosomes 4q22, 3p24 and 3q21. *Human genetics* **126**: 549-557.

Collins FS, Drumm ML, Cole JL, Lockwood WK, Vande Woude GF, Iannuzzi MC. 1987. Construction of a general human chromosome jumping library, with application to cystic fibrosis. *Science* **235**: 1046-1049.

Consortium EP. 2004. The ENCODE (ENCyclopedia Of DNA Elements) Project. *Science* **306**: 636-640.

Consortium EP. 2011. A user's guide to the encyclopedia of DNA elements (ENCODE). *PLoS biology* **9**: e1001046.

Consortium EP. 2012. An integrated encyclopedia of DNA elements in the human genome. *Nature* **489**: 57-74.

Cookson WO. 2001. The genetics of atopic dermatitis: strategies, candidate genes, and genome screens. *Journal of the American Academy of Dermatology* **45**: S7-9.

Corbel C, Lemarchandel V, Thomas-Vaslin V, Pelus AS, Agboton C, Romeo PH. 2007. Neuropilin 1 and CD25 co-regulation during early murine thymic differentiation. *Dev Comp Immunol* **31**: 1082-1094.

Correa da Rosa J, Malajian D, Shemer A, Rozenblit M, Dhingra N, Czarnowicki T, Khattri S, Ungar B, Finney R, Xu H et al. 2015. Patients with atopic dermatitis have attenuated and distinct contact hypersensitivity responses to common allergens in skin. *J Allergy Clin Immunol* **135**: 712-720.

Cuende J, Lienart S, Dedobbeleer O, van der Woning B, De Boeck G, Stockis J, Huygens C, Colau D, Somja J, Delvenne P et al. 2015. Monoclonal antibodies against GARP/TGF-beta1 complexes inhibit the immunosuppressive activity of human regulatory T cells in vivo. *Sci Transl Med* **7**: 284ra256.

d'Hennezel E, Bin Dhuban K, Torgerson T, Piccirillo CA. 2012. The immunogenetics of immune dysregulation, polyendocrinopathy, enteropathy, X linked (IPEX) syndrome. *Journal of medical genetics* **49**: 291-302.

Darsow U, Wollenberg A, Simon D, Taieb A, Werfel T, Oranje A, Gelmetti C, Svensson A, Deleuran M, Calza AM et al. 2010. ETFAD/EADV eczema task force 2009 position paper on diagnosis and treatment of atopic dermatitis. *Journal of the European Academy of Dermatology and Venereology : JEADV* **24**: 317-328.

De Heller-Milev M, Huber M, Panizzon R, Hohl D. 2000. Expression of small proline rich proteins in neoplastic and inflammatory skin diseases. *The British journal of dermatology* **143**: 733-740.

de Jongh GJ, Zeeuwen PL, Kucharekova M, Pfundt R, van der Valk PG, Blokx W, Dogan A, Hiemstra PS, van de Kerkhof PC, Schalkwijk J. 2005. High expression levels of keratinocyte

antimicrobial proteins in psoriasis compared with atopic dermatitis. *The Journal of investigative dermatology* **125**: 1163-1173.

Deckers IA, McLean S, Linssen S, Mommers M, van Schayck CP, Sheikh A. 2012. Investigating international time trends in the incidence and prevalence of atopic eczema 1990-2010: a systematic review of epidemiological studies. *PloS one* **7**: e39803.

Dehouck Y, Kwasigroch JM, Gilis D, Rooman M. 2011. PoPMuSiC 2.1: a web server for the estimation of protein stability changes upon mutation and sequence optimality. *BMC Bioinformatics* **12**: 151.

Dimas AS, Deutsch S, Stranger BE, Montgomery SB, Borel C, Attar-Cohen H, Ingle C, Beazley C, Gutierrez Arcelus M, Sekowska M et al. 2009. Common regulatory variation impacts gene expression in a cell type-dependent manner. *Science* **325**: 1246-1250.

Dinkel H, Michael S, Weatheritt RJ, Davey NE, Van Roey K, Altenberg B, Toedt G, Uyar B, Seiler M, Budd A et al. 2012. ELM--the database of eukaryotic linear motifs. *Nucleic acids research* **40**: D242-251.

Du P, Kibbe WA, Lin SM. 2008. lumi: a pipeline for processing Illumina microarray. *Bioinformatics* **24**: 1547-1548.

Eberlein-Konig B, Schafer T, Huss-Marp J, Darsow U, Mohrenschlager M, Herbert O, Abeck D, Kramer U, Behrendt H, Ring J. 2000. Skin surface pH, stratum corneum hydration, trans-epidermal water loss and skin roughness related to atopic eczema and skin dryness in a population of primary school children. *Acta dermato-venereologica* **80**: 188-191.

Eckert RL, Broome AM, Ruse M, Robinson N, Ryan D, Lee K. 2004. S100 proteins in the epidermis. *The Journal of investigative dermatology* **123**: 23-33.

Edwards JP, Fujii H, Zhou AX, Creemers J, Unutmaz D, Shevach EM. 2013. Regulation of the expression of GARP/latent TGF-beta1 complexes on mouse T cells and their role in regulatory T cell and Th17 differentiation. *Journal of immunology* **190**: 5506-5515.

Eichenfield LF, Hanifin JM, Luger TA, Stevens SR, Pride HB. 2003. Consensus conference on pediatric atopic dermatitis. *Journal of the American Academy of Dermatology* **49**: 1088-1095.

Ellinghaus D, Baurecht H, Esparza-Gordillo J, Rodriguez E, Matanovic A, Marenholz I, Hubner N, Schaarschmidt H, Novak N, Michel S et al. 2013. High-density genotyping study identifies four new susceptibility loci for atopic dermatitis. *Nature genetics* **45**: 808-812.

Elmose C, Thomsen SF. 2015. Twin Studies of Atopic Dermatitis: Interpretations and Applications in the Filaggrin Era. *Journal of allergy* **2015**: 902359.

Esparza-Gordillo J, Marenholz I, Lee YA. 2010. Genome-wide approaches to the etiology of eczema. *Current opinion in allergy and clinical immunology* **10**: 418-426.

Esparza-Gordillo J, Weidinger S, Folster-Holst R, Bauerfeind A, Ruschendorf F, Patone G, Rohde K, Marenholz I, Schulz F, Kerscher T et al. 2009. A common variant on chromosome 11q13 is associated with atopic dermatitis. *Nature genetics* **41**: 596-601.

Eyerich K, Novak N. 2013. Immunology of atopic eczema: overcoming the Th1/Th2 paradigm. *Allergy* **68**: 974-982.

Eyerich K, Pennino D, Scarponi C, Foerster S, Nasorri F, Behrendt H, Ring J, Traidl-Hoffmann C, Albanesi C, Cavani A. 2009. IL-17 in atopic eczema: linking allergen-specific adaptive and microbial-triggered innate immune response. *The Journal of allergy and clinical immunology* **123**: 59-66 e54.

Eyerich S, Zielinski CE. 2014. Defining Th-cell subsets in a classical and tissue-specific manner: Examples from the skin. *European journal of immunology* **44**: 3475-3483.

Ezell SA, Tsichlis PN. 2012. Akt1, EMSY, BRCA2 and type I IFN signaling: a novel arm of the IFN response. *Transcription* **3**: 305-309.

Fardet L, Kassar A, Cabane J, Flahault A. 2007. Corticosteroid-induced adverse events in adults: frequency, screening and prevention. *Drug safety* **30**: 861-881.

Ferreira MA, Matheson MC, Duffy DL, Marks GB, Hui J, Le Souef P, Danoy P, Baltic S, Nyholt DR, Jenkins M et al. 2011. Identification of IL6R and chromosome 11q13.5 as risk loci for asthma. *Lancet* **378**: 1006-1014.

Freedman ML, Monteiro AN, Gayther SA, Coetzee GA, Risch A, Plass C, Casey G, De Biasi M, Carlson C, Duggan D et al. 2011. Principles for the post-GWAS functional characterization of cancer risk loci. *Nature genetics* **43**: 513-518.

Fridrich S, Hahn SA, Linzmaier M, Felten M, Zwarg J, Lennerz V, Tuettenberg A, Stocker W. 2016. How Soluble GARP Enhances TGFbeta Activation. *PloS one* **11**: e0153290.

Frischmeyer-Guerrerio PA, Guerrerio AL, Oswald G, Chichester K, Myers L, Halushka MK, Oliva-Hemker M, Wood RA, Dietz HC. 2013. TGFbeta receptor mutations impose a strong predisposition for human allergic disease. *Sci Transl Med* **5**: 195ra194.

Fu J, Wolfs MG, Deelen P, Westra HJ, Fehrmann RS, Te Meerman GJ, Buurman WA, Rensen SS, Groen HJ, Weersma RK et al. 2012. Unraveling the regulatory mechanisms underlying tissue-dependent genetic variation of gene expression. *PLoS genetics* **8**: e1002431.

Fujitani Y, Kanaoka Y, Aritake K, Uodome N, Okazaki-Hatake K, Urade Y. 2002. Pronounced eosinophilic lung inflammation and Th2 cytokine release in human lipocalin-type prostaglandin D synthase transgenic mice. *Journal of immunology* **168**: 443-449.

Gabriel SB, Schaffner SF, Nguyen H, Moore JM, Roy J, Blumenstiel B, Higgins J, DeFelice M, Lochner A, Faggart M et al. 2002. The structure of haplotype blocks in the human genome. *Science* **296**: 2225-2229.

Ganem MB, De Marzi MC, Fernandez-Lynch MJ, Jancic C, Vermeulen M, Geffner J, Mariuzza RA, Fernandez MM, Malchiodi EL. 2013. Uptake and intracellular trafficking of superantigens in dendritic cells. *PloS one* **8**: e66244.

Gao PS, Rafaels NM, Hand T, Murray T, Boguniewicz M, Hata T, Schneider L, Hanifin JM, Gallo RL, Gao L et al. 2009. Filaggrin mutations that confer risk of atopic dermatitis confer greater risk for eczema herpeticum. *The Journal of allergy and clinical immunology* **124**: 507-513, 513 e501-507.

Gao PS, Rafaels NM, Mu D, Hand T, Murray T, Boguniewicz M, Hata T, Schneider L, Hanifin JM, Gallo RL et al. 2010. Genetic variants in thymic stromal lymphopoietin are associated with atopic dermatitis and eczema herpeticum. *The Journal of allergy and clinical immunology* **125**: 1403-1407 e1404.

Garmhausen D, Hagemann T, Bieber T, Dimitriou I, Fimmers R, Diepgen T, Novak N. 2013. Characterization of different courses of atopic dermatitis in adolescent and adult patients. *Allergy* **68**: 498-506.

Gauthy E, Cuende J, Stockis J, Huygens C, Lethe B, Collet JF, Bommer G, Coulie PG, Lucas S. 2013. GARP is regulated by miRNAs and controls latent TGF-beta1 production by human regulatory T cells. *PloS one* **8**: e76186.

Geers C, Gros G. 2000. Carbon dioxide transport and carbonic anhydrase in blood and muscle. *Physiol Rev* **80**: 681-715.

Genomes Project C, Auton A, Brooks LD, Durbin RM, Garrison EP, Kang HM, Korbel JO, Marchini JL, McCarthy S, McVean GA et al. 2015. A global reference for human genetic variation. *Nature* **526**: 68-74.

Giard DJ, Aaronson SA, Todaro GJ, Arnstein P, Kersey JH, Dosik H, Parks WP. 1973. In vitro cultivation of human tumors: establishment of cell lines derived from a series of solid tumors. *Journal of the National Cancer Institute* **51**: 1417-1423.

Gibbs S, Fijneman R, Wiegant J, van Kessel AG, van De Putte P, Backendorf C. 1993. Molecular characterization and evolution of the SPRR family of keratinocyte differentiation markers encoding small proline-rich proteins. *Genomics* **16**: 630-637.

Gierl MS, Karoulias N, Wende H, Strehle M, Birchmeier C. 2006. The zinc-finger factor Insm1 (IA-1) is essential for the development of pancreatic beta cells and intestinal endocrine cells. *Genes & development* **20**: 2465-2478.

Gittler JK, Shemer A, Suarez-Farinas M, Fuentes-Duculan J, Gulewicz KJ, Wang CQ, Mitsui H, Cardinale I, de Guzman Strong C, Krueger JG et al. 2012. Progressive activation of T(H)2/T(H)22 cytokines and selective epidermal proteins characterizes acute and chronic atopic dermatitis. *J Allergy Clin Immunol* **130**: 1344-1354.

Glaser R, Meyer-Hoffert U, Harder J, Cordes J, Wittersheim M, Kobliakova J, Folster-Holst R, Proksch E, Schroder JM, Schwarz T. 2009. The antimicrobial protein psoriasin (S100A7)

is upregulated in atopic dermatitis and after experimental skin barrier disruption. *The Journal of investigative dermatology* **129**: 641-649.

Glazier AM, Nadeau JH, Aitman TJ. 2002. Finding genes that underlie complex traits. *Science* **298**: 2345-2349.

Graessel A, Hauck SM, von Toerne C, Kloppmann E, Goldberg T, Koppensteiner H, Schindler M, Knapp B, Krause L, Dietz K et al. 2015. A Combined Omics Approach to Generate the Surface Atlas of Human Naive CD4+ T Cells during Early T-Cell Receptor Activation. *Mol Cell Proteomics* **14**: 2085-2102.

Greisenegger EK, Zimprich F, Zimprich A, Gleiss A, Kopp T. 2013. Association of the chromosome 11q13.5 variant with atopic dermatitis in Austrian patients. *European journal of dermatology : EJD* **23**: 142-145.

Gresch O, Engel FB, Nesic D, Tran TT, England HM, Hickman ES, Korner I, Gan L, Chen S, Castro-Obregon S et al. 2004. New non-viral method for gene transfer into primary cells. *Methods* **33**: 151-163.

Griffiths CE, van de Kerkhof P, Czarnecka-Operacz M. 2017. Psoriasis and Atopic Dermatitis. *Dermatol Ther (Heidelb)* **7**: 31-41.

Gruber R, Elias PM, Crumrine D, Lin TK, Brandner JM, Hachem JP, Presland RB, Fleckman P, Janecke AR, Sandilands A et al. 2011. Filaggrin genotype in ichthyosis vulgaris predicts abnormalities in epidermal structure and function. *The American journal of pathology* **178**: 2252-2263.

Guilloud-Bataille M, Bouzigon E, Annesi-Maesano I, Bousquet J, Charpin D, Gormand F, Hochez J, Just J, Lemainque A, Le Moual N et al. 2008. Evidence for linkage of a new region (11p14) to eczema and allergic diseases. *Human genetics* **122**: 605-614.

Gulick T. 2001. Transfection using DEAE-dextran. *Current protocols in molecular biology / edited by Frederick M Ausubel [et al]* **Chapter 9**: Unit9 2.

Haagerup A, Bjerke T, Schiotz PO, Dahl R, Binderup HG, Tan Q, Kruse TA. 2004. Atopic dermatitis -- a total genome-scan for susceptibility genes. *Acta dermato-venereologica* **84**: 346-352.

Hachem JP, Crumrine D, Fluhr J, Brown BE, Feingold KR, Elias PM. 2003. pH directly regulates epidermal permeability barrier homeostasis, and stratum corneum integrity/cohesion. *The Journal of investigative dermatology* **121**: 345-353.

Hahn SA, Neuhoff A, Landsberg J, Schupp J, Eberts D, Leukel P, Bros M, Weilbaecher M, Schuppan D, Grabbe S et al. 2016. A key role of GARP in the immune suppressive tumor microenvironment. *Oncotarget* doi:10.18632/oncotarget.9598.

Hahn SA, Stahl HF, Becker C, Correll A, Schneider FJ, Tuettenberg A, Jonuleit H. 2013. Soluble GARP has potent antiinflammatory and immunomodulatory impact on human CD4(+) T cells. *Blood* **122**: 1182-1191.

Hamid Q, Boguniewicz M, Leung DY. 1994. Differential in situ cytokine gene expression in acute versus chronic atopic dermatitis. *J Clin Invest* **94**: 870-876.

Hanifin JR, G. 1980. Diagnostic features of atopic dermatitis. *Acta Dermato-Venereologica (Stockh)* **92**: 44-47.

Hardy J, Singleton A. 2009. Genomewide association studies and human disease. *The New England journal of medicine* **360**: 1759-1768.

Hassan AS, Kaelin U, Braathen LR, Yawalkar N. 2007. Clinical and immunopathologic findings during treatment of recalcitrant atopic eczema with efalizumab. *Journal of the American Academy of Dermatology* **56**: 217-221.

He JQ, Chan-Yeung M, Becker AB, Dimich-Ward H, Ferguson AC, Manfreda J, Watson WT, Sandford AJ. 2003. Genetic variants of the IL13 and IL4 genes and atopic diseases in at-risk children. *Genes and immunity* **4**: 385-389.

Heintzman ND, Stuart RK, Hon G, Fu Y, Ching CW, Hawkins RD, Barrera LO, Van Calcar S, Qu C, Ching KA et al. 2007. Distinct and predictive chromatin signatures of transcriptional promoters and enhancers in the human genome. *Nature genetics* **39**: 311-318.

Hekkelman ML, Te Beek TA, Pettifer SR, Thorne D, Attwood TK, Vriend G. 2010. WIWS: a protein structure bioinformatics Web service collection. *Nucleic acids research* **38**: W719-723.

Hershey GK, Friedrich MF, Esswein LA, Thomas ML, Chatila TA. 1997. The association of atopy with a gain-of-function mutation in the alpha subunit of the interleukin-4 receptor. *The New England journal of medicine* **337**: 1720-1725.

Hirota T, Takahashi A, Kubo M, Tsunoda T, Tomita K, Sakashita M, Yamada T, Fujieda S, Tanaka S, Doi S et al. 2012. Genome-wide association study identifies eight new susceptibility loci for atopic dermatitis in the Japanese population. *Nature genetics* **44**: 1222-1226.

Hirschhorn JN. 2005. Genetic approaches to studying common diseases and complex traits. *Pediatric research* **57**: 74R-77R.

Hoare C, Li Wan Po A, Williams H. 2000. Systematic review of treatments for atopic eczema. *Health technology assessment* **4**: 1-191.

Hoffjan S, Stemmler S. 2015. Unravelling the complex genetic background of atopic dermatitis: from genetic association results towards novel therapeutic strategies. *Archives of dermatological research* **307**: 659-670.

Holle R, Happich M, Lowel H, Wichmann HE, Group MKS. 2005. KORA--a research platform for population based health research. *Gesundheitswesen* **67 Suppl 1**: S19-25.

Hotze M, Baurecht H, Rodriguez E, Chapman-Rothe N, Ollert M, Folster-Holst R, Adamski J, Illig T, Ring J, Weidinger S. 2014. Increased efficacy of omalizumab in atopic dermatitis patients with wild-type filaggrin status and higher serum levels of phosphatidylcholines. *Allergy* **69**: 132-135.

Howell MD. 2007. The role of human beta defensins and cathelicidins in atopic dermatitis. *Current opinion in allergy and clinical immunology* **7**: 413-417.

Howell MD, Boguniewicz M, Pastore S, Novak N, Bieber T, Girolomoni G, Leung DY. 2006. Mechanism of HBD-3 deficiency in atopic dermatitis. *Clinical immunology* **121**: 332-338.

Howell MD, Fairchild HR, Kim BE, Bin L, Boguniewicz M, Redzic JS, Hansen KC, Leung DY. 2008. Th2 cytokines act on S100/A11 to downregulate keratinocyte differentiation. *The Journal of investigative dermatology* **128**: 2248-2258.

Howell MD, Kim BE, Gao P, Grant AV, Boguniewicz M, DeBenedetto A, Schneider L, Beck LA, Barnes KC, Leung DY. 2009. Cytokine modulation of atopic dermatitis filaggrin skin expression. *The Journal of allergy and clinical immunology* **124**: R7-R12.

Howell MD, Parker ML, Mustelin T, Ranade K. 2015. Past, present, and future for biologic intervention in atopic dermatitis. *Allergy* **70**: 887-896.

Huang da W, Sherman BT, Lempicki RA. 2009. Systematic and integrative analysis of large gene lists using DAVID bioinformatics resources. *Nature protocols* **4**: 44-57.

Hunter DJ, Kraft P. 2007. Drinking from the fire hose--statistical issues in genomewide association studies. *The New England journal of medicine* **357**: 436-439.

Hwang J, Son KN, Kim CW, Ko J, Na DS, Kwon BS, Gho YS, Kim J. 2005. Human CC chemokine CCL23, a ligand for CCR1, induces endothelial cell migration and promotes angiogenesis. *Cytokine* **30**: 254-263.

Illi S, von Mutius E, Lau S, Nickel R, Gruber C, Niggemann B, Wahn U, Multicenter Allergy Study G. 2004. The natural course of atopic dermatitis from birth to age 7 years and the association with asthma. *The Journal of allergy and clinical immunology* **113**: 925-931.

International HapMap C. 2005. A haplotype map of the human genome. *Nature* **437**: 1299-1320.

Irvine AD, McLean WH, Leung DY. 2011. Filaggrin mutations associated with skin and allergic diseases. *The New England journal of medicine* **365**: 1315-1327.

Ishikawa J, Narita H, Kondo N, Hotta M, Takagi Y, Masukawa Y, Kitahara T, Takema Y, Koyano S, Yamazaki S et al. 2010. Changes in the ceramide profile of atopic dermatitis patients. *The Journal of investigative dermatology* **130**: 2511-2514.

Islam SA, Luster AD. 2012. T cell homing to epithelial barriers in allergic disease. *Nat Med* **18**: 705-715.

Jarzab J, Filipowska B, Ebracka J, Kowalska M, Bozek A, Rachowska R, Gubala E, Grzanka A, Hadas E, Jarzab B. 2009. Locus 1q21 gene expression changes in atopic dermatitis skin lesions: deregulation of SPRR1A. *Allergy* **64**: 512-512.

Jensen FC, Girardi AJ, Gilden RV, Koprowski H. 1964. Infection of Human and Simian Tissue Cultures with Rous Sarcoma Virus. *Proceedings of the National Academy of Sciences of the United States of America* **52**: 53-59.

Jensen JM, Folster-Holst R, Baranowsky A, Schunck M, Winoto-Morbach S, Neumann C, Schutze S, Proksch E. 2004. Impaired sphingomyelinase activity and epidermal differentiation in atopic dermatitis. *The Journal of investigative dermatology* **122**: 1423-1431.

Jensen JM, Proksch E. 2009. The skin's barrier. *Giornale italiano di dermatologia e venereologia : organo ufficiale, Societa italiana di dermatologia e sifilografia* **144**: 689-700.

Jin S, Park CO, Shin JU, Noh JY, Lee YS, Lee NR, Kim HR, Noh S, Lee Y, Lee JH et al. 2014. DAMP molecules S100A9 and S100A8 activated by IL-17A and house-dust mites are increased in atopic dermatitis. *Experimental dermatology* **23**: 938-941.

Jungersted JM, Scheer H, Mempel M, Baurecht H, Cifuentes L, Hogh JK, Hellgren LI, Jemec GB, Agner T, Weidinger S. 2010. Stratum corneum lipids, skin barrier function and filaggrin mutations in patients with atopic eczema. *Allergy* **65**: 911-918.

Jutel M, Akdis CA. 2008. T-cell regulatory mechanisms in specific immunotherapy. *Chemical immunology and allergy* **94**: 158-177.

Jutel M, Akdis CA. 2011. T-cell subset regulation in atopy. *Current allergy and asthma reports* **11**: 139-145.

Kabesch M, Schedel M, Carr D, Woitsch B, Fritzsch C, Weiland SK, von Mutius E. 2006. IL-4/IL-13 pathway genetics strongly influence serum IgE levels and childhood asthma. *The Journal of allergy and clinical immunology* **117**: 269-274.

Kadonaga JT, Carner KR, Masiarz FR, Tjian R. 1987. Isolation of cDNA encoding transcription factor Sp1 and functional analysis of the DNA binding domain. *Cell* **51**: 1079-1090.

Kaiser HB. 2004. Risk factors in allergy/asthma. *Allergy and asthma proceedings : the official journal of regional and state allergy societies* **25**: 7-10.

Kamsteeg M, Zeeuwen PL, de Jongh GJ, Rodijk-Olthuis D, Zeeuwen-Franssen ME, van Erp PE, Schalkwijk J. 2007. Increased expression of carbonic anhydrase II (CA II) in lesional skin of atopic dermatitis: regulation by Th2 cytokines. *The Journal of investigative dermatology* **127**: 1786-1789.

Kayserova J, Sismova K, Zentsova-Jaresova I, Katina S, Vernerova E, Polouckova A, Capkova S, Malinova V, Striz I, Sediva A. 2012. A prospective study in children with a severe form of atopic dermatitis: clinical outcome in relation to cytokine gene polymorphisms. *Journal of investigational allergology & clinical immunology* **22**: 92-101.

Kelhala HL, Palatsi R, Fyhrquist N, Lehtimaki S, Vayrynen JP, Kallioinen M, Kubin ME, Greco D, Tasanen K, Alenius H et al. 2014. IL-17/Th17 pathway is activated in acne lesions. *PLoS One* **9**: e105238.

Kezic S, Novak N, Jakasa I, Jungersted JM, Simon M, Brandner JM, Middelkamp-Hup MA, Weidinger S. 2014. Skin barrier in atopic dermatitis. *Frontiers in bioscience* **19**: 542-556.

Kniep EM, Roehlecke C, Ozkucur N, Steinberg A, Reber F, Knels L, Funk RH. 2006. Inhibition of apoptosis and reduction of intracellular pH decrease in retinal neural cell cultures by a blocker of carbonic anhydrase. *Invest Ophthalmol Vis Sci* **47**: 1185-1192.

Knight JC. 2003. Functional implications of genetic variation in non-coding DNA for disease susceptibility and gene regulation. *Clinical science* **104**: 493-501.

Knight JC. 2006. Analysis of allele-specific gene expression. *Methods in molecular biology* **338**: 153-165.

Koizumi H, Kartasova T, Tanaka H, Ohkawara A, Kuroki T. 1996. Differentiation-associated localization of small proline-rich protein in normal and diseased human skin. *The British journal of dermatology* **134**: 686-692.

Kong HH, Oh J, Deming C, Conlan S, Grice EA, Beatson MA, Nomicos E, Polley EC, Komarow HD, Program NCS et al. 2012. Temporal shifts in the skin microbiome associated with disease flares and treatment in children with atopic dermatitis. *Genome research* **22**: 850-859.

Kopfnagel V, Harder J, Werfel T. 2013. Expression of antimicrobial peptides in atopic dermatitis and possible immunoregulatory functions. *Current opinion in allergy and clinical immunology* **13**: 531-536.

Kottgen A Albrecht E Teumer A Vitart V Krumsiek J Hundertmark C Pistis G Ruggiero D O'Seaghdha CM Haller T et al. 2013. Genome-wide association analyses identify 18 new loci associated with serum urate concentrations. *Nature genetics* **45**: 145-154.

Krawczak M, Nikolaus S, von Eberstein H, Croucher PJ, El Mokhtari NE, Schreiber S. 2006. PopGen: population-based recruitment of patients and controls for the analysis of complex genotype-phenotype relationships. *Community genetics* **9**: 55-61.

Kretschmer A, Moller G, Lee H, Laumen H, von Toerne C, Schramm K, Prokisch H, Eyerich S, Wahl S, Baurecht H et al. 2014. A common atopy-associated variant in the Th2 cytokine locus control region impacts transcriptional regulation and alters SMAD3 and SP1 binding. *Allergy* **69**: 632-642.

Kryukov GV, Pennacchio LA, Sunyaev SR. 2007. Most rare missense alleles are deleterious in humans: implications for complex disease and association studies. *American journal of human genetics* **80**: 727-739.

Kypriotou M, Huber M, Hohl D. 2012. The human epidermal differentiation complex: cornified envelope precursors, S100 proteins and the 'fused genes' family. *Experimental dermatology* **21**: 643-649.

Lee CH, Marekov LN, Kim S, Brahim JS, Park MH, Steinert PM. 2000a. Small proline-rich protein 1 is the major component of the cell envelope of normal human oral keratinocytes. *FEBS Lett* **477**: 268-272.

Lee YA, Wahn U, Kehrt R, Tarani L, Businco L, Gustafsson D, Andersson F, Oranje AP, Wolkertstorfer A, v Berg A et al. 2000b. A major susceptibility locus for atopic dermatitis maps to chromosome 3q21. *Nature genetics* **26**: 470-473.

Levin J, Friedlander SF, Del Rosso JQ. 2013. Atopic dermatitis and the stratum corneum: part 2: other structural and functional characteristics of the stratum corneum barrier in atopic skin. *The Journal of clinical and aesthetic dermatology* **6**: 49-54.

Leyden JJ, Marples RR, Kligman AM. 1974. Staphylococcus aureus in the lesions of atopic dermatitis. *The British journal of dermatology* **90**: 525-530.

Leyva-Castillo JM, Hener P, Michea P, Karasuyama H, Chan S, Soumelis V, Li M. 2013. Skin thymic stromal lymphopoietin initiates Th2 responses through an orchestrated immune cascade. *Nature communications* **4**: 2847.

Li L, He S, Sun JM, Davie JR. 2004. Gene regulation by Sp1 and Sp3. *Biochem Cell Biol* **82**: 460-471.

Liu C, Xu D, Liu L, Schain F, Brunnstrom A, Bjorkholm M, Claesson HE, Sjoberg J. 2009. 15-Lipoxygenase-1 induces expression and release of chemokines in cultured human lung epithelial cells. *American journal of physiology Lung cellular and molecular physiology* **297**: L196-203.

Liu Y, Mounkes LC, Liggitt HD, Brown CS, Solodin I, Heath TD, Debs RJ. 1997. Factors influencing the efficiency of cationic liposome-mediated intravenous gene delivery. *Nat Biotechnol* **15**: 167-173.

Liu YJ. 2006. Thymic stromal lymphopoietin: master switch for allergic inflammation. *The Journal of experimental medicine* **203**: 269-273.

Maia AT, Spiteri I, Lee AJ, O'Reilly M, Jones L, Caldas C, Ponder BA. 2009. Extent of differential allelic expression of candidate breast cancer genes is similar in blood and breast. *Breast cancer research : BCR* **11**: R88.

Mali P, Yang L, Esvelt KM, Aach J, Guell M, DiCarlo JE, Norville JE, Church GM. 2013. RNA-guided human genome engineering via Cas9. *Science* **339**: 823-826.

Mallol J, Crane J, von Mutius E, Odhiambo J, Keil U, Stewart A, Group IPTS. 2013. The International Study of Asthma and Allergies in Childhood (ISAAC) Phase Three: a global synthesis. *Allergologia et immunopathologia* **41**: 73-85.

Manavalan B, Basith S, Choi S. 2011. Similar Structures but Different Roles - An Updated Perspective on TLR Structures. *Frontiers in physiology* **2**: 41.

Manz J, Rodriguez E, ElSharawy A, Oesau EM, Petersen BS, Baurecht H, Mayr G, Weber S, Harder J, Reischl E et al. 2016. Targeted resequencing and functional testing identifies low-frequency missense variants in the gene encoding GARP as significant contributors to atopic dermatitis risk. *The Journal of investigative dermatology* doi:10.1016/j.jid.2016.07.009.

Marcos-Vadillo E, Garcia-Sanchez A. 2016. Promoter Assay Using Luciferase Reporter Gene in the A549 Cell Line. *Methods in molecular biology* **1434**: 199-211.

Marenholz I, Bauerfeind A, Esparza-Gordillo J, Kerscher T, Granell R, Nickel R, Lau S, Henderson J, Lee YA. 2011. The eczema risk variant on chromosome 11q13 (rs7927894) in the population-based ALSPAC cohort: a novel susceptibility factor for asthma and hay fever. *Human molecular genetics* **20**: 2443-2449.

Marenholz I, Esparza-Gordillo J, Ruschendorf F, Bauerfeind A, Strachan DP, Spycher BD, Baurecht H, Margaritte-Jeannin P, Saaf A, Kerkhof M et al. 2015. Meta-analysis identifies seven susceptibility loci involved in the atopic march. *Nature communications* **6**: 8804.

Marenholz I, Nickel R, Ruschendorf F, Schulz F, Esparza-Gordillo J, Kerscher T, Gruber C, Lau S, Worm M, Keil T et al. 2006. Filaggrin loss-of-function mutations predispose to phenotypes involved in the atopic march. *The Journal of allergy and clinical immunology* **118**: 866-871.

Marenholz I, Volz A, Ziegler A, Davies A, Ragoussis I, Korge BP, Mischke D. 1996. Genetic analysis of the epidermal differentiation complex (EDC) on human chromosome 1q21: chromosomal orientation, new markers, and a 6-Mb YAC contig. *Genomics* **37**: 295-302.

Maston GA, Evans SK, Green MR. 2006. Transcriptional regulatory elements in the human genome. *Annu Rev Genomics Hum Genet* **7**: 29-59.

Mastrolorenzo A, Zuccati G, Massi D, Gabrielli MG, Casini A, Scozzafava A, Supuran CT. 2003. Immunohistochemical study of carbonic anhydrase isozymes in human skin. *European journal of dermatology : EJD* **13**: 440-444.

McClellan JM, Susser E, King MC. 2007. Schizophrenia: a common disease caused by multiple rare alleles. *Br J Psychiatry* **190**: 194-199.

McGirt LY, Beck LA. 2006. Innate immune defects in atopic dermatitis. *The Journal of allergy and clinical immunology* **118**: 202-208.

Mesko B, Poliska S, Nagy L. 2011. Gene expression profiles in peripheral blood for the diagnosis of autoimmune diseases. *Trends Mol Med* **17**: 223-233.

Miajlovic H, Fallon PG, Irvine AD, Foster TJ. 2010. Effect of filaggrin breakdown products on growth of and protein expression by Staphylococcus aureus. *The Journal of allergy and clinical immunology* **126**: 1184-1190 e1183.

Miller W, Rosenbloom K, Hardison RC, Hou M, Taylor J, Raney B, Burhans R, King DC, Baertsch R, Blankenberg D et al. 2007. 28-way vertebrate alignment and conservation track in the UCSC Genome Browser. *Genome research* **17**: 1797-1808.

Mills RE, Luttig CT, Larkins CE, Beauchamp A, Tsui C, Pittard WS, Devine SE. 2006. An initial map of insertion and deletion (INDEL) variation in the human genome. *Genome research* **16**: 1182-1190.

Moffatt MF. 2004. SPINK5: a gene for atopic dermatitis and asthma. *Clinical and experimental allergy : journal of the British Society for Allergy and Clinical Immunology* **34**: 325-327.

Möhrenschlager M ST, Williams HC, von der Werth J, Krämer U, Behrendt H, Ring J. 1998. Übersetzung und Validierung der britischen Diagnosekriterien des atopischen Ekzems bei 8- und 9- jährigen Schulkindern in Augsburg. *Allergol J* **7**: 373-377.

Moore MM, Rifas-Shiman SL, Rich-Edwards JW, Kleinman KP, Camargo CA, Jr., Gold DR, Weiss ST, Gillman MW. 2004. Perinatal predictors of atopic dermatitis occurring in the first six months of life. *Pediatrics* **113**: 468-474.

Mutanu Jungersted J, Hellgren LI, Hogh JK, Drachmann T, Jemec GB, Agner T. 2010. Ceramides and barrier function in healthy skin. *Acta dermato-venereologica* **90**: 350-353.

Nakane H, Ishida-Yamamoto A, Takahashi H, Iizuka H. 2002. Elafin, a secretory protein, is cross-linked into the cornified cell envelopes from the inside of psoriatic keratinocytes. *The Journal of investigative dermatology* **119**: 50-55.

Nicolae DL, Gamazon E, Zhang W, Duan S, Dolan ME, Cox NJ. 2010. Trait-associated SNPs are more likely to be eQTLs: annotation to enhance discovery from GWAS. *PLoS genetics* **6**: e1000888.

Nograles KE, Zaba LC, Shemer A, Fuentes-Duculan J, Cardinale I, Kikuchi T, Ramon M, Bergman R, Krueger JG, Guttman-Yassky E. 2009. IL-22-producing "T22" T cells account for upregulated IL-22 in atopic dermatitis despite reduced IL-17-producing TH17 T cells. *The Journal of allergy and clinical immunology* **123**: 1244-1252 e1242.

Nomura I, Gao B, Boguniewicz M, Darst MA, Travers JB, Leung DY. 2003. Distinct patterns of gene expression in the skin lesions of atopic dermatitis and psoriasis: a gene microarray analysis. *The Journal of allergy and clinical immunology* **112**: 1195-1202.

Nonomura K, Yamanishi K, Yasuno H, Nara K, Hirose S. 1994. Up-regulation of elafin/SKALP gene expression in psoriatic epidermis. *The Journal of investigative dermatology* **103**: 88-91.

Novak H, Muller A, Harrer N, Gunther C, Carballido JM, Woisetschlager M. 2007. CCL23 expression is induced by IL-4 in a STAT6-dependent fashion. *Journal of immunology* **178**: 4335-4341.

Novak N, Simon D. 2011. Atopic dermatitis - from new pathophysiologic insights to individualized therapy. *Allergy* **66**: 830-839.

Nutten S. 2015. Atopic dermatitis: global epidemiology and risk factors. *Annals of nutrition & metabolism* **66** Suppl 1: 8-16.

O'Neill EA, Fletcher C, Burrow CR, Heintz N, Roeder RG, Kelly TJ. 1988. Transcription factor OTF-1 is functionally identical to the DNA replication factor NF-III. *Science* **241**: 1210-1213.

O'Regan GM, Campbell LE, Cordell HJ, Irvine AD, McLean WH, Brown SJ. 2010. Chromosome 11q13.5 variant associated with childhood eczema: an effect supplementary to filaggrin mutations. *The Journal of allergy and clinical immunology* **125**: 170-174 e171-172.

O'Regan GM, Sandilands A, McLean WH, Irvine AD. 2008. Filaggrin in atopic dermatitis. *The Journal of allergy and clinical immunology* **122**: 689-693.

Offord V, Werling D. 2013. LRRfinder2.0: a webserver for the prediction of leucine-rich repeats. *Innate Immun* **19**: 398-402.

Olesen AB, Ellingsen AR, Larsen FS, Larsen PO, Veien NK, Thestrup-Pedersen K. 1996. Atopic dermatitis may be linked to whether a child is first- or second-born and/or the age of the mother. *Acta dermato-venereologica* **76**: 457-460.

Ong PY, Leung DY. 2006. Immune dysregulation in atopic dermatitis. *Current allergy and asthma reports* **6**: 384-389.

Ong PY, Ohtake T, Brandt C, Strickland I, Boguniewicz M, Ganz T, Gallo RL, Leung DY. 2002. Endogenous antimicrobial peptides and skin infections in atopic dermatitis. *The New England journal of medicine* **347**: 1151-1160.

Osipovich AB, Long Q, Manduchi E, Gangula R, Hipkens SB, Schneider J, Okubo T, Stoeckert CJ, Jr., Takada S, Magnuson MA. 2014. Insm1 promotes endocrine cell differentiation by modulating the expression of a network of genes that includes Neurog3 and Ripply3. *Development* **141**: 2939-2949.

Palmer CN, Irvine AD, Terron-Kwiatkowski A, Zhao Y, Liao H, Lee SP, Goudie DR, Sandilands A, Campbell LE, Smith FJ et al. 2006. Common loss-of-function variants of the epidermal barrier protein filaggrin are a major predisposing factor for atopic dermatitis. *Nature genetics* **38**: 441-446.

Park HY, Kim CR, Huh IS, Jung MY, Seo EY, Park JH, Lee DY, Yang JM. 2013. Staphylococcus aureus Colonization in Acute and Chronic Skin Lesions of Patients with Atopic Dermatitis. *Annals of dermatology* **25**: 410-416.

Pastinen T. 2010. Genome-wide allele-specific analysis: insights into regulatory variation. *Nature reviews Genetics* **11**: 533-538.

Pastinen T, Ge B, Hudson TJ. 2006. Influence of human genome polymorphism on gene expression. *Human molecular genetics* **15 Spec No 1**: R9-16.

Pastinen T, Hudson TJ. 2004. Cis-acting regulatory variation in the human genome. *Science* **306**: 647-650.

Paternoster L Standl M Waage J Baurecht H Hotze M Strachan DP Curtin JA Bonnelykke K Tian C Takahashi A et al. 2015. Multi-ancestry genome-wide association study of 21,000 cases and 95,000 controls identifies new risk loci for atopic dermatitis. *Nature genetics* **47**: 1449-1456.

Patrizi A, Raone B, Ravaioli GM. 2015. Management of atopic dermatitis: safety and efficacy of phototherapy. *Clinical, cosmetic and investigational dermatology* **8**: 511-520.

Pendaries V, Malaisse J, Pellerin L, Le Lamer M, Nachat R, Kezic S, Schmitt AM, Paul C, Poumay Y, Serre G et al. 2014. Knockdown of filaggrin in a three-dimensional reconstructed human

epidermis impairs keratinocyte differentiation. *The Journal of investigative dermatology* **134**: 2938-2946.

Pfundt R, van Ruissen F, van Vlijmen-Willems IM, Alkemade HA, Zeeuwen PL, Jap PH, Dijkman H, Fransen J, Croes H, van Erp PE et al. 1996. Constitutive and inducible expression of SKALP/elafin provides anti-elastase defense in human epithelia. *J Clin Invest* **98**: 1389-1399.

Plotz SG, Wiesender M, Todorova A, Ring J. 2014. What is new in atopic dermatitis/eczema? *Expert opinion on emerging drugs* **19**: 441-458.

Poncelet AC, Schnaper HW. 2001. Sp1 and Smad proteins cooperate to mediate transforming growth factor-beta 1-induced alpha 2(I) collagen expression in human glomerular mesangial cells. *J Biol Chem* **276**: 6983-6992.

Powell JE, Henders AK, McRae AF, Wright MJ, Martin NG, Dermitzakis ET, Montgomery GW, Visscher PM. 2012. Genetic control of gene expression in whole blood and lymphoblastoid cell lines is largely independent. *Genome research* **22**: 456-466.

Probst-Kepper M, Geffers R, Kroger A, Viegas N, Erck C, Hecht HJ, Lunsdorf H, Roubin R, Moharregh-Khiabani D, Wagner K et al. 2009. GARP: a key receptor controlling FOXP3 in human regulatory T cells. *Journal of cellular and molecular medicine* **13**: 3343-3357.

Ramasamy A, Curjuric I, Coin LJ, Kumar A, McArdle WL, Imboden M, Leynaert B, Kogevinas M, Schmid-Grendelmeier P, Pekkanen J et al. 2011. A genome-wide meta-analysis of genetic variants associated with allergic rhinitis and grass sensitization and their interaction with birth order. *The Journal of allergy and clinical immunology* **128**: 996-1005.

Regl G, Kasper M, Schnidar H, Eichberger T, Neill GW, Ikram MS, Quinn AG, Philpott MP, Frischauf AM, Aberger F. 2004. The zinc-finger transcription factor GLI2 antagonizes contact inhibition and differentiation of human epidermal cells. *Oncogene* **23**: 1263-1274.

Ring J, Abraham A, de Cuyper C, Kim K, Langeland T, Parra V, Pigatto P, Reunala T, Szczepanski R, Mohrenschlager M et al. 2008. Control of atopic eczema with pimecrolimus cream 1% under daily practice conditions: results of a > 2000 patient study. *Journal of the European Academy of Dermatology and Venereology : JEADV* **22**: 195-203.

Ring J, Alomar A, Bieber T, Deleuran M, Fink-Wagner A, Gelmetti C, Gieler U, Lipozencic J, Luger T, Oranje AP et al. 2012. Guidelines for treatment of atopic eczema (atopic dermatitis) part I. *Journal of the European Academy of Dermatology and Venereology : JEADV* **26**: 1045-1060.

Ring JPB, Ruzicka T. 2005. Handbook of atopic eczema. *Berlin, Springer*.

Risch N, Merikangas K. 1996. The future of genetic studies of complex human diseases. *Science* **273**: 1516-1517.

Robertson IB, Rifkin DB. 2013. Unchaining the beast; insights from structural and evolutionary studies on TGFbeta secretion, sequestration, and activation. *Cytokine Growth Factor Rev* **24**: 355-372.

Rodriguez E, Baurecht H, Herberich E, Wagenpfeil S, Brown SJ, Cordell HJ, Irvine AD, Weidinger S. 2009. Meta-analysis of filaggrin polymorphisms in eczema and asthma: robust risk factors in atopic disease. *The Journal of allergy and clinical immunology* **123**: 1361-1370 e1367.

Rodriguez E, Baurecht H, Wahn AF, Kretschmer A, Hotze M, Zeilinger S, Klopp N, Illig T, Schramm K, Prokisch H et al. 2014. An integrated epigenetic and transcriptomic analysis reveals distinct tissue-specific patterns of DNA methylation associated with atopic dermatitis. *The Journal of investigative dermatology* **134**: 1873-1883.

Roubin R, Pizette S, Ollendorff V, Planche J, Birnbaum D, Delapeyriere O. 1996. Structure and developmental expression of mouse Garp, a gene encoding a new leucine-rich repeat-containing protein. *The International journal of developmental biology* **40**: 545-555.

Sabo PJ, Hawrylycz M, Wallace JC, Humbert R, Yu M, Shafer A, Kawamoto J, Hall R, Mack J, Dorschner MO et al. 2004. Discovery of functional noncoding elements by digital analysis of chromatin structure. *Proceedings of the National Academy of Sciences of the United States of America* **101**: 16837-16842.

Sabo PJ, Kuehn MS, Thurman R, Johnson BE, Johnson EM, Cao H, Yu M, Rosenzweig E, Goldy J, Haydock A et al. 2006. Genome-scale mapping of DNase I sensitivity in vivo using tiling DNA microarrays. *Nature methods* **3**: 511-518.

Sandstrom MH, Faergemann J. 2004. Prognosis and prognostic factors in adult patients with atopic dermatitis: a long-term follow-up questionnaire study. *The British journal of dermatology* **150**: 103-110.

Sarris M, Andersen KG, Randow F, Mayr L, Betz AG. 2008. Neuropilin-1 expression on regulatory T cells enhances their interactions with dendritic cells during antigen recognition. *Immunity* **28**: 402-413.

Schaarschmidt H, Ellinghaus D, Rodriguez E, Kretschmer A, Baurecht H, Lipinski S, Meyer-Hoffert U, Harder J, Lieb W, Novak N et al. 2015. A genome-wide association study reveals 2 new susceptibility loci for atopic dermatitis. *The Journal of allergy and clinical immunology* **136**: 802-806.

Schalkwijk J, van Vlijmen IM, Alkemade JA, de Jongh GJ. 1993. Immunohistochemical localization of SKALP/elafin in psoriatic epidermis. *The Journal of investigative dermatology* **100**: 390-393.

Scherer WF, Syverton JT, Gey GO. 1953. Studies on the propagation in vitro of poliomyelitis viruses. IV. Viral multiplication in a stable strain of human malignant epithelial cells (strain HeLa) derived from an epidermoid carcinoma of the cervix. *The Journal of experimental medicine* **97**: 695-710.

Schmidt-Weber CB, Akdis M, Akdis CA. 2007. TH17 cells in the big picture of immunology. *The Journal of allergy and clinical immunology* **120**: 247-254.

Schmitt J, Langan S, Deckert S, Svensson A, von Kobyletzki L, Thomas K, Spuls P, Harmonising Outcome Measures for Atopic Dermatitis I. 2013. Assessment of clinical signs of atopic dermatitis: a systematic review and recommendation. *The Journal of allergy and clinical immunology* **132**: 1337-1347.

Schmitt J, Schmitt N, Meurer M. 2007. Cyclosporin in the treatment of patients with atopic eczema - a systematic review and meta-analysis. *Journal of the European Academy of Dermatology and Venereology : JEADV* **21**: 606-619.

Schmitt J, Spuls P, Boers M, Thomas K, Chalmers J, Roekevisch E, Schram M, Allsopp R, Aoki V, Apfelbacher C et al. 2012. Towards global consensus on outcome measures for atopic eczema research: results of the HOME II meeting. *Allergy* **67**: 1111-1117.

Schmitt J, Spuls PI, Thomas KS, Simpson E, Furue M, Deckert S, Dohil M, Apfelbacher C, Singh JA, Chalmers J et al. 2014. The Harmonising Outcome Measures for Eczema (HOME) statement to assess clinical signs of atopic eczema in trials. *The Journal of allergy and clinical immunology* **134**: 800-807.

Schmitt J, Williams H, Group HD. 2010. Harmonising Outcome Measures for Eczema (HOME). Report from the First International Consensus Meeting (HOME 1), 24 July 2010, Munich, Germany. *The British journal of dermatology* **163**: 1166-1168.

Schmitz R, Atzpodien K, Schlaud M. 2012. Prevalence and risk factors of atopic diseases in German children and adolescents. *Pediatric allergy and immunology : official publication of the European Society of Pediatric Allergy and Immunology* **23**: 716-723.

Schneider U, Schwenk HU, Bornkamm G. 1977. Characterization of EBV-genome negative "null" and "T" cell lines derived from children with acute lymphoblastic leukemia and leukemic transformed non-Hodgkin lymphoma. *International journal of cancer Journal international du cancer* **19**: 621-626.

Schram ME, Spuls PI, Leeflang MM, Lindeboom R, Bos JD, Schmitt J. 2012. EASI, (objective) SCORAD and POEM for atopic eczema: responsiveness and minimal clinically important difference. *Allergy* **67**: 99-106.

Schreiber S, Rosenstiel P, Albrecht M, Hampe J, Krawczak M. 2005. Genetics of Crohn disease, an archetypal inflammatory barrier disease. *Nature reviews Genetics* **6**: 376-388.

Serre D, Gurd S, Ge B, Sladek R, Sinnett D, Harmsen E, Bibikova M, Chudin E, Barker DL, Dickinson T et al. 2008. Differential allelic expression in the human genome: a robust approach to identify genetic and epigenetic cis-acting mechanisms regulating gene expression. *PLoS genetics* **4**: e1000006.

Sheng H, Goich S, Wang A, Grachtchouk M, Lowe L, Mo R, Lin K, de Sauvage FJ, Sasaki H, Hui CC et al. 2002. Dissecting the oncogenic potential of Gli2: deletion of an NH(2)-terminal fragment alters skin tumor phenotype. *Cancer research* **62**: 5308-5316.

Shevach EM. 2009. Mechanisms of foxp3+ T regulatory cell-mediated suppression. *Immunity* **30**: 636-645.

Simon D, Aeberhard C, Erdemoglu Y, Simon HU. 2014. Th17 cells and tissue remodeling in atopic and contact dermatitis. *Allergy* **69**: 125-131.

Simon D, Braathen LR, Simon HU. 2004. Eosinophils and atopic dermatitis. *Allergy* **59**: 561-570.

Skapenko A, Leipe J, Lipsky PE, Schulze-Koops H. 2005. The role of the T cell in autoimmune inflammation. *Arthritis research & therapy* **7 Suppl 2**: S4-14.

Sonesson A, Bartosik J, Christiansen J, Roscher I, Nilsson F, Schmidtchen A, Back O. 2013. Sensitization to skin-associated microorganisms in adult patients with atopic dermatitis is of importance for disease severity. *Acta dermato-venereologica* **93**: 340-345.

Soumelis V, Reche PA, Kanzler H, Yuan W, Edward G, Homey B, Gilliet M, Ho S, Antonenko S, Lauerma A et al. 2002. Human epithelial cells trigger dendritic cell mediated allergic inflammation by producing TSLP. *Nature immunology* **3**: 673-680.

Spencer CC, Su Z, Donnelly P, Marchini J. 2009. Designing genome-wide association studies: sample size, power, imputation, and the choice of genotyping chip. *PLoS genetics* **5**: e1000477.

Spergel JM. 2010a. Epidemiology of atopic dermatitis and atopic march in children. *Immunology and allergy clinics of North America* **30**: 269-280.

Spergel JM. 2010b. From atopic dermatitis to asthma: the atopic march. *Annals of allergy, asthma & immunology : official publication of the American College of Allergy, Asthma, & Immunology* **105**: 99-106; quiz 107-109, 117.

Steinbrink K, Mahnke K, Grabbe S, Enk AH, Jonuleit H. 2009. Myeloid dendritic cell: From sentinel of immunity to key player of peripheral tolerance? *Human immunology* **70**: 289-293.

Stockis J, Colau D, Coulie PG, Lucas S. 2009. Membrane protein GARP is a receptor for latent TGF-beta on the surface of activated human Treg. *European journal of immunology* **39**: 3315-3322.

Strachan DP, Wong HJ, Spector TD. 2001. Concordance and interrelationship of atopic diseases and markers of allergic sensitization among adult female twins. *The Journal of allergy and clinical immunology* **108**: 901-907.

Suarez-Farinas M, Dhingra N, Gittler J, Shemer A, Cardinale I, de Guzman Strong C, Krueger JG, Guttman-Yassky E. 2013. Intrinsic atopic dermatitis shows similar TH2 and higher TH17 immune activation compared with extrinsic atopic dermatitis. *The Journal of allergy and clinical immunology* **132**: 361-370.

Suarez-Farinas M, Tintle SJ, Shemer A, Chiricozzi A, Nograles K, Cardinale I, Duan S, Bowcock AM, Krueger JG, Guttman-Yassky E. 2011. Nonlesional atopic dermatitis skin is characterized by broad terminal differentiation defects and variable immune abnormalities. *The Journal of allergy and clinical immunology* **127**: 954-964 e951-954.

Sun LD, Xiao FL, Li Y, Zhou WM, Tang HY, Tang XF, Zhang H, Schaarschmidt H, Zuo XB, Foelster-Holst R et al. 2011. Genome-wide association study identifies two new susceptibility loci for atopic dermatitis in the Chinese Han population. *Nature genetics* **43**: 690-694.

Taylor J, Tyekucheva S, King DC, Hardison RC, Miller W, Chiaromonte F. 2006. ESPERR: learning strong and weak signals in genomic sequence alignments to identify functional elements. *Genome research* **16**: 1596-1604.

Taylor SC, Berkelman T, Yadav G, Hammond M. 2013. A defined methodology for reliable quantification of Western blot data. *Mol Biotechnol* **55**: 217-226.

Thijs J, Krastev T, Weidinger S, Buckens CF, de Bruin-Weller M, Bruijnzeel-Koomen C, Flohr C, Hijnen D. 2015. Biomarkers for atopic dermatitis: a systematic review and meta-analysis. *Current opinion in allergy and clinical immunology* **15**: 453-460.

Thomsen SF. 2015. Epidemiology and natural history of atopic diseases. *European clinical respiratory journal* **2**.

Thorey IS, Roth J, Regenbogen J, Halle JP, Bittner M, Vogl T, Kaesler S, Bugnon P, Reitmaier B, Durka S et al. 2001. The Ca2+-binding proteins S100A8 and S100A9 are encoded by novel injury-regulated genes. *J Biol Chem* **276**: 35818-35825.

Thurman RE, Rynes E, Humbert R, Vierstra J, Maurano MT, Haugen E, Sheffield NC, Stergachis AB, Wang H, Vernot B et al. 2012. The accessible chromatin landscape of the human genome. *Nature* **489**: 75-82.

Tokuhiro S, Yamada R, Chang X, Suzuki A, Kochi Y, Sawada T, Suzuki M, Nagasaki M, Ohtsuki M, Ono M et al. 2003. An intronic SNP in a RUNX1 binding site of SLC22A4, encoding an organic cation transporter, is associated with rheumatoid arthritis. *Nature genetics* **35**: 341-348.

Tran DQ, Andersson J, Wang R, Ramsey H, Unutmaz D, Shevach EM. 2009. GARP (LRRC32) is essential for the surface expression of latent TGF-beta on platelets and activated FOXP3+ regulatory T cells. *Proceedings of the National Academy of Sciences of the United States of America* **106**: 13445-13450.

Trifari S, Kaplan CD, Tran EH, Crellin NK, Spits H. 2009. Identification of a human helper T cell population that has abundant production of interleukin 22 and is distinct from T(H)-17, T(H)1 and T(H)2 cells. *Nature immunology* **10**: 864-871.

Urade Y, Hayaishi O. 2000. Biochemical, structural, genetic, physiological, and pathophysiological features of lipocalin-type prostaglandin D synthase. *Biochim Biophys Acta* **1482**: 259-271.

van der Hulst AE, Klip H, Brand PL. 2007. Risk of developing asthma in young children with atopic eczema: a systematic review. *The Journal of allergy and clinical immunology* **120**: 565-569.

Vasilopoulos Y, Cork MJ, Murphy R, Williams HC, Robinson DA, Duff GW, Ward SJ, Tazi-Ahnini R. 2004. Genetic association between an AACC insertion in the 3'UTR of the stratum corneum chymotryptic enzyme gene and atopic dermatitis. *The Journal of investigative dermatology* **123**: 62-66.

Veldhoen M, Uyttenhove C, van Snick J, Helmby H, Westendorf A, Buer J, Martin B, Wilhelm C, Stockinger B. 2008. Transforming growth factor-beta 'reprograms' the differentiation of T helper 2 cells and promotes an interleukin 9-producing subset. *Nature immunology* **9**: 1341-1346.

Wadonda-Kabondo N, Sterne JA, Golding J, Kennedy CT, Archer CB, Dunnill MG, Team AS. 2004. Association of parental eczema, hayfever, and asthma with atopic dermatitis in infancy: birth cohort study. *Archives of disease in childhood* **89**: 917-921.

Wang R, Kozhaya L, Mercer F, Khaitan A, Fujii H, Unutmaz D. 2009. Expression of GARP selectively identifies activated human FOXP3+ regulatory T cells. *Proceedings of the National Academy of Sciences of the United States of America* **106**: 13439-13444.

Wang R, Wan Q, Kozhaya L, Fujii H, Unutmaz D. 2008. Identification of a regulatory T cell specific cell surface molecule that mediates suppressive signals and induces Foxp3 expression. *PloS one* **3**: e2705.

Wang R, Zhu J, Dong X, Shi M, Lu C, Springer TA. 2012. GARP regulates the bioavailability and activation of TGFbeta. *Molecular biology of the cell* **23**: 1129-1139.

Warren ST, Zhang F, Licameli GR, Peters JF. 1987. The fragile X site in somatic cell hybrids: an approach for molecular cloning of fragile sites. *Science* **237**: 420-423.

Weber JL, David D, Heil J, Fan Y, Zhao C, Marth G. 2002. Human diallelic insertion/deletion polymorphisms. *American journal of human genetics* **71**: 854-862.

Weidinger S, Gieger C, Rodriguez E, Baurecht H, Mempel M, Klopp N, Gohlke H, Wagenpfeil S, Ollert M, Ring J et al. 2008a. Genome-wide scan on total serum IgE levels identifies FCER1A as novel susceptibility locus. *PLoS genetics* **4**: e1000166.

Weidinger S, Illig T, Baurecht H, Irvine AD, Rodriguez E, Diaz-Lacava A, Klopp N, Wagenpfeil S, Zhao Y, Liao H et al. 2006. Loss-of-function variations within the filaggrin gene predispose for atopic dermatitis with allergic sensitizations. *The Journal of allergy and clinical immunology* **118**: 214-219.

Weidinger S, Novak N. 2015. Atopic dermatitis. *Lancet* doi:10.1016/S0140-6736(15)00149-X.

Weidinger S, O'Sullivan M, Illig T, Baurecht H, Depner M, Rodriguez E, Ruether A, Klopp N, Vogelberg C, Weiland SK et al. 2008b. Filaggrin mutations, atopic eczema, hay fever, and asthma in children. *The Journal of allergy and clinical immunology* **121**: 1203-1209 e1201.

Weidinger S, Willis-Owen SA, Kamatani Y, Baurecht H, Morar N, Liang L, Edser P, Street T, Rodriguez E, O'Regan GM et al. 2013. A genome-wide association study of atopic dermatitis identifies loci with overlapping effects on asthma and psoriasis. *Human molecular genetics* **22**: 4841-4856.

Welter D, MacArthur J, Morales J, Burdett T, Hall P, Junkins H, Klemm A, Flicek P, Manolio T, Hindorff L et al. 2014. The NHGRI GWAS Catalog, a curated resource of SNP-trait associations. *Nucleic acids research* **42**: D1001-1006.

Werner Y, Lindberg M. 1985. Transepidermal water loss in dry and clinically normal skin in patients with atopic dermatitis. *Acta dermato-venereologica* **65**: 102-105.

Wichmann HE, Gieger C, Illig T, Group MKS. 2005. KORA-gen--resource for population genetics, controls and a broad spectrum of disease phenotypes. *Gesundheitswesen* **67 Suppl 1**: S26-30.

Wildin RS, Ramsdell F, Peake J, Faravelli F, Casanova JL, Buist N, Levy-Lahad E, Mazzella M, Goulet O, Perroni L et al. 2001. X-linked neonatal diabetes mellitus, enteropathy and endocrinopathy syndrome is the human equivalent of mouse scurfy. *Nature genetics* **27**: 18-20.

Williams H, Flohr C. 2006. How epidemiology has challenged 3 prevailing concepts about atopic dermatitis. *The Journal of allergy and clinical immunology* **118**: 209-213.

Williams H, Stewart A, von Mutius E, Cookson W, Anderson HR, International Study of A, Allergies in Childhood Phase O, Three Study G. 2008. Is eczema really on the increase worldwide? *The Journal of allergy and clinical immunology* **121**: 947-954 e915.

Williams HC, Burney PG, Hay RJ, Archer CB, Shipley MJ, Hunter JJ, Bingham EA, Finlay AY, Pembroke AC, Graham-Brown RA et al. 1994a. The U.K. Working Party's Diagnostic Criteria for Atopic Dermatitis. I. Derivation of a minimum set of discriminators for atopic dermatitis. *The British journal of dermatology* **131**: 383-396.

Williams HC, Burney PG, Strachan D, Hay RJ. 1994b. The U.K. Working Party's Diagnostic Criteria for Atopic Dermatitis. II. Observer variation of clinical diagnosis and signs of atopic dermatitis. *The British journal of dermatology* **131**: 397-405.

Williams HC, Strachan DP. 1998. The natural history of childhood eczema: observations from the British 1958 birth cohort study. *The British journal of dermatology* **139**: 834-839.

Wing K, Onishi Y, Prieto-Martin P, Yamaguchi T, Miyara M, Fehervari Z, Nomura T, Sakaguchi S. 2008. CTLA-4 control over Foxp3+ regulatory T cell function. *Science* **322**: 271-275.

Wollenberg A, Wetzel S, Burgdorf WH, Haas J. 2003. Viral infections in atopic dermatitis: pathogenic aspects and clinical management. *The Journal of allergy and clinical immunology* **112**: 667-674.

Wray GA. 2003. Transcriptional regulation and the evolution of development. *The International journal of developmental biology* **47**: 675-684.

Wray GA, Hahn MW, Abouheif E, Balhoff JP, Pizer M, Rockman MV, Romano LA. 2003. The evolution of transcriptional regulation in eukaryotes. *Molecular biology and evolution* **20**: 1377-1419.

Wu K, Bi Y, Sun K, Wang C. 2007. IL-10-producing type 1 regulatory T cells and allergy. *Cellular & molecular immunology* **4**: 269-275.

Xu J, Rogers MB. 2007. Modulation of Bone Morphogenetic Protein (BMP) 2 gene expression by Sp1 transcription factors. *Gene* **392**: 221-229.

Yan H, Yuan W, Velculescu VE, Vogelstein B, Kinzler KW. 2002. Allelic variation in human gene expression. *Science* **297**: 1143.

Zheng T, Yu J, Oh MH, Zhu Z. 2011. The atopic march: progression from atopic dermatitis to allergic rhinitis and asthma. *Allergy, asthma & immunology research* **3**: 67-73.

Ziegler SF, Artis D. 2010. Sensing the outside world: TSLP regulates barrier immunity. *Nature immunology* **11**: 289-293.

Table I: Gene transcripts with genome-wide significant differential expression (P$_{FDR}$ <0.05, Diff >1/fold change >2) in non-lesional skin (AN) vs. controls (NN)

Probe ID	ACCESSION	GENE SYMBOL	CHR	PROBE_COORDINATES	mean.NN	mean.AN	Diff. AN_NN	Pvalue AN_NN	P.FDR AN_NN
1470630	NM_001014291.2	SPRR2G	1	151388896-151388945	12.1830581	14.4206001	2.237541952	6.89E-12	1.43E-07
510468	NM_006163.1	NFE2	12	54685936-54685985	8.56888232	9.58762828	1.018745957	1.20E-07	0.000287001
6550500	NM_002963.3	S100A7	1	153431424-153431473	10.4863025	13.647205	3.160902476	5.47E-07	0.000813691
7000408	NM_205545.1	LYPD2	8	143832477-143832526	7.58456185	9.18073336	1.596171515	1.73E-06	0.001389269
6620121	NM_005623.2	CCL8	17	29672323-29672372	8.19215603	9.27392777	1.081771742	2.19E-06	0.001527058
2230500	NM_001014450.1	SPRR2F	1	153084780-153084829	10.7182116	12.7947996	2.076588021	2.20E-06	0.001527058
3180392	NM_006770.3	MARCO	2	119468445-119468494	7.11962196	8.24922342	1.129601466	7.39E-06	0.003343195
5910019	NM_000491.3	C1QB	1	22860377-22860426	9.93917007	10.9893564	1.050186334	1.26E-05	0.004170382
2060674	NM_000067.1	CA2	8	86580533-86580582	10.7949068	12.1015985	1.306691655	1.51E-05	0.004762649
5390220	NM_002965.2	S100A9	1	151599776-151599825	11.234989	13.1291932	1.894204129	2.93E-05	0.007006314
6110343	NM_145898.1	CCL23	17	34340185-34340234	7.19830442	8.62516053	1.426856114	8.10E-05	0.013116939
1050168	NM_002638.2	PI3	20	43238123-43238172	7.67497724	9.59719345	1.922216209	0.00014823	0.01750098
1820379	NM_000954.5	PTGDS	9	138994544-138994557:138995106-138995128:138995852-138995864	11.4620938	10.1179332	-1.344160688	0.00044829	0.031738518
5890193	NM_148975.1	MS4A4A	11	59832420-59832469	7.99580028	9.15575596	1.159955681	0.00078119	0.041903012

Table II: Gene transcripts with genome-wide significant differential expression (P$_{FDR}$ <0.05, Diff >1/fold change >2) in lesional skin (AL) vs. controls (NN)

ProbeID	ACCESSION	GENE SYMBOL	CHR	PROBE_COORDINATES	mean.NN	mean.AL	Diff. AL.NN	Pvalue AL_NN	P.FDR AL_NN
1470630	NM_001014291.2	SPRR2G	1	151388896-151388945	12.1830581	14.6726778	2.48961966	3.11E-13	2.33E-09
5310722	NM_004441.3	EPHB1	3	134978917-134978966	9.56688415	8.0007743	-1.5661098	3.93E-12	2.05E-08
6040017	NM_017931.2	TTC38	22	45068374-45068423	10.301	9.18866531	-1.1123347	9.82E-12	2.56E-08
50129	NM_013241.2	FHOD1	16	67263502-67263538:67263539-67263551	9.04722886	10.0869794	1.03975058	1.62E-11	3.06E-08
3990170	NM_005532.3	IFI27	14	93652556-93652605	11.4749484	13.761614	2.28666563	2.38E-11	4.14E-08
1450309	NM_017931.1	FLJ20699	22	45068302-45068351	9.60360464	8.53240844	-1.0711962	3.04E-11	4.52E-08
2230500	NM_001014450.1	SPRR2F	1	153084780-153084829	10.7182116	13.8121514	3.09393973	2.39E-10	1.99E-07
1850156	NM_194284.2	CLDN23	8	8561463-8561512	10.9659435	9.49734767	-1.4685958	5.35E-10	3.48E-07
6550500	NM_002963.3	S100A7	1	153431424-153431473	10.4863025	14.5364773	4.05017474	9.59E-10	5.23E-07
4760338	NM_004358.3	CDC25B	20	3734490-3734539	10.5307032	11.624768	1.09406474	1.17E-09	5.64E-07
3990433	NM_018404.2	ADAP2	17	26310214-26310263	10.220023	11.4836254	1.26360238	1.25E-09	5.93E-07
840364	NM_001039948.2	SGSM1	22	23652660-23652709	8.74820111	7.52185739	-1.2263437	1.75E-09	7.43E-07
160270	NM_022003.1	FXYD6	11	117213021-117213070	8.65421415	7.64198744	-1.0122267	2.47E-09	8.43E-07
3450537	NM_032564.2	DGAT2	11	75190079-75190128	9.93040472	8.86530646	-1.0650983	3.27E-09	9.87E-07
3130128	NM_001004051.1	GPRASP2	X	101858979-101859028	9.81812494	8.8097311	-1.0083938	3.68E-09	1.04E-06
5390220	NM_002965.2	S100A9	1	151599776-151599825	11.234989	14.3953461	3.16035702	4.49E-09	1.21E-06
4260243	NM_004225.2	MFHAS1	8	8785016-8785065	8.55208551	9.8218106	1.26972509	5.54E-09	1.41E-06
5270367	NM_001814.2	CTSC	11	87666917-87666966	9.98170142	11.6073005	1.62559908	6.59E-09	1.58E-06
1580333	NM_020853.1	KIAA1467	12	13127273-13127322	8.78370979	7.62733817	-1.1563716	1.25E-08	2.57E-06
3120370	NM_001251.1	CD68	17	7426110-7426153	11.1227389	12.3662866	1.24354768	1.49E-08	2.75E-06
840553	NM_001012761.1	RGMB	5	98159946-98159995	10.9161133	9.75227203	-1.1638413	1.60E-08	2.89E-06
7550358	NM_006159.1	NELL2	12	43188674-43188723	9.39239266	11.3547547	1.96236207	1.77E-08	3.10E-06
4860093	XM_936251.2	LOC653888			8.8198475	10.0733976	1.25355006	1.79E-08	3.10E-06
3450138	NM_001814.2	CTSC	11	87666842-87666891	10.7175025	12.0846805	1.36717798	2.23E-08	3.59E-06
4070091	NM_001001523.1	RORC	1	151778900-151778949	9.93908335	7.87754138	-2.061542	3.07E-08	4.44E-06
4920075	NM_003245.2	TGM3	20	2269595-2269644	11.8933638	13.0281365	1.13477271	3.82E-08	5.13E-06
2510338	NM_003878.1	GGH	8	64092673-64092722	11.3539224	12.5295279	1.17560549	4.07E-08	5.33E-06
3830563	NM_025184.3	EFHC2	X	44037623-44037672	9.11083422	8.04033367	-1.0705005	4.19E-08	5.45E-06
2060674	NM_000067.1	CA2	8	86580533-86580582	10.7949068	12.5061066	1.71119978	4.41E-08	5.63E-06
6220343	NM_021098.2	CACNA1H	16	1211052-1211101	9.48008646	7.59065035	-1.8894361	4.41E-08	5.63E-06
4890553	NM_001001523.1	RORC	1	151778990-151779039	9.34729046	7.50103285	-1.8462576	5.20E-08	6.41E-06
3780092	NM_014452.3	TNFRSF21	6	47307455-47307504	10.5451407	11.7817734	1.23663267	5.26E-08	6.41E-06
7050082	NM_001611.2	ACP5	19	11546718-11546767	8.69986414	9.73125419	1.03139005	6.60E-08	7.41E-06
5700735	NM_031458.1	PARP9	3	123729903-123729952	9.10976569	10.5961811	1.48641546	6.74E-08	7.46E-06
6840390	NM_153350.2	FBXL16	16	742824-742873	9.30241881	8.17995474	-1.1224641	6.84E-08	7.53E-06
1470382	NM_004029.2	IRF7	11	613117-613117:613206-613254	6.85538167	8.0214102	1.16602854	8.01E-08	8.30E-06
5910847	NM_000418.2	IL4R	16	27283393-27283442	9.07514691	10.6237766	1.54862966	8.22E-08	8.43E-06
2350504	NM_001953.2	ECGF1	22	49311047-49311064:49311065-49311096	10.7402434	12.7282181	1.98797472	8.70E-08	8.84E-06
7210717	NM_173558.2	FGD2	6	37104771-37104820	10.4015026	11.4153394	1.0138368	9.02E-08	9.03E-06
4220259	NM_001336.2	CTSZ	20	57003862-57003911	11.1273105	12.1809863	1.05367585	9.58E-08	9.23E-06
5360376	NM_006762.1	LAPTM5	1	30978154-30978203	9.58694365	10.7788385	1.19189481	9.73E-08	9.29E-06

6770474	NM_030622.6	CYP2S1	19	41713266-41713315	7.69226623	8.9986203	1.30635407	1.06E-07	9.67E-06
3890228	NM_005797.2	MPZL2	11	118124223-118124272	12.2305557	13.4447745	1.2142188	1.13E-07	1.02E-05
150202	NM_144765.1	MPZL2	11	118127813-118127862	8.71094243	9.74884555	1.03790313	1.16E-07	1.03E-05
2340725	BM715829	HS.8038	5	179271343-179271392	8.59430105	7.52290351	-1.0713975	1.16E-07	1.03E-05
4260253	NM_001031716.1	OBFC2A	2	192259631-192259680	9.61810716	11.0714274	1.45332028	1.30E-07	1.08E-05
870468	NM_014505.4	KCNMB4	12	69111174-69111223	9.39044778	8.04931419	-1.3411336	1.31E-07	1.08E-05
130681	NM_005615.4	RNASE6	14	20320082-20320131	7.84964012	8.99781081	1.14817069	1.35E-07	1.09E-05
5670687	NM_015993.1	PLLP	16	55847785-55847834	11.0276749	9.73822044	-1.2894544	1.40E-07	1.12E-05
2350762	NM_020375.2	C12orf5	12	4331958-4332007	7.38476447	8.74579096	1.36102649	1.53E-07	1.20E-05
5090445	NM_024539.3	RNF128	X	105926593-105926642	9.51552553	8.2115671	-1.3039584	1.93E-07	1.40E-05
6060315	NM_031471.4	FERMT3	11	63747749-63747798	8.53401421	9.7334116	1.19939739	2.13E-07	1.51E-05
1570661	NM_000775.2	CYP2J2	1	60359237-60359286	10.4366003	8.99105633	-1.445544	2.14E-07	1.51E-05
780528	NM_001827.1	CKS2	9	91119989-91120032:91121108-91121113	9.72977438	10.8120497	1.08227528	2.20E-07	1.53E-05
1050168	NM_002638.2	PI3	20	43238123-43238172	7.67497724	12.6738132	4.99883592	2.22E-07	1.53E-05
4480148	NM_001113411.1	FGGY	1	60228233-60228256:60228257-60228282	10.089645	8.99363106	-1.096014	3.22E-07	2.00E-05
730358	NM_020215.2	C14orf132	14	95629766-95629815	11.4743984	10.2703976	-1.2040008	3.48E-07	2.11E-05
2750280	NM_003885.2	CDK5R1	17	27841663-27841712	7.98797905	9.1983039	1.21032486	3.64E-07	2.16E-05
4850440	NM_182922.2	HEATR3	16	48693699-48693748	7.19867242	8.28038194	1.08230952	3.65E-07	2.16E-05
870711	NM_001039503.2	POL3S	16	31094879-31094928	7.94091652	10.8205039	2.87958743	3.70E-07	2.18E-05
6940102	NM_002160.1	TNC	9	116822907-116822956	10.0734962	11.8082419	1.73474569	4.04E-07	2.29E-05
6400176	NM_004029.2	IRF7	11	612640-612644:612645-612689	8.38674896	9.87145681	1.48470784	4.06E-07	2.29E-05
3420541	NM_014573.2	TMEM97	17	23679301-23679350	11.8395885	10.5645383	-1.2750502	4.21E-07	2.35E-05
2480730	NM_015162.3	ACSBG1	15	78463394-78463443	12.2917285	10.2323142	-2.0594143	4.43E-07	2.44E-05
7570673	NM_003364.2	UPP1	7	48114453-48114479:48114480-48114502	8.75089818	10.4364665	1.68556834	4.83E-07	2.60E-05
5910019	NM_000491.3	C1QB	1	22860377-22860426	9.93917007	11.4489187	1.50974862	5.86E-07	2.98E-05
1990593	NM_024335.2	IRX6	16	53922097-53922146	9.88546853	8.58591427	-1.2995543	6.78E-07	3.33E-05
3890523	XM_937367.1	IL7R			8.28051285	10.2120978	1.93158494	6.83E-07	3.35E-05
430259	NM_020248.2	CTNNBIP1	1	9908549-9908598	11.8650526	10.6681141	-1.1969385	7.03E-07	3.43E-05
5560246	NM_001018004.1	TPM1	15	61141526-61141529:61141828-61141873	11.6933504	10.6574905	-1.0358599	7.08E-07	3.44E-05
7550500	NM_002229.2	JUNB	19	12764585-12764629:12764630-12764634	8.4568016	9.65053743	1.19373583	7.21E-07	3.48E-05
2900348	NM_003407.2	ZFP36	19	39899714-39899763	11.1023374	12.2430459	1.14070847	7.36E-07	3.48E-05
4480288	NM_022767.2	ISG20L1	15	86976380-86976429	8.63942998	9.81050712	1.17107714	7.58E-07	3.56E-05
3120196	NM_001031806.1	ALDH3A2	17	19521034-19521083	12.2663261	11.0198962	-1.2464299	7.97E-07	3.67E-05
3420739	NM_021021.2	SNTB1	8	121619351-121619400	9.10257551	8.0641125	-1.038463	8.32E-07	3.80E-05
6840075	NM_000270.1	NP	14	20014881-20014930	9.02467347	10.405094	1.38042054	1.11E-06	4.63E-05
6020424	NM_005572.3	LMNA	1	154374205-154374254	10.3861794	11.4071907	1.02101129	1.28E-06	5.08E-05
3710373	NM_001048197.1	SNHG3-RCC1	1	28737782-28737831	7.94847103	8.99315061	1.04467957	1.29E-06	5.10E-05
5670424	NM_002068.1	GNA15	19	3114544-3114593	10.2569754	11.4339889	1.17701346	1.40E-06	5.41E-05
940220	NM_022162.1	NOD2	16	49324082-49324131	9.67723489	10.7921182	1.11488328	1.53E-06	5.77E-05
3460020	AK095707	HS.374278	16	79981590-79981639	12.618312	11.1509084	-1.4674036	1.57E-06	5.90E-05
5960343	NM_033405.2	PRIC285	20	61660011-61660060	9.57681655	10.7250822	1.14826567	1.83E-06	6.46E-05
6330725	NM_005178.2	BCL3	19	49954947-49954996	9.17492677	10.3369919	1.16206512	1.89E-06	6.59E-05
5700725	NM_033255.2	EPSTI1	13	43462293-43462342	8.02139897	10.0185173	1.9971183	1.95E-06	6.77E-05
5360070	NM_004701.2	CCNB2	15	57204299-57204348	8.21180176	9.52008022	1.30827846	1.99E-06	6.86E-05
610519	NM_001018020.1	TPM1	15	61141496-61141529:61141828-61141843	11.5938683	10.5898917	-1.0039766	1.99E-06	6.86E-05

2690709	NM_004624.2	VIPR1	3	42553981-42554030	11.0715933	10.007398	-1.0641954	2.11E-06	7.11E-05
6200382	NM_178177.2	NMNAT3	3	140761829-140761878	10.1072707	9.03485462	-1.0724161	2.17E-06	7.25E-05
3930343	NM_001629.2	ALOX5AP	13	30236347-30236396	10.7749828	11.8317688	1.05678595	2.18E-06	7.27E-05
5910402	XR_015970.1	MGC102966	17	20345444-20345493	10.1090055	13.4765265	3.36752098	2.22E-06	7.38E-05
4830674	NM_032621.2	BEX2	X	102564441-102564490	10.4678945	9.34355586	-1.1243387	2.26E-06	7.43E-05
6620437	NM_019102.2	HOXA5	7	27181334-27181383	10.8790322	9.59499525	-1.284037	2.33E-06	7.61E-05
5270674	NM_003485.3	GPR68	14	91699107-91699156	8.1592265	9.59769114	1.43846464	2.71E-06	8.57E-05
6370228	AB074162	HS.554507	9	126462570-126462619	8.67407277	7.33505465	-1.3390181	2.85E-06	8.87E-05
1230348	NM_001042476.1	CARHSP1	16	8948804-8948853	10.1157534	11.3930712	1.27731779	3.13E-06	9.52E-05
520114	NM_004564.1	PET112L	4	152811510-152811559	9.1358057	10.2675194	1.13171366	3.72E-06	0.00010714
3120437	NM_000755.2	CRAT	9	130897121-130897170	9.02535087	7.3854773	-1.6398736	3.75E-06	0.00010768
3840491	NM_021255.2	PELI2	14	55837274-55837323	9.74679119	8.45684569	-1.2899455	3.97E-06	0.00011237
4150048	NM_001444.1	FABP5	8	82192820-82192830:82192831-82192869	12.1026842	13.4625298	1.35984563	4.09E-06	0.00011523
2360020	NM_013402.3	FADS1	11	61323986-61324035	11.0646054	9.17568789	-1.8889175	4.10E-06	0.00011526
3850754	NM_025249.1	KIAA1683	19	18228925-18228974	9.16182612	7.9792506	-1.1825755	4.22E-06	0.00011774
460102	NM_000560.3	CD53	1	111243722-111243771	7.6686019	8.9701347	1.3015328	4.31E-06	0.00011896
1580411	NM_001040651.1	CD3D	11	118209860-118209876:118209877-118209909	8.66829498	10.2828833	1.61458833	4.36E-06	0.00011981
6590228	NM_006725.2	CD6	11	60544218-60544267	7.12592453	8.48245373	1.3565292	4.38E-06	0.00012024
2650608	NM_001237.2	CCNA2	4	122958685-122958734	7.66896545	8.90527237	1.23630692	4.43E-06	0.00012151
2640768	NM_001814.2	CTSC	11	87710365-87710414	7.64937949	8.94831053	1.29893105	4.45E-06	0.00012154
4490520	NM_004951.3	EBI2	13	98745378-98745427	8.31573618	9.65988229	1.3441461	4.80E-06	0.00012777
7400017	NM_004445.2	EPHB6	7	142278751-142278779:142278780-142278800	11.6130559	10.4996836	-1.1133723	4.91E-06	0.00012987
6960274	NM_002108.2	HAL	12	96367930-96367979	9.08525956	10.409275	1.32401549	5.05E-06	0.0001324
2650156	NM_018833.2	TAP2	6	32906458-32906507	6.94183941	8.05280168	1.11096226	5.05E-06	0.0001324
1010592	NM_001001548.1	CD36	7	80143770-80143819	9.73210299	10.9358097	1.20370672	5.68E-06	0.00014385
2650164	NM_018291.2	FLJ10986	1	59912323-59912372	10.6294731	9.47828637	-1.1511868	5.75E-06	0.00014529
7000408	NM_205545.1	LYPD2	8	143832477-143832526	7.58456185	9.11811239	1.53355054	5.88E-06	0.00014793
20129	NM_001803.2	CD52	1	26519273-26519322	8.83704062	10.0886524	1.25161179	6.02E-06	0.00015058
4230196	NM_002266.2	KPNA2	17	63469563-63469577:63469678-63469712	6.89751321	8.19773343	1.30022022	6.42E-06	0.00015812
4780411	NM_017522.3	LRP8	1	53711532-53711581	7.15690858	8.41612758	1.259219	6.69E-06	0.00016278
10487	NM_052901.2	SLC25A25	9	129911123-129911172	9.5808639	10.7103824	1.12951848	6.69E-06	0.00016278
7570148	NM_032737.2	LMNB2	19	2428328-2428377	9.4253036	10.4851756	1.05987196	6.84E-06	0.00016591
6840408	NM_004271.3	LY86	6	6599837-6599859:6599860-6599886	7.07430134	8.08776361	1.01346228	6.92E-06	0.0001673
610598	NM_004000.2	CHI3L2	1	111586462-111586509:111586510-111586511	7.25934426	9.57934594	2.32000168	6.97E-06	0.00016822
5550279	NM_001098175.1	ENTPD1	10	97604334-97604383	7.81182626	8.81710895	1.00528269	7.02E-06	0.00016911
5670605	NM_139354.2	MATK	19	3777979-3778028	7.35519725	8.94197259	1.58677535	7.66E-06	0.0001793
6840468	NM_002108.2	HAL	12	96367248-96367297	11.1819832	12.3414951	1.15951195	7.84E-06	0.0001812
7400102	NM_020437.3	ASPHD2	22	25169156-25169172:25169173-25169205	6.99102966	8.01653888	1.02550922	7.97E-06	0.00018267
3140707	NM_031458.1	PARP9	3	123729671-123729720	8.77744608	10.0127123	1.23526619	8.12E-06	0.00018561
3840554	NM_014767.1	SPOCK2	10	73488877-73488926	8.22033551	9.48339024	1.26305473	8.75E-06	0.00019486
3440754	NM_001012633.1	IL32	16	3058184-3058233	8.12557276	9.65474175	1.52916899	8.76E-06	0.00019486
6330132	NM_002201.4	ISG20	15	86999776-86999825	9.19610725	10.2994179	1.10331065	9.47E-06	0.00020827
4210619	NM_001767.2	CD2	1	117113051-117113100	7.99140592	9.43604258	1.44463666	9.49E-06	0.00020851

1170671	NM_000732.4	CD3D	11	118210491-118210540	8.41005463	9.95349385	1.54343922	1.05E-05	0.00022306
7100093	NM_001025580.1	AMMECR1	X	109438952-109439001	7.09100385	8.29794865	1.2069448	1.06E-05	0.00022395
6560291	NM_018099.3	FAR2	12	29377858-29377907	9.90996142	7.91397169	-1.9959897	1.06E-05	0.00022502
2100196	NM_005101.1	ISG15	1	939540-939589	8.44648641	9.69561344	1.24912703	1.07E-05	0.00022571
290739	NM_004944.2	DNASE1L3	3	58178504-58178530:58179070-58179092	8.90474598	10.0414972	1.13675125	1.07E-05	0.00022577
5810612	NM_001150.1	ANPEP	15	88129409-88129458	9.20223584	10.2427328	1.04049698	1.14E-05	0.00023642
4040037	NM_004951.3	EBI2	13	98745149-98745198	7.2579792	8.48029997	1.22232077	1.19E-05	0.00024364
4150189	NM_001912.3	CTSL1	9	89535894-89535943	10.7901072	12.0995324	1.30942517	1.21E-05	0.00024606
1980689	NM_172245.1	CSF2RA	XY	1369261-1369310	7.60603526	8.69314347	1.08710821	1.26E-05	0.00025375
7510537	NM_005138.1	SCO2	22	49308992-49309041	9.77005415	11.1420797	1.37202555	1.27E-05	0.00025468
5810154	NM_001039131.1	ALOX15B	17	7892930-7892979	10.8840256	8.92787186	-1.9561538	1.28E-05	0.00025601
6110343	NM_145898.1	CCL23	17	34340185-34340234	7.19830442	9.02380193	1.82549752	1.30E-05	0.00025868
3890689	NM_198053.1	CD247	1	165666584-165666633	8.10126072	9.61864748	1.51738676	1.32E-05	0.00026174
630315	NM_005771.3	DHRS9	2	169660803-169660852	9.19186267	10.3641202	1.17225754	1.32E-05	0.00026181
520678	NM_000560.3	CD53	1	111243720-111243769	7.17279232	8.37981226	1.20701994	1.34E-05	0.00026434
2230379	NM_005746.2	NAMPT	7	105893542-105893591	8.17980242	9.83036322	1.6505608	1.49E-05	0.0002846
1690066	NM_002462.2	MX1	21	41752921-41752970	11.2476963	12.3102451	1.06254886	1.57E-05	0.00029596
5810743	NM_207376.1	LOC387882	12	104288777-104288826	9.36495526	10.389616	1.02466072	1.61E-05	0.00030048
2810673	NM_152739.3	HOXA9	7	27202174-27202223	11.7468686	10.1732894	-1.5735792	1.65E-05	0.00030727
7560632	NM_005546.3	ITK	5	156614228-156614277	7.16565349	8.57811076	1.41245726	1.84E-05	0.00032927
3990259	NM_001042595.1	TMEM91			11.5660868	10.4537069	-1.1123799	1.93E-05	0.00034112
3170270	NM_005764.3	PDZK1IP1	1	47649561-47649610	8.71338026	9.74689213	1.03351186	1.94E-05	0.00034173
4260386	NM_145918.2	CTSL1	9	89535884-89535933	11.1741502	12.4047619	1.23061167	1.98E-05	0.00034871
580739	NM_001996.2	FBLN1	22	44337731-44337780	13.1384683	12.1148712	-1.0235971	2.02E-05	0.00035374
2940110	NM_001048201.1	UHRF1	19	4912360-4912409	8.59711048	9.80852316	1.21141268	2.10E-05	0.00036228
1690240	NM_032385.3	C5orf4	5	154198595-154198644	9.72428337	8.51357069	-1.2107127	2.12E-05	0.00036362
1500139	NM_006042.1	HS3ST3A1	17	13445168-13445171:13445172-13445217	7.18903291	8.65626779	1.46723488	2.20E-05	0.00037359
1010672	NM_000901.1	NR3C2	4	149219673-149219722	9.6738986	8.64444399	-1.0294546	2.27E-05	0.00038333
110180	NM_001080157.1	ARHGAP9	12	57866149-57866198	8.65002763	9.75771279	1.10768516	2.30E-05	0.00038594
6290400	NM_000734.2	CD247	1	165666606-165666655	8.01344624	9.43849888	1.42505264	2.33E-05	0.0003909
110719	NM_004207.2	SLC16A3	17	77790597-77790646	8.1942474	9.57542763	1.38118023	2.34E-05	0.00039236
3190112	NM_030666.2	SERPINB1	6	2834064-2834113	9.68703304	10.7927029	1.10566988	2.45E-05	0.00040513
650753	NM_001025108.1	AFF3	2	100163843-100163892	8.80184924	7.76715493	-1.0346943	2.49E-05	0.00040982
6060468	NM_002964.3	S100A8	1	153362613-153362662	11.9339613	14.1807222	2.2467609	2.58E-05	0.00041993
630619	NM_006665.3	HPSE	4	84442360-84442409	8.22297748	9.81229941	1.58932193	2.58E-05	0.00041958
3840564	NM_206938.1	MS4A7	11	59918446-59918495	7.7228982	8.81201385	1.08911565	2.59E-05	0.00042084
2490537	NM_001066.2	TNFRSF1B	1	12191715-12191764	8.93685177	10.0352999	1.09844817	2.63E-05	0.00042449
5720369	NM_000361.2	THBD	20	23026506-23026555	8.2280792	9.47679647	1.24871727	2.79E-05	0.00044452
4810020	NM_002664.1	PLEK	2	68477871-68477920	8.99437241	10.1804082	1.18603579	2.87E-05	0.00045259
1300408	NM_005335.3	HCLS1	3	122833112-122833161	9.3296501	10.3903037	1.06065363	3.07E-05	0.00047677
730440	NM_006509.2	RELB	19	45541112-45541161	7.53546646	8.7041101	1.16864364	3.09E-05	0.00047909
6220538	NM_003974.2	DOK2	8	21822473-21822522	7.27764554	8.30212658	1.02448104	3.44E-05	0.00051378
7040035	NM_001032409.1	OAS1	12	111839789-111839838	6.83748638	7.88180044	1.04431406	3.63E-05	0.00053375
4260368	NM_181800.1	UBE2C	20	43877911-43877959:43878755-43878755	8.83926071	9.98217586	1.14291515	3.65E-05	0.0005353
2630561	NM_001024662.1	RPL6	12	112847219-112847268	8.11773393	9.25552031	1.13778638	4.34E-05	0.00060561

2640619	NM_003430.2	ZNF91	19	23542438-23542487	12.0979268	10.7817213	-1.3162055	4.36E-05	0.00060812
110382	NM_002872.3	RAC2	22	37621465-37621514	9.73434575	10.8352023	1.10085651	4.49E-05	0.00062114
1050706	NM_001786.2	CDC2	10	62221918-62221967	7.88799076	9.02510881	1.13711806	4.50E-05	0.00062208
150072	NM_002163.2	IRF8	16	84513378-84513427	9.46981857	10.5072831	1.03746451	4.54E-05	0.00062439
4010719	NM_172249.1	CSF2RA	XY	1367531-1367535:1367412-1367456	7.46298892	8.56437664	1.10138771	4.60E-05	0.00063014
4730037	NM_018990.2	SASH3	X	128756617-128756666	6.72915681	7.93095936	1.20180255	4.63E-05	0.00063175
2490309	NM_018986.3	SH3TC1	4	8242502-8242551	7.15489485	8.22306249	1.06816764	4.72E-05	0.00064121
1820379	NM_000954.5	PTGDS	9	138994544-138994557:138995106-138995128:138995852-138995864	11.4620938	10.2210995	-1.2409943	4.76E-05	0.00064463
4810026	NM_144765.1	MPZL2	11	118130913-118130916:118133153-118133198	7.19932402	8.19943332	1.0001093	4.89E-05	0.00065574
5310471	NM_181803.1	UBE2C	20	43875503-43875510:43877900-43877923:43877924-43877941	8.80578409	9.85046535	1.04468125	5.07E-05	0.00067281
160494	NM_020980.2	AQP9	15	56265152-56265201	11.2185161	9.35478472	-1.8637314	5.19E-05	0.00068402
3420044	NM_133625.3	SYN2	3	12199855-12199872:12203046-12203077	8.64138615	7.56098138	-1.0804048	5.49E-05	0.00071145
360619	NM_005248.2	FGR	1	27938933-27938982	8.38104339	9.45640684	1.07536345	5.51E-05	0.00071315
1500010	NM_001255.2	CDC20	1	43601340-43601387:43601388-43601389	8.87936562	10.1237821	1.24441648	5.76E-05	0.00073414
1470500	NM_002147.3	HOXB5	17	46668690-46668739	9.6476268	8.63303406	-1.0145927	5.81E-05	0.0007389
2140278	NM_198289.1	CIDEA	18	12264206-12264255	8.96317766	7.59627361	-1.366904	6.19E-05	0.00077253
5360670	NM_002658.2	PLAU	10	75346964-75347013	9.74375397	10.8620101	1.11825615	6.21E-05	0.00077405
520273	NM_022904.1	RASAL3	19	15562460-15562509	8.13202272	9.15375163	1.02172891	6.23E-05	0.00077457
6900209	NM_033274.2	ADAM19	5	156904841-156904890	8.16849319	9.58072911	1.41223592	6.91E-05	0.0008345
5870164	NM_001045557.1	SLA	8	134118227-134118276	8.48269596	9.57508852	1.09239256	7.23E-05	0.00086089
4590767	NM_003125.2	SPRR1B	1	151271513-151271562	10.4146596	12.288436	1.87377644	7.48E-05	0.00088367
5670674	NM_000902.3	MME	3	154900904-154900953	7.41936896	8.44757995	1.02821099	7.92E-05	0.00092429
1820750	NM_007315.2	STAT1	2	191548824-191548858:191549811-191549825	8.49809534	9.77937652	1.28128118	9.19E-05	0.00102545
10240	NM_002558.2	P2RX1	17	3800020-3800069	8.77784586	7.76138203	-1.0164638	0.00010309	0.00110936
3310471	NM_145274.2	TMEM99	17	36244673-36244722	11.4103073	10.4028374	-1.0074699	0.00010383	0.00111505
6520180	NM_003853.2	IL18RAP	2	102435293-102435342	6.7697598	8.01177826	1.24201845	0.00011197	0.0011779
2630541	BX107250	HS.445442	11	7979819-7979868	8.99603159	7.98421969	-1.0118119	0.00012087	0.00124396
2680382	NM_001003679.1	LEPR	1	65873604-65873653	12.3805206	10.8850618	-1.4954588	0.00012331	0.00126304
1010246	NM_022872.2	IFI6	1	27994780-27994829	8.14555767	9.43839138	1.29283371	0.00014375	0.00141796
7550484	NM_002727.2	SRGN	10	70533801-70533850	9.3059468	10.6626199	1.35667307	0.00015848	0.00152147
6400392	NM_000561.2	GSTM1	1	110037838-110037887	13.0706632	12.0597967	-1.0108665	0.00017354	0.00161541
2570079	NM_139266.1	STAT1	2	191548621-191548670	11.0373896	12.050272	1.01288244	0.00017386	0.00161761
6860240	BC070337	HS.546375	14	22017757-22017762:22086287-22086330	7.48527408	8.49163185	1.00635777	0.00017602	0.00163233
50725	NM_178349.1	LCE1B	1	151051950-151051999	13.6944153	12.6017848	-1.0926305	0.00018167	0.00167013
5310634	NM_004104.4	FASN	17	80036214-80036263	12.2663223	11.2004547	-1.0658676	0.00018972	0.00172438
5890193	NM_148975.1	MS4A4A	11	59832420-59832469	7.99580028	9.24261825	1.24681797	0.00019486	0.00175805
6200168	NM_006875.2	PIM2	X	48655729-48655778	7.78666455	8.83275498	1.04609043	0.00019626	0.00176613
6510377	NM_016639.1	TNFRSF12A	16	3012033-3012082	8.49060718	9.70658507	1.21597789	0.00021891	0.00191685
6660475	NM_001042729.1	FGR	1	27938871-27938920	8.63069446	9.71621719	1.08552273	0.00022383	0.00194935
6250064	NM_002198.1	IRF1	5	131846773-131846822	9.0944359	10.3219719	1.22753602	0.00022883	0.00198378
5290397	NM_013246.2	CLCF1	11	67131876-67131925	6.84471561	7.85330818	1.00859257	0.00023079	0.00199487
6620121	NM_005623.2	CCL8	17	29672323-29672372	8.19215603	9.78932105	1.59716502	0.00023367	0.00201315

2000300	NM_006332.3	IFI30	19	18149528-18149574:18149659-18149661	8.1915393	9.27450353	1.08296423	0.00023909	0.0020469
6200255	NM_018441.3	PECR	2	216612179-216612228	8.65517094	7.4698103	-1.1853606	0.00025923	0.00217498
2030767	NM_001778.2	CD48	1	160648718-160648767	8.03351422	9.09459317	1.06107895	0.00026779	0.00222783
1440736	NM_000527.2	LDLR	19	11105336-11105385	11.3716682	12.4003303	1.02866207	0.00029104	0.0023841
4810341	NM_003650.2	CST7	20	24888342-24888348:24888349-24888391	6.92309369	8.04832501	1.12523132	0.00029212	0.00239014
780725	NM_001109.3	ADAM8	10	134926186-134926235	6.97718321	8.24991604	1.27273283	0.00029286	0.00239145
3180392	NM_006770.3	MARCO	2	119468445-119468494	7.11962196	8.20255248	1.08293052	0.00029436	0.00239996
360500	NM_002727.2	SRGN	10	70526868-70526917	9.4398174	10.7390694	1.29925199	0.00032443	0.00256767
1580161	NM_018092.3	NETO2	16	47115854-47115903	7.8661606	8.87475362	1.00859302	0.00033119	0.00260833
2470017	NM_006864.2	LILRB3	19	59412606-59412655	7.31920651	8.46456538	1.14535887	0.00036366	0.00281403
1440709	NM_003613.2	CILP	15	63275926-63275975	12.2383556	11.1207629	-1.1175927	0.00043236	0.00321995
1850709	NM_001149.2	ANK3	10	61788362-61788411	10.2637634	9.1526784	-1.111085	0.00047643	0.00346757
2490017	NM_025079.1	ZC3H12A	1	37722267-37722316	9.04534194	10.0496068	1.00426489	0.00049544	0.00356602
2710575	NM_001781.1	CD69	12	9796674-9796723	7.29600553	8.85989877	1.56389324	0.00051631	0.00366682
5050162	NM_001040280.1	CD83	6	14136583-14136632	8.2115902	9.31056826	1.09897807	0.00053608	0.00377504
3180528	NM_004994.2	MMP9	20	44078320-44078369	8.23221179	9.73284272	1.50063093	0.00065816	0.00440654
2350465	NM_000992.2	RPL29	3	52029908-52029957	7.57489392	8.91175186	1.33685794	0.00078878	0.00503675
6450129	NM_004867.3	ITM2A	X	78615324-78615973	9.64886509	8.11512293	-1.5337422	0.00088117	0.00547396
3360634	NM_013322.2	SNX10	7	26379697-26379746	7.71226192	8.82945617	1.11719424	0.00088678	0.00549525
5260047	NM_001444.1	FABP5	8	82195737-82195773:82196108-82196120	11.778017	12.8666217	1.08860469	0.00095429	0.00578153
3420612	NM_006144.2	GZMA	5	54441606-54441655	7.66518078	8.85079281	1.18561203	0.00111566	0.00652749
5310053	NM_002341.1	LTB	6	31656373-31656422	9.05651683	10.2462659	1.18974904	0.00125352	0.00709488
7160474	NM_002123.2	HLA-DQB1	6	32736001-32736004:32737102-32737147	8.14584018	9.47536379	1.32952361	0.00149615	0.00811784
3710553	NM_175840.1	SMOX	20	4116158-4116207	7.72647678	8.8449074	1.11843062	0.00155709	0.00837163
2140242	NM_007115.2	TNFAIP6	2	151934982-151935008:151938309-151938331	9.20047183	10.2713499	1.07087808	0.00161366	0.00861348
1740050	XM_495863.3	GVIN1	11	6691459-6691508	8.06489193	9.08844113	1.0235492	0.00177694	0.00929914
5080131	NM_145792.1	MGST1	12	16408108-16408157	11.0645486	9.8762913	-1.1882573	0.00216247	0.0108295
3060341	NM_001013714.1	LOC440993	3	196913288-196913337	9.34737181	8.31392344	-1.0334484	0.00231797	0.01141068
830682	XM_937508.2	LOC387934	-	-	11.8383399	12.8542502	1.01591037	0.00271504	0.01293416
1010546	XM_944822.1	LOC649143			9.38507881	10.7492967	1.36421789	0.00373203	0.01658244
5810685	NM_003246.2	THBS1	15	37676117-37676166	8.07641212	9.38476145	1.30834933	0.0037724	0.0167169
1450471	XM_371783.3	LOC202134	5	175486440-175486489	9.49894878	8.37778631	-1.1211625	0.0050176	0.02092559
6660398	NM_002003.2	FCN1	9	137801465-137801514	7.68070275	8.77411034	1.09340759	0.01078258	0.03770372
3170128	NM_171827.2	CD8A	2	86865488-86865537	7.4604068	8.47213572	1.01172892	0.01282294	0.04312906

Table III: Gene transcripts with genome-wide significant differential expression (P$_{FDR}$ <0.05, Diff >1/fold change >2) in lesional skin (AL) vs. non-lesional skin (AN)

ProbeID	ACCESSION	GENE SYMBOL	CHR	PROBE_COORDINATES	mean.NN	mean.AN	mean.AL	Diff. AL_AN	Pvalue AL_AN	P.FDR AL_AN
4150048	NM_001444.1	FABP5	8	82192820-82192830:82192831-82192869	12.1026842	12.2308666	13.4625298	1.23166318	1.33E-06	0.00122574
3310471	NM_145274.2	TMEM99	17	36244673-36244722	11.4103073	11.6029982	10.4028374	-1.2001607	3.05E-06	0.00134514
160494	NM_020980.2	AQP9	15	56265152-56265201	11.2185161	11.1640315	9.35478472	-1.8092468	5.25E-06	0.00137548
5670687	NM_015993.1	PLLP	16	55847785-55847834	11.0276749	10.8675112	9.73822044	-1.1292907	6.02E-06	0.0014047
3460020	AK095707	HS.374278	16	79981590-79981639	12.618312	12.3514816	11.1509084	-1.2005732	8.57E-06	0.00145052
7570673	NM_003364.2	UPP1	7	48114453-48114479:48114480-48114502	8.75089818	9.21698121	10.4364665	1.21948531	1.17E-05	0.00162388
4780411	NM_017522.3	LRP8	1	53711532-53711581	7.15690858	7.32423954	8.41612758	1.09188804	1.34E-05	0.00173182
6840075	NM_000270.1	NP	14	20014881-20014930	9.02467347	9.31473164	10.405094	1.09036237	1.61E-05	0.00181443
4070091	NM_001001523.1	RORC	1	151778900-151778949	9.93908335	9.08024021	7.87754138	-1.2026988	2.85E-05	0.00218793
1850156	NM_194284.2	CLDN23	8	8561463-8561512	10.9659435	10.5390615	9.49734767	-1.0417138	2.88E-05	0.00218793
4890553	NM_001001523.1	RORC	1	151778990-151779039	9.34729046	8.57082213	7.50103285	-1.0697893	4.24E-05	0.00256579
2680382	NM_001003679.1	LEPR	1	65873604-65873653	12.3805206	12.4387343	10.8850618	-1.5536724	4.78E-05	0.00268708
1050168	NM_002638.2	PI3	20	43238123-43238172	7.67497724	9.59719345	12.6738132	3.07661971	4.84E-05	0.00268708
6940102	NM_002160.1	TNC	9	116822907-116822956	10.0734962	10.5180401	11.8082419	1.29020173	5.07E-05	0.00276705
4590767	NM_003125.2	SPRR1B	1	151271513-151271562	10.4146596	10.6438201	12.288436	1.64461592	5.14E-05	0.00278069
3990170	NM_005532.3	IFI27	14	93652556-93652605	11.4749484	12.4563046	13.761614	1.30530941	5.32E-05	0.00280786
780079	XM_943677.1	LOC654053			8.52005792	8.72207494	7.64165779	-1.0804172	6.60E-05	0.00306746
870711	NM_001039503.2	POL3S	16	31094879-31094928	7.94091652	8.88535855	10.8205039	1.9351454	8.45E-05	0.0034708
6510377	NM_016639.1	TNFRSF12A	16	3012033-3012082	8.49060718	8.63688854	9.70658507	1.06969653	8.65E-05	0.00349859
5270674	NM_003485.3	GPR68	14	91699107-91699156	8.1592265	8.57783796	9.59769114	1.01985317	9.72E-05	0.00378225
1230348	NM_001042476.1	CARHSP1	16	8948804-8948853	10.1157534	10.3378441	11.3930712	1.05522706	9.76E-05	0.00379143
5910402	XR_015970.1	MGC102966	17	20345444-20345493	10.1090055	10.84047	13.4765265	2.63605646	0.0001033	0.00389185
1690066	NM_002462.2	MX1	21	41752921-41752970	11.2476963	11.2660593	12.3102451	1.04418583	0.00011715	0.00411376
2100196	NM_005101.1	ISG15	1	939540-939589	8.44648641	8.44541288	9.69561344	1.25020056	0.00013331	0.00433723
3190112	NM_030666.2	SERPINB1	6	2834064-2834113	9.68703304	9.7740542	10.7927029	1.01864873	0.00013684	0.00438963
1450471	XM_371783.3	LOC202134	5	175486440-175486489	9.49894878	9.72407637	8.37778631	-1.3462901	0.00017382	0.00489121
2350504	NM_001953.2	ECGF1	22	49311047-49311064:49311065-49311096	10.7402434	11.348607	12.7282181	1.37961112	0.00018258	0.00501984
1690240	NM_032385.3	C5orf4	5	154198595-154198644	9.72428337	9.52488884	8.51357069	-1.0113181	0.00021775	0.00545545
1500139	NM_006042.1	HS3ST3A1	17	13445168-13445171:13445172-13445217	7.18903291	7.3419209	8.65626779	1.31434689	0.00023922	0.00570587
1580161	NM_018092.3	NETO2	16	47115854-47115903	7.8661606	7.86269504	8.87475362	1.01205858	0.00028027	0.00626869
6220343	NM_021098.2	CACNA1H	16	1211052-1211101	9.48008646	9.00377192	7.59065035	-1.4131216	0.00032925	0.0068554
6900209	NM_033274.2	ADAM19	5	156904841-156904890	8.16849319	8.45045317	9.58072911	1.13027594	0.00033227	0.0068859
7550484	NM_002727.2	SRGN	10	70533801-70533850	9.3059468	9.5601494	10.6626199	1.10247047	0.00041793	0.00773561
360500	NM_002727.2	SRGN	10	70526868-70526917	9.4398174	9.57357639	10.7390694	1.165493	0.00053478	0.0087683
7550358	NM_006159.1	NELL2	12	43188674-43188723	9.39239266	9.82608235	11.3547547	1.52867238	0.00062615	0.00968546
5700725	NM_033255.2	EPSTI1	13	43462293-43462342	8.02139897	8.61482136	10.0185173	1.40369591	0.00064617	0.00985734

6370228	AB074162	HS.554507	9	126462570-126462619	8.67407277	8.33614911	7.33505465	-1.0010945	0.00076132	0.01086568
2350465	NM_000992.2	RPL29	3	52029908-52029957	7.57489392	7.75574736	8.91175186	1.15600449	0.0007645	0.01089077
3890326	NM_001024465.1	SOD2	6	160103621-160103670	10.3341532	10.3003982	11.3005498	1.00015156	0.00090534	0.01173294
450615	NM_005953.2	MT2A	16	55200021-55200068:55200069-55200070	11.2929319	10.967983	11.9973211	1.02933804	0.00098438	0.01226674
730047	NM_001002236.1	SERPINA1	14	93916997-93917046	7.19301102	6.82037625	7.98323374	1.16285749	0.00104811	0.01261649
1010246	NM_022872.2	IFI6	1	27994780-27994829	8.14555767	8.21478823	9.43839138	1.22360315	0.00140447	0.0149516
3890523	XM_937367.1	IL7R			8.28051285	9.15377521	10.2120978	1.05832259	0.00201488	0.01845836
3180528	NM_004994.2	MMP9	20	44078320-44078369	8.23221179	8.38357176	9.73284272	1.34927097	0.00210351	0.01888801
2230500	NM_001014450.1	SPRR2F	1	153084780-153084829	10.7182116	12.7947996	13.8121514	1.01735171	0.00217959	0.01923936
5080450	NM_006006.4	ZBTB16	11	113626419-113626468	9.90043354	10.4751902	9.38797892	-1.0872113	0.00223436	0.01942635
6380484	NM_001002235.1	SERPINA1	14	93914546-93914595	7.57854628	7.25436055	8.54000868	1.28564813	0.00229766	0.01980193
6660398	NM_002003.2	FCN1	9	137801465-137801514	7.68070275	7.40121291	8.77411034	1.37289743	0.00263765	0.02155358
5390220	NM_002965.2	S100A9	1	151599776-151599825	11.234989	13.1291932	14.3953461	1.26615289	0.00303617	0.02357279
1240474	NM_001018011.1	ZBTB16	11	113626269-113626318	8.4562956	9.01965357	7.86990629	-1.1497473	0.00439995	0.02975762
2230379	NM_005746.2	NAMPT	7	105893542-105893591	8.17980242	8.80259931	9.83036322	1.02776391	0.00479348	0.0313635
6060468	NM_002964.3	S100A8	1	153362613-153362662	11.9339613	13.1546167	14.1807222	1.0261055	0.0273489	0.09353885
610598	NM_004000.2	CHI3L2	1	111586462-111586509:111586510-111586511	7.25934426	8.46357665	9.57934594	1.11576929	0.03607531	0.11199948

Table IV: Functional Annotation Cluster derived from DAVID gene enrichment analysis for non-lesional skin (AN) vs. controls (NN)

	Term	Count	P-value	Genes	ES	P_{BH}
				Cluster 1: Epidermis development ES=2.53		
	Common genes:			S100A7, SPRR2G, SPRR2F (ALL)		
1	GO:0060429~epithelium development (BP)	4	6.96E-04	CA2	19.86	0.1282
2	GO:0030216~keratinocyte differentiation (BP)	3	0.0013		51.24	0.0599
3	GO:0009913~epidermal cell differentiation (BP)	3	0.0015		46.97	0.0570
4	GO:0030855~epithelial cell differentiation (BP)	3	0.0053		24.69	0.1383
5	GO:0008544~epidermis development (BP)	3	0.0093		18.38	0.1546
6	GO:0007398~ectoderm development (BP)	3	0.0109		16.99	0.1640
				Cluster 2: Defense response ES=2.29		
	Common genes:			CCL23, S100A9, CCL8 (ALL); C1QB (1,3,7); PTGDS (2,4)		
1	GO:0006952~defense response (BP)	5	0.0011	S100A7	9.17	0.1010
2	GO:0007626~locomotory behavior (BP)	4	0.0012		16.46	0.0759
3	GO:0006954~inflammatory response (BP)	4	0.0020		13.87	0.0625
4	GO:0007610~behavior (BP)	4	0.0055		9.61	0.1281
5	GO:0006935~chemotaxis (BP)	3	0.0071		21.14	0.1449
6	GO:0042330~taxis (BP)	3	0.0071		21.14	0.1449
7	GO:0009611~response to wounding (BP)	4	0.0078		8.51	0.1429
8	GO:0007267~cell-cell signaling (BP)	3	0.0829		5.64	0.7039
				Cluster 3: Immune response ES=2.15		
	Common genes:			C1QB, CCL23, CCL8 (ALL); S1009A (1,2,3); S1007A (1,4,6); CA2 (4,5,7); PI3 (4,5)		
1	GO:0006952~defense response (BP)	5	0.0011		9.17	0.1010
2	GO:0006954~inflammatory response (BP)	4	0.0020		13.87	0.0625
3	GO:0009611~response to wounding (BP)	4	0.0078		8.51	0.1429
4	GO:0005576~extracellular region (CC)	7	0.0095	PTGDS	3.18	0.3488
5	GO:0044421~extracellular region part (CC)	5	0.0131		4.76	0.2560
6	GO:0006955~immune response (BP)	4	0.0160		6.54	0.2172
7	GO:0005615~extracellular space (CC)	4	0.0293		5.33	0.3597

ES=enrichment score, P_{BH}=Benjamini-Hochberg corrected P-value

Table V: Functional Annotation Cluster derived from DAVID gene enrichment analysis for lesional skin (AL) vs. controls (NN)

	Term	Count	P-value	Genes	ES	P_BH
				Cluster 1: Defense response ES=4.83		
	Common genes of terms:			IL18RAP, S100A8, LY86, S100A9, CCL8, GPR68, C1QB, TNFAIP6, TNFRSF1B, CCL23, P2RX1, IRF7, THBS1 **(ALL)**		
1	*GO:0006952~defense response (BP)*	25	5.4x10⁻⁷	ITK, FGR, S100A7, RNASE6, IL32, CD48, CD83, NOD2, TAP2, LILRB3, BCL3, MX1	3.27	4.4x10⁻⁴
2	*GO:0009611~response to wounding (BP)*	21	8.5x10⁻⁶	PLEK TNC, TPM1, CD36, THBD, PLLP, ENTPD1, PLAU	3.19	0.0046
3	*GO:0006954~inflammatory response (BP)*	13	7.1x10⁻⁴		3.22	0.1102
				Cluster 2: Extracellular space ES=3.93		
	Common genes of terms:			LDLR, MMP9, LEPR, LY86, CILP, GGH, CHI3L2, CCL8, IL32, FXYD6, C1QB, FBLN1, CCL23, THBD, ISG15, CLCF1, FCN1, LRP8, CA2, THBS1, LTB, SRGN **(ALL)**; SPOCK2, TNC, ENTPD1, PI3 **(2,3)**		
1	*GO:0005615~extracellular space (CC)*	22	8.0x10⁻⁵	CD8A, S100A7, NELL2, IFI30, IL7R, CTSL1, EPHB6, TNFRSF1B, HPSE, IL4R, CD2, PLEK, GZMA, POL3S, RNASE6, PTGDS, CST7, PLAU	2.63	0.0090
2	*GO:0005576~extracellular region (CC)*	44	9.1x10⁻⁵		1.79	0.0069
3	*GO:0044421~extracellular region part (CC)*	26	2.2x10⁻⁴		2.22	0.0123
				Cluster 3: Plasma membrane ES=2.99		
	Common genes of terms:			KCNMB4, AQP9, LDLR, CD8A, MME, CD52, ANPEP, GPR68, VIPR1, EPHB1, MARCO, CD48, EPHB6, LAPTM5, CD69, IL4R, TAP2, CD2, ENTPD1, CD6, ADAM8, SLC16A3, CD83, THBD, CD36, P2RX1, LILRB3 **(ALL)**; RGM **(1,2,4)**; CDK5R1, GNA15, S100A7, FERMT3, ANK3, IL7R, CD247, CD3D, SNTB1, CA2, GZMA, PLEK, CLDN23, THBS1, TGM3, LRP8, CACNA1H, SYN2, TPM1, ALDH3A2 **(1,4)**		
1	*GO:0044459~plasma membrane part (CC)*	48	4.0x10⁻⁵		1.79	0.0090
2	*GO:0031226~intrinsic to plasma membrane (CC)*	28	0.0014		1.89	0.0394
3	*GO:0005887~integral to plasma membrane (CC)*	27	0.0022		1.86	0.0439
4	*GO:0005886~plasma membrane (CC)*	61	0.0087	LYPD2, LY86, LEPR, CD53, NOD2, TNFRSF12A, FXYD6, TNFRSF1B, CD68, ITK, LMNA, ADAP2, PLAU	1.32	0.1166
				Cluster 4: Immune cell activation ES=2.75		
	Common genes of terms:			BCL3 **(1-12,14)**; RELB, IRF1 **(1-12)**; IL7R **(1-10,13,14)**; CD8A, CD3D **(1-10,13)**; CLCF1 **(1-4,6-10,14)**; PLEK **(1-4)**; CD48, CD2 **(4,5,9,10)**; MMP9 **(1-3,6)**; HCLS1, IRF8, HOXA9 **(1-3)**; LTB **(1,2,4)**; CCNB2 **(1,2)**		
1	*GO:0048534~hemopoietic or lymphoid organ development (BP)*	14	2.0x10⁻⁵		4.34	0.0083
2	*GO:0002520~immune system development (BP)*	14	3.8x10⁻⁵	IL7R	4.08	0.0124

3	*GO:0030097~hemopoiesis (BP)*	12	1.67E-04			4.09	0.0447
4	*GO:0001775~cell activation (BP)*	13	2.3×10^{-4}	P2RX1, ENTPD1		3.65	0.0531
5	*GO:0042110~T cell activation (BP)*	8	0.0010			5.11	0.1322
6	*GO:0002521~leukocyte differentiation (BP)*	8	0.0012			4.92	0.1399
7	*GO:0030217~T cell differentiation (BP)*	6	0.0012			7.43	0.1340
8	*GO:0030098~lymphocyte differentiation (BP)*	7	0.0017			5.47	0.1533
9	*GO:0046649~lymphocyte activation (BP)*	9	0.0033			3.64	0.2093
10	*GO:0045321~leukocyte activation (BP)*	9	0.0104			2.99	0.4042
11	*GO:0046632~alpha-beta T cell differentiation (BP)*	3	0.0125			17.26	0.4109
12	*GO:0046631~alpha-beta T cell activation (BP)*	3	0.0204			13.42	0.4976
13	*hsa05340:Primary immunodeficiency (KEGG)*	4	0.0207	TAP2		6.68	0.4549
14	*GO:0042113~B cell activation (BP)*	3	0.2413			3.18	0.9303

		Cluster 5: Epidermis development ES=2.57				
	Common genes:	SPRR1B, SPRR2G, SPRR2F **(ALL)**; TGM3, LCE1B **(1-7)**; S100A7 **(1,2,4-7)**; HOXB5, DHRS9 **(2,6)**; LTB, ALDH3A2, FABP5 **(5,7)**				
1	*GO:0030216~keratinocyte differentiation (BP)*	6	0.0013		7.32	0.1340
2	*GO:0030855~epithelial cell differentiation (BP)*	8	0.0015		4.70	0.1467
3	*GO:0031424~keratinization (BP)*	5	0.0019		9.36	0.1591
4	*GO:0009913~epidermal cell differentiation (BP)*	6	0.0019		6.71	0.1543
5	*GO:0008544~epidermis development (BP)*	9	0.0020		3.94	0.1528
6	*GO:0060429~epithelium development (BP)*	10	0.0020	HOXA5, CA2	3.55	0.1473
7	*GO:0007398~ectoderm development (BP)*	9	0.0033		3.64	0.2093
8	*GO:0001533~cornified envelope*	3	0.0288		11.17	0.2823

		Cluster 6: Lysosome ES=2.43				
	Common genes:	CTSZ, CD68, LAPTM5, ACP5, CTSC, CTSL1 **(ALL)**; HPSE, GGH, IFI30, SRGN **(1-3)**				
1	GO:0000323~lytic vacuole (CC)	10	0.0011		3.88	0.0478
2	GO:0005764~lysosome (CC)	10	0.0011		3.88	0.0478
3	GO:0005773~vacuole (CC)	10	0.0036		3.25	0.0612
4	hsa04142:Lysosome (KEGG)	6	0.0472		3.00	0.6505

	Term	Count	P-value	Genes	ES	P_BH
				Cluster 7: Cellular component ES=2.38		
				CYP2J2, FADS1, CYP2S1, DHRS9, OAS1, ACSBG1, DGAT2, MGST1 **(ALL)**; AQP9 **(1-5)**; ANK3, TAP2 **(1-3,6)**; PLEK, MME, CD52, CD36, CD68, CCNB2, TNFRSF1B, RAC2, , SLC16A3, P2RX1 **(1-3)**; LMNA **(1,2)**		
1	GO:0005626~insoluble fraction (CC)	22	0.0012		2.15	0.0447
2	GO:0000267~cell fraction (CC)	26	0.0013	ANPEP, CTSL1, HAL, FBLN1	1.97	0.0408
3	GO:0005624~membrane fraction (CC)	21	0.0018		2.13	0.0409
4	GO:0005792~microsome (CC)	9	0.0083		3.11	0.1184
5	GO:0042598~vesicular fraction (CC)	9	0.0098		3.02	0.1166
6	GO:0005783~endoplasmic reticulum (CC)	20	0.0233	CTSZ, S100A7, NR3C2, CRAT, ALDH3A2, FAR2, PTGDS, ALOX5AP, ASPHD2, CTSC	1.71	0.2454

ES=enrichment score, P_BH=Benjamini-Hochberg corrected P-value

Table VI: Functional Annotation Cluster derived from DAVID gene enrichment analysis for lesional (AL) vs. non-lesional skin (AN)

	Term	Count	P-value	Genes	ES	P_BH
				Cluster 1: Extracellular space ES=2.34		
	Common genes:			ISG15, MMP9, LEPR, FCN1, LRP8, SERPINA1, SRGN (ALL); TNC, PI3 (1,3)		
1	GO:0044421~extracellular region part (CC)	9	0.0020		3.63	0.1727
2	GO:0005615~extracellular space (CC)	7	0.0064		3.96	0.2565
3	GO:0005576~extracellular region (CC)	12	0.0074	POL3S, NELL2, IL7R	2.31	0.2061
				Cluster 2: Extracellular matrix ES=1.77		
	Common genes:			TNC, MMP9, PI3, SERPINA1 (ALL)		
1	GO:0044421~extracellular region part (CC)	9	0.0020	ISG15, LEPR, FCN1, LRP8, SRGN	3.63	0.1727
2	GO:0005578~proteinaceous extracellular matrix (CC)	4	0.0452		4.84	0.6586
3	GO:0031012~extracellular matrix (CC)	4	0.0543		4.49	0.6462

ES=enrichment score, P_BH=Benjamini-Hochberg corrected P-value

Table VII: Sequences of used primers and EMSA oligonucleotides

primer code	5' → 3' sequence	Product length (bp)	purpose
9_RV primer_for	ctagcaaaataggctgtccc		sequencing inserts pGL4.23/pGL4.12
11_pGL4.12[luc2CP] Sequ. rev	catagcttctgccagccgaac		sequencing inserts pGL4.23/pGL4.12
rs2155219_for_BglII	ttttagatctgagcttccactatttgcctg	459/1142	insert luciferase assay
rs2155219_459bp_rev_HindIII	ttttaagcttcttctagaggcctcagggtt	459	insert luciferase assay
rs2155219_1142bp_rev_HindIII	ttttaagctttggattctgacggagcagaa	1142	insert luciferase assay
rs2155219_1142bp_for_inv_BglII	tttttagatcttggattctgacggagcagaa	1142	insert luciferase assay
rs2155219_rev_inv_HindIII	ttttaagcttgagcttccactatttgcctg	1142	insert luciferase assay
rs2155219mut_for_major	gttaatatttgtctggggtgtttttatttcatcc	1142	Mutagenisis primer
rs2155219mut_rev_major	ggatgaaataaaacaccccagacaaatattaac	1142	Mutagenisis primer
rs11236797mut_for_major	ataaagttatttccttcgtatgctgcgcgg	1142	Mutagenisis primer
rs11236797mut_rev_major	ccgcgcagcatacgaaggaaataactttat	1142	Mutagenisis primer
C11orf30Prom_844_for_BglII	ttttagatctcccttgacagagatagcacg	844	insert luciferase assay
C11orf30Prom_844_rev_HindIII	ttttaagctttcttcccaggaccctgcct	844	insert luciferase assay
LRRC32Prom_711_for_BglII	ttttagatctcctgccaggacccaccagagt	711	insert luciferase assay
LRRC32Prom_711_rev_HindIII	ttttaagcttagtgcgcccccccgagggccg	711	insert luciferase assay
1142bp_enh_KpnI_for	ttttggtaccgagcttccactatttgcctg	1142	insert luciferase assay
1142bp_enh_SacI_rev	ttttgagctctggattctgacggagcagaa	1142	insert luciferase assay
C11orf30Prom844_Enh_CS_rev*	ggtagtgatatctcgtgcta		sequencing insert pGL4.12/C11orf30Prom
LRRC32Prom711_Enh_CS_rev*	aaggaaatgacccttcgctg		sequencing insert pGL4.12/LRRC32Prom
LRRC32_cds_XhoI_for	ttttctcgagatgagaccccagatcctgct	2054	insert expression vector
LRRC32_cds_SacII_rev	ttttccgcggttaggctttatactgttggttaaac	2054	insert expression vector
rs79525962_mut_mi_for	ccatacaccttttccaatctggcca	1142	Mutagenisis primer
rs79525962_mut_mi_rev	tggccagattggaaaaggtgtatgg	1142	Mutagenisis primer
SeqFor1_LRRC32	aatgggcggtaggcgtgtac	1162	sequencing insert pIRES2-AcGFP1
SeqRev1_LRRC32	cctcaaaggtccgcaagcag	1162	sequencing insert pIRES2-AcGFP1
SeqFor2_LRRC32	cccagctcttgaatctggat	1095	sequencing insert pIRES2-AcGFP1
SeqRev2_LRRC32	acagatggctggcaactaga	1095	sequencing insert pIRES2-AcGFP1
rs79525962_mutqc_mi_for	gcccccatacacctttttccaatctggccagcct		Quickchange mutagenisis
rs79525962_mutqc_mi_rev	aggctggccagattggaaaaggtgtatggggc		Quickchange mutagenisis
C11orf30eSNP_rs2282611_seq_for	gtgagtccttggtacatcta	556	sequencing eSNP

C11orf30eSNP_rs2282611_seq_rev	taacatcggatccggtagaa	556	sequencing eSNP
LRRC32eSNP_rs3781701_seq_for	cagctaactaatgccatagg	493	sequencing eSNP
LRRC32eSNP_rs3781701_seq_rev	cttgtgatgtgatagctgag	493	sequencing eSNP
rs3781701_LRRC32_f_seq	gaatgagagaatgcaagagc	90	sequencing eSNP
rs3781701_LRRC32_r_seq	tcctccttctctgcctgttt	90	sequencing eSNP
rs7927894_seq_for	tctgcagaatggatgttaaga	457	sequencing
rs7927894_seq_rev	tcctgcatccctagatctaa	457	sequencing
C11orf30_300bp_for	atcctctatgaagatttcac	300	allelic expression analysis
C11orf30_300bp_rev	agttgtgaaccactatacaa	300	allelic expression analysis
C11orf30_Snapshot_for	aggttgggtttcaacaacagtgact		allelic expression analysis
C11orf30_Snapshot_rev	taaaaataccctccgaggtctagga		allelic expression analysis
LRRC32_354bp_for	ctgatctttaccactgcagg	354	allelic expression analysis
LRRC32_354bp_for	gaggctctgtataagctctc	354	allelic expression analysis
LRRC32_Snapshot_16bp_for	gcctgtttccctcctc	16	allelic expression analysis
LRRC32_Snapshot_16bp_rev	aacccacaccagggtggaaaggaag	16	allelic expression analysis
For_rs2155219_Ma_G	Cy5-ttaatatttgtctggggtgttttatttcatc	31	EMSA
Rev_rs2155219_Ma_G	gatgaaataaaacaccccagacaaatattaa	31	EMSA
K_For_rs2155219_Ma_G	ttaatatttgtctggggtgttttatttcatc	31	EMSA
For_rs2155219_Mi_T	Cy5-ttaatatttgtctggtgtgtttttatttcatc	31	EMSA
Rev_rs2155219_Mi_T	gatgaaataaaacacaccagacaaatattaa	31	EMSA
K_For_rs2155219_Mi_T	ttaatatttgtctggtgtgtttttatttcatc	31	EMSA
For_SP1 (Briggs et al. 1986)	CY5-attcgatcggggcggggcgag	22	EMSA
Rev_SP1	gctcgccccgccccgatcgaat	22	EMSA
For_Oct1 (O'Neill et al. 1988)	CY5-tgtcgaatgcaaatcactagaa	22	EMSA
Rev_Oct1	ttctagtgatttgcattcgaca	22	EMSA
hLRRC32_for	atgagaccccagatcctgct	2054	RT-PCR
hLRRC32_rev	ttaggctttatactgttggttaaac	2054	RT-PCR
hβ-actin_for	ggattcctatgtgggcgacgagg	884	RT-PCR
hβ-actin_rev	cacggagtacttgcgctcaggagg	884	RT-PCR

*9_RV primer_for is used as forward primer; for= forward; rev= reverse; Ma= major; Mi= minor; Enh= enhancer; inv= invers

7.2 Figures
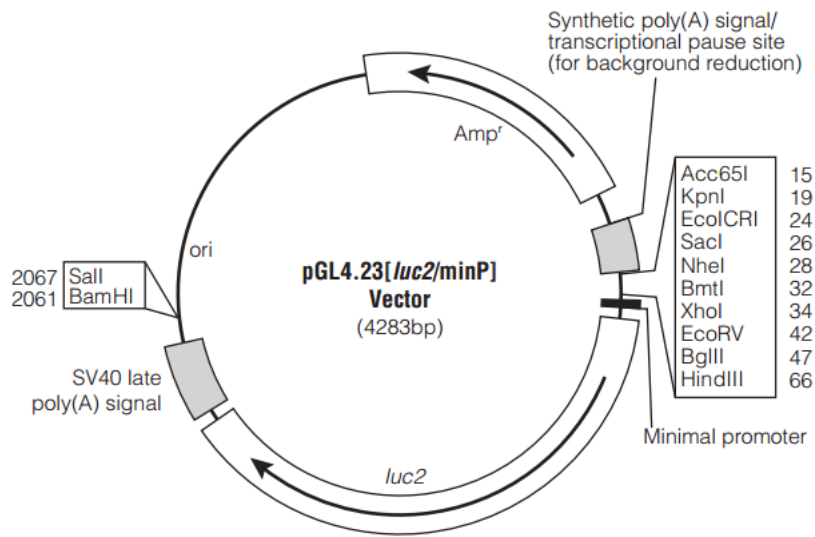
**Figure I: Vector map of pGL4.23[*luc2/minP*] vector (Promega)**
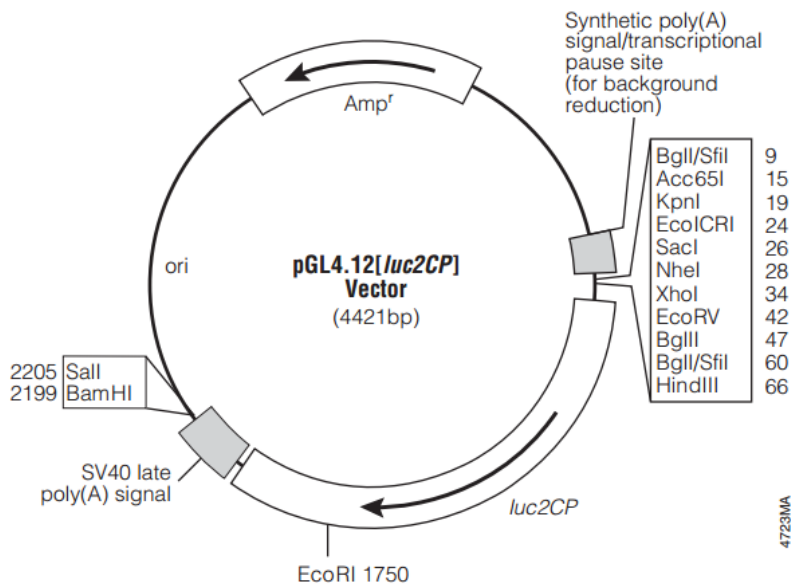
**Figure II: Vector map of pGL4.12[*luc2CP*] vector (Promega)**
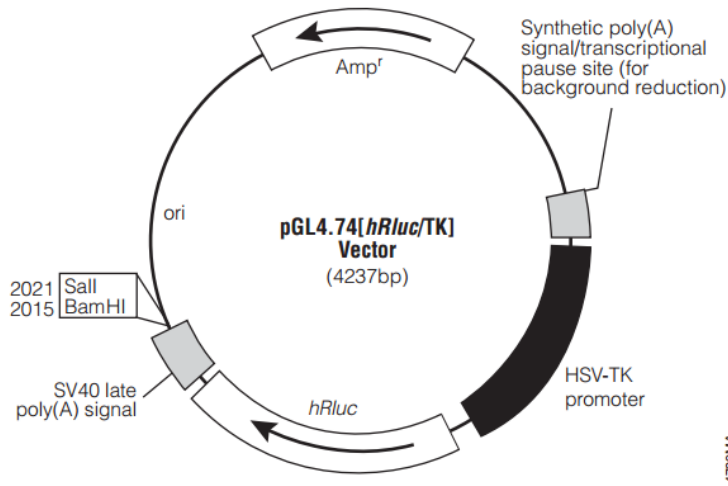
**Figure III: Vector map of pGL4.74[*hRluc/TK*] vector (Promega)**
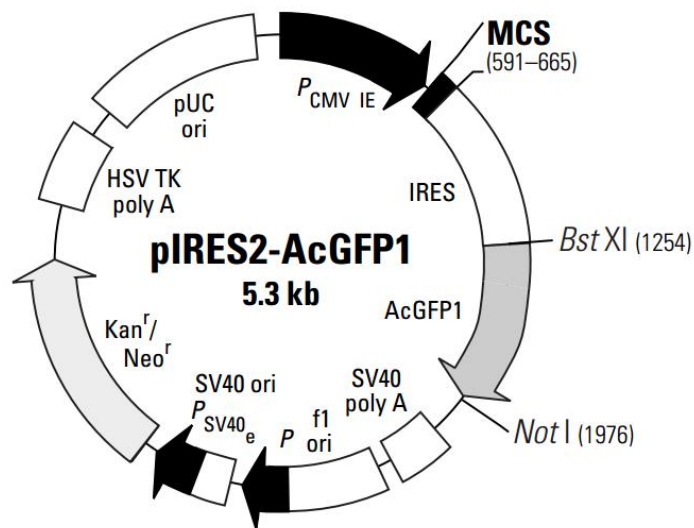
Figure IV: Vector map of pIRES2-AcGFP1 vector (Clontech Laboratories)

LIST OF PUBLICATIONS AND PRESENTATIONS

Publications included in this thesis

Manz J*, Rodríguez E*, ElSharawy A*, Oesau EM, Petersen BS, Baurecht H, Mayr G, Weber S, Harder J, Reischl E, Schwarz A, Novak N, Franke A, Weidinger S.: Targeted Resequencing and Functional Testing Identifies Low-Frequency Missense Variants in the Gene Encoding GARP as Significant Contributors to Atopic Dermatitis Risk. J Invest Dermatol 2016 Dec;136(12):2380-2386. doi: 10.1016/j.jid.2016.07.009. *joint first authors

Publications not included in this thesis

Amos CI, Dennis J, Wang Z, Byun J, Schumacher FR, Gayther SA, Casey G, Hunter DJ, Sellers TA, Gruber SB, Dunning AM, Michailidou K, Fachal L, Doheny K, Spurdle AB, Li Y, Xiao X, Romm J, Pugh E, Coetzee GA, Hazelett DJ, Bojesen SE, Caga-Anan C, Haiman CA, Kamal A, Luccarini C, Tessier D, Vincent D, Bacot F, Van Den Berg DJ, Nelson S, Demetriades S, Goldgar DE, Couch FJ, Forman JL, Giles GG, Conti DV, Bickeböller H, Risch A, Waldenberger M, Brüske-Hohlfeld I, Hicks BD, Ling H, McGuffog L, Lee A, Kuchenbaecker K, Soucy P, **Manz J**, Cunningham JM, Butterbach K, Kote-Jarai Z, Kraft P, FitzGerald L, Lindström S, Adams M, McKay JD, Phelan CM, Benlloch S, Kelemen LE, Brennan P, Riggan M, O'Mara TA, Shen H, Shi Y, Thompson DJ, Goodman MT, Nielsen SF, Berchuck A, Laboissiere S, Schmit SL, Shelford T, Edlund CK, Taylor JA, Field JK, Park SK, Offit K, Thomassen M, Schmutzler R, Ottini L, Hung RJ, Marchini J, Amin Al Olama A, Peters U, Eeles RA, Seldin MF, Gillanders E, Seminara D, Antoniou AC, Pharoah PD, Chenevix-Trench G, Chanock SJ, Simard J, Easton DF.: The OncoArray Consortium: A Network for Understanding the Genetic Architecture of Common Cancers. Cancer Epidemiol Biomarkers Prev. 2017 Jan;26(1):126-135. doi: 10.1158/1055-9965.EPI-16-0106.

Allegri M, De Gregori M, Minella CE, Klersy C, Wang W, Sim M, Gieger C, **Manz J**, Pemberton IK, MacDougall J, Williams FM, Van Zundert J, Buyse K, Lauc G, Gudelj I, Primorac D, Skelin A, Aulchenko YS, Karssen LC, Kapural L, Rauck R, Fanelli G; PainOMICS Group.: 'Omics' biomarkers associated with chronic low back pain: protocol of a retrospective longitudinal study. BMJ Open 2016 Oct 19;6(10):e012070. doi: 10.1136/bmjopen-2016-012070.

Marinelli M, Pappa I, Bustamante M, Bonilla C, Suarez A, Tiesler CM, Vilor-Tejedor N, Zafarmand MH, Alvarez-Pedrerol M, Andersson S, Bakermans-Kranenburg MJ, Estivill X, Evans DM, Flexeder C, Forns J, Gonzalez JR, Guxens M, Huss A, van IJzendoorn MH, Jaddoe VW, Julvez J, Lahti J, López-Vicente M, Lopez-Espinosa MJ, **Manz J**, Mileva-Seitz VR, Perola M, Pesonen AK, Rivadeneira F, Salo PP, Shahand S, Schulz H, Standl M, Thiering E, Timpson NJ, Torrent M, Uitterlinden AG, Smith GD, Estarlich M, Heinrich J, Räikkönen K, Vrijkotte TG, Tiemeier H, Sunyer J. Heritability and Genome-Wide Association Analyses of Sleep Duration in Children: The EAGLE Consortium. Sleep. 2016 Oct 1;39(10):1859-1869.

Baurecht H, Hotze M, Rodríguez E, **Manz J**, Weidinger S, Cordell HJ, Augustin T, Strauch K.: Compare and Contrast Meta Analysis (CCMA): A Method for Identification of Pleiotropic Loci in Genome-Wide Association Studies. PLoS One 2016 May 5;11(5):e0154872. doi: 10.1371/journal.pone.0154872. eCollection 2016.

Day FR, Ruth KS, Thompson DJ, Lunetta KL, Pervjakova N, Chasman DI, Stolk L, Finucane HK, Sulem P, Bulik-Sullivan B, Esko T, Johnson AD, Elks CE, Franceschini N, He C, Altmaier E, Brody JA, Franke LL, Huffman JE, Keller MF, McArdle PF, Nutile T, Porcu E, Robino A, Rose LM, Schick UM, Smith JA, Teumer A, Traglia M, Vuckovic D, Yao J, Zhao W, Albrecht E, Amin N, Corre T, Hottenga JJ, Mangino M, Smith AV, Tanaka T, Abecasis GR, Andrulis IL, Anton-Culver H, Antoniou AC, Arndt V, Arnold AM, Barbieri C, Beckmann MW, Beeghly-Fadiel A, Benitez J, Bernstein L, Bielinski SJ, Blomqvist C, Boerwinkle E, Bogdanova NV, Bojesen SE, Bolla MK, Borresen-Dale AL, Boutin TS, Brauch H, Brenner H, Brüning T, Burwinkel B, Campbell A, Campbell H, Chanock SJ, Chapman JR, Chen YD, Chenevix-Trench G, Couch FJ, Coviello AD, Cox A, Czene K, Darabi H, De Vivo I, Demerath EW, Dennis J, Devilee P, Dörk T, Dos-Santos-Silva I, Dunning AM, Eicher JD, Fasching PA, Faul JD, Figueroa J, Flesch-Janys D, Gandin I, Garcia ME, García-Closas M, Giles GG, Girotto GG, Goldberg MS, González-Neira A, Goodarzi MO, Grove ML, Gudbjartsson DF, Guénel P, Guo X, Haiman CA, Hall P, Hamann U, Henderson BE, Hocking LJ, Hofman A, Homuth G, Hooning MJ, Hopper JL, Hu FB, Huang J, Humphreys K, Hunter DJ, Jakubowska A, Jones SE, Kabisch M, Karasik D, Knight JA, Kolcic I, Kooperberg C, Kosma VM, Kriebel J, Kristensen V, Lambrechts D, Langenberg C, Li J, Li X, Lindström S, Liu Y, Luan J, Lubinski J, Mägi R, Mannermaa A, **Manz J**, Margolin S, Marten J, Martin NG, Masciullo C, Meindl A, Michailidou K, Mihailov E, Milani L, Milne RL, Müller-Nurasyid M, Nalls M, Neale BM, Nevanlinna H, Neven P, Newman AB, Nordestgaard BG, Olson JE, Padmanabhan S, Peterlongo P, Peters U, Petersmann A, Peto J, Pharoah PD, Pirastu NN, Pirie A, Pistis G, Polasek O, Porteous D, Psaty BM, Pylkäs K, Radice P, Raffel LJ, Rivadeneira F, Rudan I, Rudolph A, Ruggiero D, Sala CF, Sanna S, Sawyer EJ, Schlessinger D, Schmidt MK, Schmidt F, Schmutzler RK, Schoemaker MJ, Scott RA, Seynaeve CM, Simard J, Sorice R, Southey MC, Stöckl D, Strauch K, Swerdlow A, Taylor KD, Thorsteinsdottir U, Toland AE, Tomlinson I, Truong T, Tryggvadottir L, Turner ST, Vozzi D, Wang Q, Wellons M, Willemsen G, Wilson JF, Winqvist R, Wolffenbuttel BB, Wright AF, Yannoukakos D, Zemunik T, Zheng W, Zygmunt M, Bergmann S, Boomsma DI, Buring JE, Ferrucci L, Montgomery GW, Gudnason V, Spector TD, van Duijn CM, Alizadeh BZ, Ciullo M, Crisponi L, Easton DF, Gasparini PP, Gieger C, Harris TB, Hayward C, Kardia SL, Kraft P, McKnight B, Metspalu A, Morrison AC, Reiner AP, Ridker PM, Rotter JI, Toniolo D, Uitterlinden AG, Ulivi S, Völzke H, Wareham NJ, Weir DR, Yerges-Armstrong LM; PRACTICAL Consortium.; kConFab Investigators.; AOCS Investigators.; Generation Scotland.; EPIC-InterAct Consortium.; LifeLines Cohort Study., Price AL, Stefansson K, Visser JA, Ong KK, Chang-Claude J, Murabito JM, Perry JR, Murray A.: Large-scale genomic analyses link reproductive aging to hypothalamic signaling, breast cancer susceptibility and BRCA1-mediated DNA repair. Nat Genet. 2015 Nov;47(11):1294-303. doi: 10.1038/ng.3412. Epub 2015 Sep 28.

Meldrum SJ, Heaton A, Li Y, Zhang G, D'Vaz N, **Manz J**, Reischl E, Koletzko BV, Susan L. Prescott SL, Simmer K.: Polymorphisms in the fatty acid desaturase (FADS) gene cluster alter the effects of fish oil supplementation on plasma and erythrocyte fatty acid profiles. British Journal of Nutrition. Submitted

Dagostino C, De Gregori M, Gieger C, **Manz J**, Gudelj I, Lauc G, Divizia L, Wang W, Sim M, Pemberton IK, MacDougall J, Williams F, Van Zundert J, Primorac D, Aulchenko Y, Kapural L, Allegri M; PainOmics Group.: Validation of standard operating procedures in a multicenter retrospective study to identify -omics biomarkers for chronic low back pain. PLoS One 2017 May 1;12(5):e0176372. doi: 10.1371/journal.pone.0176372. eCollection 2017.

McKay* JD*, Hung RJ*, Han Y, Zong X, CarrerasTorres R, Christiani DC, Caporaso N, Johansson M, Xiao X, Li Y, Byun J, Dunning A, Pooley K, Qian DC , Ji X, Liu G, Timofeeva M, Bojesen SE, Wu X, Le Marchand L, Albanes D, Bickebölller H, Aldrich MC, Bush WS, Tardon A, Rennert G, Dawn Teare M, Field JK, Kiemeney LA, Lazarus P, Haugen A, Lam S, Schabath MB, Andrew AS, Shen H, Hong YC, Yuan JM, Bertazzi PA, Pesator AC, Ye Y, Diao N, Su L, Zhang R, Brhane Y, Leighl N,. Johansen JS, Mellemgaard A, Saliba W, Haiman C, Wilkens L, Fernandez-Somoano A, Fernandez-Tardon G, van der Heijden H, Hee Kim J, Dai J, Hu Z, Davies M, Marcus MW, Brunnström H, Manjer J, Melander O, Muller DC, Overvad K, Trichopoulou A, Tumino R, Doherty J, Barnett M, Chen C, Goodman G, Cox A, Taylor F, Woll P, Brüske I, Wichmann HE, **Manz J**, Muley T, Risch A, Rosenberger A, Grankvist K, Johansson M, Shepherd FA, Tsao MS, Arnold SM, Haura EB, Bolca C, Holcatova I, Janout V, Kontic M, Lissowska J, Mukeria A, Ognjanovic S, Orlowski TM, Scelo G, Swiatkowska B, Zaridze D, Bakke P, Skaug V, Zienolddiny S, Duell EJ, Butler LM, Koh WP, Gao YT, Houlston R, McLaughlin J, Stevens V, Joubert P, Lamontagne M, Nickle DC, Obeidat M, Timens W, Zhu B, Song L, Kachuri L, Soler Artigas M, Tobin MD, Wain LV, SpiroMeta Consortium, Rafnar T, Thorgeirsson TE, Reginsson GW, Stefansson K, Hancock DB, Bierut LJ, Spitz MR, Gaddis NC, Lutz SM, Gu F, Johnson EO, Kamal A, Pikielny C, Zhu D, Lindströem S, Jiang X, Tyndale RF, Chenevix-Trench G, Beesley J, Bossé Y, Chanock S, Brennan P, Landi MT, Amos CI.: Large scale genetic analysis identifies novel loci and histological variability in susceptibility to lung cancer. Nat Genet. 2017. Submitted

Poster presentations:

Judith Manz, Anja Kretschmer, Gabriele Möller, Annette Peters, Jerzy Adamski, Melanie Waldenberger, Eva Reischl , Stephan Weidinger: *An atopy-associated variant in the 11q13.5 locus regulates promoter activity*. ASHG 2014 Annual meeting, San Diego, USA

Oral presentations

"Characterization of a susceptibility locus for atopic dermatitis and inflammatory bowel disease.", 4th Workshop of Genetic Epidemiology, 2014

DANKSAGUNG (ACKNOWLEDGEMENTS)

CURRICULUM VITAE

Persönliche Daten:

Name: Judith Manz

Werdegang:

03/2012 – 08/2016	Naturwissenschaftliche Doktorandin (Dr. rer. nat.) am Helmholtz Zentrum München, Institut für Epidemiologie II, Abteilung für molekulare Epidemiologie, Arbeitsgruppe *Complex Diseases*
10/2009 – 02/2012	Masterstudiengang (M.Sc.) der Ernährungs-wissenschaft an der Technischen Universität München Masterarbeit: "Analysis of the molecular basis of inter-individual differences in A-SAA levels"
10/2006 – 07/2009	Bachelorstudiengang (B.Sc.) der Ernährungs-wissenschaft an der Technischen Universität München Bachelorarbeit: „Entwicklung von Reporter-gensystemen zur Untersuchung ER-Stress assoziierter Genexpression von Grp-78 und CHOP in Darmepithelzelllinien
03/2004 – 07/2006	Duale Ausbildung zur Biologielaborantin an der Julius Maximilian Universität Würzburg, Institut für Pharmakologie und Toxikologie
2003	Abitur am Gymnasium im Ellental, Bietigheim-Bissingen